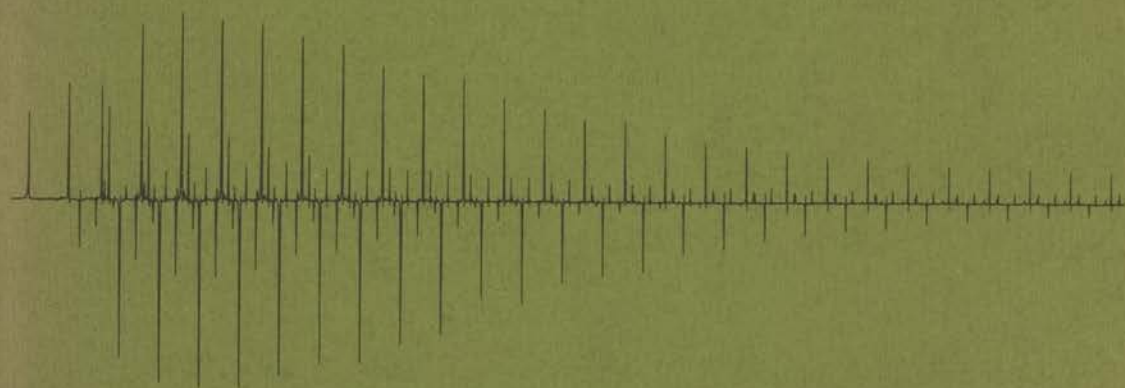


CHEMICALLY INDUCED DYNAMIC  
NUCLEAR POLARIZATION



R. KAPTEIN

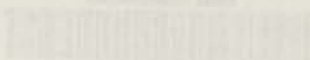
RIJKSUNIVERSITEIT LEIDEN



0922 4085

CHEMICALLY INDUCED DYNAMIC NUCLEAR POLARIZATION

UNIVERSITY LIBRARY



022 4585

# CHEMICALLY INDUCED DYNAMIC NUCLEAR POLARIZATION

PROEFSCHRIFT  
TER VERKRIJGING VAN DE GRAAD VAN DOCTOR IN  
DE WISKUNDE EN NATUURWETENSCHAPPEN AAN  
DE RIJKSUNIVERSITEIT TE LEIDEN, OP GEZAG VAN  
DE RECTOR MAGNIFICUS DR. C. SOETEMAN,  
HOGLERAAR IN DE FACULTEIT DER LETTEREN,  
TEN OVERSTAAN VAN EEN COMMISSIE UIT DE SENAAT  
TE VERDEDIGEN OP WOENSDAG 12 MEI 1971  
TE KLOKKE 15.15 UUR

DOOR

**ROBERT KAPTEIN**

GEBOREN TE 's-GRAVENHAGE IN 1941

1971

BRONDER-OFFSET N.V.  
ROTTERDAM

# CHEMICALLY INDUCED DYNAMIC NUCLEAR POLARIZATION

PROMOTOR: PROF. DR. L.J. OOSTERHOFF

TER VERKRIJGING VAN DE GRAAD VAN DOCTOR IN  
DE WISKUNDE EN NATUURWETENSCHAPPEN AAN  
DE RIJKSUNIVERSITEIT TE LEIDEN, OP BEZAG VAN  
DE RECTOR MAGNIFICUS DR. C. ROZEMAN,  
HOOGLEERAAR IN DE FACULTEIT DER LETTEREN,  
TEH OORSTAAN VAN EEN COMMISSIE UIT DE SENAAT  
TE VERDEELDEN OP WOENSDAG 13 MEI 1971  
TE KLOKKE 16.15 UUR

DOOR

ROBERT KAPTEIN

- GEBOREN TE GRAVENHAGE IN 1941

## STELLINGEN

### I

Het kan voordelen bieden om CIDNP experimenten uit te voeren, waarbij het spectrum wordt opgenomen tijdens de reactie in zeer lage magneet velden (b.v. het aardveld). De enorme versterkings factoren ( $10^6$  à  $10^7$ ), die hierbij kunnen optreden, maken dit mogelijk.

### II

De opmerking van Buchachenko et al., dat CIDNP zou ontstaan tijdens de elementaire stappen van chemische reacties (het maken of verbreken van chemische bindingen), suggereert een verkeerd beeld van de werkelijkheid.

A.L. Buchachenko, S.V. Rykov, and A.V.Kessenich,  
Zh. Fiz. Khim., 44, 876 (1970).  
S.V. Rykov, A.L. Buchachenko, A.V.Kessenich,  
Spectr. Letters, 3, 55 (1970).

### III

Theorieën van de chemisch geïnduceerde electronen-spin polarisatie zullen rekening moeten houden met het dynamische karakter van dit verschijnsel.

P.W. Atkins, R.C.Gurd, K.A. Mc Lauchlan, and A.F. Simpson,  
Chem.Phys.Letters, 8, 55 (1971).  
Dit proefschrift, hoofdstuk II:

## IV

Uit de manier waarop Matsen schrijft over "popular misconceptions about spin", blijkt, dat hij geen hoge dunk heeft van organisch chemici.

F.A. Matsen, J. Am. Chem. Soc., 92, 3525 (1970)

## V

De door Dahlberg, Anderson en Dayton gemeten emissie van de tweede positieve groep van  $N_2 - C^3\Pi_u \rightarrow B^3\Pi_g$  - in een bundelexperiment, waar bij protonen op  $N_2(X^1\Sigma_g^+)$  worden geschoten, is voornamelijk het gevolg van secundaire processen.

D.A. Dahlberg, D.K. Anderson, en I.E. Dayton,  
Phys. Rev. 164, 20, (1967).

J.F.M. Aarts en F.J. de Heer, Chem. Phys. Letters, 4, 116 (1969)

## VI

Gilbert en Hybart, die tijdsafhankelijke osmotische hoogten meten, menen ten onrechte dat de naar het tijdstip nul geëxtrapoleerde hoogte de ware osmotische druk voorstelt.

M. Gilbert and F.J. Hybart, J. Polymer Science, 9, 222 (1971).

## VII

Het is waarschijnlijk, dat de gesubstitueerde  $C_5$ -ring in de door Hoxmeier et al. beschreven verbinding als een carbeen complex voorkomt.

R. Hoxmeier, B. Deubzer, H.D. Kaesz, J. Amer. Chem. Soc., 93,  
536 (1971).

VIII

Het model, waarmee Glasel zijn deuterium kernspin-relaxatie metingen aan oplossingen van polymethacrylzuur in  $D_2O$  interpreteert, is aanvechtbaar.

J.A. Glasel, J.Amer.Chem.Soc., 92, 375 (1970).

IX

De methode van Freed om in de theorie van stralingsloze overgangen irreversibiliteit af te leiden is aan bedenkingen onderhevig.

K.F.Freed, J.Chem.Phys., 52, 1345 (1970).

X

Het stimuleren van het ping-pong spel zou een goed alternatief kunnen zijn van de tot nu toe gevolgde politiek voor het verre oosten van sommige grootmachten.

R. Kaptein

Leiden, 12 mei 1971

... ..  
... ..  
... ..

F. A. Cotton, *J. Chem. Phys.*, **10**, 413 (1942).

... ..  
... ..  
... ..

G. A. Baker, *J. Chem. Phys.*, **10**, 413 (1942).

*Phys. Rev.*, **55**, 20 (1942).

J. F. O'Connell and F. J. O'Connell, *J. Chem. Phys.*, **10**, 413 (1942).

... ..

... ..  
... ..  
... ..

F. J. O'Connell and F. J. O'Connell, *J. Chem. Phys.*, **10**, 413 (1942).

... ..  
... ..  
... ..

F. J. O'Connell and F. J. O'Connell, *J. Chem. Phys.*, **10**, 413 (1942).

... ..

... ..

CHAPTER IV	CIDRP, TRIPLET AND SINGLET STATE PHOTODIMERIZATION OF NITROXINE DECOMPOSITIONS	27
CHAPTER V	CIDRP V. SPIN EMPLOYMENTS IN ORGANICAL PRODUCTS	35
CHAPTER VI	CIDRP. HIGH REVERSED OF THE POLARIZATION IN THE REACTION OF NITROXINE WITH WITH DIMETHYLACETONE	41
CHAPTER VII	CIDRP VII. PHOTOACTIVATIONS OF ALIPHATIC NITROXIDES	51
71	GENERAL INTRODUCTION	
72	1. Introduction	52
73	2. Photoactivation of nitroxine	53
74	3. The present status of nitroxine	54
75	4. References	55
76	CHAPTER I CIDRP IN FIVE WAVELENGTHS	
77	1. Introduction	56
78	2. Results and discussion	57
79	3. Conclusions	58
80	4. References	59
81	CHAPTER VIII. SPIN EMPLOYMENTS IN ORGANICAL PRODUCTS	65
82	1. Introduction	66
83	2. Results and discussion	67
84	3. Conclusions	68
85	4. References	69
86	CHAPTER II CIDRP II. RELATIONSHIP BETWEEN CIDRP AND PHOTODIMERIZATION	
87	1. Introduction	70
88	2. Photoactivation of nitroxine	71
89	3. Photoactivation of nitroxine	72
90	4. Photoactivation of nitroxine	73
91	5. References	74
92	3. Conclusions	75
93	CHAPTER III CIDRP III. AMINOACETONE RADICAL COUPLED AND DIMERIZATION PRODUCTS	
94	1. Introduction	76
95	2. Theory	77
96	3. Results and discussion	78
97	4. Conclusions	79
98	5. References	80
99	CHAPTER V CIDRP V. SPIN EMPLOYMENTS IN ORGANICAL PRODUCTS	
100	1. Introduction	81
101	2. Results and discussion	82
102	3. Conclusions	83
103	4. References	84

voor Saskia  
Marcel en  
Sebastiaan.

## CONTENTS

	page
GENERAL INTRODUCTION	11
The Radical Pair Model.	12
What can be learned from CIDNP?	15
The present status and prospects.	17
CHAPTER I    CIDNP IN FIVE ALKYL RADICALS	19
1. Introduction	19
2. Results and discussion	20
References	25
CHAPTER II    CIDNP II. RELATION WITH ANOMALOUS ESR SPECTRA	26
1. Introduction	26
2. Population rates	26
3. Relaxation in alkyl radicals	27
4. Discussion	28
References	28
CHAPTER III    CIDNP III. ANOMALOUS MULTIPLETS OF RADICAL COUPLING AND DISPROPORTIONATION PRODUCTS	29
1. Introduction	29
2. Theory	29
3. Enhancement factor $V_{\max}$	30
4. Discussion	30
References	31

		page
CHAPTER IV	CIDNP. TRIPLET AND SINGLET STATE PHOTOSENSITIZATION OF PEROXIDE DECOMPOSITIONS	32
CHAPTER V	CIDNP V. NMR ENHANCEMENTS IN BIRADICAL PRODUCTS	35
CHAPTER VI	CIDNP. SIGN REVERSAL OF THE POLARIZATION IN THE REACTION OF ISOBUTYRYL PEROXIDE WITH BROMOTRICHLOROMETHANE	41
CHAPTER VII	CIDNP VII. PHOTOREACTIONS OF ALIPHATIC KETONES	46
	1. Introduction	46
	2. Photolysis of diisopropyl ketone in $\text{CDCl}_3$	47
	3. The photoreaction of diisopropyl ketone with $\text{CCl}_4$	50
	References	54
CHAPTER VIII	CIDNP VIII. SPIN DYNAMICS AND DIFFUSION OF RADICAL PAIRS	55
	1. Introduction	55
	2. The Spin Hamiltonian and S-T <sub>0</sub> mixing	58
	2.1 The exchange term	59
	2.2 The Zeeman terms	61
	2.3 The hyperfine terms	61
	2.4 Other terms	61
	2.5 S-T <sub>0</sub> mixing	63
	3. Diffusion and recombination of radical pairs	65
	3.1 S precursor	66
	3.2 T precursor	66
	3.3 F precursor	67
	3.4 Thermal equilibrium	69
	4. CIDNP intensities and enhancement factors	70
	4.1 Recombination products	71
	4.2 Escape products	73

	page
4.3 Structure of CIDNP spectra	75
4.4 Simple rules	77
4.5 Second order spectra and computer simulation	79
5. Examples	80
5.1 Ethylchloride at 15.1 Mc	80
5.2 2-Cyanopropane	81
5.3 Isobutane	83
Conclusion	84
APPENDIX A. Spin-orbit coupling in radical pairs	84
APPENDIX B. Free radical encounters	85
References	88
CHAPTER IX	
CIDNP IX. REACTIONS COMPETITIVE WITH GEMINATE RECOMBINATION OF RADICAL PAIRS	92
1. Introduction	92
2. Theory	93
2.1 Competitive reactions	93
2.2 S precursor	94
2.3 T precursor	98
2.4 Enhancement factors and product yields	100
2.5 Memory effect	101
3. Stereospecific homolytic rearrangements	102
3.1 S precursor	103
3.2 T precursor	104
4. Discussion of experimental examples	105
4.1 Radical scavenging	105
4.2 Fragmentation	106
4.3 Rearrangements of radicals	108
4.4 Conclusions	109
References	110

CHAPTER X	CIDNP X. ON THE MAGNETIC FIELD	
	DEPENDENCE	112
	1. Introduction	112
	2. General formalism	113
	2.1 Radical pair theory	113
	2.2 Stage a. The Hamiltonian matrix	114
	2.3 Stage b. The populations in $H_T$	118
	2.4 Stage c. The populations in $H_0$	122
	3. Qualitative features and predictions	
	of the theory	123
	3.1 Effects of $S-T_{\pm}$ mixing	123
	3.2 The zero-field case	126
	4. Experimental examples	129
	4.1 Photolysis of propionyl peroxide	129
	4.2 Photolysis of diisopropyl ketone	
	in $CCl_4$	132
	4.3 Thermal and photochemical decomposition of acetyl peroxide	139
	4.4 Other work	140
	5. Conclusions	141
	APPENDIX. Populations of zero-field	
	levels.	142
	References	144
CHAPTER XI	CIDNP XI. THERMAL DECOMPOSITION OF ACETYL	
	PEROXIDE	146
	1. Introduction	146
	2. Acetyl peroxide	148
	2.1 CIDNP spectra	148
	2.2 Origin of the ethane polarization	150
	2.3 Enhancement factors provided by the DP center	151
	3. 2,2'-Di-carbon-13-acetyl peroxide	154
	3.1 $^1H$ -spectrum	154
	3.2 $^{13}C$ -spectrum	156
	3.3 50/50 Mixture enriched/non-enriched	
	acetyl peroxide	158

	page
4. Dideutero-acetyl peroxide	160
4.1 <sup>1</sup> H-spectrum	160
4.2 <sup>2</sup> D-spectrum	161
5. Hexadeutero-acetyl peroxide	163
6. Conclusions	164
7. Experimental section	164
References	166
CHAPTER XII	CIDNP XII. THERMAL DECOMPOSITION OF
	ALIPHATIC ACYL PEROXIDES
	168
1. Introduction	168
2. Aliphatic acyl peroxides	171
2.1 Propionyl peroxide	172
2.2 Butyryl peroxide	176
2.3 Isobutyryl peroxide	177
2.4 Isovaleryl peroxide	179
2.5 Pivaloyl peroxide	180
3. Alicyclic acyl peroxides	181
3.1 Cyclopropanecarbonyl peroxide	183
3.2 Cyclobutanecarbonyl peroxide	186
3.3 Cyclopentanecarbonyl peroxide	187
3.4 Cyclopropylacetyl peroxide	189
4. $\alpha$ -Unsaturated acyl peroxides	194
4.1 Acrylyl peroxide	195
4.2 Methacrylyl peroxide	197
4.3 <u>trans</u> -Crotonyl peroxide	199
5. <u>t</u> -Butylperpivalate	200
6. Conclusions	202
7. Experimental section	203
References	204
SAMENVATTING	208
ACKNOWLEDGEMENT	211
CURRICULUM VITAE	212

## GENERAL INTRODUCTION.

The subject of this thesis is the study of nuclear magnetic resonance (nmr) spectra of reacting systems. In 1967 Bargon, Fischer and Johnson<sup>1</sup> and independently Ward and Lawler<sup>2</sup> reported the discovery of nmr emission and enhanced absorption during free radical reactions. These effects have been named "Chemically Induced Dynamic Nuclear Polarization" (CIDNP). This name reflects the early theories, which have been advanced<sup>1b,2b</sup>, and which treated the phenomena in a way similar to the well-understood "Dynamic Nuclear Polarization" (DNP) effects, induced by microwave irradiation. Although it has turned out that the polarization, induced by chemical reactions, has a completely different origin, the name CIDNP has been kept, to designate the phenomenon.

One of the very first papers<sup>2a</sup> on CIDNP contained already an example of the "multiplet effect", by which is meant the occurrence of both emission and enhanced absorption within a multiplet of a nucleus, coupled to a group of other nuclei. This effect could not be explained by the DNP theory, since it required a strong correlation between the nuclei in the radicals, which is not provided by the DNP cross-relaxation mechanism. This and other mysteries showed that the DNP model was inadequate in case of polarization<sup>3</sup> induced by chemical reactions. However, it was clear that CIDNP could develop into a valuable new tool for the study of reaction mechanisms, once it became properly understood.

Thus, we took up the challenge and started the present investigation, soon after the appearance of the first papers<sup>1,2</sup>. As we were primarily interested in the physical principles underlying the polarization phenomena, the systems that we have studied experimentally, were chosen mainly from the field of simple acyl peroxide decompositions. These constitute a class of well-documented homolytic reactions (actually some of these systems turned out to be not so simple). Furthermore, the magnetic parameters of the alkyl radicals, generated during decomposition, were known from electron spin resonance (esr) in most cases.

A preliminary account of this experimental work has been published in 1968 and is reproduced in chapter I. A noteworthy result was the observed dependence of the polarization upon type of reaction, which also did not follow from the DNP model. Since the correct CIDNP mechanism was not yet discovered, the discussion of this paper in terms of the DNP model are somewhat obsolete now; they demonstrate how poorly understood the effects were at that time. However, this first paper contains a remark on electron spin-exchange during radical encounters, and although the import was not yet fully recognized, the pursuit of this point has proven to be very fruitful.

Chapters II and III consist of papers published in 1969, in which the base is laid for the "radical pair model", the basic ideas of which were independently published by Closs<sup>4</sup>. Electron spin polarization (CIDEP), which was known<sup>5</sup> long before CIDNP but had not received much attention, is considered in part II. The possible connection with nuclear spin polarization via cross-relaxation (noted in II) has not been substantiated by further work; this is probably not important as a polarization mechanism for nuclei. A completely satisfactory theory for CIDEP does not yet seem to exist.

#### The radical pair model.

Chapter III is concerned with nuclear polarization in recombination products and explains the multiplet effect in terms of nuclear spin dependent singlet (S) - triplet (T) mixing in radical pairs. In high

magnetic fields only S- $T_0$  mixing ( $T_0$  is the triplet state with  $M_S = 0$ ) is important and therefore no nuclei are "flipped"<sup>6</sup>. However, they determine the rate of intersystem-crossing (S- $T_0$  mixing) and thus the reaction probability of the pair, since reaction occurs usually only from the S-state. This process has been called "spin-selection"<sup>7</sup>. Although this is an appropriate name for the case of reactions in high magnetic field, it does not correctly describe the low field case, since nuclear spins undergo transitions there.

It may seem improbable that the tiny magnetic interactions between electrons and nuclei ( $10^{-5}$  kcal/mole) are capable of influencing the course of chemical reactions. This becomes more understandable, when it is realized that these interactions mix S and T states only effectively by virtue of the fact, that the energy gap between these states becomes of the same order magnitude or less in a diffusing radical pair. Moreover, even when the reaction is only slightly (say for 1%) controlled by nuclear spins, this results in enormous polarization enhancements (factor 1000), because of the small thermal nuclear polarization (about  $10^{-5}$  in a field of 23 kG).

As was mentioned above, mixing of S with  $T_+$  and  $T_-$  states can be neglected in high fields, in spite of the fact that for certain separations of the pair S and  $T_-$  states will become degenerate (see figure 1 of chapter VIII). This can be understood by noting that radical pairs (being quantum mechanical systems) behave like cars on a highway (e.g. the S-level), running with considerable speed. This high speed makes it impossible for them to make the sharp turns into the cross-roads (dotted line to the  $T_-$  level). Only when roads have a nearly parallel course, some of the cars are able to make the turn (S  $\rightarrow$   $T_0$  transitions). The theory for high fields is substantially simplified by this feature.

In chapters IV to VII the radical pair model is applied to a number of photochemical and thermal reactions. In IV the photolysis of some acyl peroxides provides an illustration of the role of the precursor multiplicity (S or T) in CIDNP spectra. The peroxide decompositions are photosensitized by T state ketones and, notably, also by excited S state anthracene.

CIDNP effects in the products of a biradical are presented in chapter V.

In chapter VI the thermal decomposition of isobutyryl peroxide in the presence of various concentrations of the radical trap  $\text{CCl}_3\text{Br}$  is discussed. It shows a unique feature of CIDNP: products of geminate pairs (with a common precursor) can be distinguished from those of non-geminate pairs (F-pairs, i.e. pairs formed by encounters of free, uncorrelated radicals).

Chapter VII describes some CIDNP spectra, obtained during photolysis of diisopropyl ketone, a representative of the  $\alpha$ -branched aliphatic ketones. In contrast to most solvents, a singlet reaction predominates in  $\text{CCl}_4$ . It involves probably the formation of a complex of  $^1n, \pi^*$  ketone with  $\text{CCl}_4$ .

The radical pair theory of CIDNP in high magnetic fields is critically reexamined in chapter VIII. A model is developed, in which the role of diffusion of radical pairs is more properly taken into account, by employing a random walk diffusion model<sup>8</sup>; a similar idea has been conceived by Adrian<sup>9</sup>, although our treatment differs from his in some respects. It turns out that all qualitative predictions of the theory follow from two simple rules (presented in section 4.4 of VIII): one for net polarization and the other for multiplet effects.

In chapters IX and X extensions of the theory of VIII are given. Fast reactions, that compete with geminate recombination of radical pairs, are the subject of chapter IX. Application of CIDNP to the determination of rate constants of these fast reactions is an intriguing possibility, although at present the uncertainties are rather large. In chapter X, the model is generalized to include the case of reactions in low magnetic fields; some examples of low field reactions are discussed as well. The theory becomes somewhat more involved, due to the fact that mixing of S with all three T states must be taken into account. However, the field dependence of CIDNP yields additional information (e.g. the sign of the effective exchange integral in our model) and applies a severe test to the theoretical models, that have been developed.

Chapters XI and XII deal with the thermal decomposition of acyl peroxides. Acetyl peroxide and carbon-13, as well as deuterium substituted acetyl peroxides are discussed in chapter XI; a series of other acyl peroxides in chapter XII. Some of these systems provide examples of competitive reactions, such as, for instance, the decarboxylation of acyloxy radicals, and the rearrangement of the cyclopropylcarbonyl radical.

#### What can be learned from CIDNP?

Information can be obtained (i) on the reaction mechanism and (ii) on the structure of radicals and products. Starting with (i) we list a few specific points and mention some examples:

- (1) Products showing CIDNP are formed by a radical mechanism.

Trivial as it may seem, this information can be highly useful in organic chemistry. The first paper by Ward and Lawler<sup>2</sup> established the radical nature of the reactions of alkylhalides with alkyllithium compounds.

- (2) The radical pair from which the products are formed can be identified. If a product can be formed by two or more routes, CIDNP may discriminate between these.

A nice example is provided by the work by Closs and Paulson<sup>10</sup> on the formation of benzaldehyde from benzoin.

- (3) The multiplicity of the precursor of radical pairs (S or T) can be established.

We mentioned already the photosensitization of peroxide decompositions by both S and T excited states (chapter IV).

- (4) Geminate products from S-pairs can be distinguished from non-geminate products (from F-pairs).

A first example has been reported by Closs and Trifunac<sup>11</sup>, who observed opposite polarization in products from the same radical pairs, but generated differently (S- and F- pairs).

- (5) Reactions can be detected, which are difficult to detect by other means, in particular in cases where reactant and product are the same.

Examples are the thermoneutral iodine atom exchange in the reaction of alkyl radicals with alkyl iodides<sup>12</sup> and the reversible addition of radicals to styrene<sup>13</sup>.

(6) Fast, competitive reactions and dynamical processes in radicals can be studied.

Examples of radical scavenging, rearrangement and fragmentation are given in chapter IX.

(7) Minor reaction pathways can be detected, which often give rise to larger polarization than the main reaction.

The first example<sup>1</sup> of CIDNP (benzene from benzoyl peroxide) is a case, where the polarization results from a sidepath, that accounts for only 4% of the reaction<sup>14</sup>.

(8) Diffusive behaviour of radical pairs in solution can be studied.

This facet has not yet been explored.

Regarding point (ii) the information is similar to and supplements that obtained by conventional magnetic resonance techniques:

(9) Signs (and sometimes magnitudes) of hyperfine coupling constants in radicals can be determined.

e.g. the sign of the  $\alpha$ -hydrogen coupling constant in the cyclopropyl radical is negative (cf. XII).

(10) Signs of g-factor differences (and sometimes magnitudes of g-factors) follow from CIDNP spectra.

e.g. the g-factor of the acetoxy radical (life-time shorter than  $10^{-9}$  sec) was found to be 2.0058 (cf. XI).

(11) Signs of nuclear spin-spin coupling constants in the products can be determined.

e.g. cyclopropene gives rise to a  $A_2X_2$  spectrum with  $J_{AX} = +1.8$  Hz (cf. XII).

(12) Spin-lattice relaxation of radicals can be studied.

Closs and Paulson<sup>10</sup> obtained relaxation times of the order  $10^{-3}$ - $10^{-4}$  sec for benzyl type radicals.

(13) Relaxation behaviour in products can also be studied.

Apart from determination of "relaxation times", this point has not yet been investigated in detail.

Some of the information regarding signs of coupling constants and precursor multiplicities can be obtained "at a glance", by making use of the rules given in chap. VIII section 4.4. However, ambiguities may exist, since the polarization is determined by a product of several quantities. Thus it may occur, that if two signs are unknown, CIDNP will only yield their product.

A further quantity, that affects CIDNP intensities, is the rate of formation of radical pairs, which should not be too low. Precursor half-lives are usually in the range 2-30 min. If chain reactions occur, only the initiation and termination steps would give rise to polarization. Moreover, relaxation times of the product should not be too short, which restricts the observation of CIDNP effects to systems, where short-lived radicals occur as intermediates.

#### The present status and prospects.

Evidence for the radical pair mechanism is now so abundant, that the theory can be used with some confidence to derive information of the type delineated above, from CIDNP spectra. In fact, there seems to be no evidence against it at present. However, this may be partly due to the fact, that radical chemistry is conveniently complex, so that up to now one could always invoke some radical pair and make it responsible for the observed polarization. Therefore, the few ambiguous observations, that may exist, deserve a closer study, in order to see if other mechanisms contribute to nuclear polarization in chemical reactions.

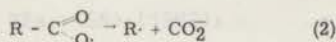
Although there is not yet complete agreement as to the best quantitative description of the effects, we might say that CIDNP has reached a stage of puberty and is rapidly progressing to become grown-up. The recently developed pulsed nmr techniques (Fourier Transform nmr) are very suitable for quantitative CIDNP studies, and will undoubtedly be applied in the near future. Furthermore the study of nuclei other than protons (especially  $^{13}\text{C}$ ) seem to be particularly fruitful<sup>15</sup>.

It is not to be expected that CIDNP will replace any of the techniques used in mechanistic chemistry or magnetic resonance; rather, it constitutes a valuable supplement to the arsenal of the chemist, and is an interesting phenomenon in its own right.

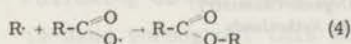
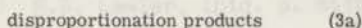
## References.

- 1.(a) J. Bargon, H. Fischer and U. Johnsen, Z. Naturforsch., 22a, 1551 (1967);  
(b) J. Bargon and H. Fischer ibid. p. 1556.
- 2.(a) H.R. Ward and R.G. Lawler, J. Am. Chem. Soc., 89, 5518 (1967);  
(b) R.G. Lawler, ibid. p. 5519.
3. Following common usage in the field, the term "polarization" is used throughout this work to denote all deviations from thermal equilibrium populations. It includes, therefore, population distributions in which no "net polarization" occurs, which would resemble situations of "alignment", and which give rise to the multiplet effect.
4. G.L. Closs, J. Am. Chem. Soc., 91, 4552 (1969).
5. R.W. Fessenden and R.H. Schuler, J. Chem. Phys., 39, 2147 (1963).
6. The operator responsible for the mixing,  $S_{12}^I$  is diagonal in the nuclear spin states.
7. H.R. Ward, presented at the CIDNP symposium of the ACS meeting in Houston, Feb. (1970).
8. R.M. Noyes, "Progress in Reaction Kinetics" ed. G. Porter, Pergamon, Oxford, Vol. 1. (1961), pp. 129 - 160
- 9.(a) F.J. Adrian, J. Chem. Phys., 53, 3374 (1970),  
(b) F.J. Adrian, personal communication.
10. G.L. Closs and D.R. Paulson, J. Am. Chem. Soc., 92, 7229 (1970).
11. G.L. Closs and A.D. Trifunac, ibid., 92, 2186 (1970).
- 12.(a) H.R. Ward, R.G. Lawler and R.A. Cooper, Tetrahedron Lett., 527 (1969);  
(b) A.R. Lepley, Chem. Comm., 1460 (1969).
- 13.(a) W.G.B. Huysmans, presented at the CIDNP symposium of the Belgian Chemical Society, March (1971).  
(b) W.G.B. Huysmans and R. Kaptein, to be published.
14. B. Blank and H. Fischer, personal communication.
15. E. Lippmaa, T. Pehk, A.L. Buchachenko and S.V. Rykov, Chem. Phys. Lett., 5, 521 (1970).

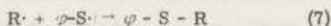
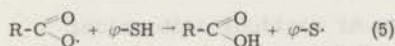




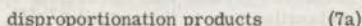
or



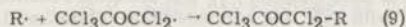
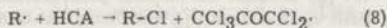
In thiophenol:



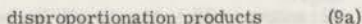
or



In HCA:

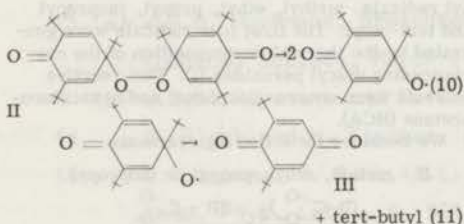


or



Induced decomposition will not be considered here, firstly because under the conditions of the experiments it will probably not be very important and secondly because in a chain reaction polarization of protons in subsequent radicals is expected to be small (it has been observed in a one step transfer reaction (7)), unless the reactions are extremely fast. In our cases the radicals are actually also secondary radicals.

For the tert-butyl radical a more convenient source was found to be bis(1, 3, 5-tri-tert-butyl-2, 5-cyclohexadien-4-one)peroxide (II)\*.



\* A more detailed account of the thermal decomposition of II will be given elsewhere.

and reactions (3a), (6), (7a), (8) and (9a) for R = tert-butyl.

The NMR spectra have been recorded on a Varian HA 100-IL spectrometer (100 MHz,  $H_0 = 23$  kgauss) and a Varian DA 60-IL spectrometer (60 MHz,  $H_0 = 14$  kgauss and 15 MHz,  $H_0 = 3.5$  kgauss). A lock signal was obtained from a capillary containing  $\text{H}_2\text{SO}_4$ . Chemical shifts are given in ppm from TMS. The spectra presented in the figures are all 100 MHz spectra of 0.1 M peroxide solutions, recorded 90 seconds after the sample had been inserted in the preheated probe, when maximum enhanced signals occurred. This time corresponded to the time required for the heating up of the sample. The first three peroxides decomposed at a convenient rate at 110°C, diisobutyl peroxide at 80°C and II at 130°C.

## 2. RESULTS AND DISCUSSION

### 2.1. Methyl.

The results for the decomposition of diacetyl peroxide ( $\delta = 2.14$  ppm) are summarized in table 1. Enhancement factors could not be measured very accurately, but are in the range 10-20 at 100 MHz, somewhat less for methane. The acetyl groups in acetic acid and methylacetate do not give enhanced signals, probably due to a too short mean lifetime of the acetate radicals (estimated at  $10^{-10} - 10^{-9}$  sec [8]). It is a remarkable fact that both E and A occur. These and other experiments with diacetyl peroxide [9] also indicate that it is a rule for methyl radicals that products from radical-radical coupling reactions (3), (4), (7), (9) show E, while products from reactions with diamagnetic molecules (6), (8) give A.

If this proves to be a general rule, the observation of E in methylacetate would demonstrate that this compound is mainly formed by reaction (4) and not by induced decomposition.

An explanation for this difference in behaviour (and generally for A in methyl radicals) is not easily given, but possibly electron spin exchange during triplet encounters of radicals, which do not lead to a combination reaction, modulates the scalar field at the protons strongly enough to act as a polarizing mechanism, accounting for A in products of reactions (6) and (8). This mechanism could of course not operate at singlet encounters, which lead to a combination reaction. In this case the omnipresent dipolar mechanism could result in E.

The distinction between triplet and singlet encounters has been made by several authors in the theory of radical recombination reactions [10, 11].

Table 1  
The decomposition of diacetyl peroxide

$\delta$ (ppm)	Assignment	Product of reaction
thiophenol:		
0.13 A	methane	6
1.84 N	acetic acid	CH <sub>3</sub> 5
2.24 E	thioanisole	CH <sub>3</sub> 7
HCA:		
0.83 E	ethane	3
1.69 E	1, 1, 1, 3, 3-pentachlorobutanone	9
1.96 N	methylacetate	(acetate CH <sub>3</sub> ) 4
3.54 E	methylacetate	OCH <sub>3</sub>
2.94 A	methylchloride	8

A: enhanced absorption. E: emission. N: normal, not enhanced.

It does not seem to be in accordance with the assumption by Nelsen and Bartlett [12] of a very fast singlet-triplet interconversion of radical pairs.

A more quantitative treatment is necessary before something definite could be said about this point.

## 2.2. Ethyl.

The assignments of the spectra recorded dur-

ing the decomposition of dipropionyl peroxide in thiophenol (fig. 1) and in HCA (fig. 2) are given in table 2. The spectrum of thiophenole (fig. 1) would be expected if the CH<sub>2</sub> protons of the ethyl radical are polarized by a dipolar mechanism and the CH<sub>3</sub> protons by a scalar mechanism (e.g. modulation of the scalar coupling by rotation around the C-C axis). This does not seem unreasonable. The spectrum of ethylchloride (fig. 2) is more confusing; low field lines of the CH<sub>2</sub> quartet A,

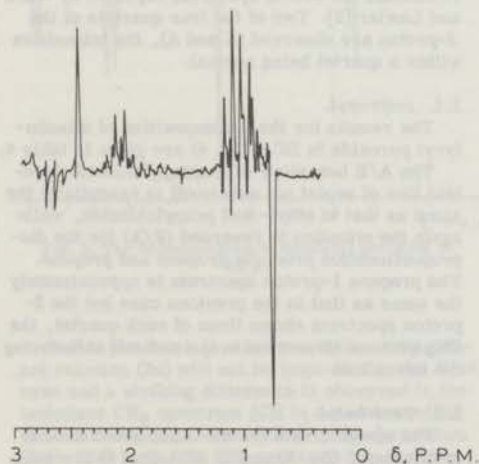


Fig. 1. The decomposition of dipropionyl peroxide in thiophenol.

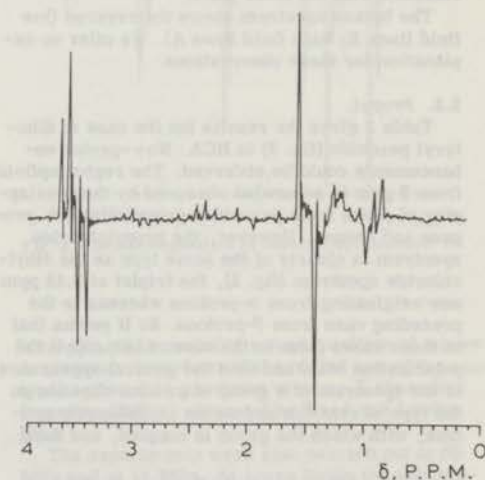


Fig. 2. The decomposition of dipropionyl peroxide in HCA.

Table 2  
The decomposition of dipropionyl peroxide

$\delta$ (ppm)	Assignment	Product of reaction
thiophenol: fig. 1		
0.75 E	ethane	6
0.93 triplet N	propionic acid CH <sub>3</sub>	5
2.09 quartet N	" CH <sub>2</sub>	
0.95 triplet N	dipropionyl peroxide CH <sub>3</sub>	-
2.12 quartet N	" CH <sub>2</sub>	
1.12 triplet A	thiophenetole CH <sub>3</sub>	7
2.68 quartet E	" CH <sub>2</sub>	
2.45	spinning side band of solvent SH peak	
HCA: fig. 2		
0.90 triplet E/A	butane CH <sub>3</sub>	3
1.30 E/A	" CH <sub>2</sub>	
1.21 triplet N	dipropionyl peroxide CH <sub>3</sub>	-
2.40 quartet N	" CH <sub>2</sub>	
1.47 triplet A/E	ethylchloride CH <sub>3</sub>	8
3.52 quartet A/E	" CH <sub>2</sub>	

high field lines E and the same for the CH<sub>3</sub> triplet, the central line not being enhanced\*. In addition the outer lines of the CH<sub>2</sub> quartet are more enhanced than the inner lines.

The butane spectrum shows the reverse (low field lines E, high field lines A). We offer no explanation for these observations.

### 2.3. Propyl.

Table 3 gives the results for the case of dibutyl peroxide (fig. 3) in HCA. No  $\gamma$ -proton enhancements could be observed. The region upfield from 2 ppm is somewhat obscured by the overlapping of peaks from peroxide, propylchloride, propane and hexane. However, the propylchloride spectrum is clearly of the same type as the ethylchloride spectrum (fig. 2), the triplet at 3.44 ppm now originating from  $\alpha$ -protons whereas in the preceding case from  $\beta$ -protons. So it seems that in these cases (also in the case of isopropyl) the polarization state and thus the general appearance of the spectrum of a group of protons depends on the type of reaction and on the neighbouring protons, with which the group is coupled, and does

\* The central line shows actually a very small emission.

not depend on the place ( $\alpha$  or  $\beta$ ) in the radical precursor.

The spectrum of the vinyl protons of propene resembles the butene spectrum reported by Ward and Lawler [3]. Two of the four quartets of the 2-proton are observed (E and A), the intensities within a quartet being normal.

### 2.4. Isopropyl.

The results for the decomposition of diisobutyl peroxide in HCA (fig. 4) are given in table 4.

The A/E behaviour of isopropylchloride (central line of septet not enhanced) is essentially the same as that of ethyl- and propylchloride, while again the situation is reversed (E/A) for the disproportionation products propane and propene. The propene 1-proton spectrum is approximately the same as that in the previous case but the 2-proton spectrum shows lines of each quartet, the CH<sub>3</sub> protons ( $\beta$ -protons in the radical) influencing the intensities.

### 2.5. Tert-butyl.

The spectral data for the decomposition of II in thiophenol (fig. 5) and in HCA (fig. 6) are summarized in table 5. The high field part of the spectra are shown in the figures.

Table 3  
The decomposition of dibutyl peroxide in HCA

$\delta$ (ppm)		Assignment	Product of reaction
0.8 - 1.5		hexane and propane	3, 3a
1.02 triplet	N	dibutyl peroxide CH <sub>3</sub>	-
1.67 sextet	N	" $\beta$ -CH <sub>2</sub>	-
2.30 triplet	N	" $\alpha$ -CH <sub>2</sub>	-
1.02 triplet	N	propylchloride CH <sub>3</sub>	8
1.82 sextet	A/E	" $\beta$ -CH <sub>2</sub>	-
3.44 triplet	A/E	" $\alpha$ -CH <sub>2</sub>	-
4.84	E/A	propene 1-CH <sub>2</sub>	3a
5.70 two quartets	E/A	" 2-CH	-

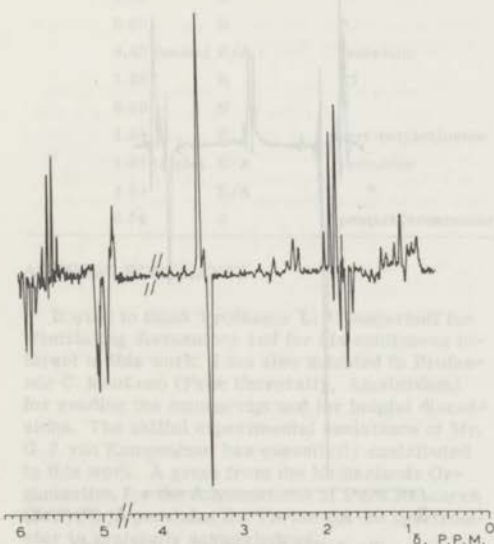


Fig. 3. The decomposition of dibutyl peroxide in HCA.

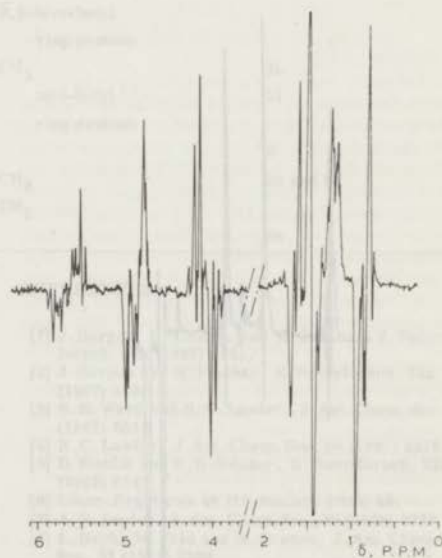


Fig. 4. The decomposition of diisobutyl peroxide in HCA.

Due to the much greater reactivity of thiophenol reaction (3a) will not be important in the first case and a striking difference is observed in the isobutane CH<sub>3</sub> spectrum (CH is not observed) in the two cases (fig. 5 reaction (6), fig. 6 reaction (3a)). The isobutene CH<sub>2</sub> spectrum is not shown but is very similar to the CH<sub>3</sub> spectrum, except that there are more lines. The isobutene spec-

trum (fig. 6) is probably a superposition of a pure A spectrum (reactions (7a) and (9a) are of the same type) and an E/A spectrum of more E character (reaction (3a)) as observed by Ward and Lawler [3].

The experiments were also carried out at 60 MHz and at 15 MHz. At lower fields the enhancement factors were greater (see ref. [2]). At 15

Table 4  
The decomposition of diisobutryl peroxide in HCA

$\delta$ (ppm)	Assignment	Product of reaction
0.85 triplet E/A	propane CH <sub>3</sub>	3a
1.32 E/A	" CH <sub>2</sub>	"
1.18 doublet N	diisobutryl peroxide CH <sub>3</sub>	"
2.57 septet N	(not shown) "	"
1.46 doublet A/E	isopropylchloride CH <sub>3</sub>	8
4.12 septet A/E	" CH	"
1.67 doublet E/A	propene CH <sub>3</sub>	3a
4.84 E/A	" 1-CH <sub>2</sub>	"
5.70 E/A	" 2-CH	"

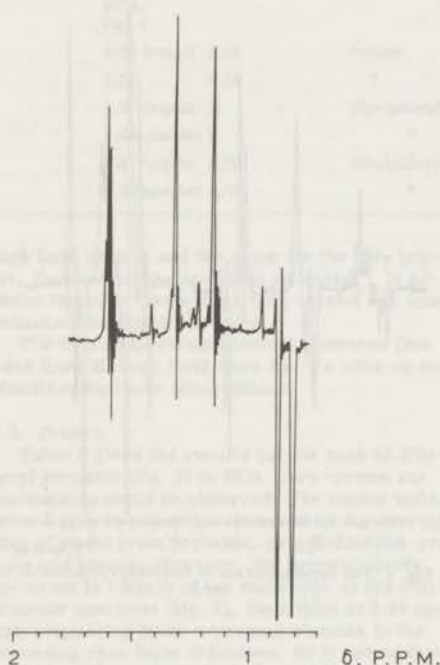


Fig. 5. The decomposition of II in thiophenol.

MHz they were estimated to be up to 100 in some cases. This is primarily due to the  $H_0^2$  dependence of the  $g$ -tensor mechanism, making the polarizing mechanism, whatever it may be, relatively stronger at lower fields. The 15 MHz spectra

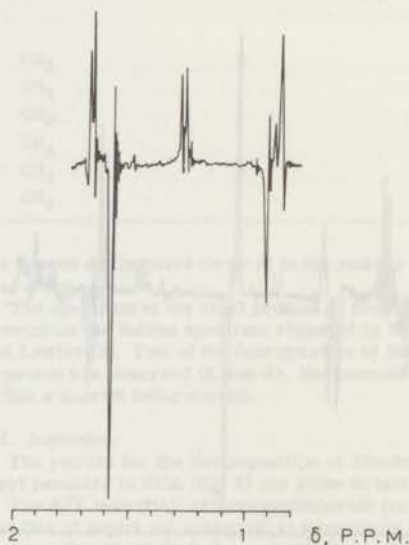


Fig. 6. The decomposition of II in HCA.

were complicated by the overlapping of lines and the appearance of more lines in the multiplets. However, in the simpler cases (diacetyl peroxide, dipropionyl peroxide and II in HCA) the relative intensities of E and A lines were unaltered, an exception being the isobutene spectrum, which obtained more E character at 15 MHz, indicating that the E/A mechanism has a longer correlation time than the A mechanism in this case.

Table 5  
 The decomposition of II

$\delta$ (ppm)	Assignment		Product of reaction
thiophenol: fig. 5			
0.84 doublet E	isobutane	CH <sub>3</sub>	6
0.88 N	II	1-tert-butyl	-
1.32 N	"	3,5-tert-butyl	-
1.18 N	III	tert-butyl	11
1.64 triplet A	isobutene	CH <sub>3</sub>	7a
4.55 A	"	CH <sub>2</sub>	-
HCA fig. 6			
0.87 N	II	1-tert-butyl	-
1.26 N	"	3,5-tert-butyl	-
6.60 N	"	ring protons	-
0.88 doublet E/A	isobutane	CH <sub>3</sub>	3a
1.28 N	III	tert-butyl	11
6.40 N	"	ring protons	-
1.58 E	tert-butylchloride	-	8
1.67 triplet E/A	isobutene	CH <sub>3</sub>	3a and 9a
4.60 E/A	"	CH <sub>2</sub>	-
6.74 A	pentachloroacetone	-	9a

## ACKNOWLEDGEMENTS

It wish to thank Professor L. J. Oosterhoff for stimulating discussions and for his continuous interest in this work. I am also indebted to Professor C. MacLean (Free University, Amsterdam) for reading the manuscript and for helpful discussions. The skilful experimental assistance of Mr. G. J. van Kampenhout has essentially contributed to this work. A grant from the Netherlands Organization for the Advancement of Pure Research (Z.W.O.) to purchase the Varian DA-60 spectrometer is gratefully acknowledged.

## REFERENCES

- [1] J. Bargon, H. Fischer and U. Johnsen, *Z. Naturforsch.* 22a (1967) 1551.
- [2] J. Bargon and H. Fischer, *Z. Naturforsch.* 22a (1967) 1556.
- [3] H. R. Ward and R. G. Lawler, *J. Am. Chem. Soc.* 89 (1967) 5518.
- [4] R. G. Lawler, *J. Am. Chem. Soc.* 89 (1967) 5519.
- [5] D. Stehlik and K. H. Hauser, *Z. Naturforsch.* 22a (1967) 914.
- [6] *Chem. Eng. News* 46 (15 January 1968) 40.
- [7] A. R. Lepley, *J. Am. Chem. Soc.* 80 (1968) 2710.
- [8] L. Herk, M. Feld and M. Szwarc, *J. Am. Chem. Soc.* 83 (1961) 2998.
- [9] R. Kaptein, unpublished results.
- [10] R. K. Lyon, *J. Am. Chem. Soc.* 86 (1964) 1907.
- [11] C. W. Pyun, *J. Chem. Phys.* 48 (1968) 1306.
- [12] F. Nelson and P. D. Bartlett, *J. Am. Chem. Soc.* 88 (1966) 143.

## CHAPTER II

## CHEMICALLY INDUCED DYNAMIC NUCLEAR POLARIZATION II

(Relation with anomalous ESR spectra)

R. KAPTEIN and J. L. OOSTERHOFF

*Department of Theoretical Organic Chemistry,  
University of Leiden, P.O. Box 75, The Netherlands*

Received 11 August 1969

A mechanism is proposed to account for observations by Fessenden and Schuler and Smaller et al. of ESR emission during radiolysis experiments. The same mechanism supplemented by spin relaxation may explain anomalous CIDNP multiplets.

## 1. INTRODUCTION

The phenomenon of enhanced NMR absorption (A) and emission (E) during radical reactions has been called CIDNP [1,2]. Since its discovery a number of effects have been published [2-6] which could not be explained by the theory given by Bargon and Fischer [1b]. We mention in particular the occurrence of both E and A within a multiplet (multiplet effect).

In a preceding paper [3] some NMR spectra were given, recorded during the thermal decomposition of peroxides. It was observed that alkyl radical products of displacement (D) reactions showed the (A/E) multiplet effect (low field A, high field E). At least for D products of primary radicals this has also been observed by others [4b, c, 5b, c].

Anomalous spin state populations have also been observed in the ESR spectra of radicals formed during radiolysis experiments by Fessenden and Schuler [7] and recently by Smaller et al. [8].

In this letter we wish to propose a mechanism, which may lead to an explanation of both types of anomalies\*: if during formation of the radicals the population rates of the free radical energy levels are not uniform but dependent on the nuclear spin states, transient ESR emission and absorption would be expected and together with a suitable relaxation mechanism this could lead to the observed nuclear polarizations.

\* Fischer and Bargon [6b] have also suggested a relation between the ESR results and the CIDNP multiplet effect. However, they do not give a foundation.

## 2. POPULATION RATES

To show how differences in population rates may arise we consider the dissociation of a simple (hypothetical)  $H_2$  like molecule H-X (X having no nuclear spin) but the treatment can easily be extended to more complex systems. The dissociation is approximated by a two-step process



During the first step the H-X bond is broken and a radical pair is formed. After a mean time  $\tau$  the pair is completely dissociated in the second step.

For the description of the radical pair we take as a basis:

$$S \alpha_N, T_{+1} \alpha_N, T_0 \alpha_N, T_{-1} \alpha_N, S \beta_N, T_{+1} \beta_N, T_0 \beta_N, T_{-1} \beta_N$$

where S and T are the valence bond singlet and triplet functions,  $\alpha_N$  and  $\beta_N$  representing the nuclear spin states.

The effective Hamiltonian for the radical pair could be written:

$$H = H_Z^e + H_Z^N + H_{ex} + H_{SS} + H_{SI}$$

$H_Z^e$  and  $H_Z^N$  are the electron and nuclear Zeeman terms,  $H_{ex}$  is the exchange term,  $H_{SS}$  is the electron-electron dipolar coupling term and  $H_{SI}$  the hyperfine coupling term. We will include here only the scalar interactions and only the secular

part  $H_{SI}^Z$  of  $H_{SI}$ , which mixes S with  $T_0$  states\*.

$H_N^Z$  is also not important here. Thus the truncated Hamiltonian becomes:

$$H = H_{SI}^Z + H_{EX} + H_{SI}^Z = \omega_e (S_1^Z + S_2^Z) - J(I_{\frac{1}{2}} + 2S_1 S_2) + (8\pi/3)g\beta g_N \beta_N \hbar^{-1} I^Z [S_1^Z \delta(r_1) + S_2^Z \delta(r_2)]. \quad (1)$$

$J$  is the exchange integral (angular frequency units are used).

In this model we assume that in the first step  $J$  changes suddenly to a value comparable to the hyperfine coupling constant  $A$ , the system being in a singlet state initially. If the proton has  $\alpha$  spin, we can describe the state of the radical pair after the first step by

$$\varphi^+(t) = [c_S(t) S + c_T(t) T_0] \alpha_N.$$

From  $i \partial \varphi / \partial t = H \varphi$  we get the coupled equations

$$i \dot{c}_S = J c_S + a c_T$$

$$i \dot{c}_T = a c_S - J c_T$$

where  $a = \frac{1}{2}A$ . With the initial conditions  $c_S(0) = 1$ ,  $c_T(0) = 0$  this gives

$$\varphi^+(t) = [\cos \omega t S - i \omega^{-1} \sin \omega t (JS + aT_0)] \alpha_N \quad (2a)$$

where  $\omega = (J^2 + a^2)^{\frac{1}{2}}$  and by the same procedure

$$\varphi^-(t) = [\cos \omega t S - i \omega^{-1} \sin \omega t (JS - aT_0)] \beta_N. \quad (2b)$$

This gives an oscillating spin density at the H-atom given by

$$\rho^\pm(t) = 2 \langle \varphi^\pm | S_1^Z \delta(r_1) + S_2^Z \delta(r_2) | \varphi^\pm \rangle = \pm 2aJ \omega^{-2} \sin^2 \omega t. \quad (3)$$

Thus there is on the average a preference for one kind of electron spin at the H-atom, depending on the nuclear spin state and the probabilities of finding  $\alpha$  or  $\beta$  electron spin at the H-atom after the second step will not be equal.

If a selectivity parameter  $\Delta$  is given by (3) averaged over a distribution of lifetimes of the radical pair, this gives

$$\Delta^\pm = \frac{1}{\tau} \int_0^\infty \rho^\pm(t) e^{-t/\tau} dt = \pm \frac{4aJ\tau^2}{1+4\omega^2\tau^2}. \quad (4)$$

For long  $\tau$  ( $4\omega^2\tau^2 \gg 1$ ), (4) becomes  $\pm aJ/(J^2+a^2)$

\* The nonsecular part of  $H_{SI}$  mixes S with  $T_{\pm 1}$  states, but this is less important due to the larger energy differences.

which has a maximum value  $\frac{1}{2}$  when  $J = a$ . The sign depends on the relative signs of  $J$  and  $a$ . The population rate constants for the  $\alpha\alpha_N$ ,  $\alpha\beta_N$ ,  $\beta\alpha_N$  and  $\beta\beta_N$  levels of the H-atom could be expressed as  $\frac{1}{4}k(1+\Delta)$ ,  $\frac{1}{4}k(1+\Delta)$ ,  $\frac{1}{4}k(1-\Delta)$ ,  $\frac{1}{4}k(1-\Delta)$  respectively where  $k$  is a chemical rate constant.

The observations of Fessenden and Schuler [7] and of Smaller et al. [8] (low field ESR lines emission, high field lines absorption, immediately after formation of the radicals) can be explained with this mechanism if it is assumed that  $J$  is positive at the distances involved, meaning that the triplet state has the lower energy<sup>†</sup>. We come back to this point later.

It may be noted that the differences in population rates do not give a net electron or nuclear polarization.

### 3. RELAXATION IN ALKYL RADICALS

It is reasonable to assume that 1-protons in alkyl radicals are relaxed by a dipolar mechanism. Thus for short correlation times of the tumbling motion the  $\Delta m = 2$  relaxation rate  $W_2$  is the largest for these protons. For 2-protons however, the dipolar coupling tensor is much less anisotropic and furthermore it is probable that a scalar mechanism is acting, the isotropic hyperfine interaction being modulated by a fast rotation of the group of 2-protons with respect to the 2p orbital carrying the unpaired electron. In this case the  $\Delta m = 0$  relaxation rate  $W_0$  is the largest for 2-protons.

In fig. 1 the energy levels are drawn for a radical with two protons A and B, which could be a model for alkyl radicals.  $A_A$  is positive as is well known for 2-protons and  $A_B$  is negative (1-protons). The relative values of the population rates are in accordance with the arguments pointed out above (indicated by the thickness of the levels).

The largest relaxation rates are then  $W_0^A$  and  $W_2^B$  and for clarity only these are indicated in the figure. It can be seen that by the relaxation process the  $\alpha_N\beta_N$  and  $\beta_N\alpha_N$  levels are filled and the  $\alpha_N\alpha_N$  and  $\beta_N\beta_N$  levels depleted. If the radical does not live longer than its relaxation time ( $\approx 10^{-5}$  sec) and if furthermore the nuclear

<sup>†</sup> In radiolysis experiments there is also the possibility that molecules dissociate from an excited triplet state. In that case a negative value of  $J$  would be needed to explain the results. However, Fischer [9] has recently observed the same trend in the ESR spectra of alkyl radicals formed by a chemical reaction, where the system is in a singlet state initially.

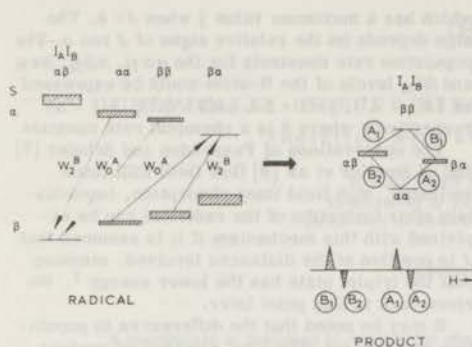


Fig. 1. Energy level scheme of a radical with two protons ( $A_A > 0$ ,  $A_B < 0$ ) and of reaction product. The most important relaxation transitions are drawn. The NMR spectrum of the product is indicated.

polarization is transferred to the D product, this gives rise to the (A/E) multiplets in the NMR spectrum of this product, provided the nuclear-nuclear spin coupling constant is positive.

#### 4. DISCUSSION

For alkyl radicals  $\alpha \approx 10^8$  rad/sec. If we take  $J = 5 \times 10^6$  rad/sec and  $\tau = 10^{-9}$  sec then we have from eq. (4)  $\Delta^\pm = \pm 0.1$ , a value which is large enough to account for the ESR and CIDNP results. Apparently rather large values of  $\tau$  are needed, but in a pair of alkyl radicals where more protons are present, the value of  $\alpha$  becomes accordingly larger for some nuclear states and smaller values of  $\tau$  ( $\approx 10^{-10}$  sec) would still give large enough values of  $\Delta$ . It is seen that  $\Delta$  depends rather critically on the lifetime of the radical pair and our model would predict a negligible effect in the gas phase. The positive sign of  $J$  that is needed is somewhat puzzling but we are not aware of experimental evidence on the sign of  $J$  in a loose radical pair\*.

\* The situation is different from the biradical cases where negative  $J$ 's have been found [10, 11].

For 2p electron radicals the sign of the exchange integral depends on the relative orientation and probably also on the exchange mechanism (direct or indirect via solvent molecules).

We realize that the process of dissociation of molecules into radicals is more complicated than the model described above and we intend to study this process and that of association of radicals in more detail.

We wish to thank Dr. H. Fischer for a preprint and for stimulating discussions.

#### REFERENCES

- [1] a. J. Bargon, H. Fischer and U. Johnsen, *Z. Naturforsch.* 22a (1967) 1551;  
b. J. Bargon and H. Fischer, *Z. Naturforsch.* 22a (1967) 1556;
- [2] a. H. R. Ward and G. R. Lawler, *J. Am. Chem. Soc.* 89 (1967) 5518;  
b. R. G. Lawler, *J. Am. Chem. Soc.* 89 (1967) 5519.
- [3] R. Kaptein, *Chem. Phys. Letters* 2 (1968) 261.
- [4] a. A. R. Lepley, *J. Am. Chem. Soc.* 90 (1967) 2710;  
b. A. R. Lepley, *Chem. Commun.* (1969) 64;  
c. A. R. Lepley and R. L. Landau, *J. Am. Chem. Soc.* 91 (1969) 748, 749;  
d. A. R. Lepley, *J. Am. Chem. Soc.* 91 (1969) 1237.
- [5] a. H. R. Ward, R. G. Lawler and H. Y. Loken, *J. Am. Chem. Soc.* 90 (1968) 7359;  
b. H. R. Ward, R. G. Lawler and R. A. Cooper, *J. Am. Chem. Soc.* 91 (1969) 746;  
c. H. R. Ward, R. G. Lawler and R. A. Cooper, *Tetrahedron Letters* 69 (1969) 527.
- [6] a. J. Bargon and H. Fischer, *Z. Naturforsch.* 23a (1968) 2109;  
b. H. Fischer and J. Bargon, *Accounts Chem. Res.* 2 (1969) 110.
- [7] R. W. Fessenden and R. H. Schuler, *J. Chem. Phys.* 39 (1963) 2147.
- [8] B. Smaller, J. R. Remko and E. C. Avery, *J. Chem. Phys.* 48 (1968) 5174.
- [9] H. Fischer, private communication.
- [10] S. H. Glarum and J. H. Marshall, *J. Chem. Phys.* 47 (1967) 1374.
- [11] H. Lemaire, *J. Chim. Phys.* (1967) 559.



$$c_S^i(t) = \cos \omega t - \frac{iJ}{\omega} \sin \omega t,$$

$$c_T^i(t) = -i \frac{a_i}{\omega} \sin \omega t,$$

$$\omega = (J^2 + a_i^2)^{\frac{1}{2}}.$$

The mixing coefficients  $a_i$  for the four nuclear states  $\omega_i$  are shown in table 1.

Table 1

$\chi_i$	$a_i = \langle S\chi_i   H   T_0 \chi_i \rangle$
$\alpha \alpha$	$\frac{1}{4} (A_1 - A_2)$
$\alpha \beta$	$\frac{1}{4} (A_1 + A_2)$
$\beta \alpha$	$-\frac{1}{4} (A_1 + A_2)$
$\beta \beta$	$-\frac{1}{4} (A_1 - A_2)$

If it is assumed that the product of  $P^*$  can not be formed from a triplet state, the rate of  $P^*$  is proportional to

$$|c_S^i(t)|^2 = 1 - (a_i^2/\omega^2) \sin^2 \omega t$$

and depends on the nuclear states. Averaging this expression over a distribution of lifetimes of the radical pair with a mean lifetime  $\tau$ , the population rates of the nuclear levels of  $P^*$  will be proportional to

$$P_i = 1 - \frac{2a_i^2\tau^2}{1+4\omega^2\tau^2}. \quad (3)$$

If  $A_1$  and  $A_2$  have the same sign this will lead to larger population rates for the  $\alpha\alpha$  and  $\beta\beta$  levels than for the  $\alpha\beta$  and  $\beta\alpha$  levels of  $P^*$  and if the chemical shifts of  $H_1$  and  $H_2$  in  $P^*$  are not identical and the nuclear-nuclear spin coupling constant  $J_{12}$  is positive, this gives rise to two (E/A) doublets for the NMR spectrum of this product.

One might also say that it will take a longer time (smaller value of  $|J|$ ) for the radical pairs with  $\alpha\alpha$  and  $\beta\beta$  nuclear spins to go over to the  $T_0$  state than for the others.

This will be the case only if no other (stronger) S-T mixing mechanisms such as spin-orbit interactions are present. At least for alkyl radicals these will not be larger than the hyperfine interactions as evidenced by the small  $g$ -tensor anisotropies.

If more nuclei are present in the radicals this mechanism will also lead to larger population rates for the levels of  $P^*$  with higher  $|m_i|$  ( $z$ -component of total nuclear spin)†.

### 3 ENHANCEMENT FACTOR $V_{\max}$

The maximum enhancement factor is defined [3]

$$V_{\max} = \frac{I - I_0}{I_0} \approx \frac{I}{I_0},$$

where  $I$  is the maximum intensity of an NMR line and  $I_0$  the intensity it should have if the spin system were in equilibrium. If it is assumed that only  $P^*$  contributes to the enhanced signals and not  $P$  the enhancement factor can be calculated.

Using the steady state conditions for the reactions in scheme (1) the steady state concentration of  $P^*$  becomes

$$P^* = \frac{k_1 k_2 T_1}{k_2 + k_3} [A_m].$$

where  $[A_m]$  is the concentration of  $A$  at the time at which maximum enhancement occurs ( $t_{\max}$ ).

The enhancement factor for an NMR transition between states  $\chi_i$  and  $\chi_j$  is then

$$V_{\max}^{ij} = \frac{(P_j - P_i)}{\sum_R P_R} \times \frac{k_1 k_2 T_1}{(k_2 + k_3)} \times \frac{lkT}{g_N \beta_N H_0} \times \frac{[A_m]}{[P_m]} \quad (4)$$

where  $[P_m]$  denotes the total concentration of  $P$  at  $t_{\max}$ , which can be measured in principal at least, by interrupting the reaction.  $l$  is the number of nuclear levels of  $P$ ,  $P_i$  is given by eq. (3) and the other symbols have their usual meaning.

### 4. DISCUSSION

If we consider the hypothetical case of two identical alkyl radicals with one proton, generated at 110°C. e.g. from a peroxide, in a field of 23.5 kGauss, we have the following values

$$\frac{kT}{g_N \beta_N H_0} = 8 \times 10^4, \quad k_1 = 5 \times 10^{-3} \text{ sec}^{-1},$$

$$l = 4, \quad T_1 \approx 10 \text{ sec}$$

$$\frac{1}{2}A \approx 2 \times 10^8 \text{ rad/sec}, \quad [A_m]/[P_m] \approx 10.$$

† This would also have consequences for the population rates of the free radical levels, because these are complementary. As this would lead to larger population rates for lower  $|m_i|$  values, this could be an alternative explanation for the A/E multiplets of D products of these radicals, provided that the radical lifetimes are short so that the nuclear polarization is not destroyed by the relaxation process.

The values of the other quantities which enter eq. (4) are known less precisely but the following tentative values do not seem unreasonable

$$\frac{k_2}{k_2 + k_3} = 0.02 \quad (\text{"cage effect"}),$$

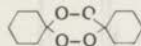
$$\tau = \frac{1}{k_2 + k_3} = 10^{-9} \text{ sec},$$

$$|J| = 5 \times 10^8 \text{ rad/sec}.$$

With these values  $V_{\max} \approx 30$ , which has the right order of magnitude for the cases studied in I. It will be clear that much larger values of  $V_{\max}$  can be attained and that the limiting value of 658 for the Overhauser enhancements does not apply here.

It may be noted that there are several arguments in favour of the mechanism we propose:

- In I we observed that R products of simultaneously formed radicals showed the (E/A) multiplets and products from secondary radicals did not (see also ref. [4]).
- Recently we observed [5] the same (E/A) patterns in decene, a disproportionation product from the decamethylene biradical [6], which is an intermediate during the thermal decomposition of dispiro [5, 2, 5, 2]-7, 8, 15, 16-tetraoxa-hexadecane



In this case, which is the first example of an intramolecularly biradical showing DIDNP, we know that the spins remain correlated, because they are not allowed to diffuse away.

- If the radical pair is generated in the triplet state, the theory predicts the reverse multiplet effect. Recent experiments by Closs [7] confirm this.

#### ACKNOWLEDGEMENT

We thank Dr. G. L. Closs for preprints of his work.

#### REFERENCES

- R. Kaptein and L. J. Oosterhoff, Chem. Phys. Letters 4 (1969)
- R. Kaptein, Chem. Phys. Letters 2 (1968) 261.
- J. Bargon and H. Fischer, Z. Naturforsch. 22a (1967) 1556.
- H. R. Ward, R. G. Lawler and R. A. Cooper, Tetrahedron Letters 69 (1969) 527.
- R. Kaptein, M. Fráter-Schröder and L. J. Oosterhoff, to be published.
- P. R. Story, D. D. Denson, C. E. Bishop, B. C. Clark and J. C. Farine, J. Am. Chem. Soc. 90 (1968) 817.
- G. L. Closs and L. E. Closs, in press.
- G. L. Closs, in press.

## Chemically Induced Dynamic Nuclear Polarization. Triplet and Singlet State Photosensitization of Peroxide Decompositions

By R. KAPTEIN,\* J. A. DEN HOLLANDER, D. ANTHEUNIS, and L. J. OOSTERHOFF

(Department of Theoretical Organic Chemistry, University of Leiden, P.O. Box 75, Leiden, The Netherlands)

**Summary** Nuclear spin polarization in photolysis products of peroxides in the presence of ketones is opposite to the polarization in products both from direct photolysis and from thermal decomposition.

ONE prediction of the current theory of CIDNP<sup>1-3</sup> is that the nuclear polarization found in cage recombination products from radical pairs will depend upon the multiplicity of the electronic state, singlet (*S*) or triplet (*T*), of the precursor from which the pair is generated. Thus both net polarization [emission (*E*) or enhanced absorption (*A*)] and multiplet effects (*E/A* or *A/E* within a multiplet) will be reversed for products from *T* pairs as compared to products from *S* pairs. This opposite behaviour will hold also for the polarization of transfer products from radicals escaping from the cage of formation, provided that the free-radical lifetimes are not much longer than the nuclear spin-lattice relaxation times in the radical (ca.  $10^{-6}$  s).<sup>1b</sup> This suggests<sup>2b</sup> that the observation of CIDNP during photochemical reactions could yield valuable information on the multiplicity of precursors of radical pairs or biradicals.<sup>†</sup> However, there is an ambiguity here because the theory also predicts<sup>2d</sup> that combination (or disproportionation) products of secondary radical encounters will be polarized like *T*-pair products, so that when *T*-pair polarization is observed one has *a priori* two alternative explanations for its origin: (i) primary cage recombination of a *T* pair or (ii) combination from secondary encounters of free radicals. In the second case the spin-state of the radical precursor could not be determined. Closs *et al.*<sup>2</sup> explain their results for the reactions of carbenes and benzophenones with alkylbenzenes as cage recombinations from *T* pairs [case (i)]. Although this interpretation may turn out to be correct (there can be little doubt about the spin-states of the precursors in these systems), the second possibility should be considered also, since the chemistry of the systems indicates that the radicals are mainly consumed by secondary encounters.

Here we show unambiguously the role of the precursor multiplicity. We studied <sup>1</sup>H n.m.r. spectra during photolysis of some peroxides in the presence of photosensitizers. Several authors have shown that the decomposition of peroxides can be photosensitized.<sup>4</sup> Two examples will be discussed here. The experiments were carried out on a Varian DA-60 spectrometer, modified in order to irradiate the sample in the probe with the light of an Osram HBO 1000 w high-pressure mercury arc, filtered with a CuSO<sub>4</sub> solution (transparent in the region 310–600 nm).

The spectra in Figure 1a–c were obtained from a solution of 0.26 M-benzoyl peroxide (BPO) (δ 8.2–7.3 p.p.m.) in CCl<sub>4</sub> before, during, and after irradiation. The *E* lines in Figure 1b (δ 7.25 p.p.m.) belong to chlorobenzene. Figure 1d–f shows a similar series for the same solution, to which 0.11 M-acetophenone was added. Chlorobenzene clearly shows enhanced absorption in this case. In addition some

emission lines (δ 7.0–7.2 p.p.m.) can be seen, that could be assigned to phenyl benzoate. The *A* effect is larger in Figure 1e than the *E* effect in Figure 1b due to a higher rate of decomposition of peroxide in the presence of acetophenone. In solutions containing 0.008 M-acetophenone, *A* can still be observed for chlorobenzene.

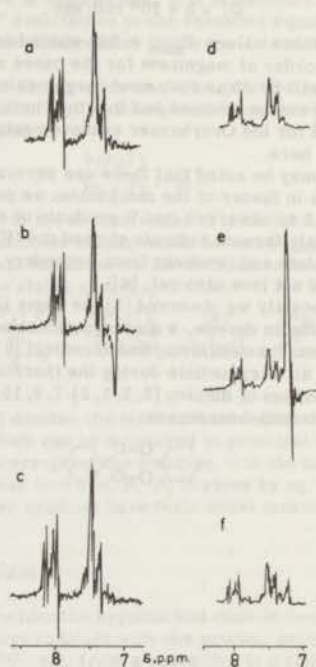


FIGURE 1. 60 MHz n.m.r. spectra of 0.23 M-benzoyl peroxide in CCl<sub>4</sub> (a) before, (b) during, (c) after irradiation and of the same solution with 0.11 M-acetophenone added (d) before, (e) during, and (f) after irradiation. The spectra (c) and (f) were run after a time long enough for thermal equilibrium to be established.

This reversal can be observed also in the spectra of Figure 2a and b recorded during the photolysis of 0.13 M-propionyl peroxide [δ (CH<sub>2</sub>) 2.37, δ (CH<sub>3</sub>) 1.18 p.p.m.] in CCl<sub>4</sub> and the same solution containing 0.11 M-acetophenone [δ (CH<sub>2</sub>) 2.53 p.p.m.]. The effect can be seen most clearly in the ethyl chloride lines [δ (CH<sub>2</sub>) 3.52, δ (CH<sub>3</sub>) 1.42 p.p.m., *A/E* multiplets in Figure 2a, *E/A* multiplets in Figure 2b],<sup>‡</sup> but also in the butane CH<sub>2</sub> lines (δ 0.90 p.p.m.). The spectra of Figures 1b and 2a are similar to spectra that we obtained during thermal decomposition of the peroxides in CCl<sub>4</sub> at 85° (cf. refs. 5 and 6).

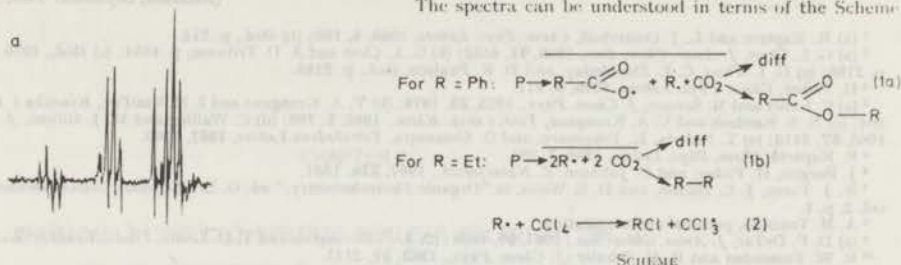
\* The observation of CIDNP in biradical products has been mentioned in ref. 1b and will be published shortly in more detail.

† The high-field line of the ethyl chloride CH<sub>2</sub> triplet overlaps with the low-field line of the peroxide CH<sub>2</sub> triplet.

The similarity to the thermal decomposition indicates that the direct photolysis proceeds via an excited singlet state and the reversal of the polarization in the presence of

assumption by Walling and Gibian<sup>4d</sup> of sensitization by triplet anthracene. This result is in accord with suggestions of sensitization of peroxide decompositions by excited  $S$ -states of benzene,<sup>4</sup> toluene,<sup>4b</sup> and naphthalene.<sup>4c</sup>

The spectra can be understood in terms of the Scheme



$P$  represents peroxide ( $S_0$ ) in the thermal decomposition, peroxide ( $S_1$ ) in the direct photolysis, a triplet precursor, e.g. peroxide ( $T_1$ ) or some peroxide-sensitizer ( $T_1$ ) complex, in the photosensitized decomposition in the presence of ketones and similarly a singlet precursor in the presence of anthracene. Diffusion from the cage (indicated by a bar, is denoted by "diff." For BPO a second and probably major reaction path<sup>9</sup> yielding two benzyloxy-radicals-escaping from the cage will not give the reversal of nuclear polarization. As the benzyloxy-radical is expected to have a larger  $g$  value than the phenyl radical and the hyperfine coupling constants are positive in the phenyl radical, theory<sup>4c</sup> predicts  $A$  in phenyl benzoate for cage recombination from an  $S$  pair (equation 1a) and  $E$  in the transfer reaction product chlorobenzene (equation 2) from phenyl radicals that escaped from the primary cage by diffusion.<sup>1b</sup> For  $T$  pairs: phenyl benzoate  $E$ , chlorobenzene  $A$ .

The formation of propionyloxy-radicals followed by rapid decarboxylation before appreciable diffusion from the cage has occurred is also possible. The hyperfine coupling constants in the ethyl radical have opposite signs [ $A(\text{CH}_2) = 27\text{G}$ ,  $A(\text{CH}_3) = -22\text{G}$ ].<sup>10</sup> The observed phases for the multiplet effects in Figure 2a are in accordance with the theory for recombination from an  $S$  pair of ethyl radicals (butane,  $E/A$ ) and diffusion followed by rapid transfer reaction (ethyl chloride,  $A/E$ ). For  $T$  pairs: butane  $A/E$ , ethyl chloride  $E/A$ . Other interpretations such as combination and diffusion from secondary encounter pairs are very unlikely in these cases. We note that the diffusive process and also the hyperfine-coupling-induced intersystem-crossing rate, yielding polarization *via* selection in the second part of (equation 1), will be very similar for  $S$  and  $T$  pairs so that n.m.r. intensities are expected to be opposite but similar in magnitude for equal rates of decomposition, although chemically the amount of cage effect may differ.

The observations described here firmly support the recent theory of CIDNP<sup>1-3</sup> and suggest that the early experiments by Bargon and Fischer<sup>5</sup> (thermal decomposition of BPO in cyclohexanone) should be explained in a similar way and that cross-relaxation in free radicals does

FIGURE 2. 60 MHz n.m.r. spectra of 0.13 M-propionyl peroxide in  $\text{CCl}_4$  (a) during irradiation and of the same solution with 0.11 M-acetophenone added (b) during and (c) after irradiation.

acetophenone is direct evidence for photosensitization of the decomposition by triplet acetophenone.<sup>4d</sup> With benzophenone we observed the same effects, but weaker, which is probably due to a lower triplet energy<sup>7</sup> of benzophenone ( $E_T$  69 kcal/mole) compared with acetophenone ( $E_T$  74 kcal/mole). With fluorenone ( $E_T$  53 kcal/mole) we did not observe the reversal of polarization §

Surprisingly, addition of 0.07 anthracene resulted in an increase of the emission signal for chlorobenzene by a factor of 5 and of  $A/E$  for ethyl chloride and  $E/A$  for butane by a factor of 9, indicating sensitization by excited singlet anthracene<sup>6</sup> ( $E_S$  76,  $E_T$  42 kcal/mole), contrary to the

§ Trozzolo<sup>8</sup> has recently observed  $A$  for the benzene line during photolysis of BPO in cyclohexanone. We have verified this and we observed  $A$  for benzene also in cyclopentanone and acetone using a  $\text{NiSO}_4$  filter solution (transparent below 310 nm). With a  $\text{CuSO}_4$  filter, however, benzene shows  $E$  in these solvents. Apparently there is competition of direct photolysis with triplet-sensitized decomposition in these systems.

¶ In accordance with this conclusion we observed the quenching of anthracene fluorescence by benzoyl peroxide.

not play a significant role in this case. It may be noted that a suggested<sup>11</sup> mechanism of polarization by transfer reaction (equation 2) cannot be reconciled with the observed reversal of polarization.

We thank the Netherlands Organization for the Advancement of Pure Research (Z.W.O.) for a grant to purchase the Varian DA-60 spectrometer and for a fellowship (to D.A.).

(Received, September 14th, 1970; Com. 1564.)

- <sup>1</sup> (a) R. Kaptein and L. J. Oosterhoff, *Chem. Phys. Letters*, 1969, **4**, 195; (b) *ibid.*, p. 214.
- <sup>2</sup> (a) G. L. Closs, *J. Amer. Chem. Soc.*, 1969, **91**, 4552; (b) G. L. Closs and A. D. Trifunac, p. 4554; (c) *ibid.*, 1970, **92**, 2183; (d) *ibid.*, p. 2186; (e) G. L. Closs, C. E. Doubleday, and D. R. Paulson, *ibid.*, p. 2185.
- <sup>3</sup> H. Fisher, *Chem. Phys. Letters*, 1970, **4**, 611.
- <sup>4</sup> (a) C. Luner and M. Szwarc, *J. Chem. Phys.*, 1955, **23**, 1978; (b) V. A. Krongauz and I. N. Vasil'ev, *Kinetika i Kataliz*, 1963, **4**, 67, 204; (c) N. S. Kardash and V. A. Krongauz, *Teor. i eksp. Khim.*, 1965, **1**, 796; (d) C. Walling and M. J. Gibian, *J. Amer. Chem. Soc.*, 1965, **87**, 3413; (e) T. Nakata, K. Tokumaru, and O. Simamura, *Tetrahedron Letters*, 1967, 3303.
- <sup>5</sup> R. Kaptein, *Chem. Phys. Letters*, 1968, **2**, 261.
- <sup>6</sup> J. Bargon, H. Fisher, and U. Johnson, *Z. Naturforsch.*, 1967, **22a**, 1551.
- <sup>7</sup> N. J. Turro, J. C. Dalton, and D. S. Weiss, in "Organic Photochemistry," ed. O. L. Chapman, Marcel Dekker, New York, 1969, vol. 2, p. 1.
- <sup>8</sup> A. M. Trozzolo, personal communication.
- <sup>9</sup> (a) D. F. DeTar, *J. Amer. Chem. Soc.*, 1967, **89**, 4058; (b) J. C. Bevington and T. D. Lewis, *Trans. Faraday Soc.*, 1958, **54**, 1340.
- <sup>10</sup> R. W. Fessenden and R. H. Schuler, *J. Chem. Phys.*, 1963, **39**, 2147.
- <sup>11</sup> F. Gerhart and G. Osterman, *Tetrahedron Letters*, 1969, 4705.



CHAPTER V

CHEMICALLY INDUCED DYNAMIC NUCLEAR POLARIZATION V.  
NMR ENHANCEMENTS IN BIRADICAL PRODUCTS<sup>1</sup>.

By R. Kaptein, M. Fráter-Schröder  
and L.J. Oosterhoff

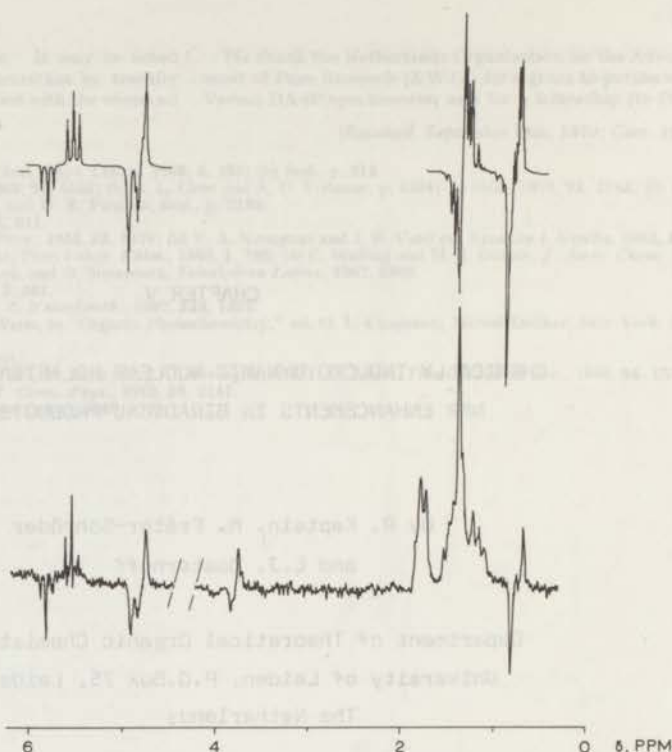
Department of Theoretical Organic Chemistry,  
University of Leiden, P.O.Box 75, Leiden,  
The Netherlands

Sir:

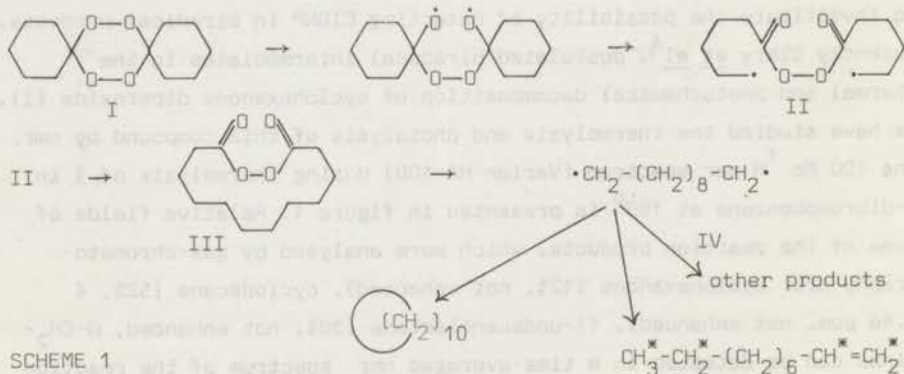
Observations of nmr emission (E) and enhanced absorption (A) during radical reactions can be interpreted in terms of processes occurring in radical pairs<sup>2,3</sup> rather than in free radicals. Because of the close relationship between radical pairs and biradicals it seemed worthwhile to investigate the possibility of detecting CIDNP in biradical products. Recently Story *et al*<sup>4</sup> postulated biradical intermediates in the thermal and photochemical decomposition of cyclohexanone diperoxide (I). We have studied the thermolysis and photolysis of this compound by nmr; the 100 Mc <sup>1</sup>H nmr spectrum (Varian HA-100) during thermolysis of I in m-dibromobenzene at 180<sup>o</sup> is presented in figure 1. Relative fields of some of the reaction products, which were analysed by gas-chromatography are: cyclohexanone (12%, not enhanced), cyclodecane (52%,  $\delta$  1.48 ppm, not enhanced), 11-undecanolactone (30%, not enhanced, O-CH<sub>2</sub>-lines can be detected in a time-averaged nmr spectrum of the reaction

fig. 1

100 Mc nmr spectrum during thermal decomposition of 0.2 M cyclohexanone diperoxide (I) in m-dibromobenzene at 180°. A Computer simulated CIDNP spectrum of 1-decene, formed from bi-radical IV, is shown at the top.



mixture at  $\delta$  4.13 ppm) and 1-decene (6%, vinyl-protons,  $\delta$  4.8-6.0 ppm,  $\text{CH}_3$ -protons,  $\delta$  0.86 ppm, E/A multiplets). Another E/A multiplet is observed at 3.90 ppm, that may be due to the  $\text{O-CH}_2$ -group of  $\epsilon$ -caprolactone<sup>5</sup>; the mechanism by which it is formed, however is not clear and we will not discuss it further. Cyclodecane and 1-decene can be accounted for by the reaction sequence presented in scheme 1 (c.f. ref 4).



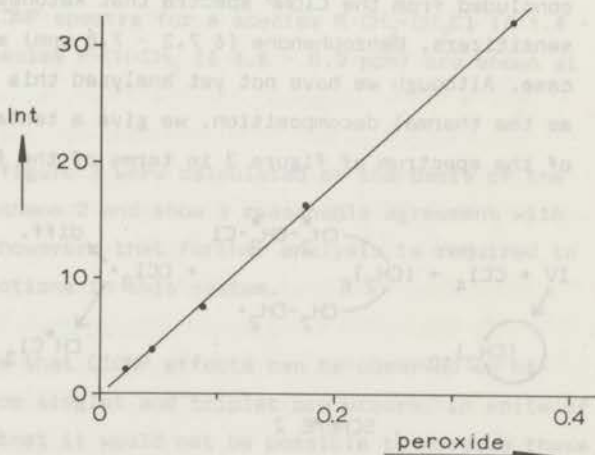
SCHEME 1

The starred protons are polarized. Although formation of 1-decene during thermolysis of pure peroxide I has not been mentioned by Story *et al.*, we have strong indications that the observed E/A multiplets in the vinyl- and methyl-region must be assigned to 1-decene, formed by internal disproportionation from the decamethylene biradical (IV):

- (i) Mass spectral analysis (MS-12/glc combination) unambiguously showed 1-decene to be present in the reaction mixture. No low boiling products like pentene or pentane, which might be formed from disproportionation of II and subsequent reaction, could be detected.
- (ii) Intensities of the enhanced lines were found to depend linearly on the concentration of peroxide I (see figure 2), showing that the polarized species is formed from I in a first order reaction.
- (iii) The CIDNP patterns are in accordance with the theoretically expected spectrum for disproportionation of biradical IV, formed from a singlet precursor, as can be seen in figure 1 from the satisfactory agreement between the observed and computer-simulated spectrum<sup>7</sup> (the CH<sub>2</sub>-region around  $\delta$  1.40 ppm is obscured by absorptions of peroxide I and other products).

fig. 2

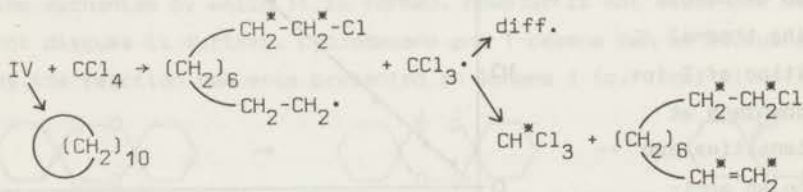
Maximum intensity of the emission line at 0.92 ppm versus concentration of peroxide I during thermal decomposition of I in *m*-dibromobenzene at 180°. Intensities are plotted on an arbitrary scale.



The absence of polarization in the single line of cyclodecane is also predicted by the theory ( $\Delta g = 0$  : no net effect). The absence of polarization in 11-undecanolactone is in accord with its formation by carboxy inversion from the cyclic peroxide III, as suggested in ref.4.

The vinyl-proton part of the spectrum in figure 1 is essentially the same as the butene spectrum obtained by Ward and Lawler<sup>9</sup> in the reaction of butyllithium and butylbromide and the propene spectrum (quartets instead of triplets for the methine proton) that we previously obtained<sup>10</sup> during decomposition of-butyryl peroxide. This strongly indicates that these products are formed by a cage disproportionation reaction from a singlet radical pair. The biradical IV has approximately the same size as the nitroxide biradicals that have been studied by Glarum and Marshall<sup>11a</sup> and by Lemaire<sup>11b</sup>. Hence the average exchange interaction between the two unpaired electrons is also expected to be of the same order of magnitude *viz.* 20 - 50 G (depending on the temperature), which is comparable to the hyperfine interactions, thus satisfying a necessary condition to obtain polarization.

We have also studied the photolysis of I. We could not detect any CIDNP effects during direct photolysis of I in several solvents. However, when benzophenone (0.3 M) was added to a 0.1 M solution of I in CCl<sub>4</sub>, CIDNP could be observed (figure 3). In a recent communication<sup>12</sup> we discussed the photosensitization of peroxide decompositions and concluded from the CIDNP spectra that ketones serve as triplet sensitizers. Benzophenone ( $\delta$  7.3 - 7.8 ppm) acts similarly in this case. Although we have not yet analysed this system in the same detail as the thermal decomposition, we give a tentative explanation of part of the spectrum of figure 3 in terms of the following reactions<sup>13</sup>:



SCHEME 2

The multiplets at 1.54 and 3.42 ppm have the correct chemical shift for a species R-CH<sub>2</sub>-CH<sub>2</sub>Cl, and the E/A multiplet effect indicates a triplet biradical precursor. The vinyl-proton signals (methine  $\delta$  5.60 ppm, E, methylene  $\delta$  5.00 ppm, A) and chloroform ( $\delta$  7.25 ppm, E) indicate disproportionation of R-CH<sub>2</sub>-CH<sub>2</sub> with CCl<sub>3</sub> ( $g = 2.0091$ )<sup>14</sup> from the cage of formation (triplet precursor) or from encounter pairs of free radicals.



**Figure 3** 60 Mc nmr spectrum during photolysis of 0.1 M peroxide I in  $\text{CCl}_4$  with 0.3 M benzophenone. A  $\text{CuSO}_4$  filter solution was used. Computer simulated CIDNP spectra for a species  $\text{R-CH}_2\text{-CH}_2\text{Cl}$  ( $\delta$  1.4 - 3.5 ppm) and for a species  $\text{R-CH=CH}_2$  ( $\delta$  4.8 - 6.0 ppm) are shown at the top.

The simulated spectra in figure 3 were calculated on the basis of the reactions postulated in scheme 2 and show a reasonable agreement with experiment. It is clear, however, that further analysis is required to elucidate the complex reactions in this system.

The present work shows that CIDNP effects can be observed in biradical products, both from singlet and triplet precursors, in spite of a supposition by Closs<sup>3b</sup> that it would not be possible to observe these effects in the case of singlet biradicals. It should be emphasized, however, that polarization in biradical products such as 1-decene can only be observed by virtue of a competing reaction path, independent of the electronic multiplicity of the biradical, e.g. transfer reactions with the solvent (indicated by "other products" in scheme 1). In the case of radical pairs this competing process generally is diffusion from the cage.

Acknowledgement. We wish to thank Mr. J.A. den Hollander and Mr. D. Antheunis for assistance with the photochemical experiments and Mr. F.J.J. de Kanter for carrying out the computer calculations.

References and Footnotes

- 1) Presented in part at the CIDNP Symposium of the ACS meeting in Houston, February 1970.
- 2) R. Kaptein and L.J. Oosterhoff, Chem. Phys. Letters, 4, 195, 214 (1969).
- 3) (a) G.L. Closs, J. Amer. Chem. Soc., 91, 4452 (1969);  
(b) G.L. Closs and A.D. Trifunac, ibid., 91, 4454 (1969);  
(c) ibid., 92, 2183 (1970).
- 4) P.R. Story, D.D. Denson, C.E. Bishop, B.C. Clark and J.C. Farine, ibid., 90, 817 (1968).
- 5) Authentic  $\epsilon$ -caprolactone, synthesized from cyclohexanone by oxidation with perbenzoic acid<sup>6</sup> has  $\delta(\text{OCH}_2) = 3.88$  ppm in m-dibromobenzene.
- 6) S.L. Friess, ibid., 71, 2571 (1949).
- 7) The computer program is a modified nmr. spectrum simulation program. Populations of nuclear spin energy levels are calculated according to the CIDNP theory<sup>2,3</sup>. The hyperfine coupling constants used for biradical IV are those reported for the octyl radical<sup>8</sup>  $A = -22\text{G}$ ,  $A = +28\text{G}$ . Details of the procedure will be published elsewhere.
- 8) A. Hudson and R.A. Jackson, Chem. Comm., 1323 (1969).
- 9) H.R. Ward and R.G. Lawler, J. Amer. Chem. Soc., 89, 5518 (1967).
- 10) R. Kaptein, Chem. Phys. Letters, 2, 261 (1968).
- 11) (a) S.H. Glarum and J.H. Marshall, J. Chem. Phys., 47, 1374 (1967);  
(b) H. Lemaire, J. Chim. Phys., 559 (1967).
- 12) R. Kaptein, J.A. den Hollander, D. Antheunis and L.J. Oosterhoff, Chem. Comm., 1887 (1970).
- 13) Similar reactions are conceivable for biradical II and products would give similar CIDNP effects.
- 14) A. Hudson and H.A. Hussein, Mol. Phys., 16, 199 (1969).

CHAPTER VI

CHEMICALLY INDUCED DYNAMIC NUCLEAR POLARIZATION.  
SIGN REVERSAL OF THE POLARIZATION IN THE REACTION OF  
ISOBUTYRYL PEROXIDE WITH BROMOTRICHLOROMETHANE.

By R. Kaptein<sup>\*</sup>, F.W. Verheus and L.J. Oosterhoff

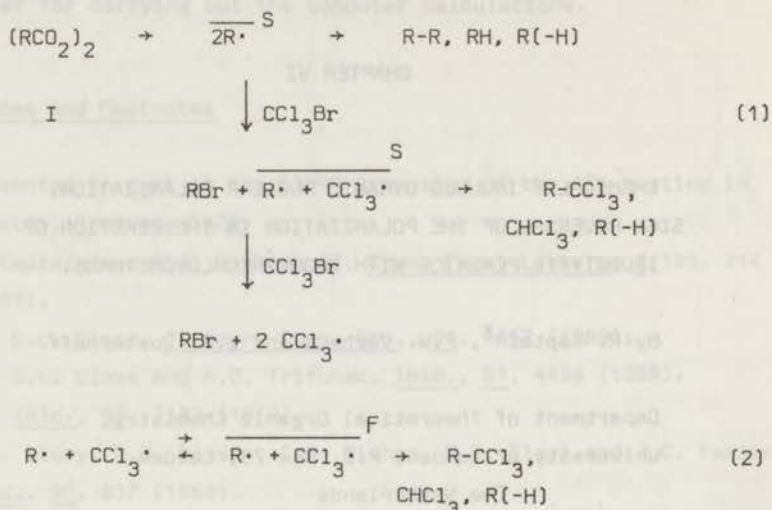
Department of Theoretical Organic Chemistry,  
University of Leiden, P.O. Box 75, Leiden,  
The Netherlands

**Summary** Sign reversal of chloroform polarization at 0.1 M  $\text{CCl}_3\text{Br}$ , added as a scavenger for isopropyl radicals is indicative of long-time spin-correlation effects of radical pairs in solution.

**CIDNP** offers the possibility of studying the problem of spin-correlation in radical pairs<sup>1,2</sup>. An important question is: how long does a pair of freely diffusing radicals, formed in a single event, retain its identity as a pair? With regard to observable CIDNP effects, meaningful conditions for this are: (i) there must still be some chance of geminate recombination, and (ii) the electron spins of the pair have not yet lost their phase relationship. The thermal decomposition of isobutryl peroxide (I) in the presence of bromotrichloromethane allowed us to investigate this problem. The CIDNP spectrum of the decomposition of I in hexachloroacetone was reported previously<sup>3</sup>. It is consistent with formation and subsequent reactions of a pair of isopropyl radicals;

apart from ionic pathways, which do not give rise to CIDNP effects, this in accord with other studies<sup>4,5</sup>.

The reactions of I in the presence of bromotrichloromethane are presented in the scheme.



SCHEME.

R· is the isopropyl radical and S and F denote pairs from a singlet precursor and from free radical encounters respectively. Products from S and F pairs give opposite polarization<sup>2b</sup>. The 100 Mc nmr spectrum taken during decomposition at 80° of a 0.2 M solution of I in hexachlorobutadiene, containing 5 M CCl<sub>3</sub>Br, is shown in figure 1.

Enhanced absorption (A) and emission (E) occur for the products chloroform ( δ 7.27 ppm, A ), propene ( methine δ 5.70 ppm, E + E/A; methylene δ 4.90 ppm, A + E/A ), isopropylbromide ( methine δ 4.19 ppm, A + A/E; methyl δ 1.69 ppm, E + A/E ), 2-trichloromethyl-propane ( methine δ 2.70 ppm, E; methyl δ 1.27 ppm, A ), propane and 2,3-dimethylbutane ( methyl δ 0.85 ppm E/A ), and some unidentified products. These polarization patterns are completely in accord with reactions (1) of the scheme (coupling and disproportionation of and escape from both S-pairs), showing that CCl<sub>3</sub>Br interferes with geminate recombination of isopropyl radicals in this high concentration range.

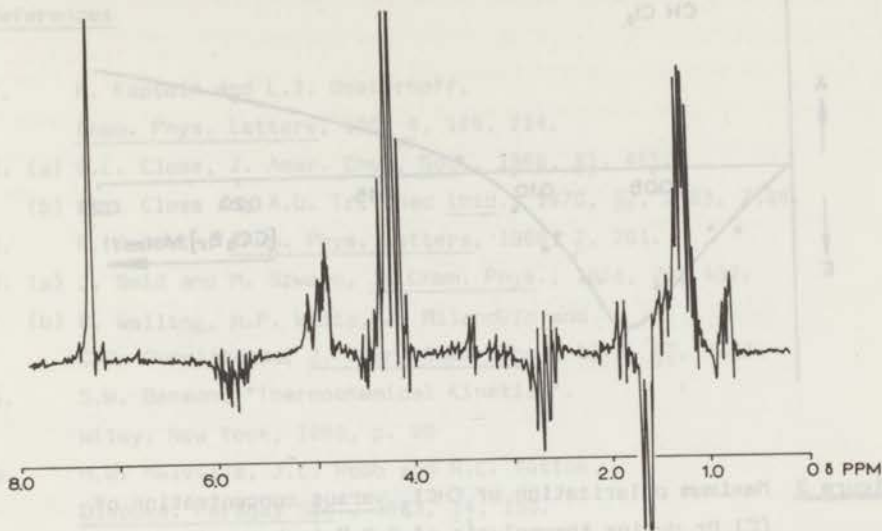


Figure 1 100 Mc nmr spectrum during thermolysis of 0.2 M isobutyryl peroxide in hexachlorobutadiene with 5 M  $\text{CCl}_3\text{Br}$  at  $80^\circ$ .

At lower  $\text{CCl}_3\text{Br}$  concentrations the propene and isopropylbromide lines acquire more E/A and A/E character, i.e. polarization becomes determined by reactions of the first pair (c.f. ref. 3).

The chloroform signal exhibited the behaviour shown in figure 2; it changed sign at 0.11 M  $\text{CCl}_3\text{Br}$  indicating, that effects of reactions (1) and (2) just cancel at this concentration. Below 0.11 M reaction (2) predominates (F-pairs). At first sight it may seem to be unlikely, that the transfer reaction with  $\text{CCl}_3\text{Br}$  in the range of 0.1 M is fast enough to yield a pair with appreciable probability of geminate recombination. This process is usually thought to occur within a time  $10^{-10}$ - $10^{-9}$  sec; to compete on this time-scale the transfer reaction ought to have a rate constant  $k_{tr}$  in the range  $10^9$  -  $10^{10}$  1/mole, sec (close to diffusion controlled) which is unreasonably large for this reaction<sup>5</sup>. Indeed, for a somewhat similar radical ( $\text{CCl}_3\text{CH}_2\dot{\text{C}}\text{HOCOCCH}_3$ ),  $k_{tr}$  for this reaction has been measured<sup>6</sup> and would have a value of  $2.2 \cdot 10^4$  1/mole, sec at  $80^\circ$ .

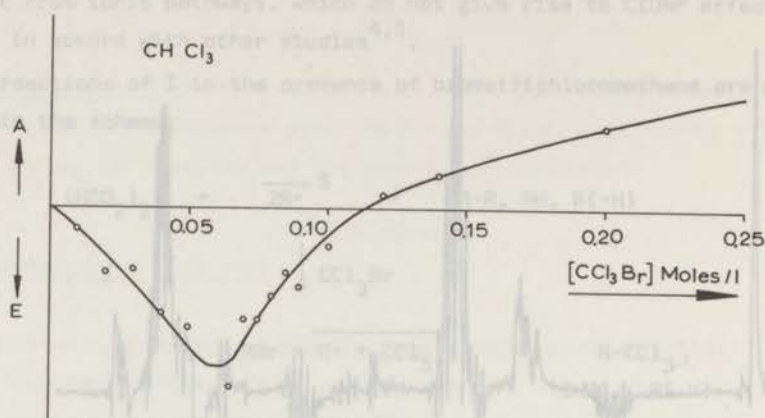


Figure 2 Maximum polarization of  $\text{CHCl}_3$  versus concentration of  $\text{CCl}_3\text{Br}$  during thermolysis of 0.2 M isobutyryl peroxide in hexachlorobutadiene.

Furthermore, for  $k_{tr}$  in the range  $10^9 - 10^{10}$  1/mole, sec the life-time of  $R\cdot$  would be so short, that reaction (2) would not be competitive. Thus there seems to be a discrepancy. However, by applying a quantitative theory of DIDNP based on a random walk model for the diffusive motion of radical pairs, it can be shown<sup>7</sup> that even at 0.1 M  $\text{CCl}_3\text{Br}$  chloroform formed in (1) would still give an observable enhancement for  $k_{tr} = 5 \cdot 10^6 - 5 \cdot 10^7$  1/mole, sec, giving life-times for  $R\cdot$  of the order of microseconds (a larger value of  $k_{tr}$  for the isopropyl radical than for the vinyl acetate derived radical does not seem to be unrealistic). Essentially this longer time-scale for polarization in the diffusion model is due to the dependence of both product formation and polarization on  $\sqrt{k_{tr} [S]}$ , where  $[S]$  is the concentration of scavenger. A more detailed discussion will be given elsewhere<sup>7</sup>. Although calculations are tentative because of lack of information on rate constants, the present work seems to show that spin-correlation effects of radical pairs in solution can be of rather long duration (microseconds). This observation would support our view that CIDNP arises from S-T mixing in freely diffusing radical pairs.

References

1. R. Kaptein and L.J. Oosterhoff,  
Chem. Phys. Letters, 1969 4, 195, 214.
2. (a) G.L. Closs, J. Amer. Chem. Soc., 1969, 91, 4552  
(b) G.L. Closs and A.D. Trifunac ibid., 1970, 92, 2183, 2188.
3. R. Kaptein, Chem. Phys. Letters, 1968, 2, 261.
4. (a) J. Smid and M. Szwarc, J. Chem. Phys., 1958, 29, 432;  
(b) C. Walling, H.P. Waits, J. Milanovic and  
C.G. Pappiaonou, J. Amer. Chem. Soc., 1970, 92, 4927.
5. S.W. Benson, "Thermochemical Kinetics".  
Wiley, New York, 1968, p. 99
6. H.W. Melville, J.C. Robb and R.C. Tutton,  
Discuss. Faraday Soc., 1953, 14, 150.
7. R. Kaptein, to be published.

## CHAPTER VII

### CHEMICALLY INDUCED DYNAMIC NUCLEAR POLARIZATION VII. PHOTOREACTIONS OF ALIPHATIC KETONES.\*

By J.A. den Hollander, R. Kaptein and  
P.A.T.M. Brand.

(Department of Theoretical Organic Chemistry, University of  
Leiden, P.O. Box 75, Leiden, The Netherlands)

#### 1. Introduction.

The photochemistry of ketones has been thoroughly investigated. It has been established that for aliphatic ketones, which have no  $\gamma$ -hydrogen atoms, the major reaction is the "Norrish type I" split into an acyl/alkyl radical pair<sup>1</sup>. The question of the excited state from which this process occurs has only recently received some attention. Quenching studies<sup>2,3</sup> have shown that in the case of *t*-butyl alkyl ketones the type I reaction proceeds from both singlet (S) and triplet (T)  $n, \pi^*$  states. We have studied the photoreactions of aliphatic ketones with CIDNP in order to further elucidate the role of the excited state. It follows from the radical pair theory of CIDNP<sup>4,5</sup> and it has been demonstrated experimentally<sup>4,6</sup> that CIDNP spectra depend strongly upon the multiplicity of the precursors of radical pairs.

---

\* Presented at the CIDNP Symposium of the Belgian Chemical Society in Brussels, March 1971.

In this preliminary account we will discuss some reactions of diisopropyl ketone (DIK), which are typical of the reactions of  $\alpha$ -branched ketones. 60 Mc CIDNP spectra were obtained during photolysis in the modified probe of a Varian DA-60 nmr spectrometer. Samples were irradiated with an Osram HBO 1000 high-pressure mercury arc, in pyrex sample tubes (spectra did not change qualitatively in a quartz set-up).

Photolysis of DIK in two solvents will be discussed:

- (i) deuteriochloroform, representing an "inert" solvent (inert as to the primary photochemical steps) and
- (ii) carbontetrachloride. In the latter solvent a novel photoreaction was discovered.

## 2. Photolysis of Diisopropylketone (DIK) in $\text{CDCl}_3$ .

During irradiation of a 0.5 M solution of DIK in  $\text{CDCl}_3$  the CIDNP spectrum shown in figure 1 was obtained. Enhanced absorption (A) or emission (E) occurred for the following products: isobutyraldehyde (aldehyde H,  $\delta$  9.60 ppm, A + A/E),  $\text{CHCl}_3$  ( $\delta$  7.26, E),  $\text{CH}_2\text{Cl}_2$  ( $\delta$  5.30 ppm, E), propene (methine H,  $\delta$  5.75 ppm, A/E + A; methylene group  $\delta$  4.90 ppm, A/E + E;

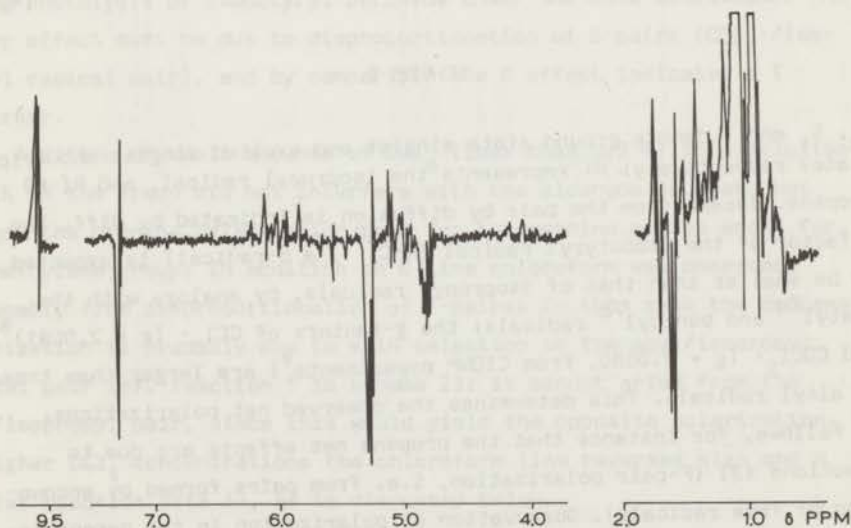
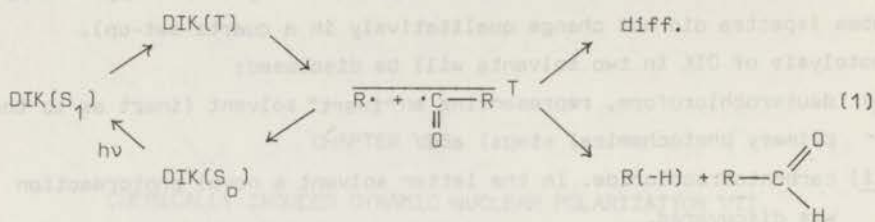


Figure 1 60 Mc nmr spectrum during photolysis of 0.5 M diisopropyl ketone in  $\text{CDCl}_3$ .

methyl group  $\delta$  1.70 ppm, A/E + E), propane and/or 2,2-dimethylbutane (methyl groups  $\delta$  0.85 ppm, A/E), DIK (methyl groups  $\delta$  1.02 ppm A + A/E). The spectrum is compatible with radical pair formation from T-state



SCHEME I.

$S_0$ ,  $S_1$  and T denote ground state singlet and excited singlet and triplet states respectively;  $\text{R}\cdot$  represents the isopropyl radical, and  $\text{R}(-\text{H})$  propene. Escape from the pair by diffusion is indicated by diff. The g-factor of the isobutyryl radical ( $\text{R}-\text{C}(=\text{O})\cdot$ , a  $\sigma$ -radical) is expected to be smaller than that of isopropyl radicals, by analogy with the acetyl<sup>7a</sup> and benzoyl<sup>7b</sup> radicals; the g-factors of  $\text{CCl}_3\cdot$  ( $g = 2.0091$ )<sup>8</sup> and  $\text{CCl}_2\cdot$  ( $g = 2.0080$ , from CIDNP experiments<sup>9</sup>) are larger than those of alkyl radicals. This determines the observed net polarizations; it follows, for instance that the propene net effects are due to reactions (3) (F-pair polarization, i.e. from pairs formed by encounters of free radicals). Observation of polarization in the parent ketone is remarkable and parallels a similar observation by Closs and Paulson<sup>10</sup> in the case of desoxybenzoin<sup>11</sup>.

The A effect in the aldehyde and A/E effects in propene and propane were also observed in a variety of other solvents: benzene, hexane, cyclohexane, fluorotrichloromethane, 1,1,2-trichlorotrifluoroethane.

It can easily be verified by applying the simple rules derived previously<sup>12</sup>, that the polarizations of figure 1 are in accord with the reactions of scheme I; however, since CIDNP effects are qualitatively the same for products from T-pairs and F-pairs<sup>4b</sup>, other reactions are possible, which would give similar polarizations. Thus A/E effects in propane and propene could arise from a T state isopropyl radical pair formed by rapid loss of CO from the acyl radical (cf. ref.3). Also, the polarization of the aldehyde might be due to acyl/alkyl F-pairs. It is not easy to exclude the latter possibility definitely, because it is hard to find radical scavengers, which do not interfere with the photochemistry of the ketone; furthermore, triplet quenching experiments<sup>10</sup> are not entirely unambiguous in our case, since quenchers like piperylene are effective alkyl radical traps as well. Our assumption of the intermediacy of T state ketones rests on the following evidence:

(i) photolysis of DIK in  $\text{CF}_2\text{Cl}-\text{CFCl}_2$  in the presence of 0.3 M  $\text{CCl}_3\text{Br}$  resulted in an E line for  $\text{CHCl}_3$ , whereas this product showed an A effect during photolysis of isobutyryl peroxide under the same conditions. The latter effect must be due to disproportionation of S-pairs ( $\text{CCl}_3\cdot/\text{isopropyl radical pair}$ ), and by comparison the E effect indicates a T precursor.

(ii) Addition of small amounts of  $\text{CCl}_4$  (less than 0.2 M) to a solution of DIK in the freon did not interfere with the aldehyde doublet, but changed the propene polarization to E for the methine proton and A for the methylene group; in addition an E line chloroform was observed, presumably from disproportionation of F-pairs. In this case the propene polarization is probably due to spin selection in the acyl/isopropyl radical pair (cf. reaction 1 in scheme I); it cannot arise from the  $\text{CCl}_3/\text{isopropyl pair}$ , since this would yield the opposite polarization. At higher  $\text{CCl}_4$  concentrations the chloroform line reverses sign and a singlet reaction sets in, as is discussed below.

The observed behaviour can be explained by assuming pair formation chiefly from T state ketone; it would be hard to reconcile with a

reaction mainly from the  $S_1$  state and polarization from F-pairs. This conclusion is in accordance with the findings of Yang and Feit<sup>2</sup> in the case of *t*-butyl alkyl ketones, where the type I split occurred predominantly from the T state.

### The Photoreaction of Diisopropyl ketone with $CCl_4$ <sup>13</sup>

The CIDNP spectrum obtained during irradiation of a 0.5 M solution of DIK in  $CCl_4$  is shown in figure 2b. The assignments, product yields, relaxation times ( $T_1$ ) and enhancement factors  $V$  are given in Table I.

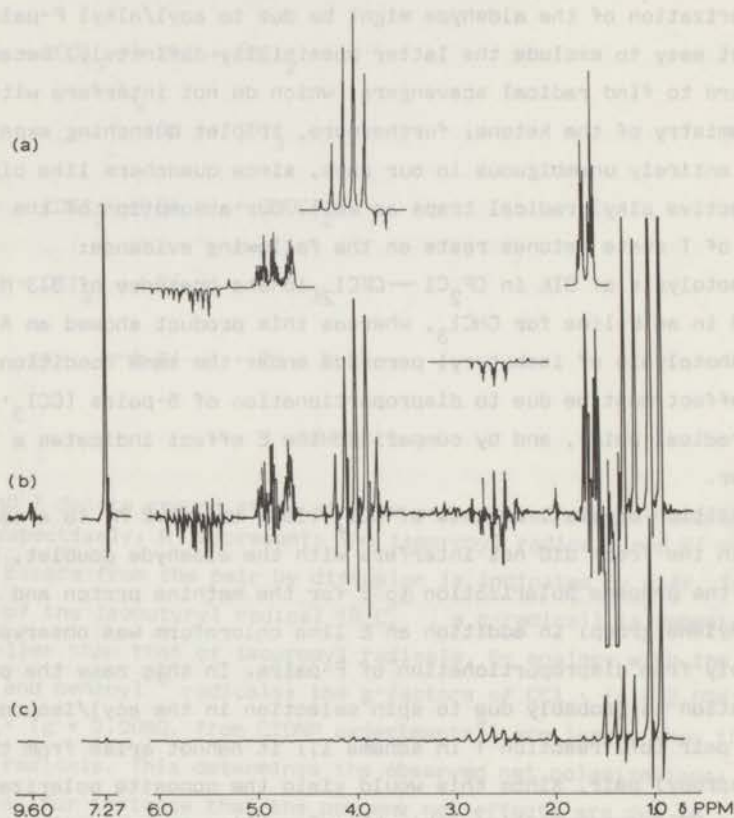


Figure 2 60 Mc nmr spectrum during (b) and after (c) photolysis of 0.5 M diisopropyl ketone in  $CCl_4$ . Spectrum (c) was recorded at a gain reduced by a factor 2.5 after 8 min. irradiation. Computer simulations are shown on top (a).

**Table I** Assignments, yields, relaxation times and enhancement factors for products from the photoreaction of diisopropyl ketone in  $\text{CCl}_4$ .

product	$\delta$ (ppm)	"yield"(%)(a)	$T_1$ (sec)	$V^{(b)}$
isobutyraldehyde		(c)		
$-\overset{\text{O}}{\parallel}{\text{C}}-\text{H}$	9.60	A		
chloroform	7.27	A	19	69
propene CH	5.73	E	1.0 <sup>(d)</sup>	85
CH <sub>2</sub> (cis)	4.97	A		62
(trans)	4.88			
CH <sub>3</sub>	1.72	A		36
isopropylchloride CH	4.13	A	31	53
CH <sub>3</sub>	1.54	E		14
trichloroisobutane CH	2.73	E	3.5 <sup>(e)</sup>	
CH	1.30	A		26
isobutyrylchloride CH <sup>3</sup>	2.92	N <sup>(g)</sup>	45	
CH <sub>3</sub>	1.30	N		
diisopropyl ketone CH	2.71	N		
CH <sub>3</sub>	1.04	N		

(a) nmr intensities (normalized to one proton) of products after 30 min irradiation in a sealed tube.

(b) enhancement factors calculated from  $V = I_t/I_0 T_1$  (see text); estimated error  $\pm 20\%$ .

(c) not observable after irradiation.

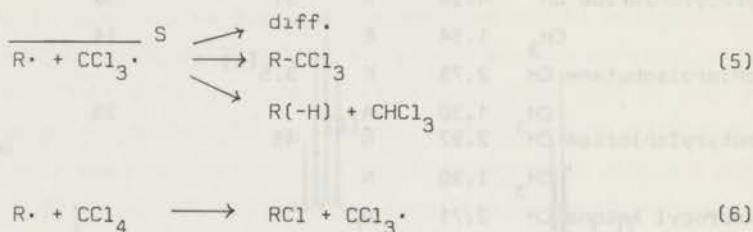
(d) yield is low probably due to secondary reactions of propene. On the basis of the CIDNP spectrum one would estimate the ratio disproportionation to coupling to be 2.5:1, assuming equal enhancement factors for propene and trichloroisobutane.

(e) determined from methyl doublet at 1.30 ppm after converting isobutyrylchloride into the acid by reaction with  $\text{H}_2\text{O}$ .

(f) enhanced doublet is assigned to the coupling product and not to isobutyrylchloride by analogy with the propene polarization. Furthermore the CH proton of isobutyrylchloride is not polarized.

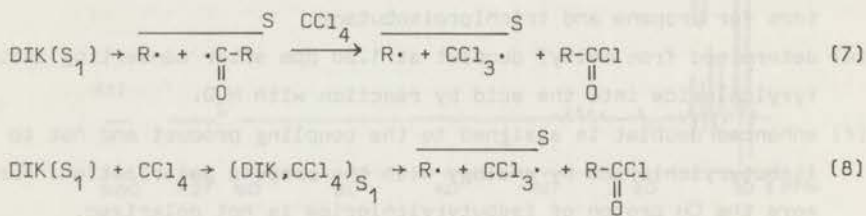
(g) N: not enhanced.

Yields were determined by integration of 100 Mc nmr spectra of irradiated samples. The enhancement factors are calculated from the formula  $V = It/I_0 T_1$ , where  $I$  is the intensity during irradiation and  $I_0$  the normal intensity of the product, after a total irradiation time  $t$ . From a comparison with the spectrum of figure 1, it will be obvious that  $CCl_4$  cannot be regarded as an "inert" solvent. The spectrum of fig. 2b can be completely accounted for by assuming formation of a  $CCl_3\cdot$ /isopropyl radical pair from a singlet state precursor, in contrast to the previous case, where reaction occurred from the T state. Reactions are shown in scheme II.



SCHEME II

Recombination (5) and transfer (6) after diffusion from the pair give rise to the observed polarizations, except for the aldehyde A effect, which must originate from a T reaction (1). One might speculate on the mechanism by which the pair is formed from  $DIK(S_1)$ . It should be noted, however, that CIDNP cannot give information on this point, beyond establishing the singlet nature of the precursor. Two possible pathways are indicated in scheme III:



SCHEME III

Reaction (7) involves a type I split from the  $S_1$  state followed by an extremely rapid transfer reaction with  $CCl_4$ . The rapidity of this step could be rationalized by the excess energy of the acyl radical<sup>1</sup> but it would be hard to explain the high selectivity of this reaction; the only other compound that we have found to exhibit the singlet reaction with DIK is hexachloroethane in deuterated benzene; compounds like  $CCl_3$ ,  $CHCl_3$ ,  $CFCl_3$ ,  $CCl_3Br$ ,  $CF_2Cl-CFCl_2$  did not show this reaction. Therefore, we favour the mechanism (8) involving the nonradiative decay of a complex formed from  $DIK(S_1)$  and  $CCl_4$  (exciplex). It would not be unreasonable to assume that special requirements for complex formation could render this reaction highly selective. In support of this mechanism we observed that the fluorescence of DIK is quenched when  $CCl_4$  is added to a solution of the ketone in  $CF_2Cl-CFCl_2$ . The use of this freon as a solvent precluded the possibility of fluorescence quenching by an intermolecular chlorine heavy atom effect<sup>1</sup>. The aldehyde A signal at 9.60 ppm in fig. 2b shows that intersystem-crossing in the ketone is not suppressed completely; a small fraction of  $S_1$  ketones arrives apparently in the T state and gives the type I reaction. We do not know of other cases, where CIDNP effects from both S- and T-pairs, derived from the same parent compound, appear in one spectrum.

Finally we note that the computer simulations shown in fig. 2a appear to be far from perfect. This can be seen most clearly in the case of the isopropylchloride septet at 4.13 ppm, where two high field lines have the wrong sign. The calculations were based on a g-value of 2.0091 for the  $CCl_3\cdot$  radical<sup>8</sup>. A better fit would have been obtained by using values in the range 2.0140-2.0150. Although a g-value of 2.014 has been reported<sup>14</sup> for  $CCl_3\cdot$  in a solid matrix, we consider the value 2.0091 to be more realistic. In our opinion the reason for this discrepancy lies in the neglect of nuclear relaxation in the products. When both net polarization and multiplet effects are present, it can be shown that e.g. a dipolar relaxation mechanism may tend to increase the apparent net effect.

### Acknowledgement.

We wish to thank Prof. L.J. Oosterhoff for his continuous interest in this work, Mr. J.G. Lammers for the fluorescence measurements and Mr. D. Antheunis for experimental assistance in the early stage of this work. Support from the Netherlands Organization for the Advancement of Pure Research (Z.W.O.) is gratefully acknowledged. We are indebted to Prof. H. Fischer and Prof. G.L. Closs for communicating results prior to publication.

### References and Footnotes.

1. J.G. Calvert and J.N. Pitts, "Photochemistry", John Wiley, New York, 1966, chap. 5.
2. N.C. Yang and E.D. Feit, J. Am. Chem. Soc., **90** (1968) 504.
3. N.C. Yang, E.D. Feit, M.H. Hui, N.J. Turro and J.C. Dalton, ibid., **92** (1970), 6974.
- 4.a G.L. Closs, ibid., **91** (1969), 4552;
- 4.b G.L. Closs and A.D. Trifunac, ibid., **92** (1970) 2183, 2186.
5. R. Kaptein and L.J. Oosterhoff, Chem. Phys. Letters, **4** (1969) 195, 214.
6. R. Kaptein, J.A. den Hollander, D. Antheunis and L.J. Oosterhoff, Chem. Comm., (1970) 1687.
- 7.a J.E. Bennet, B. Mile and B.Ward, ibid., (1969) 13.
- 7.b P.J. Krusic and T.A. Rettig, J. Am. Chem. Soc., **92** (1970) 722.
8. A. Hudson and H.A. Hussain, Mol. Phys., **16** (1969) 199.
9. M. Lehnig and H. Fischer, Z. Naturforsch., **25a** (1970) 1963.
10. G.L. Closs and D.R. Paulson, J. Am. Chem. Soc., **92** (1970) 7229.
11. We have observed this also in the case of pinacolone (methyl t-butyl ketone): A for the t-butyl group and E for the methyl group, showing that the sign of the hyperfine coupling constant ( $A_H$ ) in the acetyl radical is positive.
12. R. Kaptein, to be published.
13. Trozzolo and coworkers have made observations similar to those reported here. However, their interpretations differ from ours, cf. T. Do Minh and A.M. Trozzolo, paper presented at the CIDNP Symposium of the Belgian Chemical Society in Brussels, March 1971.
14. R.M. Leblanc, F.C. Thyron and J.A. Herman, Can. J. Chem., **46** (1968) 1625.

## CHAPTER VIII

### CHEMICALLY INDUCED DYNAMIC NUCLEAR POLARIZATION VIII

#### SPIN DYNAMICS AND DIFFUSION OF RADICAL PAIRS.

By R. Kaptein.

Department of Theoretical Organic Chemistry

University of Leiden, P.O. Box 75, Leiden.

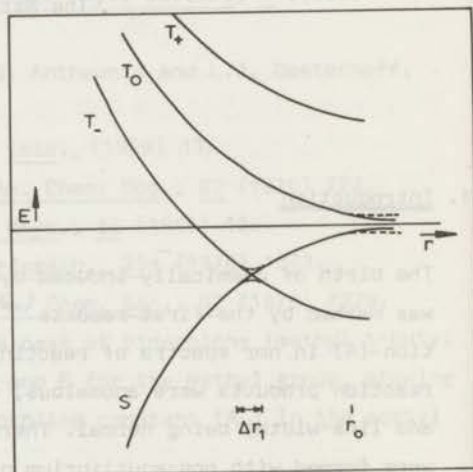
The Netherlands.

#### 1. Introduction

The birth of chemically induced dynamic nuclear polarization (CIDNP) was marked by the first reports<sup>1,2</sup> of emission (E) and enhanced absorption (A) in nmr spectra of reacting systems. Only intensities of the reaction products were anomalous, other characteristics (line-frequencies and line-width) being normal. Therefore it was obvious that the products were formed with non-equilibrium nuclear spin state populations. First ideas on the mechanism of this effect<sup>1b,2b</sup> invoked electron-nuclear cross-relaxation in free radicals to explain the enhanced polarization in a way similar to the Overhauser effect. A number of phenomena, however, were inexplicable or even in conflict with these early theories, viz. multiplet effects<sup>2,3,4</sup> (both E and A in the multiplet of a nucleus); dependence on type of reaction<sup>4</sup> (products formed by recombination behaved

opposite to transfer reaction products); dependence on the electronic state multiplicity of the precursor in photochemical reactions<sup>5,6</sup>; observation of polarization, when the reaction was run in zero magnetic field<sup>7</sup>; the magnitude of the enhancement found to be larger than the Overhauser limit in some cases<sup>5</sup>; polarization found in systems where radical life times were much larger than relaxation times in the radicals<sup>2,8</sup>. Although there is no reason why the originally proposed mechanism should not contribute to the polarization in some favourable cases, this mechanism, however is usually overshadowed by the more powerful radical pair mechanism, independently proposed by Closs<sup>5,9</sup> and by Kaptein and Oosterhoff<sup>10</sup>. This recent theory was rather successful, because it could qualitatively account for all published CIDNP spectra, with the possible exception of one or two pathological cases. The essentials of the radical pair mechanism can be discussed with the aid of figure 1, showing schematically the energy levels of singlet (S) and triplet (T) states of radical pair in a magnetic field for separations in the range of a few molecular diameters.

Figure 1 Energies of singlet and triplet states of a radical pair in a magnetic field versus separation ( $r$ ). The broken lines are the adiabatic energy levels. The S-T<sub>-</sub> mixing region is denoted by  $\Delta r_1$ ; the S-T<sub>0</sub> mixing occurs when  $r > r_0$ .



When a pair separates after its birth or after a collision, the S-T energy gap  $2J$  ( $J$  is the exchange integral) becomes smaller and at distances where degeneracies or near-degeneracies occur the S and T

states are mixed by hyperfine (hf.) interactions of electrons with nuclei, provided the time spent in a mixing (or transition) region is sufficiently long. It will be shown in the next section that for the region  $Ar_1$  in high fields (higher than a few thousand Gauss) this time is too short to allow appreciable S-T mixing, so that the system zips essentially unchanged (non-adiabatically) through this region. However, the time spent in the S-T mixing region  $r > r_0$  ( $r_0$  roughly given by the condition that J is of the order of the hf. parameters) is much larger and S-T transitions may occur. As these transitions are nuclear spin dependent, so is product formation, when this occurs only from the S state. This process has been appropriately called "spin selection"<sup>11,12</sup>. The operator for S-T<sub>0</sub> mixing is of the form  $(S_{z1} - S_{z2}) I_z$ . As the nuclear spin part ( $I_z$ ) is diagonal no nuclear spins are "flipped" and no polarization is generated in the sample considered as a whole. Only polarization for specific products results from this process. Therefore nuclear polarization in recombination products opposes that of the escaping radicals and hence of transfer reaction products. It will be clear that the magnitude of the polarization will be closely bound up with the motion of the pair; thus it depends on the dynamics of the "cage" processes. A satisfactory description of the "cage" reaction has been developed by Noyes<sup>13</sup>. He makes the distinction<sup>13b</sup> of primary cage reactions (reactions of a pair of next neighbours, surrounded by a cage of solvent molecules) and secondary recombinations of original partners, after some relative diffusion has occurred. Both processes are frequently lumped together in the name "cage" reactions. The distinction is, however, important for us, because the short time span of primary cage reactions ( $10^{-11}$  sec) will not allow nuclear spin dependent intersystem-crossing to occur and the polarization is due to spin selection in subsequent encounters of the pair. Hence the time-scale of CIDNP is limited by that of "geminate" recombination. Accordingly we shall employ Noyes approach to the kinetic description of geminate recombination<sup>14</sup> in section 3 and incorporate the dynamics of the spin system, treated in section 2. Thus relative diffusion of radical pairs is explicitly taken into account in our model. In this respect it differs from other kinetic schemes<sup>12,15,16</sup> including our previous simplified treatment<sup>10b</sup>, where the processes of product formation and escape of radical pairs are discussed in terms of time-independent rate constants.

and "mean life times". These rate constants have only a formal meaning but cannot easily be correlated with solvent properties and diffusive behaviour of radical pairs.

In section 4 the link is made with the actual CIDNP spectra and it will be shown that all qualitative predictions can be made with but two simple rules, one for net effects (E or A) and one for multiplet effects. If one is concerned with details or if spectra are too complicated one has to resort to computer simulation techniques, some results of which are discussed in section 5. In this paper we shall be concerned only with the high field case, where reactions are run in fields of a few thousand Gauss or larger. In a following paper<sup>17</sup> this restriction will be removed and the formalism will be extended to include the effects of S-T<sub>0</sub> mixing, which have to be considered in low fields.

## 2. The Spin Hamiltonian and S-T<sub>0</sub> mixing

Intersystem-crossing in a radical pair can be conveniently described in terms of a Spin Hamiltonian. Itoh *et al.*<sup>18</sup> have recently shown how this Spin Hamiltonian can be obtained from the total Hamiltonian for cases of near degeneracies of S and T states. The total Hamiltonian can be written:

$$\underline{H} = \underline{H}_e + \underline{H}_{LS} + \underline{H}_{HL} + \underline{H}_{HS} + \underline{H}_{SS} + \underline{H}_{SI} + \underline{H}_{HI} \quad (1)$$

where  $\underline{H}_e$  is the electronic energy term:

$$\underline{H}_e = \underline{H}_e^a + \underline{H}_e^b + \underline{H}_e^{ab} \quad (2)$$

$\underline{H}_e^a$  and  $\underline{H}_e^b$  describing the radicals *a* and *b* and  $\underline{H}_e^{ab}$  their mutual interaction.  $\underline{H}_{LS}$  is the spin-orbit coupling term;  $\underline{H}_{HL}$ ,  $\underline{H}_{HS}$  and  $\underline{H}_{HI}$  denote the interaction of the magnetic field with electronic orbital motion, electron spin and nuclear spin respectively;  $\underline{H}_{SS}$  is the electron spin-spin interaction term and  $\underline{H}_{SI}$  the nuclear hyperfine interaction term. Following the perturbation procedure of Itoh *et al.*<sup>18</sup>, the Spin Hamiltonian can be obtained containing terms appropriate for the S and T states of the radical pair and terms connecting these states:

$$H_{RP} = H_{ex} + H_{ZS} + H_{hf} + H_D + H_{ZI} \quad (3)$$

The various terms will now be discussed.

## 2.1 The exchange term.

The action of  $H_e^{ab}$  together with the Pauli exclusion principle gives rise to an energy difference between S and T states,  $\Delta E_{ST}$ . In Valence Bond (VB) theory the energy expression is:

$$E_{S/T} = 2E_0 + \frac{C \pm J}{1 \pm S_{ab}} \quad (4)$$

where  $E_0$  is the energy of the two fragments without interaction;  $C$ ,  $J$  and  $S_{ab}$  are Coulomb, exchange and overlap integrals. As the VB theory gives a very good approximation to the electronic energy at large separations and as the condition  $S_{ab}^2 \ll 1$  is also satisfied at large  $r$  we may identify  $\Delta E_{ST} = 2J$  for our purposes<sup>19</sup>. The Dirac exchange operator

$$H_{ex} = -J (\frac{1}{2} + 2S_1 \cdot S_2) \quad (5)$$

in the Spin Hamiltonian will reproduce this energy difference ( $S_1$  and  $S_2$  are electron spin operators). The exchange integral is

$$J = \langle \psi_a(1)\psi_b(2) | H_e^{ab} | \psi_b(1)\psi_a(2) \rangle \quad (6)$$

where  $\psi_a$  and  $\psi_b$  are the orbitals carrying the unpaired electrons. It is enlightening to consider the expression for  $J$  in the case of two H-atoms:

$$J_{H_2} = \frac{e^2 S_{ab}^2}{r_{ab}} - 2S_{ab} \langle \psi_a(1) | \frac{e^2}{r_{b1}} | \psi_b(1) \rangle + \langle \psi_a(1)\psi_b(2) | \frac{e^2}{r_{12}} | \psi_b(1)\psi_a(2) \rangle \quad (7)$$

In this case the second term prevails, making  $J$  negative, which places the S state below the T state.  $J$  decreases exponentially with distance<sup>22</sup>, giving the behaviour sketched in figure 1. For radicals in general

a similar expression will hold. If there is a  $\pi$ -electron radical present, which is usually the case, there will be orientations for which  $S_{ab} = 0$  and  $J$  is positive. This is confirmed by recent calculations<sup>23</sup>. So  $J$  will then depend both on separation and orientation. For freely tumbling and diffusing radicals this means that  $J$  fluctuates (correlation time of reorientation  $\tau_c = 10^{-11} - 10^{-10}$  sec) within an exponential envelop. In addition there may be contributions from indirect exchange mechanisms via intervening solvent molecules. Calculations indicate that  $|J|$  becomes of the order of the hf. coupling constants at about  $6 \text{ \AA}$  for H-atom 1s orbitals<sup>22</sup> and about  $10 \text{ \AA}$  for 2p and 2s orbitals<sup>23</sup>. Experiments show that  $r_0$  may be even smaller. Hirota and Weissman<sup>24</sup> found a negligible  $J$  at separations of  $5 - 6 \text{ \AA}$  in ion pairs. A value  $r_0 = 6 \text{ \AA}$  is quoted by Ferruti et al.<sup>25</sup> For nitroxide biradicals and from the work of Itoh et al.<sup>18</sup> a value of  $7 \text{ \AA}$  can be deduced. So it seems reasonable to assume that  $J$  drops to a value comparable to the hf. constants after only a few diffusive displacements.

We have previously<sup>10</sup> approximated the time dependence of  $J$  by a step function, changing  $J$  suddenly at  $t = 0$  from a very large to a low (constant) value and we shall do the same here. It has the great advantage of making the effective Hamiltonian time-independent. We considered only S-T<sub>0</sub> mixing. These simplifications are justified if

- (i) we can neglect S-T<sub>±</sub> transitions.
- (ii) the time necessary to reach a separation  $r = r_0$  is short compared to the time spent in the S-T<sub>0</sub> mixing region  $r > r_0$ .
- (iii) the residual fluctuations of  $J$  around a mean value are small.

If we anticipate that the transition probabilities for short times<sup>26</sup> are of the order  $a^2 t^2$ , where  $a = |\langle \Psi_S | H_{RP} | \Psi_T \rangle| \sim 10^8$  radians/sec, and that the thermal equilibrium polarization is about  $10^{-5}$  we see that we need times  $t > 10^{-10}$  sec to give appreciable enhancements. This is longer than the time needed for a few displacements (a few times  $10^{-11}$  sec) and the time spent in  $\Delta r_1$ , which is even shorter. So conditions (i) and (ii) seem to be satisfied. We do not really know very much about  $J$  for  $r > r_0$  so it is simplest to assume that (iii) will hold also.

Glarum<sup>27</sup> has worked out the problem with an exponential model for  $J$  and  $r(t) = vt$ . It seems that this overestimates somewhat the S-T<sub>±</sub> transition probabilities, for which there are no experimental indications in high

fields. In view of the neglect of fluctuations in J and the simplified description of the motion of the pair, we are of the opinion that this model<sup>27</sup> does not necessarily provide a better description than the present diffusion model.

## 2.2 The Zeeman terms.

The combined effects of  $\underline{H}_{LS}$  and  $\underline{H}_{HL}$  give rise<sup>18,28</sup> to a term linear in the field  $H_0$  and  $S_1, S_2$ :

$$\underline{H}_{ZS} = \beta_e H_0 \cdot \underline{g}_a \cdot S_1 + \beta_e H_0 \cdot \underline{g}_b \cdot S_2 \quad (8)$$

The anisotropy of the g-tensors,  $\underline{g}_a$  and  $\underline{g}_b$  is averaged out by the tumbling motion of the radicals, which is usually faster ( $\tau_c \sim 10^{-11} - 10^{-10}$  sec) than intersystem-crossing. We may therefore neglect the anisotropic terms:

$$\underline{H}_{ZS} = \beta_e H_0 (g_a S_{1z} + g_b S_{2z}) \quad (9)$$

Although the nuclear Zeeman term  $\underline{H}_{ZI} = \sum_i g_N \beta_N I_{zi} H_0$  is comparable to the hf. terms in high fields, it may be ignored, because it simply shifts the zero of energy, if only S-T<sub>0</sub> mixing is considered. Of course it is also unimportant in low fields.

## 2.3 The hyperfine terms.

The term  $\underline{H}_{SI}$  in (1), averaged over the space part of the wave function, leads to the hf. term describing the interaction of electrons with nuclei  $I_j$ :

$$\underline{H}_{hf} = S_1 \cdot \sum_j^a A_j I_j + S_2 \cdot \sum_k^b A_k I_k \quad (10)$$

The sum  $\sum^a$  runs over the nuclei of radical a.  $A_j$  are the isotropic hf. coupling constants; we have again neglected the anisotropic contributions. Eq. (10) is valid when the density of  $\Psi_a$  at the nuclei of b is negligible, which certainly is the case at separations  $r > r_0$ .

## 2.4 Other terms.

The electron dipolar coupling term  $\underline{H}_D = S_1 \cdot \underline{D} \cdot S_2$  is obtained by integrating

$\underline{H}_{SS}$  over the space part of the wave function. It is important to note that  $\underline{H}_D$  cannot induce S-T transitions (it mixes only T states). The tensor  $\underline{D}$  is completely anisotropic. In our case its main effects will be to modulate the energy of the T states; reorientation of the interrational vector may not be fast enough to average this out to zero. However, the uncertainty in J will be larger than the effects of  $\underline{H}_D$ , so we may as well disregard this term.

Other interactions that might mix S and T states are effects of spin-orbit coupling that have not yet been included in (8) and of spin-rotation interactions, which act during reorientation of a radical. Because they are zero on the average and have extremely short correlation times ( $10^{-14}$ - $10^{-15}$  sec)<sup>29</sup>, spin-rotation interactions will not be very important. Spin-orbit coupling is considered in Appendix A, where it is shown that it is probably not important at  $r > r_0$ , although it may play a role at shorter distances. This is important because no cross-terms with terms included in eq.(3) will appear in our results, in this way assuring that g-factor differences and hf. parameters can be obtained with some confidence from CIDNP spectra.

We are left with the effective Spin Hamiltonian of the radical pair, which can be written in the form:

$$\underline{H}_{RP} = \underline{H}^0 + \underline{H}^{\prime} \quad (11)$$

$$\begin{aligned} \underline{H}^0 = \frac{1}{2}(g_a + g_b)\beta_e \mathcal{H}^{-1} H_0 (S_{1z} + S_{2z}) - J(\frac{1}{2} + 2S_1 \cdot S_2) \\ + \frac{1}{2}(S_1 + S_2) \cdot (\sum_j^a A_{j^2} I_j + \sum_k^b A_{k^2} I_k) \quad (11a) \end{aligned}$$

$$\begin{aligned} \underline{H}^{\prime} = \frac{1}{2}(g_a - g_b)\beta_e \mathcal{H}^{-1} H_0 (S_{1z} - S_{2z}) \\ + \frac{1}{2}(S_1 - S_2) \cdot (\sum_j^a A_{j^2} I_j - \sum_k^b A_{k^2} I_k) \quad (11b) \end{aligned}$$

Angular frequency units are used ( $10^8$  radians/sec = 6 G =  $6 \cdot 10^{-4}$  cm<sup>-1</sup>).  $\underline{H}^0$  is diagonal in a basis of S and T functions and  $\underline{H}^{\prime}$  non-diagonal.

## 2.5 S-T<sub>0</sub> mixing.

For the description of time-dependent mixing of S and T<sub>0</sub> states we shall use a direct product basis of electronic S and T functions,  $S = 2^{-\frac{1}{2}}(\alpha_1\beta_2 - \beta_1\alpha_2)$ ;  $T_0 = 2^{-\frac{1}{2}}(\alpha_1\beta_2 + \beta_1\alpha_2)$  and nuclear spin product functions  $\chi_n$ . A nuclear state n is characterized by a collection of nuclear spin quantum numbers:  $n = (\dots M_j, M_k \dots)$ . We shall make use of magnetic equivalence factoring, the conditions being in our case: (i) the nuclei must be magnetically equivalent in the reaction product in the usual sense of having the same chemical shifts and the same coupling constants to other nuclei and (ii) they must have the same hf. coupling constant and reside in the same radical. These nuclei are first coupled (e.g. in case of two equivalent nuclei we make symmetric and anti-symmetric combinations) and summations over j and k run over all composite nuclei. As in III<sup>10b</sup> the wave function is expanded as

$$\phi_n(t) = \{C_{S_n}(t)S + C_{T_n}(t)T_0\}\chi_n \quad (12)$$

The time-dependence is given by  $i\frac{\partial\phi}{\partial t} = H_{RP}\phi$ . This leads to two coupled equations; solving these with initial conditions  $C_S(0)$  and  $C_T(0)$  we find

$$C_{S_n}(t) = C_S(0)\{\cos \omega t - \frac{iJ}{\omega}\sin \omega t\} - C_T(0)a_n \sin \omega t \quad (13)$$

where  $\omega = (J^2 + a_n^2)^{\frac{1}{2}}$  and

$$a_n = \langle S\chi_n | \underline{H} | T_0\chi_n \rangle = \frac{1}{2}i\Delta g\beta_e N^{-1}H_0 + \sum_j^a A_j M_j - \sum_k^b A_k M_k \quad (14)$$

with  $\Delta g = g_a - g_b$ . The probability of finding the pair in the singlet state is

$$|C_{S_n}(t)|^2 = |C_S(0)|^2 + |C_T(0)|^2 - |C_S(0)|^2(a_n/\omega)^2 \sin^2 \omega t \quad (15)$$

which gives for the special case of a singlet precursor with

$$C_S(0) = 1, C_T(0) = 0:$$

$$|C_{S_n}^S(t)|^2 = 1 - (a_n/\omega)^2 \sin^2 \omega t \quad (16a)$$

and for a triplet precursor:

$$|c_{S_n}^T(t)|^2 = (a_n/\omega)^2 \sin^2 \omega t \quad (16b)$$

It may be argued that our initial conditions imply that the functions  $\chi_n$  are eigenfunctions of the precursor, which may not generally be correct. In a following paper<sup>17</sup> we will give the general proof that mixing of the  $\chi_n$  in the precursor does not affect the results whatsoever; therefore we may as well start with the  $\chi_n$ .

A further condition for the validity of our treatment is that the radicals keep their phase relationship during the diffusive excursions, except for the effect of  $H$ . This condition seems to be satisfied because spin-lattice relaxation in radicals, which might destroy the spin correlation, is several orders of magnitude slower ( $T_1 \sim 10^{-5} - 10^{-4}$  sec) than the process of geminate recombination. In the following it will be assumed that recombination occurs only from the singlet state, so its probability is proportional to  $|c_{S_n}(t)|^2$ . This basic assumption of radical pair theory is certainly justified, when the triplet state is repulsive as in the case of the coupling of two H-atoms or alkyl radicals. Apparently it holds also for most disproportionation reactions, because the resulting CIDNP spectra can be treated on an equal footing. There are, however, reactions known where products are formed in a triplet state, notably in radiolysis<sup>30</sup>, where fragments dissociate and recombine with large excess energy and in certain reactions of peroxy radicals where triplet state ketones are formed, as evidenced by chemiluminescence<sup>30,31</sup>.

We have previously<sup>10</sup> averaged eq.(16) over a distribution of life-times  $\tau$  of the pair, and obtained for the probability of product formation

$$P_n^S \approx 1 - \frac{2a_n^2 \tau^2}{1 + 4\omega^2 \tau^2} \quad (17a)$$

$$P_n^T \approx \frac{2a_n^2 \tau^2}{1 + 4\omega^2 \tau^2} \quad (17b)$$

These formulae may still be useful in the case of biradicals<sup>32</sup> and other cases where the fragments disappear by first order kinetics. For freely diffusing radical pairs, however, the recombination reaction cannot strictly be described with first order rate constant and we will now examine this process in more detail.

### 3. Diffusion and Recombination of Radical Pairs.

At large separations the motion of the pair can be treated classically and is governed by stochastic processes. Using the theory of random flights<sup>33</sup>, Noyes<sup>13c</sup> showed that the probability of the first reencounter between  $t$  and  $t + dt$  for a pair, separating from an encounter at  $t = 0$  is  $f(t) dt$  where:

$$f(t) = mt^{-\frac{3}{2}} e^{-\frac{\pi m^2}{\rho^2 t}} \quad (18)$$

$p$  (Noyes: $\beta$ ) is the total probability of at least one reencounter:  $p = \int_0^{\infty} f(t) dt$ . For long times  $f(t) \sim mt^{-3/2}$ . The exponential factor ascertains that  $f(t)$  drops to zero for  $t = 0$ ; the exact behaviour at short times, however, is not very important. Both  $p$  and  $m$  can be expressed in the basic quantities  $\rho$  (the encounter diameter),  $\sigma$  (the rms displacement for relative diffusive motion) and  $v$  (the frequency of relative diffusive displacements)

$$p = 1 - \left(\frac{1}{2} + \frac{3\rho}{2\sigma}\right)^{-1} \quad (19)$$

$$m = 1.036 \frac{(1-p)^2}{v^{\frac{1}{2}}} \left(\frac{\rho}{\sigma}\right)^2 \quad (20)$$

For small radicals in ordinary solvent  $v$  will be about  $10^{11} \text{ sec}^{-1}$ ;  $\sigma$  will be equal to  $\rho$  or may be smaller, giving  $0.5 \leq p < 1$  and  $m \sim 10^{-6} \text{ sec}^{\frac{1}{2}}$  (the ratio  $\rho/\sigma$  does not affect  $m$  very much).

Let  $\lambda$  be the probability for recombination during a singlet encounter, then for small S-T transition probabilities, the chance of product formation during a first reencounter at time  $t$  is  $\lambda |C_{Sn}(t)|^2 f(t)$ .

Radicals of a pair that fails to react during the first reencounter

start again their random walk and have a new chance of meeting each other. Setting  $\lambda_n(t) = \lambda |C_{Sn}(t)|^2$ , the probability for recombination in the interval  $(t, t + dt)$  becomes  $P_n(t)dt$  with

$$P_n(t) = \lambda_n(t)f(t) + \int_0^t dt_1 \lambda_n(t-t_1)\{1-\lambda_n(t_1)\}f(t-t_1)f(t_1) + \int_0^t dt_2 \lambda_n(t-t_2)f(t-t_2) \int_0^{t_2} dt_1 \{1-\lambda_n(t_2-t_1)\}\{1-\lambda_n(t_1)\}f(t_2-t_1)f(t_1) + \dots \quad (21)$$

where  $t_1, t_2 \dots$  are times of the first, second... unsuccessful encounters. We shall discuss approximations to this rather unwieldy expression for the cases of S, T and F precursors (F: pairs formed by encounters of free radicals with uncorrelated spins).

### 3.1 S precursor

For small radicals both  $\lambda$  and  $|C_{Sn}^S(t)|^2$  will be close to unity so that we may neglect all but the first term in eq.(21). The total fraction of pairs with nuclear state  $n$  that recombines, becomes

$$P_n^S = \int_0^\infty \lambda |C_{Sn}^S(t)|^2 f(t) dt. \text{ This integral can be evaluated with (16a) and (18) giving} \quad P_n^S = \lambda(p - m\pi^{\frac{1}{2}} a_n^2 \omega^{-\frac{3}{2}}) = \lambda(p - x_n) \quad (22)$$

defining  $x_n$ . We have neglected terms of order  $(m^{\frac{1}{2}} a_n^2 p^{-3})$ , which are several orders of magnitude smaller than  $x_n$ . For an estimate of the polarization enhancement we use  $m = 10^{-6} \text{ sec}^{\frac{1}{2}}$ ,  $a_n = 2 \cdot 10^8 \text{ radians/sec}$ ,  $J = 6 \cdot 10^8 \text{ radians/sec}$ , giving  $x_n \sim 4 \cdot 10^{-3}$ . If  $p = \frac{1}{2}$  and the thermal polarization ( $g_N \beta_N H_0 / kT$ ) is  $10^{-5}$ , we find a respectable enhancement of about 800, which is of the order of the largest values that have been found experimentally.

### 3.2 T precursor.

As  $|C_{Sn}^T(t)|^2$  (eq.16b) remains very small we have to consider the effect of the other terms in (21). The largest contributions come from unreactive encounters at times  $t_1, t_2 \dots$  close to zero. Counting only those

contributions, we get for long times (c.f. ref.13c):

$$P_n^T(t) = \frac{1}{3} \lambda |C_{Sn}^T(t)|^2 f(t) (1 + p + p^2 + p^3 + \dots) = \frac{\lambda}{3(1-p)} |C_{Sn}^T(t)|^2 f(t) \quad (23)$$

The factor 1/3 has been included, because only one of the T states is active. The fractional population of product level n becomes:

$$P_n^T = \int_0^\infty P_n^T(t) dt = \frac{\lambda}{3(1-p)} x_n \quad (24)$$

where  $x_n$  (defined in eq.22) enters with a positive sign. From eq.(22) and (24) we find that  $P_n^S - P_m^S = -3(1-p)(P_n^T - P_m^T)$ , so that the polarization is opposite to that of the S case. If we had put  $J = 0$  we would have found  $P_n^T \propto \sqrt{|a_n|}$  a result obtained by Adrian<sup>14</sup>. However, relative line intensities calculated with this form are rather bad in most cases and we get usually much better results when intermediate values of J are used.

### 3.3 F precursor.

The case of uncorrelated free radical encounters is not so straight forward as the S and T cases. During their first encounter a fraction  $\lambda |C_S(0)|^2$  of pairs with  $M_S = 0$  combines and the remainder has a chance of meeting again, thereby giving polarization, because these pairs have more T than S character. Adrian's treatment amounts to multiplying the escaping fraction  $1 - \lambda |C_S(0)|^2$  by  $|C_{Sn}^T(t)|^2$  given in eq.(15) and averaging the result over a distribution of all possible values of  $|C_S(0)|^2$  and  $|C_T(0)|^2$ . We believe that this is not correct. We give a different procedure, the justification of which is given in Appendix B.

The product formed at the first encounter of a pair with uncorrelated spins is not polarized, because the effect of any  $S \rightarrow T$  (or lower  $\rightarrow$  upper level) transitions, that may have occurred before, is canceled by an equal number of  $T \rightarrow S$  (or upper  $\rightarrow$  lower level) transitions.

As half of the first encounter pairs will have  $M_S = 0$ , the fraction that combines is  $\frac{1}{2} \lambda \langle |C_S(0)|^2 \rangle = \frac{1}{2} \lambda$ , because the singlet fraction  $|C_S(0)|^2$  is a random number between 0 and 1, so its mean value is  $\frac{1}{2}$ .

The recombination probability at the next encounter is  $\frac{1}{2}\lambda < |C_{S_n}^F(t)|^2 > f(t)$  where

$$< |C_{S_n}^F(t)|^2 > = \frac{1}{2}\{(1 - \lambda)|C_{S_n}^S(t)|^2 + |C_{S_n}^T(t)|^2\} \quad (25)$$

Eq.(25) is derived in Appendix B;  $|C_{S_n}^S(t)|^2$  and  $|C_{S_n}^T(t)|^2$  are given by eq.(16). As an interpretation of (25) one might say that after a collision the pairs separate behaving partly as singlets and partly as triplets. Taking into account subsequent encounters with  $t_1, t_2, \dots \rightarrow 0$ , we obtain from (21): similarly to the T case

$$P_n^F(t) = \frac{\frac{1}{2}\lambda}{1 - p\{1 - \frac{1}{2}\lambda(1 - \lambda)\}} < |C_{S_n}^F(t)|^2 > f(t). \quad (26)$$

and

$$P_n^F = \frac{1}{2}\lambda + \int_0^\infty P_n^F(t) dt = \frac{1}{2}\lambda \left[ 1 + \frac{1}{1 - p\{1 - \frac{1}{2}\lambda(1 - \lambda)\}} \{p(1 - \lambda) + \lambda x_n\} \right] \quad (27)$$

where we have included the initially formed product. For  $\lambda = 1$ , eq.(27) takes the simple form

$$P_n^F = \frac{1}{2} + \frac{1}{2}(1 - p)^{-1} x_n \quad (28)$$

It is seen that the polarization per molecule of product formed is smaller than for a T precursor, but in contrast to results of other treatments<sup>12,14</sup>, it may become larger than for a S precursor. Qualitatively the polarization is similar to the T case; this is in accord with intuitive predictions by Gerhart and Ostermann<sup>34</sup> and by Closs<sup>9</sup> and with experimental results<sup>9,15b</sup>.

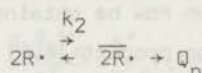
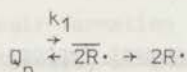
A remark on the viscosity dependence of the polarization seems to be in order. The quantity  $p$  can be estimated by various models<sup>13c</sup>, leading to expressions similar to eq.(19). All models will agree that  $p$  becomes larger (closer to unity) when the viscosity increases, because  $\sigma$  (the diffusion step) decreases. This has been confirmed experimentally in studies on the cage effect<sup>35</sup>. The quantity  $m$  (eq.20) will not be very much affected by viscosity. Consequently our model predicts, that for a S precursor CIDNP intensities will not change very much by changing

viscosity (whereas cage recombination yields may increase). However, polarization in the F and T case is predicted to become larger in more viscous solvents, due to the additional factor depending on  $p$  (in the T case  $(1 - p)^{-1}$ ).

In the remainder of this section the special case of thermal equilibrium is discussed in the light of the diffusion model. Reactions competing with geminate recombination are treated in a subsequent paper<sup>36</sup>.

### 3.4 Thermal equilibrium.

When a dimer (Q) is in thermal equilibrium with its radical monomers, there can be no enhanced polarization according to general thermodynamic principles. Hence polarization originating from geminate recombinations (S case) must be exactly canceled by that of free radical encounters (F case). We have the situation depicted in scheme 1.



Scheme 1

We shall neglect Boltzmann differences and consider the case where the life-time of the radicals is much longer than their relaxation times, so we can neglect polarization in the free radicals. The rate of formation of encounter pairs  $r_2$  is then independent of  $n$ . We can write the steady state condition for the populations of Q:

$$\frac{d}{dt} Q_n = -k_1(1 - P_n^S)Q_n - (Q_n - Q_n^0)T_1^{-1} + P_n^F r_2 = 0$$

$$Q_n = \frac{Q_n^0 + P_n^F r_2 T_1}{(1 - P_n^S)k_1 T_1 + 1} \quad (29)$$

$Q_n^0 = Q^0$  is the equilibrium population of the levels of  $Q$  and  $T_1$  is a relaxation time. We consider the case where  $\lambda = 1$ , because eq.(22) is strictly valid only for this case, so  $P_n^S = p - x_n$  and  $P_n^F$  is given by eq.(28). The steady state assumption imposes a further condition on  $Q^0$ :

$$k_1(1-p)Q^0 = \frac{1}{2}r_2 \quad (30)$$

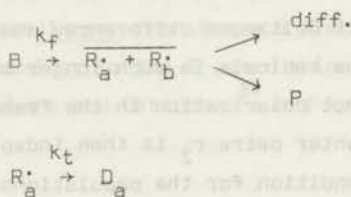
Substituting (22), (28) and (30) in (29) we have the result:

$$Q_n = \frac{r_2}{4(1-p)k_1} \frac{\{1 + (1-p+x_n)k_1T_1\}}{\{1 + (1-p+x_n)k_1T_1\}} = Q^0 \quad (31)$$

and indeed there is no polarization. Thus our model reproduces the expectations made on general thermodynamic grounds for this case. Note that this result (31) would not have been obtained if other forms for  $P_n^F$  had been used<sup>14</sup>.

#### 4. CIDNP Intensities and Enhancement factors.

All relevant quantities can now be obtained from the  $P_n$ , the fractional population of recombination product level  $n$ , calculated in the preceding section. Recombination products (P) and products of radicals that escape the "cage" by diffusion (D products) are treated respectively (see scheme 2.)



Scheme 2

We shall first consider first-order spectra, where the functions  $x_n$  are correct eigenfunctions for the product and afterwards see how second-order effects can be handled.

#### 4.1 Recombination and Disproportionations products (P).

Usually the nmr signal of a quasi-steady state concentration of polarized product is measured. The intensity versus time curve goes through a maximum: it is built up in a time corresponding to the relaxation time of the product,  $T_1^P$  (photochemical reactions) or to the sample warming-up time (thermal reactions) if this time is longer than  $T_1^P$ ; it falls off due to consumption of initiator. The intensity  $I_{mn}$  is proportional to the population difference of levels m and n,  $I_{mn} \propto N_m - N_n$ . The steady state condition for this difference is:

$$\frac{d}{dt}(N_m - N_n) = r_f(P_m - P_n) - \frac{\{(N_m - N_n) - (N_m^0 - N_n^0)\}}{T_{1mn}^P} = 0 \quad (32)$$

$$(N_m - N_n) - (N_m^0 - N_n^0) = r_f T_{1mn}^P (P_m - P_n) \quad (33)$$

$r_f$  is the rate of radical pair formation and  $T_{1mn}^P$  is the nuclear relaxation time of line mn of P (usually in the range 2 - 20 sec). The population difference at thermal equilibrium of the accumulated product at time  $t'$  is:

$$N_m^0 - N_n^0 = \frac{\sum_n^P}{L} \frac{g_N \beta_N H_0}{kT} \int_0^{t'} r_f(t) dt \quad (34)$$

where  $L = \sum_i (2I_i + 1)$ , the total number of levels of P. From (33) and (34) we obtain for the intensity enhancement at the maximum of the curve (at time  $t'$ ):

$$\frac{I_{mn} - I_{mn}^0}{I_{mn}^0} = V_{mn} T_{1mn}^P f \quad (35)$$

$I_{mn}^0$  is the intensity after quenching of the reaction;

$f = r_f(t') / \int_0^{t'} r_f(t) dt$ ;  $V_{mn}$  is the theoretical enhancement factor per molecule P formed, first introduced by Closs<sup>5,37,38</sup>:

$$V_{mn} = \frac{(P_m - P_n)}{\sum_n^P} \frac{LkT}{g_N \beta_N H_0} \quad (36)$$

with  $P_n$  given in eq.(22) and (24). For the S case  $\sum_n P_n = L \lambda p$  for  $x_n \ll p$ , hence

$$V_{mn}^S = \frac{(x_m - x_n)}{p} \cdot \frac{kT}{g_N \beta_N H_0} \quad (37)$$

For the T case:

$$V_{mn}^T = \frac{(x_m - x_n)}{\sum_n x_n} \cdot \frac{kT}{g_N \beta_N H_0} \quad (38)$$

As  $\sum_n x_n$  is of the same order as  $(x_m - x_n)$ , enormous enhancement factors ( $10^4 - 10^5$ ) result from this definition. This is, however, rather meaningless, when there are contributions from intersystem-crossing via other pathways. This difficulty could be avoided by defining an enhancement factor per radical pair formed:

$$V_{mn}' = (P_m - P_n) \frac{kT}{g_N \beta_N H_0} \quad (39)$$

which could be related to the loss of precursor signal intensity,

$I_{mn}(B_0) - I_{mn}(B_t)$ :

$$\frac{I_{mn} - I_{mn}^0}{I_{mn}(B_0) - I_{mn}(B_t)} = V_{mn}' T_{1mn}^P f \quad (40)$$

Unfortunately,  $I(B_0) - I(B_t)$  is often more difficult to obtain experimentally than  $I^0$ , the intensity of a newly formed product.

In photochemical reactions,  $r_f$  is frequently independent of the precursor concentration and the CIDNP signal is constant over an extended time range. In that case  $\int_0^{t'} r_f(t) dt = r_f t'$  and  $f = 1/t'$ ; furthermore if  $I_{mn} \gg I_{mn}^0$ , the relation of  $V_{mn}$  with experimental quantities is particularly simple:

$$V_{mn} = \frac{I_{mn}}{I_{mn}^0} \cdot \frac{t'}{T_{1mn}^P} \quad (41)$$

where  $I_{mn}^0$  is measured at  $t' \gg T_{1mn}^P$ . This form has been used recently

by Lehnig and Fischer<sup>15b</sup>. For thermal reactions (S case) one may use  $f = k_f B_{t'} / (B_0 - B_{t'})$ ,  $B_0$  and  $B_{t'}$  being the precursor concentrations at  $t = 0$  and  $t = t'$ . Eq.(40) then takes the simple form:

$$V'_{mn} = \frac{I_{mn}}{I_{mn}(B_{t'}) T_{1mn}^P k_f} \quad (42)$$

relating  $V'$  with the intensity of a precursor transition at time  $t'$ . This expression (42) can be conveniently used in thermal reactions.

For the F case  $r_f$  is a function of  $k_f B_{t'}$ , radical concentrations and the rate constants for diffusion controlled encounters.

In eq.(32) we have assigned a relaxation time  $T_{1mn}^P$  to every line mn in the spectrum of P. This is a simplification because relaxation cannot generally be described with a single time constant for a transition mn; one should actually solve the coupled relaxation equations, which presents a formidable problem in complex spectra (c.f. ref.39).

Instead one often makes the further simplification of setting  $T_{1mn}^P = T_1^P$  where  $T_1^P$  is an "average" relaxation time, and indeed this procedure can be a serious source of errors, when calculated relative intensities are compared with experimental ones. As is discussed elsewhere<sup>17</sup> this problem is most serious when both net effects and multiplet effects are present and it renders the precise determination of g-values difficult.

#### 4.2 Escape products (D)

We mentioned that radicals escaping from geminate recombination carry a polarization opposite to that of P. Frequently this polarization is transferred to products of radical transfer reactions, but it may also appear in combination products<sup>16</sup>, if it is not overshadowed by F-type polarization. We treat the case where the subsequent reaction can be described with a first order rate constant  $k_t$  (c.f. scheme 2). The steady state condition for the populations of radical a escaping the "cage" is

$$\frac{d}{dt} (R_{ma} - R_{na}) = r_f \{ (1 - P_{ma}) - (1 - P_{na}) \} - (R_{ma} - R_{na}) \{ (T_{1mn}^R)^{-1} + k_t + k_c \} = 0 \quad (43)$$

with  $T_{1mn}^R$ , the relaxation time for transition mn in the radical,  $k_c$  describing all other path by which the radical may disappear and

$$P_{ma} = \sum_{k, M_k}^b P_m \quad (44)$$

where the summation runs over all nuclear states of radical b. Similarly for product D:

$$\frac{d}{dt} (D_{ma} - D_{na}) = k_t (R_{ma} - R_{na}) - \frac{\{ (D_{ma} - D_{na}) - (D_{ma}^0 - D_{na}^0) \}}{T_{1mn}^D} = 0$$

$$(D_{ma} - D_{na}) - (D_{ma}^0 - D_{na}^0) = - \frac{(P_{ma} - P_{na}) r_f k_t T_{1mn}^D}{(T_{1mn}^R)^{-1} + k_t + k_c} \quad (45)$$

where  $(D_{ma}^0 - D_{na}^0)$  is given by

$$D_{ma}^0 - D_{na}^0 = \frac{\sum_n (1 - P_n)}{L_a} \cdot \frac{g_N \beta_N H_a}{kT} \cdot \frac{k_t}{k_t + k_c} \cdot \int_0^t r_f(t) dt \quad (46)$$

Thus we have for the intensity enhancement of D:

$$\frac{I_{mn} - I_{mn}^0}{I_{mn}^0} = V_{mn}^D \frac{(k_t + k_c)}{(1/T_{1mn}^R + k_t + k_c)} f \quad (47)$$

with

$$V_{mn}^D = - \frac{(P_{ma} - P_{na})}{\sum_n (1 - P_n)} \cdot \frac{L_a kT}{g_N \beta_N H_a} \quad (48)$$

By substituting (44) with (22), (24) or (27) formulae for the S, T and F cases are obtained. Comparing eq.(48) with (36) it is seen that D polarization has the opposite sign as to the states of fragment a.

In addition to nuclear relaxation in D, the intensities (47) depend

further on relaxation in the radical, which tends to decrease the polarization in the simple treatment given here. Again the relaxation problem is more complex<sup>40</sup> and as noted in II<sup>10a</sup> there may also be effects due to electron polarization, which might even increase nuclear polarization via cross-relaxation. However, there are not many experimental indications as to the importance of these effects, and it is surprising that eq.(47) with the further assumption of equal relaxation times for different transitions,  $T_{1mn}^D = T_1^D$  and  $T_{1mn}^R = T_1^R$ , often reproduces relative intensities rather well (c.f. figure 2).

Formulae equivalent to (47) have recently been used<sup>15b,16,41</sup> to estimate the magnitude of  $T_1^R$  from CIDNP experiments. Values in the range  $10^{-4} - 10^{-3}$  sec were found, somewhat larger than commonly obtained in esr experiments. The reason may well be that  $T_1^R$  is strongly field dependent, because the correlation times are of the order of  $\omega_S^{-1}$  ( $\omega_S = g\beta H_0 \hbar^{-1} = 6 \cdot 10^{10}$  radians/sec for  $H_0 = 3300G$ ), so that  $T_1^R$  increases in the higher nmr fields.

#### 4.3 Structure of CIDNP spectra.

When  $J^2 \gg a_n^2$  intensities (33) and enhancement factors (36) are proportional to  $a_m^2 - a_n^2$ . We examine this case, because it reveals some features, which remain valid in the more general case. If we look at the spectrum of nucleus *i* of fragment a, and consider a transition from  $m = (\dots M_i, M_j, M_k \dots)$  to  $n = (\dots M_i - 1, M_j, M_k \dots)$  we obtain from (14):

$$I_{mn} \propto (a_m^2 - a_n^2) = \frac{1}{2} A_i [\Delta g \beta_e H_0 \hbar^{-1} + \sum_{j \neq i}^a A_j M_j - \sum_k^b A_k M_k + A_i (M_i - \frac{1}{2})] \quad (49)$$

Except for the last term this expression has also been given by others<sup>27,15,12</sup>. It is instructive to consider the effect of the various terms of (49):

The first term gives rise to a net effect, E or A, depending on the sign of  $\Delta g A_i$  (note that  $\Delta g = g_a - g_b$ , so that this effect is opposite for nuclei of fragments a and b). As long as  $J^2 \gg a_n^2$  for all  $a_n$ , eq. (49) predicts that  $I_{mn}$  increases linearly with the field  $H_0$  ( $V_{mn}$  independent of  $H_0$ ). However, when  $J^2$  is comparable to or smaller than  $a_n^2$ , the theory predicts a decrease of  $I_{mn}$  for higher fields (c.f. ref.1).

Thus there will be a maximum<sup>42</sup> in the curve of  $I_{mn}$  versus  $H_0$ .

The second term gives the multiplet effect: it depends on the sign of  $A_i A_j M_j$  and in a multiplet of nucleus  $i$  coupled to  $j$ , the lines are labeled according to  $M_j = I_j, -I_j + 1, \dots, +I_j$ . The "Phase" of the multiplet effect (E/A or A/E) depends further on the absolute sign<sup>43</sup> of the coupling constant  $J_{ij}$ , because this determines, whether lines with positive  $M_j$  appear low or high field in the multiplet of  $i$ .

The third term gives a multiplet effect of opposite phase, for coupling of  $i$  to a nucleus of radical  $b$ . As to the field dependence of multiplet effects,  $I_{mn}$  is independent of  $H_0$  and  $V_{mn} \propto (H_0)^{-1}$ .

The last term is of no importance in pure first order spectra, because transitions with  $M_i > \frac{1}{2}$  and  $M_i < \frac{1}{2}$  are degenerate and the effects cancel. However, in spectra exhibiting second order effects (which is common in case of proton nmr) polarization due to this term appears. For instance, consider the A lines in  $A_n B$  spectra. If  $I_B = \frac{1}{2}$  and  $n > 1$  several transitions contribute to the A "doublet" and the degeneracy of these transitions is always lifted in such a way<sup>44</sup> that transitions with  $M_i > \frac{1}{2}$  appear inside and with  $M_i < \frac{1}{2}$  outside the "doublet" or vice versa depending on the sign of  $J_{AB}$ . Thus the lines of the doublet acquire e.g. A/E and E/A character, irrespective as to whether nucleus B was present in the pair or not. This might be called a "second order" multiplet effect, which may be superimposed on a "first order" multiplet effect. Examples hereof are given below (c.f. fig.3 and 4).

For D products we find, carrying out the summation of eq.(44):

$$P_{ma} - P_{na} = - \frac{\lambda m \pi^{\frac{1}{2}}}{\omega^{3/2}} \frac{1}{2} A_i \{ \Delta g \beta_e H_0 \mathcal{H}^{-1} + \sum_{j \neq i}^a A_j M_j + A_i (M_i - \frac{1}{2}) \} L_b \quad (50)$$

and as  $\sum_n (1 - P_n) = L(1 - \lambda p)$  and  $L = L_a L_b$  we have for the S case:

$$V_{mn}^D = - \frac{\lambda}{(1 - \lambda p)} \frac{m \pi^{\frac{1}{2}}}{\omega^{3/2}} \frac{kT}{g_N \beta_N H_0} \frac{1}{2} A_i \{ \Delta g \beta_e H_0 \mathcal{H}^{-1} + \sum_{j \neq i}^a A_j M_j + A_i (M_i - \frac{1}{2}) \} \quad (51)$$

Thus  $D_a$  product polarization is not affected by the presence of nuclei in radical  $b$ . Incidentally eq.(51) shows that if there is no recombination ( $\lambda = 0$ ) the D product is not polarized.

We may now give a summary of the predictions of radical pair theory for high field CIDNP spectra:

1. S precursor polarization is opposite to polarization of T and F precursors.
2. D product polarization is opposite to polarization in P products. Spectra of fragment  $D_a$  are independent of the presence of nuclei in radical  $b$ .
3. Net effect  $\propto \Delta g A_i$ . Sign is different for nuclei of fragment  $a$  and  $b$ .
4. Multiplet effect  $\propto A_i^a A_j^a$  or  $\propto -A_i^a A_k^b$ . Sign depends further on the sign of  $J_{ij}$  and  $J_{ik}$ .
5. "Second order" multiplet effects may appear in spectra of magnetically equivalent nuclei, even when coupled to a nucleus not present in the radical pair. Sign depends on the sign of  $J_{ij}$  but not on the sign of  $A_i$ .

#### 4.4 Simple Rules.

The first four results can be taken together in two rules containing all sign reversals. Qualitative features of CIDNP spectra can be described with the signs of two quantities,  $\Gamma_{ne}$  for net effects, and  $\Gamma_{me}$  for multiplet effects:

$$\Gamma_{ne} = \mu \epsilon \Delta g A_i \quad \begin{cases} + & : A \\ - & : E \end{cases} \quad (52a)$$

$$\Gamma_{me} = \mu \epsilon A_i A_l J_{il} \sigma_{il} \quad \begin{cases} + & : E/A \\ - & : A/E \end{cases} \quad (52b)$$

where it is to be understood that the spectrum of nucleus  $i$  of fragment  $a$  is considered.  $\mu$ ,  $\epsilon$  and  $\sigma_{il}$  are labels indicating precursor multiplicity, P or D product and presence of  $i$  and  $l$  in the same or different radicals:

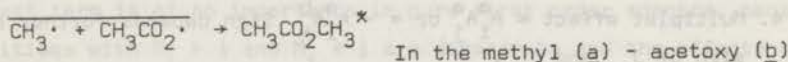
$$\mu = \begin{cases} + & \text{for T and F precursor} \\ - & \text{for S precursor} \end{cases}$$

$$\epsilon \begin{cases} + & \text{for P products (recombination).} \\ - & \text{for D products (escape).} \end{cases}$$

$$\sigma_{il} \begin{cases} + & \text{when i and l reside in the same radical} \\ - & \text{when i and l reside in different radicals} \end{cases}$$

It is a striking fact that in almost all cases, where reaction conditions are unambiguous, CIDNP spectra can be qualitatively explained by the two simple rules (52). We have found them quite useful for instant determination of precursor multiplicities, signs of hf. parameters etc. from the spectra. The use of these rules will be illustrated with two examples:

- (i) Methyl acetate formed during thermal decomposition of acetyl peroxid was reported<sup>4</sup> to show emission for the methoxy group:

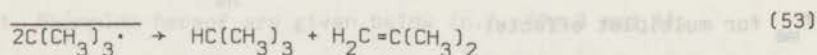


radical pair, the acetoxy radical undoubtedly has the larger g-value, due to the presence of the oxygen atoms, so  $\Delta g$  is negative.

$A_1$  is also negative in the methyl radical and we are looking at a recombination product from a singlet precursor, so

$\Gamma_{ne} = - + - - = -$ , hence E. For the D product, methylchloride we have all minus signs, hence A.

- (ii) From the decomposition of a cyclohexadienone peroxide<sup>4</sup> two t-butyl radicals are formed, which disproportionate to give isobutane and isobutene, both showing E/A multiplet effects:



For the t-butyl radical A is positive. In isobutane  $J_{11}$  is positive and the methine H is abstracted from the other radical so

we have  $\Gamma_{me} = - + + + - = +$ , E/A. For isobutene  $J_{11}$  is negative<sup>45</sup> and the splitting is due to protons of the same fragment, giving

$\Gamma_{me} = - + + + - + = +$ , hence also E/A (but for different reasons).

When a small multiplet effect is superimposed on a large net effect, rule (52b) may break down, because the apparent multiplet effect may be reversed. In that case and in the case of strongly coupled spectra it is better to employ computer simulation techniques.

#### 4.5 Second order spectra and computer simulation.

When chemical shift differences are not much larger than the coupling constants  $J_{ij}$ , second order effects appear in nmr spectra. The functions  $\chi_n$  are then not eigenfunctions of the nuclear Hamiltonian of the product:

$$\underline{H}_P = \sum_i h_i I_{iz} + \sum_{i < j} J_{ij} I_{iz} \cdot I_{jz} \quad (54)$$

where  $h_i$  are chemical shifts relative to a reference signal. To describe the spectrum the eigenvalues  $\Omega_\nu^P$  of  $\underline{H}_P$  are obtained by the transformation:

$$\underline{S}^{-1} \underline{H}_P \underline{S} = \underline{Q}^P \quad (\underline{Q}^P \text{ diagonal}) \quad (55)$$

The eigenfunctions are:

$$\chi_\nu = \sum_n S_{n\nu} \chi_n \quad (56)$$

Line frequencies are given by  $\Omega_\mu^P - \Omega_\nu^P$  and relative intensities by  $^{46}$

$$I_{\mu\nu} \propto |\langle \chi_\mu | \sum_i \gamma_i I_{xi} | \chi_\nu \rangle|^2 (P_\mu - P_\nu) \quad (57)$$

The populations  $P_\nu$  of the mixed states are calculated from the projections of  $\phi_n(t)$  (eq.12) on the state  $\chi_\nu$

$$|C_{S\nu}(t)|^2 = \sum_n |\langle S_{X\nu} | \phi_n(t) \rangle|^2 = \sum_n S_{n\nu}^2 |C_{Sn}(t)|^2 \quad (58)$$

where the last step follows from (56) and the orthogonality of the  $\chi_n$ . Along the lines of sections 3 this leads to

$$P_\mu - P_\nu = \sum_n (S_{n\mu}^2 - S_{n\nu}^2) P_n \quad (59)$$

with  $P_n$  given by (22), (24) or (27) for S,T and F cases. A nmr spectrum simulation program was modified  $^{47}$  by incorporating (57) with (59) for relative CIDNP intensities. A few examples of computer simulations are shown below.

5. Examples.

5.1 Ethylchloride at 15.1 Mc.

The 100 Mc CIDNP spectrum of the thermal decomposition of propionyl peroxide (PPD) in hexachloroacetone has been given in I<sup>4</sup>. The spectrum shows A/E and E/A multiplet effects for ethylchloride and butane respectively and is in accord with the formation of two ethyl radicals (R) giving the reactions:

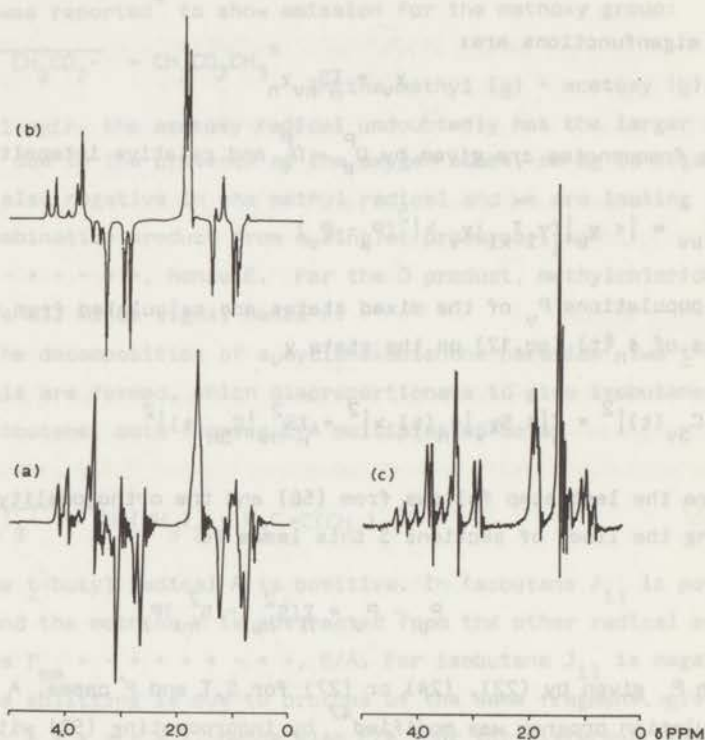
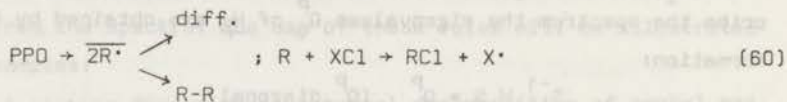


Figure 2 (a) 15.1 Mc nmr spectrum obtained during thermal decomposition of propionyl peroxide in hexachloroacetone, (b) computer simulated spectrum of ethylchloride and (c) normal 15.1 Mc spectrum of ethylchloride.

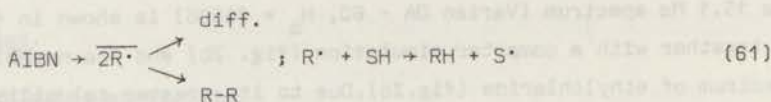
The 15.1 Mc spectrum (Varian DA - 60,  $H_0 = 3550G$ ) is shown in figure 2a together with a computer simulation (fig. 2b) and the normal 15 Mc spectrum of ethylchloride (fig. 2c). Due to its greater solubility at the temperature of the reaction ( $110^{\circ}$ ), ethylchloride appeared much stronger in the 100 Mc spectrum than butane; this is even more pronounced at 15.1 Mc because of cancelation of opposite polarization effects in nearly degenerate butane lines, so the spectrum of figure 2a is almost completely that of ethylchloride. The enhancement factor is  $2500 \pm 1000$  (difficult to estimate for gases). It is about a factor 7 larger than at 100 Mc as expected for multiplet effects. The hf. coupling constants of the ethyl radical are  $A(CH_3) = 26.9 G$ ,  $A(CH_2) = -22.4 G$ . For the simulated spectrum the best fit was obtained with  $|J| = 6 \cdot 10^8$  radians/sec, but higher values did not change the spectrum dramatically. Values of  $|J| < 10^8$  radians/sec gave worse results. Differences in relaxation times were not taken into account. The agreement with experiment is satisfactory, the largest deviations occurring in the region around 1 ppm, where butane may contribute (fig. 2a). The following can be inferred from the good agreement:

- (i)  $S-T_{\pm}$  transitions do not contribute to the polarization. This was observed in several other systems run at 15 Mc as well. So these transitions are certainly unimportant in the higher field (14 and 23.5 kG), where CIDNP spectra are usually recorded.
- (ii) Relaxation effects in the radical are probably not important.
- (iii) Relaxation in the product also does not affect relative intensities in this case.

Lines involving transitions between isolated levels, such as the strong line at 1.47 ppm, are expected to have a longer  $T_1$  than others. This line, however, has completely vanished in a pure multiplet spectrum, because it has  $M_j = 0$ . If the mean time for escape of gaseous products from the sample is shorter than  $T_1^0$ , there would also be little dependence on relaxation.

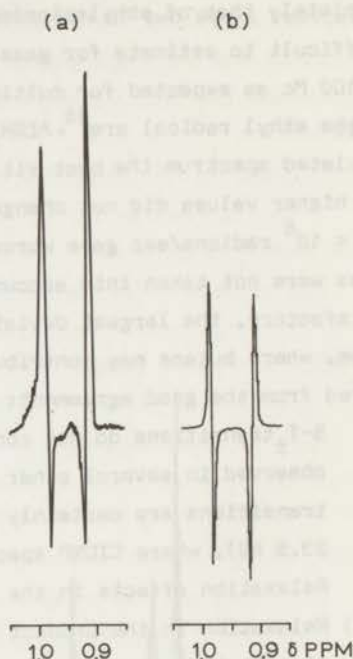
## 2-Cyanopropane

The 100 Mc spectrum (Varian HA - 100 spectrometer) shown in figure 3a, is obtained during thermal decomposition of azo-bisisobutyronitril (AIBN) in thiophenol (SH). The reactions are:



where  $\text{R}\cdot = (\text{CH}_3)_2\dot{\text{C}}\text{CN}, A(\text{CH}_3) = 20.3 \text{ G}^{49}$  and RH is 2-cyanopropane, normally giving a somewhat broadened doublet for the methyl groups at 0.95 ppm.

Figure 3 (a) 100 Mc nmr spectrum obtained during thermal decomposition of azo-bisisobutyronitril in thiophenol and (b) computer simulated spectrum of 2-cyanopropane.



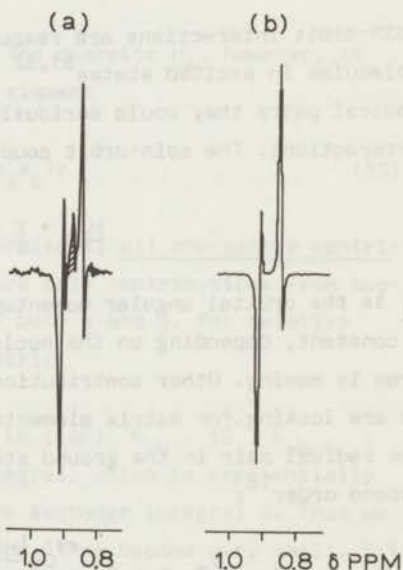
According to simple first order arguments one would not expect polarization at all, because the splitting of the equivalent methyl groups is due to a proton not present in the pair. So we have a case of a pure second order multiplet effect of the type discussed in section 4.3, caused by the term  $A_i^2(M_i - \frac{1}{2})$  in eq.(49). The "Phase" is such as expected for an  $A_B B$  spectrum of a D product with positive  $J_{AB}$ , as can be seen from the computer simulation (fig.3b). The experimental spectrum seems to have A character, but this is due to underlying unpolarized product, the enhancements being not very large in this case. The abstracted proton did not show polarization. Neither this nor other cases

provide indications of polarization resulting from a transfer reaction itself<sup>34</sup>. Emission of chloroform ascribed to such a process<sup>12,50</sup> is better explained by a radical disproportionation reaction (F-case) of  $\text{CCl}_3$  with alkyl radicals.

### 5.3 Isobutane

In I<sup>4</sup> we studied a reaction involving a pair of *t*-butyl radicals,  $A(\text{CH}_3) = 22.7 \text{ G}^{48}$ , reaction (53). The 100 Mc spectrum of the isobutane methyl groups is presented in figure 4a.

Figure 4 (a) High field part of 100 Mc nmr spectrum of isobutane, formed from disproportionation of *t*-butyl radicals. The shaded signal is due to the precursor. (b) computer simulation.



Superimposed on the E/A doublet is a second order multiplet effect, not to be confused with wiggles. The sign is opposite to that of figure 3, because isobutane is a P product. The simulated spectrum of figure 4b reproduces both of these effects. It may be noted that for the problem of two *t*-butyl radicals (20 spins!) the use of magnetic equivalence factoring is imperative.

## Conclusion.

Radical pair theory can account for the coarse structure of CIDNP spectra, as well as for details of complex spectra.

## APPENDIX A

### Spin-Orbit Coupling in Radical Pairs.

Spin-orbit interactions are responsible for intersystem-crossing in molecules in excited states<sup>51,52</sup>. If they were equally important in radical pairs they could seriously detract from the effects of the hf. interactions. The spin-orbit coupling Hamiltonian may be written

$$\underline{H}_{LS} = \sum_i \zeta_i \underline{L}_i \cdot \underline{S}_i \quad (A1)$$

$\underline{L}_i$  is the orbital angular momentum operator for electron  $i$  and  $\zeta_i$  is a constant, depending on the nucleus, in the field of which the electron is moving. Other contributions to  $\underline{H}_{LS}$  are usually negligible<sup>51,52</sup>. We are looking for matrix elements  $\underline{H}_{ST}$  connecting S and T states of the radical pair in the ground state electronic configuration. Up to second order<sup>18</sup>:

$$\underline{H}_{ST} = \langle \Psi_{OS} | \underline{H} | \Psi_{OT} \rangle - \sum_j \frac{\langle \Psi_{OS} | \underline{H} | \Psi_j \rangle \langle \Psi_j | \underline{H} | \Psi_{OT} \rangle}{E_j - E_0} \quad (A2)$$

where  $\Psi_{OS}$  and  $\Psi_{OT}$  are ground state singlet and triplet wave functions (space and spin) and  $\underline{H}$  is the full Hamiltonian of eq.(1). There are no first order contributions of  $\underline{H}_{LS}$  because this term mixes the ground state only with excited configurations. In second order the combined effects of  $\underline{H}_{LS}$  and  $\underline{H}_{HL}$  leads to deviations of the g-values from the free electron value ( $\Delta g$  term), which have already been considered. Furthermore we have to worry about terms involving  $\underline{H}_{LS}$  and  $\underline{H}_a$  (eq.2) because these may become relatively large:

$$\underline{H}_{ST} = - \sum_j \frac{\langle \psi_{OS} | \underline{H}_{LS} | \psi_{jT} \rangle \langle \psi_{jT} | \underline{H}_e | \psi_{OT} \rangle}{E_j - E_0} \quad (A3)$$

Consider a pair of radicals a and b with localized electrons. The angular momentum operators  $L_{ui}^a$  ( $u = x, y, z$  at centre a) are axial vectors, that are antisymmetric with respect to reflection in a plane that contains the axis  $u$ . Hence  $L_{ui}^a$  mixes only symmetric ( $\sigma$ ) with antisymmetric ( $\alpha$ ) states (local space symmetry at a). We need only consider one-centre contributions of  $L_{ui}^a$ ; if the wave functions are labeled according to their spacial symmetry by  $x_a x_b$  ( $x_a = \sigma$  or  $\alpha$ ), non-vanishing matrix elements of  $\underline{H}_{LS}$  are

$$\langle \psi_{OS}(\sigma_a x_b) | L_{ui}^a S_i | \psi_{jT}(\alpha_a x_b) \rangle \quad (A4)$$

and similar expressions for centre b. The operator  $\underline{H}_e$ , however, is symmetric. Therefore, when its matrix element

$$\langle \psi_{jT}(\alpha_a x_b) | \underline{H}_e | \psi_{OT}(\sigma_a x_b) \rangle \quad (A5)$$

is expanded in integrals over atomic orbitals, all one-centre contributions vanish by symmetry and there are only contributions from two-centre integrals involving orbitals of both a and b, for relative orientations such that  $x_b$  is non-symmetric.

The order of magnitude of  $\underline{H}_{ST}$  in (A1) is  $\zeta(\Delta E)^{-1} K_{ab} - 10^{-3} K_{ab}$  where  $K_{ab}$  is an electron repulsion integral, which is exponentially dependent on distance, similarly to the exchange integral  $J$ . Thus we conclude that at distances  $r > r_0$ , where  $J$  has become very small, S-T mixing by spin-orbit coupling of the type discussed here will be negligible. At short distances it might become relatively more important.

## APPENDIX B

### Free Radical Encounters.

We wish to examine the process of product forming encounters of free radicals with initially uncorrelated spins. We make use of evolution operators  $U(t, t_0)$  to describe the time-evolution of wave functions<sup>53</sup>:

$$\Psi(t) = U(t, t_0) \Psi(t_0) \quad (B1)$$

Considering only  $M_S = 0$  encounters (others are inactive) we start with

$$\Psi(0) = C_S(0) \Psi_{OS} + C_T(0) \Psi_{OT} \quad (B2)$$

where  $\Psi_{OS}$  and  $\Psi_{OT}$  are the same as in Appendix A (space and spin functions). The wave function after an encounter of duration  $t_0$  is

$$\Psi(t_0) = U_{enc}(t_0) \Psi(0) = e^{-i \int_0^{t_0} H_{enc}(t) dt} \Psi(0) \quad (B3)$$

where  $H_{enc}$  represents the Hamiltonian during the encounter, describing the process of product formation by energy transfer to surrounding solvent molecules, which we do not consider explicitly. When product formation occurs only from the singlet state, the action of  $U_{enc}$  on  $\Psi_{OS}$  and  $\Psi_{OT}$  can be described as follows:

$$U_{enc}(t_0) \Psi_{OS} = e^{-i\alpha} (1 + \eta^2)^{-1/2} [\Psi_{OS} + \eta \Psi_{PS}] \quad (B4a)$$

$$U_{enc}(t_0) \Psi_{OT} = e^{-i\beta} \Psi_{OT} \quad (B4b)$$

where  $\Psi_{PS}$  represents a lower vibrational state of the product and  $\alpha$  and  $\beta$  are phase angles. After the encounter  $\Psi(t)$  is given by (B1) with  $U = U_{RP}(t, t_0)$ , describing S-T mixing in the radical pair. In terms of the evolution operator the coefficients of eq.(16) are:

$$C_S^S(t) = \langle \Psi_{OS} | U_{RP}(t, t_0) | \Psi_{OS} \rangle \quad (B5a)$$

$$C_S^T(t) = \langle \Psi_{OS} | U_{RP}(t, t_0) | \Psi_{OT} \rangle \quad (B5b)$$

where we have suppressed the label  $n$ . The fraction that gives product during the first encounter is:

$$|\langle \Psi_{PS} | \Psi(t_0) \rangle|^2 = \frac{\eta^2}{1 + \eta^2} |C_S(0)|^2 = \lambda |C_S(0)|^2 \quad (B6)$$

where we have used the orthogonality  $\langle \Psi_{PS} | \Psi_{OS} \rangle = 0$ . Using (B1 - 5) the

quantity of interest,  $|c_S^F(t)|^2$  can be obtained:

$$c_S^F(t) = \langle \psi_{OS} | \psi(t) \rangle = e^{-i\alpha} (1 + \eta^2)^{-\frac{1}{2}} c_S^S(0) c_S^S(t) + e^{-i\beta} c_T(0) c_S^T(t) \quad (B7)$$

$$|c_S^F(t)|^2 = (1 + \eta^2)^{-1} |c_S^S(0)|^2 |c_S^S(t)|^2 + |c_T(0)|^2 |c_S^T(t)|^2 + e^{i\gamma} (1 + \eta^2)^{-\frac{1}{2}} c_S^*(0) c_S^S(t) c_T(0) c_S^T(t) + \text{c.c.} \quad (B8)$$

where  $\gamma = \alpha - \beta$  and c.c. denotes complex conjugate. The last two terms of (B8) vanish when this expression is averaged over the random phases of  $c_S^S(0)$ ,  $c_T(0)$  and  $\gamma$ . Averaging also over all possible values of  $|c_S^S(0)|^2$  and  $|c_T(0)|^2$  and using the identity  $(1 + \eta^2)^{-1} = 1 - \lambda$  (from B6) we obtain:

$$\langle |c_S^F(t)|^2 \rangle = \frac{1}{2} [(1 - \lambda) |c_S^S(t)|^2 + |c_S^T(t)|^2] \quad (B9)$$

This expression has been used in section 3.

Footnotes.

- 1.(a) J. Bargon, H. Fischer and U. Johnsen,  
Z. Naturforsch., 22a; 1551 (1967);  
(b) J. Bargon and H. Fischer, ibid. 22a, 1556 (1967).
- 2.(a) H.R. Ward and R.G. Lawler, J. Amer. Chem. Soc., 89, 5518 (1967);  
(b) R.G. Lawler, ibid. 89, 5519 (1967).
- 3.(a) A.R. Lepley, ibid. 90, 2710 (1968);  
(b) A.R. Lepley, ibid. 91, 749 (1969).
4. R. Kaptein, Chem. Phys. Letters, 2, 261 (1968).
- 5.(a) G.L. Closs and L.E. Closs, J. Amer. Chem. Soc., 91, 4549, 4550 (1969)  
(b) G.L. Closs, ibid. 91, 4552 (1969);  
(c) G.L. Closs and A.D. Trifunac, ibid. 91, 4554 (1969).
6. R. Kaptein, J.A. den Hollander, D. Antheunis and L.J. Oosterhoff,  
Chem. Comm., 1687 (1970).
- 7.(a) H.R. Ward, R.G. Lawler, H.Y. Loken and R.A. Cooper,  
J. Amer. Chem. Soc. 91, 4928 (1969);  
(b) M. Lehnig and H. Fischer, Z. Naturforsch., 24a, 1771 (1969).
8. H. Fischer, J. Phys. Chem., 73, 3834 (1969).
9. G.L. Closs and A.D. Trifunac, J. Amer. Chem. Soc., 92, 2183,  
2186 (1970).
- 10.(a) R. Kaptein and L.J. Oosterhoff, Chem. Phys. Letters, 4 195 (1969);  
(b) R. Kaptein and L.J. Oosterhoff, ibid., 4, 214 (1969).
11. H.R. Ward, paper presented at the 159th National Meeting of  
the American Chemical Society (Houston, Feb. 1970).
12. H.R. Ward and R.G. Lawler, Accounts Chem. Research, to be  
published.
- 13(a) R.M. Noyes, J. Chem. Phys., 22, 1349 (1954);  
(b) R.M. Noyes, J. Amer. Chem. Soc., 77, 2042 (1955);  
(c) R.M. Noyes, ibid., 78, 5486 (1956);  
(d) R.M. Noyes, "Progress in Reaction Kinetics", ed. G. Porter,  
Pergamon, Oxford, Vol. 1, 1961, pp 129 - 160.
14. During the preparation of this paper F.J. Adrian informed us  
that he also has applied this type of kinetics to the CIDNP  
problem. In some respects our treatment differs from his.  
c.f. F.J. Adrian, J. Chem. Phys., 53, 3374 (1970).
- 15.(a) H. Fischer, Z. Naturforsch., 25a, 1957 (1970);

- 15.(b) M. Lehnig and H. Fischer ibid., p. 1963.
16. G.L. Closs and A.D. Trifunac, J. Amer. Chem. Soc., 92, 7227 (1970).
17. R. Kaptein and J.A. den Hollander, to be published.
18. K. Itoh, H. Hayashi and S. Nagakura, Mol. Phys., 17, 561 (1969).
19. The VB theory describes the process of homolytic dissociation quite well, because it takes account of electron correlation. In MO theory also exchange integrals appear (difference between excited S and T configurations). However, MO theory without extensive configuration interaction gives a very unreliable description at large separations<sup>20</sup> so that arguments derived from MO theory<sup>21</sup> are not suitable to deduce the sign of J, also because we are interested in S and T states of the ground state electronic configuration of the radical pair. The nature of the excited state of the precursor ( e.g. in photochemical reactions) does not seem relevant except for its multiplicity.
20. C.A. Coulson, "Valence", Oxford University Press, 1961, p. 156.
21. H. Fischer, Chem. Phys. Letters, 4, 611 (1970).
22. C. Herring and M. Flicker, Phys. Review, 134, A362 (1964).
23. J.N. Murrell and J.J.C. Teixeira - Dias, Mol. Phys., 19, 521, (1970).
24. H. Hirota and S.I. Weissman, J. Amer. Chem. Soc., 86, 2538 (1964).
25. P. Ferruti, D. Gill, M.P. Klein, H.H. Wang, G. Entine and M. Calvin, ibid., 92, 3704 (1970).
26. The Landau-Zener formula (c.f. E.E. Nikitin, in "Chemische Elementarprozesse", ed. H. Hartmann, Springer, Berlin, 1968, pp 43-77) which gives time-proportional transition probabilities is unreliable for short times or high velocities, c.f. D.R. Bates, Proc. Roy. Soc. A, 257, 22 (1960).
27. S.H. Glarum, personal communication.
28. A. Carrington and A.D. McLachlan, "Introduction to Magnetic Resonance", Harper and Row, New York, 1967 chap. 9.
29. P.W. Atkins and D. Kivelson, J. Chem. Phys., 44, 169 (1966).
30. For a recent review see J.K. Thomas in "Annual Review of Physical Chemistry" ed. H. Eyring, Annual Reviews Inc., Palo Alto, Cal, 1970, pp 17 - 38.
31. R.F. Vassil'ev, Makromol. Chem., 126, 231 (1969).

32. R. Kaptein, M. Fräter-Schröder and L.J. Oosterhoff, to be published.
33. S. Chandrasekhar, Revs. Modern Phys., **15**, 1 (1943).
34. F. Gerhart and G. Ostermann, Tetrahedron Letters, 4705 (1969).
35. c.f. O. Dobis, J.M. Pearson and M. Szwarc, J. Amer. Chem. Soc., **90**, 278, 1968.
36. R. Kaptein, to be published.
37. Closs<sup>5</sup> actually used  $V_{mn} = (P_m - P_n)/(P_m + P_n) \langle I_z \rangle_0$ , which does not seem to be properly normalized. For the S case both definitions amount to the same.
38. The enhancement factor  $V_{max}^1$ , introduced by Fischer<sup>1</sup>, is  $V_{max} = (I_{mn} - I_{mn}^0)/I_{mn}^0$ . Previously<sup>4,10b</sup> we have used this definition.
39. R. Freeman, S. Wittekoek and R.R. Ernst, J. Chem. Phys., **52**, 1529 (1970).
40. c.f. J.H. Freed and G.K. Fraenkel, J. Chem. Phys., **39**, 326 (1963).
41. G.L. Closs and D.R. Paulson, J. Amer. Chem. Soc., **92**, 7229 (1970).
42. This has actually been observed for benzene formed during decomposition of benzoyl peroxide (H. Fischer and M. Lehnig, personal communication).
43. Whereas normal nmr spectra are unaffected by a simultaneous change in sign of all  $J_{ij}$ , the CIDNP spectrum in the case of a pure multiplet effect ( $\Delta g = 0$ ) is completely reversed. The proof is easily given by an extension of the proof given by Corio for normal spectra (ref.44, p 167), by noting that the populations  $N_m \propto a_m^2$  in this case are invariant to a change in sign of all  $M_i, M_j$ , because  $a_m^2$  is a bilinear form in  $M_i M_j$ .
44. P.L. Corio, "Structure of High-Resolution NMR Spectra", Academic Press, New York, 1966, p.208.
45. J.W. Emsley, J. Feeney and L.H. Sutcliffe, "High Resolution NMR Spectroscopy" Pergamon Press, Oxford, Vol 2, 1966, chap.10.
46. P.L. Corio, loc. cit., p.164.
47. We thank Dr. C.W. Haigh for a listing of LAME, a program employing magnetic equivalence factoring. We are indebted to Mr. J.A. den Hollander for making the modification.
48. R.W. Fessenden and R.H. Schuler, J. Chem. Phys., **39**, 2147 (1963).
49. S.A. Weiner and G.S. Hammond, J. Amer. Chem. Soc., **91**, 986 (1969).

50. A.L. Buchachenko, S.V. Rykov and A.V. Kessenick, Zh. Fiz. Khim., 44, 876 (1970).
- 51.(a) H.F. Hamerka and L.J. Oosterhoff, Mol. Phys., 1, 358 (1958);  
 (b) H.F. Hamerka in "The Triplet State", ed. A. Zahlan, Cambridge University Press, 1967, p.2.
- 52.(a) J.H. van der Waals and M.S. de Groot, ibid., p.101  
 (b) W.S. Veeman and J.H. van der Waals, Mol. Phys., 18, 63 (1970).
53. A. Messiah, "Quantum Mechanics", North Holland Publishing Cy., Amsterdam, 1967, Vol.1, p.310.

## CHAPTER IX

### CHEMICALLY INDUCED DYNAMIC NUCLEAR POLARIZATION IX REACTIONS COMPETITIVE WITH GEMINATE RECOMBINATION OF RADICAL PAIRS.

By R. Kaptein

Department of Theoretical Organic Chemistry,  
University Leiden, P.O. Box 75, Leiden,  
The Netherlands.

#### 1. Introduction

Potentially CIDNP is an extremely useful tool for the study of fast reactions that compete with geminate recombination of radical pairs. It is the purpose of this paper to give a discussion of polarization effects in the case of competitive reactions, by an extension of a diffusion model for CIDNP given previously in VIII<sup>1</sup>. This model<sup>2</sup> is based on the assumption of random walk diffusion of radical pairs<sup>3</sup>.

We shall consider radical transformations, such as fragmentations (e.g. decarboxylation of acyloxy radicals), rearrangements (e.g. cyclopropyl-carbinyl  $\rightarrow$  butenyl<sup>4</sup>) and fast scavenging by transfer reactions.

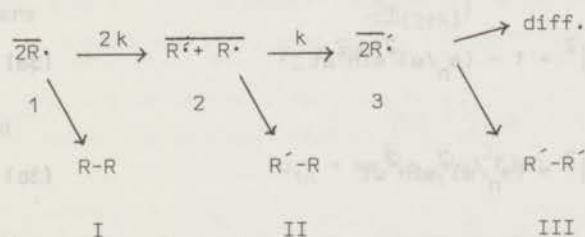
When one of the radicals of a pair undergoes a transformation, a new pair is formed, which continues the random walk and has a certain chance of recombination as well. Because of the very short time needed for the actual process of the transformation ( $10^{-13}$ - $10^{-12}$  sec), spin-correlation of the pair will not be destroyed during this process; it could only be

destroyed by magnetic interactions which have a much longer time-scale. Thus, if a pair is in the singlet (S) state just before the reaction of one of its members, the new pair will also start as a S-pair. This is important, because it implies that CIDNP effects can be expected for products of the secondary pair and of other subsequent pairs with a common precursor. A detailed discussion of this is given in section 2. The special case of stereospecificity and CIDNP during homolytic rearrangements where "reaction" is reorientation of a fragment, is treated separately (section 3). A few experimental examples are discussed in section 4.

## 2. Theory

### 2.1 Competitive Reactions.

We consider the general reaction sequence of scheme 1, where  $k$  is the unimolecular rate constant for the reaction  $R\cdot \rightarrow R'.$



Scheme 1.

The bar indicates pairs with correlated spins ("cage" in the extended sense). Radical pairs will be denoted  $P_1, P_2, P_3$  and products by  $P_I, P_{II}, P_{III}$ . We will examine what the conditions are under which polarization occurs in these products. Necessary conditions for product formation from a certain pair are (i) that the pair exists, (ii) that there is a reencounter and (iii) that the pair is in the singlet state. If no recombination occurred, the probability that the pair, born at  $t = 0$ , is present as pair 1, 2 or 3 at time  $t$  is

$$P_1(t) = e^{-2kt} \quad (1a)$$

$$P_2(t) = 2(1 - e^{-kt})e^{-kt} \quad (1b)$$

$$P_3(t) = (1 - e^{-kt})^2 \quad (1c)$$

and of course we have  $P_1(t) + P_2(t) + P_3(t) = 1$ . The probability of a first reencounter at time  $t$  after separation at  $t = 0$  is<sup>3</sup>

$$f(t) = \frac{-3}{2} \frac{\pi m^2}{p^2 t} e^{-\frac{3}{2} \frac{\pi m^2}{p^2 t}} \quad (2)$$

where  $m$  has a value of about  $10^{-6} \text{ sec}^{\frac{1}{2}}$  and  $p = \int_0^{\infty} f(t) dt$  is the probability of at least one reencounter;  $\frac{1}{2} < p < 1$ .

Furthermore, our model for S-T mixing in radical pairs<sup>1,5,6</sup> leads to the following expressions for the probability of the pair with nuclear state  $n$  being in the S-state:

$$|c_{Sn}^S(t)|^2 = 1 - (a_n/\omega)^2 \sin^2 \omega t \quad (3a)$$

$$|c_{Sn}^T(t)|^2 = (a_n/\omega)^2 \sin^2 \omega t \quad (3b)$$

where the superscripts denote the precursor multiplicities;  $a_n$  is the S-T<sub>0</sub> mixing matrix element and  $\omega = (J^2 + a_n^2)^{\frac{1}{2}}$ , with the exchange integral  $J$  (we suppress the label  $n$  for  $\omega$ ).

If probabilities for both S-T<sub>0</sub> mixing and product formation are small, we may treat these processes and the competing reaction independently. The probability of recombination at time  $t$  is then a product of the probabilities (1), (2), (3) and  $\lambda$ , the chance of reaction during a singlet encounter. The cases of S and T precursors are now treated respectively.

## 2 S precursor.

In this case the fraction of pairs with nuclear state  $n$ , present as

pair 1 in the S state will be

$$P_{1Sn}(t) = |C_{1Sn}^S(t)|^2 e^{-2kt} \quad (4)$$

and the (fractional) population of level n of product I is

$$P_{In} = \int_0^{\infty} \lambda_I P_{1Sn}(t) f(t) dt.$$

Evaluating this integral (Laplace transform) with eq.(2), (3) and (4) we obtain

$$P_{In} = \lambda_I p e^{\frac{-2m(2\pi k)^{\frac{1}{2}}}{p} - \frac{1}{2} \lambda_I p (a_{1n}/\omega)^2} \left[ e^{\frac{-2m(2\pi k)^{\frac{1}{2}}}{p}} - \frac{1}{2} e^{\frac{-2m\{2\pi(k-i\omega)\}^{\frac{1}{2}}}{p}} - \frac{1}{2} e^{\frac{-2m\{2\pi(k+i\omega)\}^{\frac{1}{2}}}{p}} \right] \quad (5)$$

which can be written

$$P_{In} = \lambda_I (y_I - q_{1n}) \quad (5a)$$

where

$$y_I = p e^{\frac{-2m(2\pi k)^{\frac{1}{2}}}{p}} \quad (6)$$

and

$$q_{1n} = m\pi^{\frac{1}{2}} (a_{1n}/\omega)^2 F(k) \quad (7)$$

with

$$F(k) = \{k + [k^2 + \omega^2]^{\frac{1}{2}}\}^{\frac{1}{2}} - (2k)^{\frac{1}{2}} \quad (8)$$

Limiting expressions for  $q_{1n}$  are

$$\text{for } k \gg \omega : q_{1n} = \frac{3}{2} m\pi^{\frac{1}{2}} a_{1n}^2 (2k)^{\frac{1}{2}} \quad (9a)$$

$$\text{and for } k \ll \omega : q_{1n} = m\pi^{\frac{1}{2}} a_{1n}^2 \omega^{\frac{3}{2}} \{1 - (2k/\omega)^{\frac{1}{2}}\} \quad (9b)$$

The latter (eq.9b) approaches  $x_n$  (eq.22 part VIII) for small k, as it should.

Neglecting product formation for the moment we can write for the second pair

$$\frac{d}{dt}P_{2n}(t) = 2kP_{1n}(t) - kP_{2n}(t) = 2k|C_{1Sn}^S(t)|^2 e^{-2kt} - kP_{2n}(t) \quad (10)$$

where we have set  $P_{1n}(t) = P_{1Sn}(t)$ , effectively neglecting any transitions back to the S state, once a pair has arrived in the  $T_0$  state, which is allowed for small transition probabilities. Furthermore, it is reasonable to assume that  $|C_{1Sn}^S(t)|^2$  reaches a stationary value before  $P_{2n}(t)$  does, so we replace it by its average value

$$\begin{aligned} \overline{|C_{1Sn}^S(t)|^2} &= 2k \int_0^{\infty} |C_{1Sn}^S(t)|^2 e^{-2kt} dt = \\ &= 1 - \frac{a_{1n}^2}{2(k^2 + \omega^2)} = 1 - \hat{x}_{1n} \end{aligned} \quad (11)$$

Integrating (10) and correcting for product formation ( $P_{In}(t)$  similarly is replaced by its stationary value  $P_{In}$  for long times) we obtain:

$$P_{2n}(t) = (1 - P_{In})(1 - \hat{x}_{1n})2(1 - e^{-kt})e^{-kt} \quad (12)$$

and for product II:

$$P_{IIIn} = \int_0^{\infty} \lambda_{II} |C_{2Sn}^S(t)|^2 P_{2n}(t) f(t) dt \quad (13)$$

Here we cannot use the function  $f(t)$  of eq.(2), which is the reencounter probability of a pair, just separated from an encounter. To determine the function  $f'(t)$  we make use of a procedure of Braun et al.<sup>7</sup>. The total encounter probability of a pair formed at a distance  $r(t_1)$  at time  $t_1$  is  $\rho \rho 1.13/r(t_1)$ , where  $r(t_1)$  is given by<sup>8</sup>  $r(t_1) = (v\sigma^2 t_1)^{1/2}$ . ( $\rho$  is the encounter diameter,  $\sigma$  and  $v$  are the mean diffusion step-length and frequency respectively). The function  $f'(t)$  is the encounter probability at  $t > t_1$ , hence

$$\int_{t_1}^{\infty} f'(t) dt = \frac{\rho \rho 1.13}{v^{1/2} \sigma t_1^{1/2}} \quad (14)$$

and by differentiating (14),

$$f'(t) = \frac{\rho\rho}{2v^{\frac{3}{2}}\sigma} t^{-\frac{3}{2}} = m't^{-\frac{3}{2}} \quad (15)$$

When  $\rho = \sigma$ ,  $m$  and  $m'$  have a similar magnitude. We can now integrate (13) with (15), obtaining the result

$$P_{IIIn} = \lambda_{II} (1 - P_{In}) (1 - \hat{x}_{1n}) (y_{II} - q_{2n}) \quad (16)$$

$$\text{where } y_{II} = 2p \left[ e^{\frac{-2m'}{p}(\pi k)^{\frac{1}{2}}} - e^{\frac{-2m'}{p}(2\pi k)^{\frac{1}{2}}} \right] \quad (17)$$

$$\text{and } q_{2n} = m'\pi^{\frac{1}{2}} [a_{2n}/\omega]^2 \{F(\frac{1}{2}k) - F(k)\} \quad (18)$$

with  $F(k)$  given by eq.(8). It has been assumed that  $f'(t)$  approaches  $f(t)$  in the limit of very large  $k$ , hence the appearance of  $p$  in eq.(17). However, in the region  $k < 10^{10} \text{sec}^{-1}$  eq.(17) becomes independent of  $p$ .

For the calculation of  $P_{IIIIn}$  we make similar approximations and for sake of simplicity we assume that  $m'$  (c.f. eq.15) is the same for pairs 2 and 3. Using the average value of  $|C_{2Sn}^S(t)|^2$

$$\begin{aligned} \overline{|C_{2Sn}^S(t)|^2} &= k \int_0^{\infty} |C_{2Sn}^S(t)|^2 e^{-kt} (1 - e^{-kt}) dt = \\ &= 1 - a_{2n}^2 \left\{ \frac{4}{k^2 + 4\omega^2} - \frac{1}{2(k^2 + \omega^2)} \right\} = 1 - \hat{x}_{2n} \end{aligned} \quad (19)$$

we arrive at

$$P_{3n}(t) = (1 - P_{In}) (1 - P_{IIIn}) (1 - \hat{x}_{1n}) (1 - \hat{x}_{2n}) (1 - e^{-kt})^2 \quad (20)$$

and the population of product III becomes

$$P_{IIIIn}^S = \int_0^{\infty} \lambda_{III} |C_{3Sn}^S(t)|^2 P_{3n}(t) f'(t) dt = \lambda_{III} (1 - P_{In}) (1 - P_{IIIn}) (1 - \hat{x}_{1n}) (1 - \hat{x}_{2n}) (y_{III} - q_{3n}) \quad (21)$$

$$\text{where } y_{III} = p \left\{ 1 - 2e^{-\frac{2m'}{p}(\pi k)^{\frac{1}{2}}} + e^{-\frac{2m'}{p}(2\pi k)^{\frac{1}{2}}} \right\} \quad (22)$$

$$\text{and } q_{3n} = m' \pi^{\frac{1}{2}} (a_{3n}/\omega)^2 \{ \omega^{\frac{1}{2}} - 2F(\frac{1}{2}k) + F(k) \} \quad (23)$$

Summarizing the results for the S case, eq.(5), (16) and (21), and neglecting products of small quantities, we get

$$P_{In}^S = \lambda_I \{ y_I - q_{1n} \} \quad (24a)$$

$$P_{IIIn}^S = \lambda_{II} (1 - P_I) \{ y_{II} (1 - \hat{x}_{1n}) - q_{2n} \} \quad (24b)$$

$$P_{IIIIn}^S = \lambda_{III} (1 - P_I) (1 - P_{II}) \{ y_{III} (1 - \hat{x}_{1n} - \hat{x}_{2n}) - q_{3n} \} \quad (24c)$$

where  $P_I$  and  $P_{II}$  are the nuclear spin independent parts<sup>9</sup> of  $P_{In}$  and  $P_{IIIn}$ . A notable result is the fact that polarization in products II and III is a sum of contributions from all preceding pairs. This might be called a "memory effect", because the effect of S-T transitions in a specific pair is stored and appears later as polarization in the recombination products of other pairs. Of course this works only if the same nuclei are present in the pairs. There are experimental examples of this effect, as will be discussed in section 4.

### 2.3 T precursor.

We make the same approximations as for the S case; only the first re-encounter is considered. Then

$$P_{In} = \int_0^{\infty} \frac{1}{3} \lambda_I |C_{1Sn}^T(t)|^2 e^{-2kt} f(t) dt = \frac{1}{3} \lambda_I q_{1n} \quad (25)$$

where we have used (3b) and  $q_{1n}$  is defined by eq.(7). Again assuming that transitions back to singlet are not important and noting that

$$|C_{1Sn}^T(t)|^2 = \hat{x}_{1n} \quad (\text{c.f. eq.11}) \text{ we have, similarly to eq.(12)}$$

$$P_{2n}(t) = (1 - \hat{x}_{1n})^2 (1 - e^{-kt}) e^{-kt} \quad (26)$$

The singlet fraction of pairs 2 is

$$P_{2Sn}(t) = \frac{1}{3} \{ |C_{2Sn}^T(t)|^2 (1 - \hat{x}_{1n}) + (1 - P_{In}) \hat{x}_{1n} \} 2(1 - e^{-kt}) e^{-kt} \quad (27)$$

where we have separately included the fraction that has crossed over from  $T_0$  to S in pair 1. In the same notation as used in eq.(24) we have:

$$P_{IIIn} = \int_0^\infty \lambda_{II} P_{2Sn}(t) f'(t) dt = \frac{1}{3} \lambda_{II} \{ q_{2n} (1 - \hat{x}_{1n}) + (1 - P_{In}) \hat{x}_{1n} y_{II} \} \quad (28)$$

$$\text{Similarly: } P_{3n}(t) = (1 - \hat{x}_{1n}) (1 - \hat{x}_{2n}) (1 - e^{-kt})^2 \quad (29)$$

$$P_{3Sn}(t) = \frac{1}{3} \{ |C_{3Sn}^T(t)|^2 (1 - \hat{x}_{1n}) (1 - \hat{x}_{2n}) + (1 - P_{IIIn}) \{ (1 - P_{In}) \hat{x}_{1n} + \hat{x}_{2n} \} \} (1 - e^{-kt})^2 \quad (30)$$

$$P_{IIIIn} = \frac{1}{3} \lambda_{III} \{ q_{3n} (1 - \hat{x}_{1n}) (1 - \hat{x}_{2n}) + y_{III} (1 - P_{IIIn}) \{ (1 - P_{In}) \hat{x}_{1n} + \hat{x}_{2n} \} \} \quad (31)$$

Neglecting products of small quantities the results for the T case (25), (28) and (31) become:

$$P_{In}^T = \frac{1}{3} \lambda_I q_{1n} \quad (32a)$$

$$P_{IIIn}^T = \frac{1}{3} \lambda_{II} \{ q_{2n} + y_{II} \hat{x}_{1n} \} \quad (32b)$$

$$P_{IIIIn}^T = \frac{1}{3} \lambda_{III} \{ q_{3n} + y_{III} (\hat{x}_{1n} + \hat{x}_{2n}) \} \quad (32c)$$

Again we have as a result that to a good approximation the polarization is a sum of contributions of all preceding pairs.

## 2.4 Enhancement factors and Product yields.

An illustration of expressions (24) for the case of a S precursor will now be given. If the extent of S-T<sub>0</sub> mixing is small, the product yields may be equated with the nuclear spin independent parts of eq.(24):

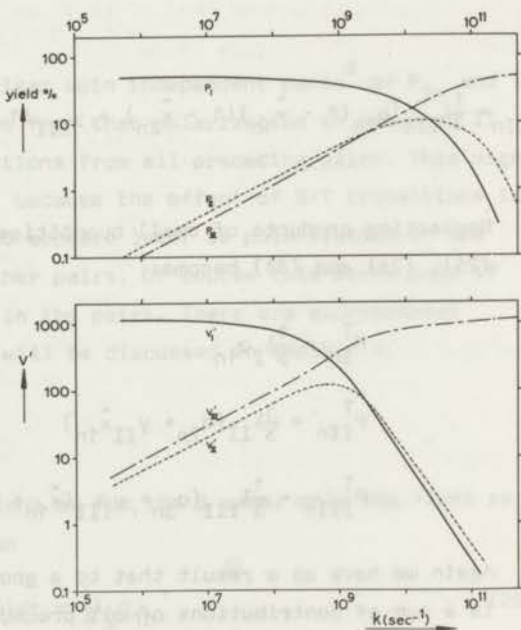
$$P_I = \lambda_I y_I \quad (33a)$$

$$P_{II} = \lambda_{II}(1 - P_I)y_{II} \quad (33b)$$

$$P_{III} = \lambda_{III}(1 - P_I)(1 - P_{II})y_{III} \quad (33c)$$

where  $y_I$ ,  $y_{II}$  and  $y_{III}$  are given by eq.(6), (17) and (22). In figure 1 these yields ( in % ) are plotted as a function of  $k$ , for the case where  $p = \frac{1}{2}$ ,  $m' = m = 10^{-6} \text{sec}^{\frac{1}{2}}$  and  $\lambda_I = \lambda_{II} = \lambda_{III} = 1$ . The maximum yield is 50% due to our choice of  $\lambda p = 0.5$ . The behaviour is as expected: for small  $k$  only product I is formed in appreciable yield and in the region of very large  $k$ , only product III.  $P_{II}$  goes through a maximum at about  $k = 2 \cdot 10^{10} \text{sec}^{-1}$ .

Figure 1. Plot of the yields  $P_I$ ,  $P_{II}$ ,  $P_{III}$  ( in % ) (a) and enhancement factors  $V_I$ ,  $V_{II}$ ,  $V_{III}$  (b) versus  $k$ . The parameters used in the calculations were the same for all three radical pairs. For their values, see the text.



In the region of small  $k$  we have  $y_{II} = 1.64 m'(\pi k)^{\frac{1}{2}}$  and  $y_{III} = 1.17 m'(\pi k)^{\frac{1}{2}}$ , and hence both  $P_{II}$  and  $P_{III}$  exhibit a  $k^{\frac{1}{2}}$  dependence<sup>3c</sup> in this region.

The enhancement factors (c.f. VIII)

$$V'_i = (P_{in} - P_{im}) \frac{kT}{g_N^{\beta} N H_0} \quad (34)$$

where  $i = I, II$  or  $III$ , have been calculated for a one-proton case (S precursor).  $V'$  is used, because this is a better measure of the observability of the effects.<sup>10</sup> Besides,  $V'$  for different products of the same precursor, is proportional to the relative CIDNP intensities of these products corrected for nuclear relaxation. The results are plotted in figure 1. In order to facilitate comparison, the magnetic parameters have been given the same values for the three radical pairs:  $A_H = 4.4 \cdot 10^8$  radians/sec,  $J = 5 \cdot 10^8$  radians/sec,  $\Delta g = -6.5 \cdot 10^{-3}$ ,  $kT/g_N^{\beta} N H_0 = 10^5$ . These values have bearing on the alkyl/trichloromethyl radical pair, which is discussed in section 4. Inspection of fig. 1b is revealing. It can be seen that the general behaviour of  $V'$  is similar to that of the product yields. However, the curves are shifted towards lower values of  $k$ . For instance, the maximum of  $V'_{II}$  occurs at about  $k = 8 \cdot 10^8 \text{ sec}^{-1}$ , a factor 25 lower than for the maximum of  $P_{II}$ . In the high  $k$  region,  $V'$  goes as  $k^{-3/2}$ , but for low values of  $k$  a  $k^{\frac{1}{2}}$  behaviour similar to  $P_{II}$  is predicted. This result is characteristic for the diffusion model. A consequence is that the polarization for products II and III drops of much slower for low values of  $k$ , than other models would predict.

Taking a value of  $k = 5 \cdot 10^8 \text{ sec}^{-1}$ , the yield of product I has decreased from 50 to 40%, whereas  $V'_I$  has dropped from 1200 to 400. A conclusion is that times of  $10^{-8}$ - $10^{-9}$  sec contribute appreciably to the polarization of geminate recombination products.

## 2.5 Memory effect.

As an example of this effect we have calculated the enhancement factors  $V'_{II}$  and  $V'_{III}$  for a one proton case, where polarization in both products II and III is due only to pair 2.

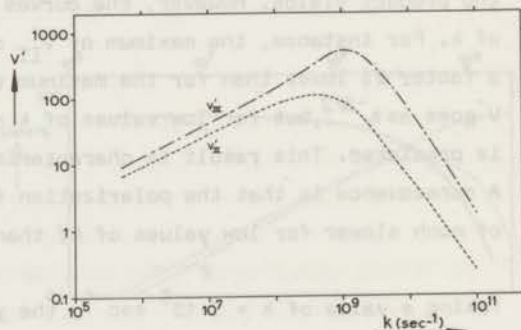
This situation is thought to occur in the decomposition of acetyl peroxide<sup>11</sup>, where emission in both methylacetate and ethane arises probably from S-T<sub>0</sub> mixing in the methyl/acetoxy radical pair. If pairs 1 and 3 cannot contribute to the polarization, we have

$$P_{II n} = \lambda_{II} (1 - P_I) \{y_{II} - q_{2n}\} \quad (35a)$$

$$P_{III n} = \lambda_{III} (1 - P_I) (1 - P_{II}) (1 - \tilde{x}_{2n}) y_{III} \quad (35b)$$

In figure 2,  $V'_{II}$  and  $V'_{III}$ , defined as in eq.(34) with (35), are plotted versus  $k$ . The values  $A_H = -4.0 \cdot 10^8$  radians/sec,  $\Delta g = -3.2 \cdot 10^{-3}$ , pertaining to the methyl/acetoxy pair<sup>11b</sup>, have been used in the calculations. This choice results in a negative polarization. Values of the other parameters are the same as those used in fig. 1. Notably,  $V'_{III}$  is everywhere larger than  $V'_{II}$ ; in the fast reaction region ( $10^9 < k < 10^{10} \text{ sec}^{-1}$ ) a factor 6 to 10 larger. Thus, in the case of rapid reactions it may even occur that polarization from pair 2 is visible only in products of pair 3.

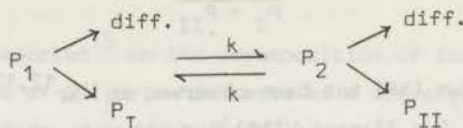
Figure 2. Plot of  $V'_{II}$  and  $V'_{III}$  versus  $k$  for the case that polarization arises only from pair 2 (memory effect).



### 3. Stereospecific Homolytic Rearrangements.

A few rearrangements of optically active compounds have been reported<sup>12,13</sup> where a high degree of retention of configuration was observed and the homolytic nature of the process was established by the observation of CIDNP. It might appear as if these observations are in conflict with

the present diffusion model, which, however, is not the case. The process of racemization, competing with recombination is depicted in scheme 2.



Scheme 2

$P_1$  and  $P_2$  are radical pairs that differ only in their relative orientation ("l" and "d" pairs) and similarly the products  $P_I$  and  $P_{II}$  (l and d products),  $P_I$  being the product with retention of configuration. The rate of racemization  $k$  is related to the tumbling frequency of the fragments. If no product formation occurred we would have

$$P_1(t) = \frac{1}{2}(1 + e^{-2kt}) \quad (36a)$$

$$P_2(t) = \frac{1}{2}(1 - e^{-2kt}) \quad (36b)$$

### 3.1 S precursor.

For  $k > \omega$  populations of the products are now given by:

$$\begin{aligned} P_{I/II} / n &= \int_0^{\infty} \lambda |C_{Sn}^S(t)|^2 \frac{1}{2}(1 \pm e^{-2kt}) f(t) dt = \\ &= \frac{1}{2} \lambda \left[ p \left( 1 \pm e^{-\frac{2m}{p}(2\pi k)} \right)^{\frac{1}{2}} - m \pi^{\frac{1}{2}} a_n^2 \left\{ \omega^{\frac{-3}{2}} \pm \frac{1}{2}(2k)^{\frac{-3}{2}} \right\} \right] \end{aligned} \quad (37)$$

Hence polarization occurs in both products, irrespective of the exact value of  $k$ . Interesting quantities are the sum and difference:

$$P_{In} + P_{IIIn} = \lambda \left\{ p - m \pi^{\frac{1}{2}} a_n^2 \omega^{\frac{-3}{2}} \right\} \quad (38)$$

$$P_{In} - P_{IIIn} = \lambda \left\{ p e^{-\frac{2m}{p}(2\pi k)} - \frac{1}{2} m \pi^{\frac{1}{2}} a_n^2 (2k)^{\frac{-3}{2}} \right\} \quad (39)$$

and the fraction of retention:

$$\frac{P_I - P_{II}}{P_I + P_{II}} = e^{-\frac{2m}{p}(2\pi k)^{\frac{1}{2}}} \quad (40)$$

Only the sum (38) has been observed so far<sup>12,13</sup>; it is equal to the normal S-case (eq.22 part VIII). For solvents of ordinary viscosity  $k$  will be not much smaller than  $10^{10} \text{ sec}^{-1}$ . If we put  $k = 10^{10} \text{ sec}^{-1}$ , we find 40 - 60% retention for  $\frac{1}{2} < p < 1$ . In fact this percentage could be even higher, because of "primary" cage recombination in the sense of Noyes, which we have not properly accounted for (c.f. ref.3b). From (39) the difference of polarization of  $P_I$  and  $P_{II}$  is expected to be very small. Observation of  $P_{In} - P_{IIn}$  requires that the nmr signals of  $P_I$  and  $P_{II}$  do not coincide. Separate signals can be observed when there is more than one asymmetric center present in the molecules<sup>14</sup>, or when an optically active solvent is used. Observation of difference polarization could provide a stringent test on the theory presented here.

### 3.2 T precursor.

The results for the T case are:

$$P_{I/II}^n = \int_0^{\infty} \frac{\lambda}{3(1-p)} |C_{Sn}^T(t)|^2 \frac{1}{2} (1 \pm e^{-kt}) f(t) dt = \frac{\lambda}{6(1-p)} m\pi^{\frac{1}{2}} a_n^2 \left[ \omega^{-\frac{3}{2}} \pm \frac{1}{2} (2k)^{-\frac{3}{2}} \right] \quad (41)$$

$$P_{In} - P_{IIn} = \frac{\lambda}{6(1-p)} m\pi^{\frac{1}{2}} a_n^2 (2k)^{-\frac{3}{2}} \quad (42)$$

$$P_{In} + P_{IIn} = \frac{\lambda}{3(1-p)} m\pi^{\frac{1}{2}} a_n^2 \omega^{-\frac{3}{2}} \quad (43)$$

$$\frac{P_I - P_{II}}{P_I + P_{II}} = 2 \frac{-5}{2} (\omega/k)^{\frac{3}{2}} \quad (44)$$

Both retention (44) and difference polarization (42) will be very small for  $k > 10^{10} \text{ sec}^{-1}$ , whereas the sum (43) is identical to eq.(24,VIII). If short distance spin-orbit coupling would contribute to the inter-system-crossing, there could be some retention.

#### 4. Discussion of Experimental Examples.

##### 4.1 Radical Scavenging.

We have previously reported<sup>15</sup> on the decomposition of isobutyryl peroxide (IBP) in the presence of  $\text{CCl}_3\text{Br}$ , which acts as a scavenger for isopropyl radicals. Chloroform, a product of the secondary isopropyl/trichloromethyl radical pair, exhibits a change of sign of the polarization, going from E to A, when the concentration of  $\text{CCl}_3\text{Br}$  is increased. The sign-change occurred at 0.11 M  $\text{CCl}_3\text{Br}$ . This phenomenon was interpreted<sup>15</sup> in terms of a competition between S-precursor polarization of spin-correlated pairs and (opposite) F-type polarization (due to free radical encounters of uncorrelated isopropyl and  $\text{CCl}_3$  radicals).

The reactions are those of scheme 1, with  $\text{R}\cdot = \text{isopropyl}$ ,  $\text{R}'\cdot = \text{CCl}_3$  and  $k = k_{\text{tr}}[\text{CCl}_3\text{Br}]$ . The value of  $k_{\text{tr}}$  for the transfer reaction  $\text{R}\cdot + \text{CCl}_3\text{Br} \rightarrow \text{RBr} + \text{CCl}_3$  is not known. For a similar radical ( $\text{CCl}_3\text{CH}_2\dot{\text{C}}\text{HOCOCCH}_3$ ) Melville et al<sup>16</sup> have found  $k_{\text{tr}} = 2 \cdot 10^4$  l/mole sec (for a reaction temperature  $80^\circ$ ). If our interpretation is correct,  $k_{\text{tr}}$  must be higher in our case. One can estimate a lower limit of  $k_{\text{tr}}$  from the theory presented here.

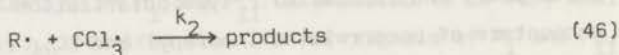
The signal intensities (I) are related to the enhancement factor  $\hat{V}$  (eq. 34) as follows (cf. eq. 42, VIII)

$$I = \hat{V} I(\text{B}_t^-) k_f T_1 \quad (45)$$

where  $I(\text{B}_t^-)$  is the intensity of a transition between the same nuclear states in the precursor at time  $t^-$ , when the maximum polarization occurs;  $k_f$  is the rate constant for the formation of pairs and  $T_1$  is the nuclear relaxation time. In our case  $k_f = 4.5 \cdot 10^{-3} \text{sec}^{-1}$  (ref. 17) and  $T_1 = 50 \text{sec}$  for chloroform. Thus, for instance, if  $\hat{V} = 2$ , the CIDNP intensity would be about half the intensity of the peroxide signal (normalized to one proton). This would be well observable. From figure 1b, it can be inferred that in the range  $k = 5 \cdot 10^5 - 5 \cdot 10^6 \text{sec}^{-1}$ , one could still have observable A effects for chloroform ( $\hat{V}_{\text{II}}$ ). This implies  $k_{\text{tr}} = 5 \cdot 10^6 - 5 \cdot 10^7$  l/mole sec, in the  $\text{CCl}_3\text{Br}$  concentration range of 0.1 M. If we put (somewhat arbitrarily)  $\lambda_{\text{I}} = \lambda_{\text{II}} = \frac{1}{2}$  and  $k = 10^6 \text{sec}^{-1}$ ,

we find  $V_{II}' = 4.6$ , while the yield would be only about 0.1%, which would be properly called a "trace".

To see whether F-type polarization can compete at 0.1 M  $\text{CCl}_3\text{Br}$ , we first estimate the steady-state concentration of  $\text{CCl}_3$  radicals. The peroxide concentration is 0.2 M. Thus the rate of formation of isopropyl radicals  $r_f = 9 \cdot 10^{-4}$  mole/l sec. Assuming that  $\frac{2}{3}$  of the radicals eventually becomes  $\text{CCl}_3$  and that these radicals disappear predominantly by bimolecular coupling:  $2\text{CCl}_3 \xrightarrow{k_1} \text{C}_2\text{Cl}_6$  with a rate constant  $k_1 = 0.5 \cdot 10^8$  l/mole sec<sup>16</sup>, we find from the steady-state condition  $[\text{CCl}_3] = 3.7 \cdot 10^{-6}$  mole/l. If the rate constant for the reaction



is taken to be  $k_2 = 2 \cdot 10^9$  l/mole sec (c.f. ref.16) the rate of disappearance of isopropyl radicals by reaction (46) would be  $k_2[\text{CCl}_3] = 7.4 \cdot 10^3 \text{ sec}^{-1}$ , or a factor 135 slower than that of the transfer reaction ( $k = 10^6 \text{ sec}^{-1}$ ). However, F-type polarization for this reaction could well be a factor 135 larger than  $V_{II}'$  ( $V_F' = -620$  is not unreasonable), thus canceling the effect of the singlet-correlated pairs.

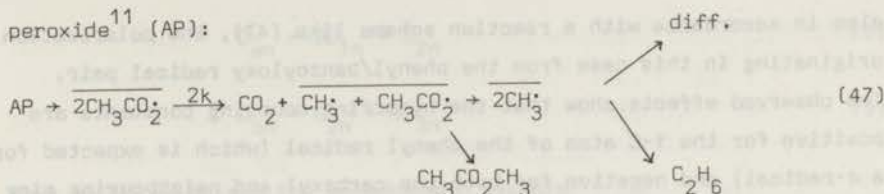
The calculations presented here are demonstrative rather than precise. They seem to indicate, however, that CIDNP effects can be observed from radical pairs, that retain their spin-correlation for rather long times, up to the microsecond region. This is anyhow about the limit for the validity of this treatment, since for longer life-times the correlation is spoiled by spin-lattice relaxation ( $T_1^R \sim 10^{-4} - 10^{-5}$  sec).

It is probable, that observation of A for pentachloroacetone, formed during decomposition of a cyclohexadienone peroxide<sup>13a</sup> (giving a pair of *t*-butyl radicals) in hexachloroacetone (HCA) similarly results from rather long-lived radical pairs.

#### 4.2 Fragmentation.

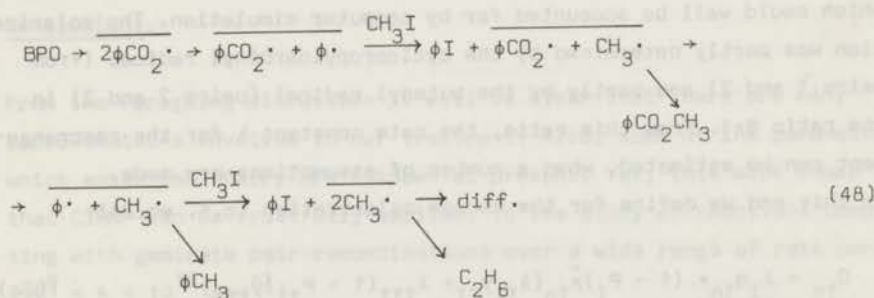
An example of this type of transformation is provided by the decarboxylation of acetoxy radicals, formed during decomposition of acetyl

peroxide<sup>11</sup> (AP):



Emission for both methylacetate ( $OCH_3$ ) and ethane was reported previously<sup>11a</sup>. We have experimental indications that both E effects are due to S-T<sub>0</sub> transitions in the methyl/acetoxy radical pair (memory effect). The value of k has been estimated<sup>7,18</sup> to be in the range  $10^9 - 10^{10} \text{ sec}^{-1}$ . The ratio  $V'_{II}/V'_{III}$  was found to be 0.26, in fair agreement with the values 0.17 - 0.10 derived from figure 2 for this range. When the experimental value of  $P_{II} = 0.32$  is used, the theoretical ratio's become 0.27 - 0.13. The theory correctly predicts larger enhancements for III than for II, in spite of the fact that the latter product is directly formed from the pair, in which polarization is generated.

In our opinion, the emission effects of ethane, toluene and methylbenzoate, observed during the decomposition of benzoyl peroxide (BPO) in the presence of methyl iodide<sup>19,20</sup> has a similar origin and is probably an extreme case of the memory effect for the fourth or fifth subsequent pair:



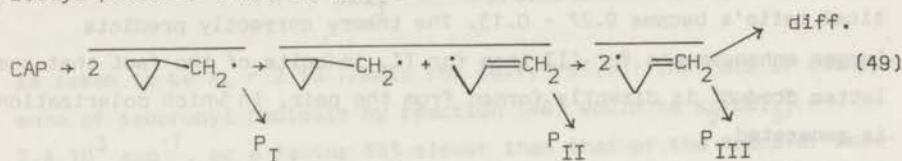
where  $\overline{\phi CO_2} \cdot$  and  $\overline{\phi} \cdot$  are the benzoyloxy and phenyl radicals and polarization is due to the benzoyloxy/methyl radical pair.

Furthermore, observations<sup>21</sup> of <sup>13</sup>C polarization during thermolysis of BPO in cyclohexanone (E for benzene and CO<sub>2</sub>, A for diphenyl and A for the three C-atoms of the  $C-C(=O)-O-C$  moiety of phenylbenzoate) are

also in accordance with a reaction scheme like (47), the polarization originating in this case from the phenyl/benzoyloxy radical pair. The observed effects show that the hyperfine coupling constants are positive for the 1-C atom of the phenyl radical (which is expected for a  $\sigma$ -radical) and negative for both the carboxyl and neighbouring ring C-atoms of the benzoyloxy radical, which is not unreasonable for an allyl-type radical.

#### 4.3 Rearrangements of Radicals.

The cyclopropylcarbinyl radical is known<sup>22</sup> to rearrange to give the 3-butenyl radical. We have studied<sup>4</sup> the decomposition of cyclopropylacetyl peroxide (CAP) in HCA at 80°. The reactions are



$P_I$ ,  $P_{II}$  and  $P_{III}$  represent coupling and disproportionation products, the CIDNP spectrum of which was not clear. However the "escape" product, 4-chloro-1-butene, resulting from transfer reaction with the solvent showed a strongly polarized spectrum (multiplet effects for all protons), which could well be accounted for by computer simulation. The polarization was partly determined by the cyclopropylcarbinyl radical (from pairs 1 and 2) and partly by the butenyl radical (pairs 2 and 3) in the ratio 8:1. From this ratio, the rate constant  $k$  for the rearrangement can be estimated, when a number of assumptions are made.

To this end we define for the escape polarization (c.f. eq.24):

$$D_{1n} = \lambda_I q_{1n} + (1 - P_I) \hat{x}_{1n} \{ \lambda_{II} y_{II} + \lambda_{III} (1 - P_{II}) y_{III} \} \quad (50a)$$

$$D_{2n} = \lambda_{II} (1 - P_I) q_{2n} + \lambda_{III} (1 - P_I) (1 - P_{II}) y_{III} \hat{x}_{2n} \quad (50b)$$

$$D_{3n} = \lambda_{III} (1 - P_I) (1 - P_{II}) q_{3n} \quad (50c)$$

and for the contributions from the cyclopropylcarbinyl and the butenyl radical respectively:

$$D_{an} = 2D_{1n} + D_{2n} \quad (51a)$$

$$D_{bn} = D_{2n} + 2D_{3n} \quad (51b)$$

from which we obtain the enhancement factors

$$V'_a = (D_{an} - D_{am}) \frac{kT}{g_N^{\beta} N^{\beta} H_0} \quad (52a)$$

$$V'_b = (D_{bn} - D_{bm}) \frac{kT}{g_N^{\beta} N^{\beta} H_0} \quad (52b)$$

$V'_a$  gives the polarization of the vinyl group and  $V'_b$  that of the methylene groups in 4-chloro-1-butene. Assuming  $\lambda_I = \lambda_{II} = \lambda_{III} = 1$ ,  $p = 0.5$ ,  $m = m' = 10^{-6} \text{ sec}^{\frac{1}{2}}$ ,  $|J| = 5 \cdot 10^8 \text{ radians/sec}$  and using known hyperfine parameters<sup>22</sup>, we calculate a ratio  $V'_a/V'_b = 8$ , for  $k = 3 \cdot 10^7 \text{ sec}^{-1}$ , in good agreement with the value  $10^8 \text{ sec}^{-1}$  estimated by others<sup>22b,23</sup>. If the life-time of the butenyl radical would be comparable to or longer than the spin-lattice relaxation time of this radical, the value  $k = 3 \cdot 10^7 \text{ sec}^{-1}$  would be a lower limit, since b-type polarization would be more affected by relaxation than a-type.

#### 4.4 Conclusions.

From the foregoing discussion it will be clear that there are many approximations involved in our treatment. Also, some of the parameters which enter the theory are unknown at present. Yet, this work shows that CIDNP can be fruitfully applied, to the study of reactions competing with geminate pair recombinations over a wide range of rate constants ( $10^6 < k < 10^{10} \text{ sec}^{-1}$ ).

The present extension of the diffusion model accounts for some experimental observations, which could otherwise hardly be explained by radical pair theory. In particular, predictions of CIDNP effects due to long-time spin-correlation effects, observed in products, which are formed in extremely low yields, are characteristic of this model.

## References and Footnotes.

1. R. Kaptein, part VIII, to be published.
2. c.f. F.J. Adrian, J. Chem. Phys., 53, 3374 (1970).
- 3.(a) R.M. Noyes, ibid., 22, 1349 (1954);  
(b) R.M. Noyes, J. Amer. Chem. Soc., 77, 2042 (1955);  
(c) R.M. Noyes, ibid., 78, 5486 (1956).
4. CIDNP effects in this system are discussed elsewhere (R. Kaptein, to be published).
5. R. Kaptein and L.J. Oosterhoff, Chem. Phys. Letters, 4, 214 (1969)
6. G.L. Closs and A.D. Trifunac, J. Amer. Chem. Soc., 92, 2183 (1970)
7. W. Braun, L. Rajbenbach and F.R. Eirich, J. Phys. Chem. 66, 1591 (1962).
8. A. Einstein, Z. Elektrochem., 14, 235 (1908).
9. The "escape" polarization arising from the factor  $(1 - P_{In})$  is only a fraction of the (opposite) polarization due to the factor  $(1 - \hat{x}_{1n})$ . Therefore, as to the polarization of  $P_{II}$ , the radicals of pair 2 cannot simply be considered as "escaped" from recombination in pair 1.
10. To obtain the enhancement factor  $V$ , related to the thermal equilibrium intensity of the product (cf. VIII), one has to divide  $V$  by the yield, which may be very small, giving very large values of  $V$  even when the signal would be too small to be detectable.
- 11.(a) R. Kaptein, Chem. Phys. Letters, 2, 261 (1968);  
(b) R. Kaptein, J. Brokken-Zijp and F.J.J. de Kanter, part XI, to be published.
12. U. Schöllkopf, U. Ludwig, G. Ostermann and M. Patsch, Tetrahedron Letters, 3415 (1969).
13. J.E. Baldwin, W.F. Erickson, R.E. Hackler and R.M. Scott, Chem. Comm. 576 (1970).
14. This experiment was suggested by Prof. J.E. Baldwin (personal communication).
15. R. Kaptein, F.W. Verheus and L.J. Oosterhoff, part VI, to be published.
16. H.W. Melville, J.C. Robb and R.C. Tutton, Discuss. Faraday Soc., 14, 150 (1953).
17. J. Smid and M. Szwarc, J. Chem. Phys., 29, 432 (1958).



CHAPTER X

CHEMICALLY INDUCED DYNAMIC NUCLEAR POLARIZATION X  
ON THE MAGNETIC FIELD DEPENDENCE.

By R. Kaptein and J.A. den Hollander.

Department of Theoretical Organic Chemistry  
University of Leiden, P.O. Box 75, Leiden.  
The Netherlands.

1. Introduction.

The magnetic field dependence of CIDNP has not yet received much attention. In particular, observation of polarization effects in the low field region (lower than a few thousand Gauss) has been reported in only a few studies<sup>1-4</sup>. In most experimental work on CIDNP, reactions are run in the nmr spectrometer probe, i.e. in fields of 14 or 23.5 kGauss. CIDNP effects have been observed also in nmr spectra after carrying out the reaction in a separate magnet<sup>1</sup>, in "zero" field<sup>2</sup> and in the low field near the spectrometer magnet<sup>3</sup> and furthermore in a spectrometer<sup>4</sup> run at fields below 100 G. Observation of zero field polarization was actually one of the most obvious pieces of evidence against the originally proposed<sup>5</sup> Overhauser-type mechanism of CIDNP. This mechanism has been replaced by the radical pair mechanism<sup>6,7,8</sup> (nuclear spin dependent singlet (S)-triplet (T) mixing in radical pairs). High field experiments can be explained by considering the mixing of S with  $T_0$  only. This simplification is no longer justified in low magnetic fields, where mixing of S with all three T states has to be considered.

Therefore, a study of low field CIDNP is of interest, because it can be expected to give more detailed information e.g. on the behaviour (and sign) of the exchange integral  $J$ , which affects the energy of S and T states of the radical pair. It may also provide a more critical test of the various theoretical models of CIDNP than the high field experiments.

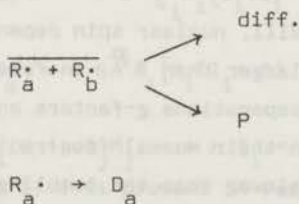
A first attempt to give a general theory of CIDNP has been made by Glarum<sup>9</sup>. It will appear, however, that his model cannot accommodate all of our experimental results.

In this paper we present an extension of a previously<sup>8</sup> given model of the radical pair mechanism, in which diffusion of radical pairs has been taken into account. Predictions of the theory will be compared with experimental CIDNP spectra in the case of some photochemical reactions, carried out in an auxiliary magnet, after rapid transfer to the spectrometer probe (Varian A-60,  $H_D = 14$  kG); spectra were run before relaxation was completed.

## 2. General Formalism.

### 2.1 Radical Pair Theory.

Radical pair theory is concerned with S-T mixing and its effects on the reaction probabilities of radical pairs. A general reaction scheme is depicted in scheme 1.



Scheme 1

The radical pair may be formed from a singlet (S) precursor, a triplet (T) precursor, or by encounters of free radicals with uncorrelated spins (F).

We have to determine the populations of the nuclear spin states of the recombination product P and of the product  $D_a$  (and similarly  $D_b$ ) formed from radicals, escaped by diffusion (diff.). As we have done previously<sup>7,8</sup>, we will describe the formation of the pair at  $t = 0$  by a sudden decrease of the exchange integral J to a low (constant) value, comparable to the hyperfine interactions. The time-dependent mixing of states follows from the Schrödinger equation, which now leads to a set of more than two coupled equations. The problem can be solved in three stages:

- a The Hamiltonian matrix for the radical pair in the magnetic field  $H_r$  (in which the reaction is carried out) is set up and diagonalized.
- b With the eigenvalues and eigenvectors obtained in stage a the populations of the product levels are calculated by a procedure similar to the one given in VIII (diffusion model).
- c From the populations calculated in the field  $H_r$ , the populations of the nuclear states in the spectrometer field  $H_0$  are determined (nuclear states in  $H_0$  may differ from those in  $H_r$ ).

There are two limiting cases for this last step<sup>9</sup>: (i) the adiabatic case (slow limit), in which populations are transferred according to the correlation diagram connecting low field with high field levels and (ii) the non-adiabatic case (fast limit), in which case populations of  $H_r$  states may be distributed over several  $H_0$  states. Experiments indicate that in practice the transfer is predominantly adiabatic.

## 2.2 Stage a. The Hamiltonian Matrix.

As we have discussed in VIII, nuclear spin dependent S-T mixing occurs probably at separations larger than  $6 \text{ \AA}$  in freely tumbling and diffusing radical pairs. At these separations g-factors and hyperfine (hf.) coupling constants ( $A_1$ ) have taken their normal free-radical values. Since intersystem-crossing is much slower than the tumbling rate in most solvents, we keep only isotropic terms in the Spin Hamiltonian<sup>8</sup>:

$$H_{RP} = H^0 + H \quad (1)$$

$$H^0 = g\beta_e H_r^{-1} H_r (S_{1z} + S_{2z}) - J(\frac{1}{2} + 2S_{1z} \cdot S_{2z}) + \frac{1}{2}(S_{1z} + S_{2z}) \cdot (\sum_j^a A_{j-j} I_j + \sum_k^b A_{k-k} I_k) \quad (1a)$$

$$\underline{H}' = \frac{1}{2} \Delta g \beta_e \mathcal{K}^{-1} H_r (S_{1z} - S_{2z}) + \frac{1}{2} (S_1 - S_2) \cdot (\sum_j^a A_j I_j - \sum_k^b A_k I_k) \quad (1b)$$

where  $g = \frac{1}{2} (g_a - g_b)$ ;  $\sum^a$  and  $\sum^b$  run over the nuclei of radical a and b respectively;  $J$  and  $A_j$  are expressed in radians/sec. We use a direct product basis of electronic singlet and triplet states  $|\sigma\rangle$  and nuclear spin states  $|n\rangle$  :  $|\sigma n\rangle = |\sigma\rangle |n\rangle$ , where  $\sigma_1$  is the singlet function  $S$  and  $\sigma_2, \sigma_3, \sigma_4$  are the triplet functions  $T_+, T_0, T_-$ ;  $|n\rangle = |\dots I_1 M_1, I_2 M_2, \dots\rangle$  are the nuclear spin product functions, where groups of magnetically equivalent<sup>8</sup> nuclei are coupled together to give resultant spins  $I_i$ . The Hamiltonian matrix is of the order  $4L$ , where  $L$  is the number of nuclear states:

$$L = L_a L_b = \prod_j^a (2I_j + 1) \prod_k^b (2I_k + 1) \quad (2)$$

The diagonal elements of  $\underline{H}_{RP}$  are:

$$\begin{aligned} E_{Sn} &= J ; E_{T_0 n} = -J ; \\ E_{T_{\pm} n} &= -J \pm g \beta_e \mathcal{K}^{-1} H_r \pm \frac{1}{2} \sum_i^{a,b} A_i M_i \end{aligned} \quad (3)$$

The non-diagonal elements are:

$$\begin{aligned} \langle T_0 n | \underline{H}' | S n \rangle &= \frac{1}{2} [\Delta g \beta_e \mathcal{K}^{-1} H_r + \sum_j^a A_j M_j - \sum_k^b A_k M_k] \\ \langle T_{\mp} m_{\pm} | \underline{H}' | S n \rangle &= \pm 8^{-\frac{1}{2}} \xi_i A_i [I_i (I_i + 1) - M_i (M_i \pm 1)]^{\frac{1}{2}} \\ \langle T_{\mp} m_{\pm} | \underline{H}' | T_0 n \rangle &= 8^{-\frac{1}{2}} A_i [I_i (I_i + 1) - M_i (M_i \pm 1)]^{\frac{1}{2}} \end{aligned} \quad (4)$$

where  $|m_{\pm}\rangle = |\dots, I_1 M_1 \pm 1, I_2 M_2, \dots\rangle$ ;  $\xi_i = +1$  if nucleus  $i$  is present in radical a,  $\xi_i = -1$  if  $i$  is present in radical b. Other matrix elements are zero. The matrix  $\underline{H}_{RP}$  is diagonalized by the orthogonal transformation

$$\underline{I}^{-1} \underline{H}_{RP} \underline{I} = \underline{\omega} \quad (5)$$

The columns of  $\underline{I}$  are the eigenvectors;  $\underline{\omega}$  is a diagonal matrix, the elements of which are the eigenvalues.

### 2.3 Stage b. The Populations in $H_r$ .

Let us first consider the populations of recombination product P, or equivalently the fraction of pairs with a certain nuclear spin state, that recombines. We make again the fundamental assumption, that only pairs in the singlet state can recombine. The time-development of each radical pair state is given by the Schrödinger equation, written in the form:

$$i\dot{\underline{C}}(t) = \underline{H}_{RP}\underline{C}(t) \quad (6)$$

$\underline{C}(t)$  is a matrix of order  $4L$ , the columns of which represent the states of the pair at time  $t$ . The solution of eq.(6), subject to initial conditions, is:

$$\underline{C}(t) = e^{-i\underline{H}_{RP}t} \underline{C}(0) = \underline{I} e^{-i\underline{\omega}t} \underline{I}^{-1} \underline{C}(0) \quad (7)$$

To obtain this result, we have used eq.(5) and a well known property of exponential operators<sup>10</sup>. For  $\underline{C}(0)$  we take a direct product:

$$\underline{C}(0) = \underline{E} \underline{S}^A \quad (8)$$

where  $E$  is the unit matrix of order 4 and  $\underline{S}^A$  is an orthogonal matrix of order  $l$ , which diagonalizes the nuclear spin Hamiltonian of the precursor:

$$(\underline{S}^A)^{-1} \underline{H}^A \underline{S}^A = \underline{\Omega}^A \quad (9)$$

In this way mixing of nuclear spin states in the precursor is accounted for in the initial conditions. However, it will be shown presently, that any mixing of nuclear spins in the precursor is irrelevant, so that we might have taken the unit matrix instead of  $\underline{S}^A$  as well. As far as the electron spins are concerned, the four initial states  $S$ ,  $T_+$ ,  $T_0$ , and  $T_-$  are included in eq. (8) and we have to select the states, pertinent to a specific problem ( $S$ ,  $T$ , or  $F$  precursor) later on. For the product P with nuclear spin Hamiltonian  $\underline{H}^P$  in the field  $H_r$  an eigenvector matrix  $\underline{S}^P$  is defined similar to (9):

$$(\underline{S}^P)^{-1} \underline{H}^P \underline{S}^P = \underline{\Omega}^P \quad (10)$$

and a matrix  $\underline{Q}^P$  representing P in 4L dimensional space:

$$\underline{Q}^P = \underline{E}_S \otimes \underline{S}^P \quad \text{with} \quad \underline{E}_S = \begin{bmatrix} 1 & & & \\ & 0 & & \\ & & 0 & \\ & & & 0 \end{bmatrix} \quad (11)$$

This expresses the assumption mentioned above that recombination occurs exclusively from the S-state. The S-states of the pair  $|v\rangle = |1v\rangle$  ( $v$  designates a nuclear state and 1 the electronic S-state), corresponding to those of P, are represented by the column vectors  $\underline{Q}_v^P$  of  $\underline{Q}^P$ . The populations of  $|v\rangle$  are determined with the help of the projections of the radical pair states, described by  $\underline{C}(t)$ , on the states  $|1v\rangle$ :

$$\underline{F}_v(t) = \tilde{\underline{C}}(t) \underline{Q}_v^P \quad (12)$$

where  $\tilde{\underline{C}}(t)$  is the transpose of  $\underline{C}(t)$ . The elements of the vector  $\underline{F}_v(t)$  are contributions of all possible initial states. A population function  $P_v^g(t)$  of the state  $|1v\rangle$ , i.e. the probability of finding the pair in the state  $|1v\rangle$ , ( $g$  denoting the type of precursor) is now given by

$$P_v^g(t) = \sum_r \underline{G}_{rr} |F_{rv}(t)|^2 = \tilde{\underline{F}}_v(t) \underline{G} \underline{F}_v^*(t) \quad (13)$$

$\tilde{\underline{F}}_v(t)$  is a row vector and  $\underline{F}_v^*(t)$  the complex conjugate. The diagonal matrix  $\underline{G}$  weights initial electronic states of a given multiplicity; all nuclear states are given equal weights.  $\underline{G}$  can be written

$$\underline{G} = \underline{E}_g \otimes \underline{I} \quad (14)$$

where  $\underline{I}$  is the unit matrix of order L;  $\underline{E}_g$  ( $g = S, T, \text{ or } F$ ) takes the form (cf. VIII)

$$\underline{E}_S = \begin{bmatrix} 1 & & & \\ & 0 & & \\ & & 0 & \\ & & & 0 \end{bmatrix}; \quad \underline{E}_T = \frac{1}{3} \begin{bmatrix} 0 & & & \\ & 1 & & \\ & & 1 & \\ & & & 1 \end{bmatrix}; \quad \underline{E}_F = \frac{1}{4} \begin{bmatrix} 1-\lambda & & & \\ & 1 & & \\ & & 1 & \\ & & & 1 \end{bmatrix} \quad (15)$$

( $\lambda$  being the probability of reaction during a singlet encounter). We have neglected Boltzmann differences and other possible population



### S-precursor.

Eq.(20) becomes in the case of a S-precursor:

$$W_{lj}^S = \sum_r T_{1r;l} T_{1r;j} \quad (23)$$

The double index  $1r'$  labels electron and nuclear functions respectively ( $r'$  runs over all nuclear states). This gives for the populations:

$$P_{\nu'}^S = \lambda (p - m \sum_{r,l,j} T_{1r;l} T_{1r;j} V_{\nu l}^P V_{\nu j}^P \sqrt{2\pi\omega_{jl}}) \quad (24)$$

### T-precursor.

In the case of T-precursor one has:

$$W_{lj}^T = \frac{1}{3} \sum_{e=2}^4 \sum_{r'} T_{er;l} T_{er;j} \quad (25)$$

giving:

$$P_{\nu'}^T = \frac{\lambda m}{3(1-p)} \sum_{e=2}^4 \sum_{r'} \sum_{l,j} T_{er;l} T_{er;j} V_{\nu l}^P V_{\nu j}^P \sqrt{2\pi\omega_{jl}} \quad (26)$$

where  $e$  runs over the T-states and where we have corrected for multiple reencounters (factor  $(1-p)^{-1}$ , cf.VIII). Combining eq.(24) and eq.(26), we obtain the result  $P_{\nu'}^S + 3(1-p)P_{\nu'}^T = \lambda p$ , or for a transition  $\nu' \rightarrow \mu'$ :

$$P_{\nu'}^S - P_{\mu'}^S = -3(1-p)(P_{\nu'}^T - P_{\mu'}^T) \quad (27)$$

showing that S and T precursors give opposite polarizations, just as in the high field case.

### F-precursor.

Proceeding as before we have from eq. (20), (14) and (15):

$$W_{lj}^F = \frac{1}{2}(\delta_{lj} - \lambda \sum_r T_{1r;l} T_{1r;j}) \quad (28)$$

which gives for F-case populations:

$$P_{\nu}^F = \frac{1}{2}\lambda [1 + c^{-1}\{p(1 - \lambda) + \lambda m \sum_r \sum_j T_{1r;1} T_{1r;j} V_{\nu 1}^P V_{\nu j}^P \sqrt{2\pi\omega_{1j}}\}] \quad (29)$$

A fraction  $\frac{1}{2}\lambda$  of unpolarized product formed during the first encounter has been included in eq.(29); a factor  $c = 1 - p(1 - \frac{1}{2}\lambda(1 - \lambda))$  accounts for the effect of multiple reencounters of pairs that fail to react during the first reencounter (cf.VIII). Comparison of eq.(29) with eq.(24) shows that F-type polarization is opposite to that from S precursors (hence similar to T-type polarization) for all magnetic fields.

#### D-products.

Polarization in products from radicals that escape from the "cage" by diffusion (D-products) can be treated similarly. Generally it is not simply related to P-product polarization as in the high field case, where P and D-products behave opposite. In the case of D-products we have to count contributions from pairs in all four electronic states, not only from the S-state as in case of P-products. Therefore, the matrices  $Q^D$  and  $V^D$  (analogous to eq.11 and 19) are defined in this case

$$Q^D = \epsilon \otimes S^D \quad (30)$$

$$V_{\nu 1}^D = \sum_n Q_{\nu n}^D T_{n 1} \quad (31)$$

where  $\epsilon$  is again the unit matrix of order 4;  $S^D = S^{D_a} S^{D_b}$ ;  $S^{D_a}$  being the eigenvector matrix (of order  $L_a$ ) of the product of fragment  $a$ :  $(S^{D_a})^{-1} H^{D_a} S^{D_a} = \Omega^{D_a}$ . The same analysis as given above leads to a quantity

$$R_{f\nu}^G(t) = \sum_{1,j} V_{f\nu;1}^D V_{f\nu;j}^D W_{1j}^G e^{i(\omega_j - \omega_1)t} \quad (32)$$

which is analogous to  $P_{\nu}^G(t)$ . We have written  $f\nu$  for  $\nu$  ( $f$  labels electronic states and  $\nu$  the nuclear state of interest). The populations  $D_{\nu}^G$  are obtained as follows (cf. footnote 26):

$$D_{\nu}^G = \int_0^{\infty} dt \left[ R_{1\nu}^G(t) f(t) (1 - \lambda) + \sum_{f=2}^4 R_{f\nu}^G f(t) \right] =$$

$$= \sum_{f=1}^4 \sum_{l,j} V_{f\nu,l}^D V_{f\nu,j}^D W_{lj}^G (p - m\sqrt{2\pi\omega_{lj}}) - P_{\nu}^G \quad (33)$$

The factor  $(1 - \lambda)$  takes into account the depletion of singlet pairs due to recombination.  $P_{\nu}^G$  is given by eq.(22) (but with  $S^D$  instead of  $S^P$ ). Substituting eq.(23) and (25) for S and T cases respectively, we arrive at the following results:

S-precursor:

$$D_{\nu}^S = p - m \sum_f \sum_{r,l,j} T_{1r,l} T_{1r,j} V_{f\nu,l}^D V_{f\nu,j}^D \sqrt{2\pi\omega_{lj}} - P_{\nu}^S \quad (34)$$

T-precursor:

$$D_{\nu}^T = p - \frac{m}{3(1-p)} \sum_f \sum_{e=2}^4 \sum_{r,l,j} T_{er,l} T_{er,j} V_{f\nu,l}^D V_{f\nu,j}^D \sqrt{2\pi\omega_{lj}} - P_{\nu}^T \quad (35)$$

It can be easily verified that eq.(34) and (35) represent polarization of opposite character also in this case. It is also to be noted that  $P_{\nu}^S$  and  $P_{\nu}^T$  depend on  $\lambda$ , while the second terms in eq.(34) and (35) do not. Therefore, it is possible to estimate  $\lambda$  from relative line intensities in the low field CIDNP spectrum of a D-product. If  $\lambda = 0$  there is still polarization in low fields, whereas in high fields there is not.

The populations of fragment a can be obtained from  $D_{\nu}^G$  through  $D_{\nu a}^G = \sum_b D_{\nu b}^G$ , where the summation extends over the nuclear states of

fragment b.

Enhancement factors can be calculated from the populations  $P_{\nu}^G$  and  $D_{\nu}^G$ , by the procedures of VIII. A computer program (Fortran IV) has been written, based on the formalism presented in this section.

## 2.4 Stage c. The Populations in $H_0$ .

Now we have to see what happens, when the sample, polarized in the field  $H_r$  is transferred to the spectrometer field  $H_0$ . Generally one will try to carry out this transfer as fast as possible, because one has to record the spectrum (or part of it) before the nuclear spins have relaxed. There are two problems associated with the rapidity of the transfer. The first, which regards the axis of quantization, can be discussed in the case of a one proton system. The directions of  $H_r$ ,  $H_0$  and of intermediate fields need not be the same. However, the magnetization follows the instantaneous field direction, if the following condition is met<sup>12</sup>:

$$\frac{dH}{dt} \ll \gamma H^2 \quad (36)$$

Thus the transfer is "adiabatic" in this sense, roughly, if the transfer time is longer than the reciprocal of the precession frequency,  $\tau = (\gamma H)^{-1}$  sec. For protons  $\gamma = 2.7 \cdot 10^4$  radians/sec G; hence, for a field of only 1 G this time  $\tau = 3.7 \cdot 10^{-5}$  sec, so that the adiabatic condition will always prevail in practice<sup>13</sup>. Accordingly we have found the spectra to be independent of the direction of  $H_r$  relative to  $H_0$ .

The second problem arises because of the fact that the eigenstates of coupled nuclei in  $H_r$  may differ from those in  $H_0$ . As mentioned above we may ask again whether the transfer occurs adiabatically or not (adiabatic in the sense of the system remaining in the same eigenstate).

For two groups of protons  $i, j$ , with coupling constant  $J_{ij}$  (in Hz) and chemical shift difference  $\delta_i - \delta_j$  (in ppm) the states are determined by the ratio  $2\pi J_{ij} / \gamma H (\delta_i - \delta_j) 10^{-6}$ .

For  $J_{ij} = 7$  Hz and  $\delta_i - \delta_j = 2$  ppm the states change appreciably in the region  $H = 200 - 5000$  G. The matrix element responsible for the mixing of nuclear states is  $\frac{1}{2} J_{ij}$ . The system behaves adiabatically during transfer if the time spent in the critical region (200 - 5000 G) is longer than  $\tau' = (\frac{1}{2} J_{ij} 2\pi)^{-1}$  sec, which is 1/22 sec in our example. This is short enough to expect adiabatic behaviour, which, indeed, has been observed experimentally (vide infra). For small coupling constants, however, there may occur deviations from this adiabatic behaviour.

In order to determine the spectrum in  $H_0$  after adiabatic transfer we have to identify the population of a state in  $H_0$  with the calculated population of the same eigenstate in  $H_r$ . In other words we have to know the correlation diagram, connecting high field with low field levels.

In the case of  $A_n B$  nmr spectra, where the highest order of sub-matrices is 2, this correlation is easily found. However, in more complex spectra, this presents a computational problem, since in the usual matrix diagonalization procedures the correlation is lost. We solved the problem by calculating a large number (k) of spectra, starting in  $H_R$  and multiplying the field each time by a factor  $x = \exp[k^{-1} \ln(H_0/H_R)]$ , ending up in  $H_0 = H_R x^k$ . In this way the correlation is found and thus the high field populations. For a complex spectrum like the propene spectrum of fig.6, the number of steps required was  $k = 300$  when  $H_R = 0.5$  G. For still higher values of k the CIDNP spectrum did not change appreciably. Therefore, this is a time-consuming, though effective procedure ( the propene problem for a single  $H_R$ , with  $k = 300$  took 45 min on a IBM 360-50 computer).

### 3. Qualitative Features and Predictions of the Theory.

#### 3.1 Effects of $S-T_{\pm}$ mixing.

The expressions for the populations  $P_V^G$  and  $D_V^G$ , derived in section 2.3, do not particularly excel in transparency. It may be asked if simpler procedures would not give similar results; these would have the additional advantage of giving more insight into the problem. For instance, a perturbation treatment has been used by Glarum<sup>9</sup>, who considered mixing of only two levels at a time. We will examine what can be learned from simpler arguments and compare predictions with those of the general formalism presented above.

The effects of  $S-T_{\pm}$  transitions will be discussed in the case of a one-proton radical pair, starting in the S-state. If the nuclear states are denoted by  $|+\rangle$  and  $|-\rangle$ , the "selection rules" (cf.eq.4) lead to the following allowed transitions from the S-level:  $|S+\rangle \rightarrow |T_0+\rangle$ ,  $|S-\rangle \rightarrow |T_0-\rangle$ ,  $|S+\rangle \rightarrow |T_+-\rangle$ , and  $|S-\rangle \rightarrow |T_+\rangle$ . The  $S-T_0$  transitions alone would not give appreciable polarization in very low fields (below about 100 G), because the  $\Delta g$  term is very small (transition probabilities are about the same for  $|+\rangle$  and  $|-\rangle$  states). Thus polarization in this field region must arise from differences in  $S-T_+$  and  $S-T_-$  transitions. These are depicted in the energy level scheme of figure 1.

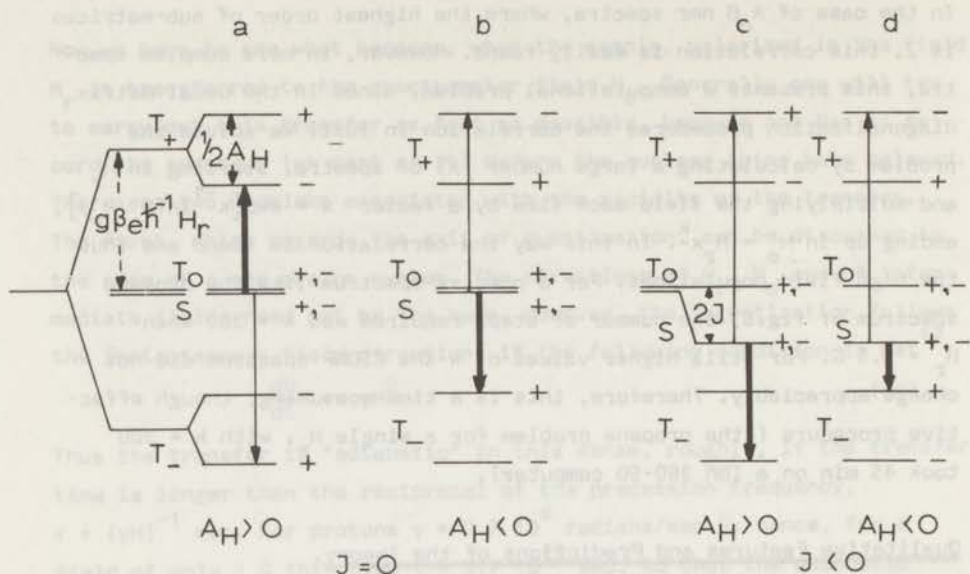


Figure 1. Energy levels of a one-proton radical pair in a magnetic field  $H_r$ . Nuclear states are designated by + and -.  $S \rightarrow T_{\pm}$  transitions are indicated; the heavier arrows represent larger transition probabilities.  $A_H$  is the hyperfine coupling constant;  $J$  is the exchange integral.

The degeneracy of the T-states is lifted by the Zeeman term; each of the  $T_+$  and  $T_-$  levels is further split by the hf. interaction. According to perturbation theory an "adiabatic transition"  $i \rightarrow j$  would have a probability

$$P_{ij} = f |H_{ij}|^2 / (E_i - E_j)^2 \quad (37)$$

where  $f$  is a dynamical factor and  $E_i$  and  $E_j$  are the zero-order energies. For  $S \rightarrow T_{\pm}$  transitions only the values of  $(E_i - E_j)$  differ. Smaller energy differences give rise to larger transition probabilities, indicated by the heavy arrows in fig.1. In the case that  $J = 0$  and  $A_H > 0$  (fig.1a) the predominance of  $|S\rangle \rightarrow |T_+\rangle$  transitions would lead to emission (E) in both recombination and "escape" products, since the  $|-\rangle$  state (upper state in the product) is preferentially populated. When  $A_H < 0$ , however,  $|S\rangle \rightarrow |T_+\rangle$  transitions are more probable,

giving enhanced absorption (A). In case of a negative  $J$  (fig.1c and d),  $S$  and  $T_0$  states are no longer degenerate and both positive and negative  $A_H$  would give A (at least when  $|J| > \frac{1}{2}|A|$ ) Thus we see that the sign of the polarization does not depend on the magnitude of  $J$  when  $A_H < 0$ , but is critically dependent on  $|J|$  when  $A_H > 0$ . For positive  $J$  the argument is reversed: positive  $A_H$  would give E, whereas for a negative  $A_H$ , A or E could occur, depending on the magnitude of  $J$ .

On the basis of this simplified treatment one would expect that these polarization effects due to  $S-T_{\pm}$  mixing would go through a maximum, when the field is increased and die out at large fields. However, computer calculations, based on the formalism of section 2, show that matters are more complicated, at least in the case of positive  $A_H$ . In figure 2 the result of some calculations for the one-proton case are presented.

The curves represent the magnetic field dependence of the enhancement factor  $V'$  for different negative values of  $J$  where

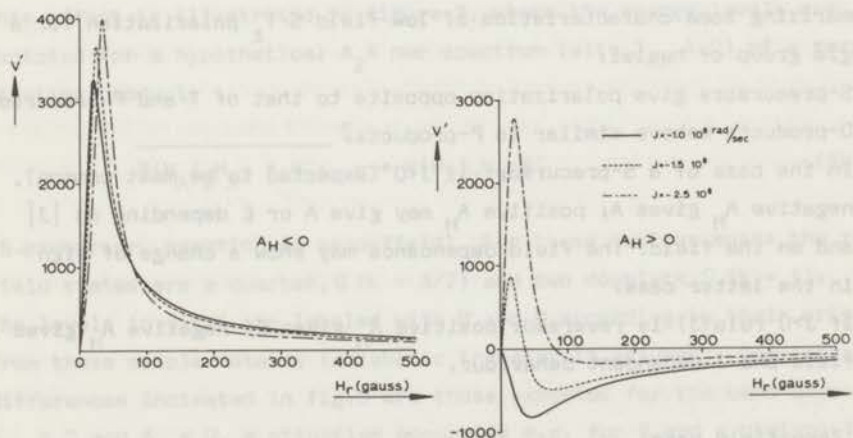


Figure 2. Polarization versus magnetic field ( $H_r$ ) calculated for a one-proton radical pair with  $A_H = -4.4 \cdot 10^8$  rad/sec (left) and  $A_H = +4.4 \cdot 10^8$  rad/sec (right). Values for the exchange integral ( $J$ ) are indicated in the figure.

$$V' = (P_{\nu}^S - P_{\mu}^S) \frac{kT}{g_N^8 H_0} \quad (38)$$

and  $|\nu\rangle = |+\rangle$ ,  $|\mu\rangle = |-\rangle$ .  $P_{\nu}^S$  is given by eq.(24). The factor  $kT/g_N^8 H_0$  has been set equal to  $10^{-5}$ . It can be seen, that when  $A_H < 0$  (fig.2a), the behaviour is "normal": only the magnitude of  $V'$  is affected by  $|J|$ . However, when  $A_H > 0$ ,  $V'$  changes sign for certain values of  $J$ . We have actually observed this peculiar behaviour (even a double change of sign, due to a  $\Delta g$  effect); an example is discussed in section 4 (cf.fig.7). Apparently it arises from an interference effect, due to the simultaneous mixing of  $S, T_0$  and  $T_+$  (or  $T_-$ ) states. Garst *et al*<sup>3</sup> have mentioned calculations of this type of oscillations. Although they do not give details, their calculations are probably similar to ours, except for a different averaging procedure.

As far as we can see, this behaviour would not follow from perturbation treatments<sup>9</sup>, allowing for mixing of only two states at a time; it seems necessary to go to second order perturbation theory, or to solve a set of coupled equations, as we have done.

Summarizing some characteristics of low field  $S-T_{\pm}$  polarization for a single group of nuclei:

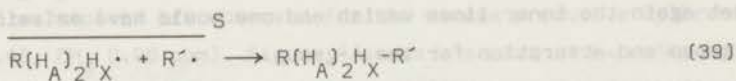
1. S-precursors give polarization opposite to that of T- and F-precursors.
2. D-products behave similar to P-products.
3. In the case of a S-precursor: if  $J < 0$  (expected to be most common), negative  $A_H$  gives A; positive  $A_H$  may give A or E depending on  $|J|$  and on the field. The field dependence may show a change of sign in the latter case.
4. If  $J > 0$  rule(3) is reversed: positive  $A_H$  gives E; negative  $A_H$  gives field and J dependent behaviour.

### 3.2 The Zero-field case.

In zero magnetic field there can be no polarization for a single nucleus, because there is no preferred direction of quantization. Polarization can only arise, when at least two coupled nuclei are present, due to unequal population of the zero-field levels of the product. These levels

are characterized by the quantum numbers  $K$  and  $M_K$ , because nuclear states are eigenstates of  $K^2$  and  $K_z$  ( $K$  is the total nuclear spin operator  $K = \sum_{i=1}^n I_i$ ). It will be shown in the Appendix that each  $K$ -manifold is uniformly populated, i.e. populations are independent of  $M_K$ . When only two coupled groups of equivalent nuclei (say  $n_i$  of type  $i$  and  $n_j$  of type  $j$ ) are present in the product and sample transfer to  $H_0$  occurs adiabatically, this leads to the so-called "n-1 multiplets": nuclei  $i$  (appearing down-field in the spectrum, say) normally exhibiting a multiplet of  $n_j + 1$  lines (for spin  $\frac{1}{2}$  nuclei) will now give rise to a multiplet of  $n_j$  lines, the high field line being absent; similarly, for the nuclei  $j$  (appearing up-field): a multiplet of  $n_i$  lines (instead of  $n_i + 1$ ), the low field line being absent. The polarizations are E for the down-field group and A for the up-field group or vice versa (see below). This phenomenon has first been noticed by Glarum<sup>9</sup>, who treated the case of two nuclear spins by explicit calculation. A more general proof (based on our formalism) of the equality of populations within the  $K$ -manifolds, giving rise to the "n-1 multiplets", will be given in the Appendix.

This effect is illustrated in figure 3, where the energy levels are depicted for a hypothetical  $A_2X$  nmr spectrum (with  $J_{AX} > 0$ ) of a recombination product:



(S-precursor, reaction in zero-field). For three nuclear spins the zero-field states are a quartet, Q ( $K = 3/2$ ) and two doublets, D ( $K = \frac{1}{2}$ ); the levels in fig.3 are labeled with Q and D according to their origin from these coupled states (adiabatic transfer is assumed). Population differences indicated in fig.3 are those expected for the case where  $A_A > 0$  and  $A_X < 0$ , a situation occurring e.g. for  $\beta$  and  $\alpha$  protons in alkyl radicals. From the assignments of transitions it can be seen that reason of the absence of the inner lines in the CIDNP spectrum is, that these lines belong to transitions between equally populated states, originating from states with the same  $K$ -multiplicity. Furthermore, it can be seen that emission and absorption effects balance, this being a general property of zero-field spectra.

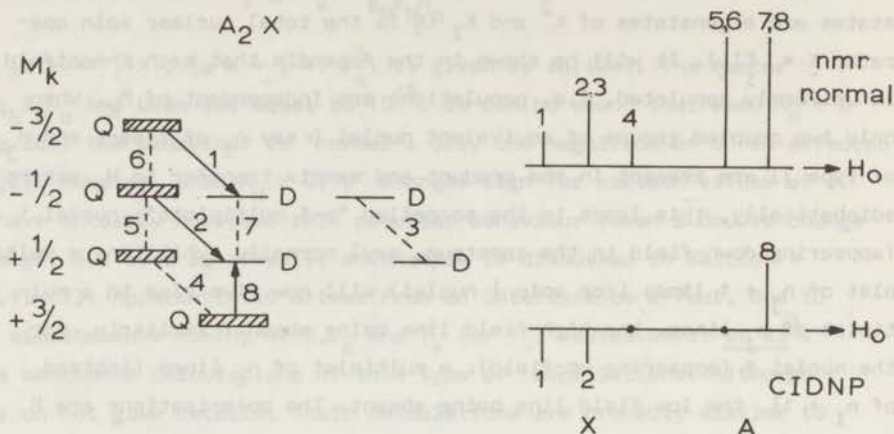


Figure 3. Energy levels and nmr spectra (normal and zero-field CIDNP) for a  $A_2X$  case, with  $J_{AX} > 0$ . Correlation with the zero-field levels is indicated by Q (quartet) and D (doublet). Numbers indicate assignment of transitions.

It should be noted, that the inner lines always are absent: when  $J_{AX}$  is negative, both the correlation with the zero-field levels and the assignment of transitions in the level diagram change in such a way, that again the inner lines vanish and one would have emission for the X-group and absorption for the A-group.

For predictions as to the sign of the effects (E for nuclei i and A for j or vice versa) one may again use the rule, which was derived in VIII for multiplet effects:

$$\Gamma_{me} = \mu \epsilon A_i A_j J_{ij} \sigma_{ij} \begin{cases} + E/A \\ - A/E \end{cases} \quad (40)$$

where the symbols have the same meaning as in VIII:  $J_{ij}$  is the nuclear coupling constant,

$$\mu \begin{cases} + & \text{T and F precursor} \\ - & \text{S precursor} \end{cases} \quad \epsilon \begin{cases} + & \text{recombination product} \\ - & \text{"escape" product} \end{cases}$$

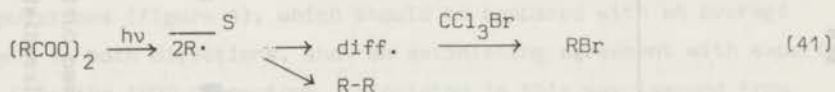
$$\sigma_{ij} \begin{cases} + & \text{nuclei i and j in the same radical} \\ - & \text{nuclei i and j in different radicals.} \end{cases}$$

E/A has to be interpreted now as E for the nuclei appearing down-field in the spectrum, and A for the up-field group. In the example of fig.2, discussed above, one would have  $\Gamma_{me} = - + + - + + = +$ , E/A. Thus, when this reaction (39) was run in a high field, one would expect E/A multiplets, whereas in zero-field it gives E and A "n - 1 multiplets" for  $I_X$  and  $I_A$  respectively. The zero-field effects discussed here remain visible to some extent, when reactions are run in low fields, but are superimposed with effects due to differences  $S-T_+$  and  $S-T_-$  mixing, as discussed in section 3.1.

#### 4. Experimental Examples.

##### 4.1 Photolysis of Propionyl Peroxide.

A solution of about 0.4 M propionyl peroxide (PPO) and 0.5 M  $CCl_3Br$  in  $CCl_4$  was irradiated in a separate magnet during 60 sec and rapidly transferred to the probe of an A-60 spectrometer. The reactions are as follows:



where  $R\cdot = CH_3CH_2\cdot$ . Pair formation occurs from a S-state. In high field (14000G) A/E multiplets are observed for the escape product ethylbromide ( $RBr$ ) ( $CH_2$  2.45,  $CH_3$  0.90 ppm). Figure 4 shows a series of experiments in different fields  $H_r$ . The spectra of  $CH_2$  and  $CH_3$ -groups of ethylbromide were recorded in separate experiments; scans in both directions (for fresh samples) are presented in figure 4. The effect of nuclear relaxation can be observed clearly from the difference between middle and lower traces. When  $H_r = 0.5$  G a spectrum results, which is almost that expected for the zero-field case: "n - 1 multiplets" (the quartet has become a triplet, the triplet appears as a doublet). The "phase" is such as predicted by rule (40) for an escape product from a S precursor. We have  $A(CH_2) = -22$  G,  $A(CH_3) = +27$  G,  $J_{ij} = +6.4$  Hz. Thus  $\Gamma_{me} = - - - + + + = -$ , A/E, and hence A for the low field  $CH_2$  - group and E for the high field  $CH_3$  - group.

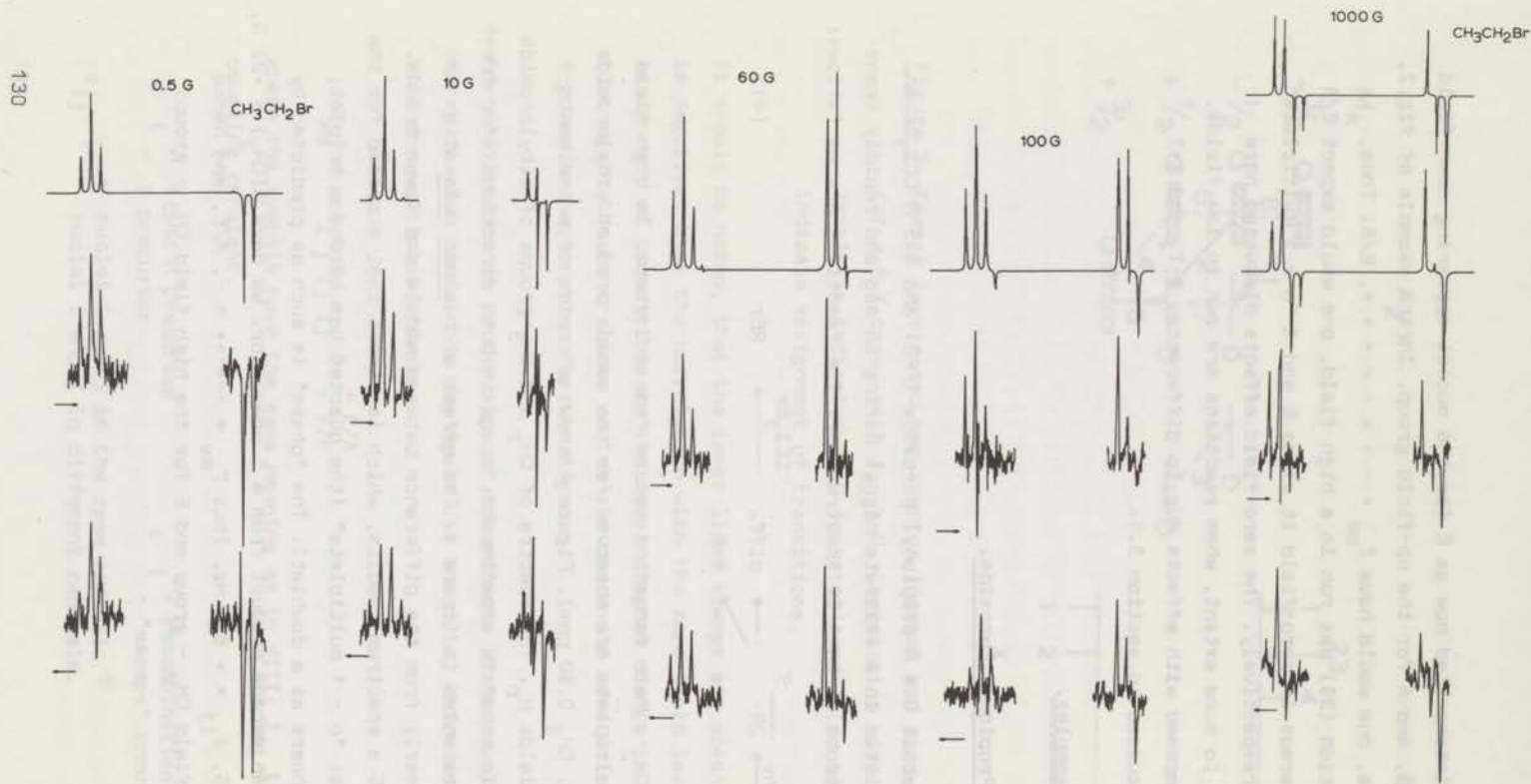


Figure 4. 60 Mc spectra of ethyl bromide formed during photolysis of 0.4 M propionyl peroxide in  $\text{CCl}_4$  in the presence of 0.5 M  $\text{CCl}_3\text{Br}$ . Irradiation was carried out in a separate magnet, in fields  $H_r$  as indicated in the figure. Scans in both directions are presented (see arrows). Computer simulations for escape from the pair  $\text{CH}_3\text{CH}_2\cdot/\text{R}\cdot$  with  $A(\text{CH}_2) = -22$  G,  $A(\text{CH}_3) = 27$  G,  $J = -5 \cdot 10^8$  rad/sec,  $\lambda = 0.75$  are shown on top. For the 1000 G top spectrum an extra nucleus  $I = 5/2$ ,  $A = 25$  G, has been added to  $\text{R}\cdot$ .

Proceeding to higher fields  $H_r$  a striking difference in behaviour of the methylene and methyl groups is observed: whereas the  $CH_2$  spectrum did not alter very much, the  $CH_3$  spectrum changed drastically, first acquiring A character and ending up as A/E multiplets at the higher fields. This reflects the different signs of the hf. coupling constants as discussed in section 3.1.

Computer calculations, based on the theory given in section 2, have been carried out for this case. As the complete problem exceeded the capabilities of our computer, we treated the problems as escape from the truncated pair  $CH_3CH_2/R\cdot$  where  $R\cdot$  is a dummy radical without nuclei ( $\Delta g = 0$ ). This was satisfactory in the low field range, but caused some deviations at intermediate fields (*vide infra*). The transfer of the sample to the probe was assumed to occur adiabatically. The values of  $J$  and  $\lambda$  were varied. The best results were obtained for  $\lambda = 0.75$  and  $J = -5 \cdot 10^8$  radians/sec. This value of  $J$  is consistent with the high field spectra of ethylchloride (cf. VIII and XII<sup>14</sup>). The final series of simulations (figure 4), which should be compared with an average of scans in both directions, show an astonishing agreement with experiment. Only the 1000 G spectrum, calculated in this way (second from top) showed more or less serious deviations, which, in our opinion, are due to the neglect of the additional nuclei in the pair. By adding an extra nucleus with spin 5/2 and with  $A = 25$  G, to the dummy radical  $R\cdot$  (the maximum that the computer could handle), the simulation improved significantly (top spectrum, 1000 G): more A character for the quartet and more E for the triplet. This influence of nuclei, which do not contribute to the nmr spectrum of the product under consideration is not observed in high field spectra. It is probably due to shifting of certain  $T_{\pm}$  levels with respect to the S level, enhancing the  $S-T_{\pm}$  transition probabilities to some extent.

Since we are dealing with an escape product, the value of  $\lambda$  affects the relative intensities in the CIDNP spectrum (cf. section 2.3). This can be seen in figure 5, where some calculations are presented for the ethylbromide  $CH_3$  - group, for reaction in a field  $H_r = 10$  G. The best value  $\lambda = 0.75$  was obtained by comparing simulations for other fields as well.

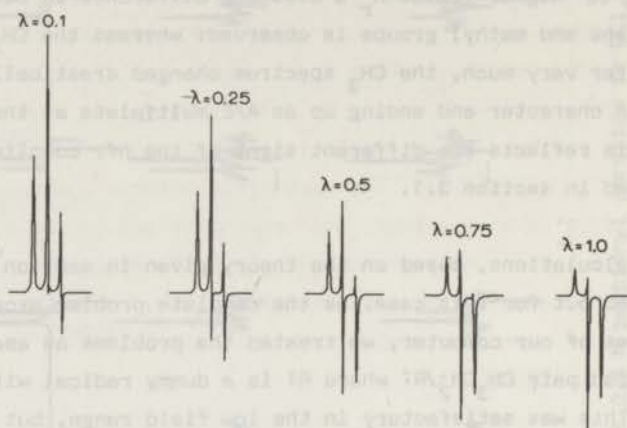
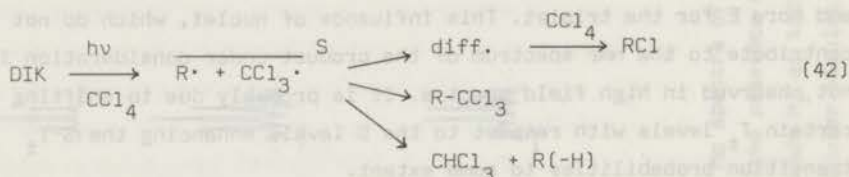


Figure 5. Simulated spectra of the  $\text{CH}_3$  - group of ethylbromide, formed in a field of 10 G, for various values of  $\lambda$ .

#### 4.2 Photolysis of Diisopropyl ketone in $\text{CCl}_4$ .

The photoreaction of diisopropyl ketone (DIK) in  $\text{CCl}_4$  has been discussed in VII<sup>15</sup> and a 60 Mc CIDNP spectrum has been presented there. The reaction probably involves complex formation of excited S state ketone with  $\text{CCl}_4$ . High field CIDNP effects could be accounted for by assuming formation and subsequent reactions of isopropyl/trichloromethyl radical pairs (S-pairs):



where  $\text{R}^\bullet = (\text{CH}_3)_2\dot{\text{C}}\text{H}$  and  $\text{R(-H)}$  is propene. Figure 6b shows a 60 Mc spectrum taken in parts after 90 sec irradiation of a solution of DIK in  $\text{CCl}_4$  in a field  $H_r = 100$  G. The traces of figure 6c are run just after those of 6b (of the same sample) and show the effect of relaxation. They represent still large polarizations, as the signals vanish almost completely, except for the parent compound ( $\delta$  1.04 ppm).

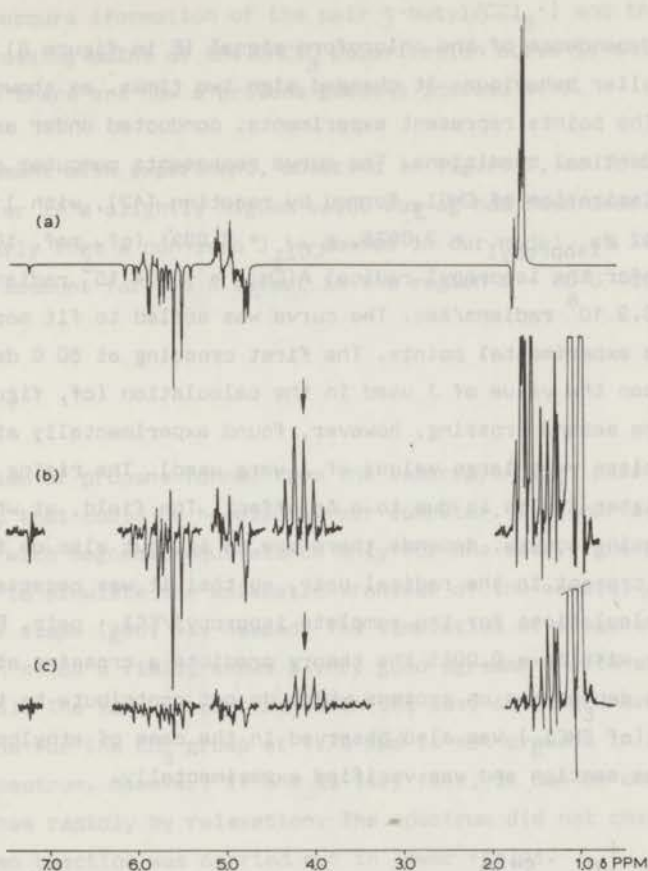


Figure 6. 60 Mc spectrum taken in parts after irradiation of diisopropyl ketone in  $\text{CCl}_4$  in a field  $H_r = 100$  G (b). Second scans of the same samples, taken just after those of (b) are shown in (c). The arrows indicate the centre line of the methine septet of isopropylchloride. A computer simulation of the propene and  $\text{CHCl}_3$  spectrum is shown on top (a) (see text).

Enhancements are observed for chloroform ( $\delta$  7.27 ppm), propene (CH 5.73,  $\text{CH}_2$  4.92,  $\text{CH}_3$  1.72 ppm), isopropylchloride (CH 4.13,  $\text{CH}_3$  1.54 ppm) and trichloroisobutane ( $\text{CH}_3$  1.30 ppm). Polarization of the first three products will now be discussed.

## Chloroform.

The field dependence of the chloroform signal ( $E$  in figure 6) exhibited a very peculiar behaviour: it changed sign two times, as shown in figure 7. The points represent experiments, conducted under as near as possible identical conditions. The curve represents computer calculations for the polarization of  $\text{CHCl}_3$  formed by reaction (42), with  $J = -1.0 \cdot 10^8$  radians/sec,  $g_{\text{isopropyl}} = 2.0026$ ,  $g_{\text{CCl}_3} = 2.0091$  (cf. ref. 16), and hf. parameters for the isopropyl radical  $A(\text{CH}_3) = +4.4 \cdot 10^8$  radians/sec,  $A(\text{CH}) = -3.9 \cdot 10^8$  radians/sec. The curve was scaled to fit more or less to the experimental points. The first crossing at 80 G depended strongly upon the value of  $J$  used in the calculation (cf. figure 2 for  $A_H > C$ ); the second crossing, however, found experimentally at 490 G, did not (unless very large values of  $J$  were used). The rising of the curve at higher fields is due to a  $\Delta g$  effect. The field, at which the second crossing occurs, depends therefore on  $\Delta g$ , but also on the number of protons present in the radical pair, so that it was necessary to make the calculations for the complete isopropyl/ $\text{CCl}_3$  pair. For a one-proton pair with  $\Delta g = 0.0065$  the theory predicts a crossing at about 200 G. This dependence on protons which do not contribute to the nmr transition (of  $\text{CHCl}_3$ ) was also observed in the case of ethylbromide in the previous section and was verified experimentally.

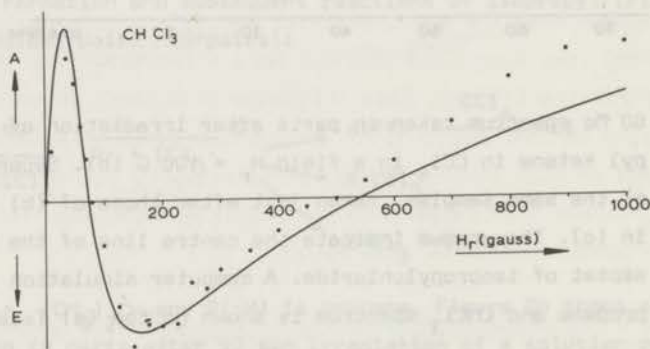


Figure 7. Polarization of  $\text{CHCl}_3$  (formed during irradiation of DIK in  $\text{CCl}_4$ ) versus magnetic field. The curve represents computer calculations ( $J = -1.0 \cdot 10^8$  rad/sec) and has been scaled to the experimental points.

When pinacolone (methyl t-butyl ketone) in  $\text{CCl}_4$  is irradiated a similar reaction occurs (formation of the pair t-butyl/ $\text{CCl}_3\cdot$ ) and the observed second crossing point of the  $\text{CHCl}_3$  polarization curve is shifted to 550 G, as there are now 9 protons present instead of 7.

The agreement with experiment, observed in figure 7, would have been even better if a slightly higher value for  $\Delta g$  had been used. It shows most clearly that a non-zero  $J$  is needed in our model, at least in this case, to account for the A effect in the region 0 - 80 G (cf. figure 2 and 7).

### Propene.

The problem of propene formed from the isopropyl/ $\text{CCl}_3\cdot$  pair was about the limit that could be handled by our computer. It comprises a g-spin problem, with magnetic equivalence only for one methyl group (cf. VIII). In order to simulate the adiabatic transfer of the sample, a large number of steps (300) was needed. The simulation of propene and  $\text{CHCl}_3$ , formed in a 100 G field, shows a very good agreement with experiment (figure 6). The same parameters as in the case of  $\text{CHCl}_3$  have been used. The E line for the  $\text{CH}_3$  group at 1.70 ppm is not present in the experimental spectrum. However, if one is very fast, it can be observed, but it vanishes rapidly by relaxation. The spectrum did not change very much, when reaction was carried out in lower fields.

The propene spectrum resulting from reaction in a field of 1500 G, and a computer simulation are shown in figure 8. There are some deviations; e.g. the A lines, predicted for the methine proton at 5.70 ppm, seem to be missing. The general behaviour of the propene spectrum, however, was reasonably well reproduced over the whole field range.

The prediction of the general theory, that S-pairs behave opposite to T and F-pairs, in low fields as well as in high fields, is borne out by the spectra presented in figure 9. In both cases reactions were run in a field  $H_r = 10$  G. Spectrum (b) shows the vinyl region of propene formed from the isopropyl/ $\text{CCl}_3\cdot$  radical pair during photolysis of DIK in  $\text{CCl}_4$  (S-case), and is similar to figure 6.

Figure 8.

60 Mc spectrum of propene, formed in a field  $H_r = 1500$  G (in the photoreaction of DIK in  $CCl_4$ ). A computer simulation is shown on top.

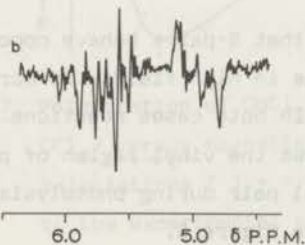
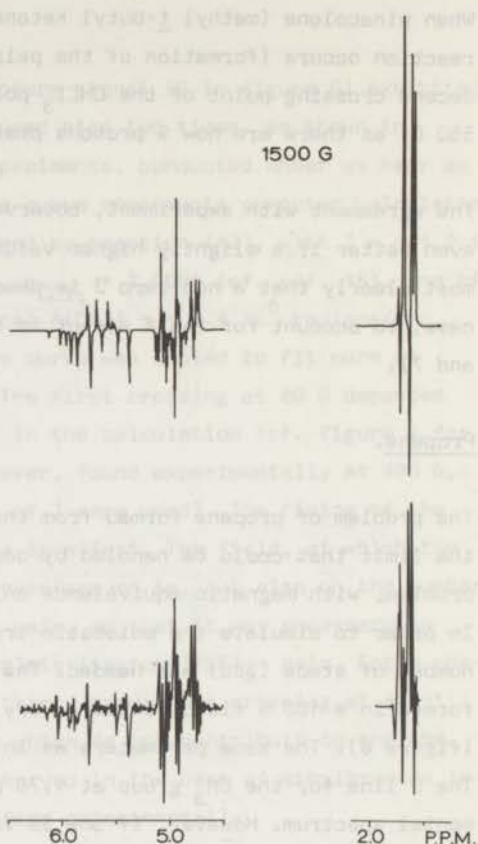


Figure 9.

Spectrum of the vinyl-region of propene, formed during photolysis of DIK in  $CF_2Cl-CFCl_2$  (a), and in  $CCl_4$  (b). Both reactions were run in a field of 10 G.

Spectrum (a) was obtained after photolysis of DIK in the freon  $\text{CF}_2\text{Cl}-\text{CFC1}_2$ , in which case propene is formed mainly from the pair of two isopropyl radicals ( F or T-case, cf. VII). The spectra (a) and (b) are almost exactly each others mirror image. They show, incidentally, that the nature of the other radical in the pair is not important in the very low field range.

#### Isopropylchloride.

The methine proton shows a "n-1 multiplet" (sextet) in very low fields, which is still visible at 100 G in figure 6b. From the lower trace in this figure (6c) it can be seen that relaxation towards thermal equilibrium is not uniform, but is faster for the low field lines of the septet (this multiplet disappears eventually). This skew relaxation seems to be particularly troublesome for this compound. Tentative calculations<sup>17</sup> indicated that it is possible that E lines of the septet are inverted due to nuclear dipole relaxation. Our failure to simulate correctly the high field spectra has been blamed to this effect (cf. VII). It seems to be even stronger in low fields<sup>18</sup>. An experimental indication for this can be observed in figure 10, which shows the isopropylchloride septet as it arises from reaction in a 1000 G field of a separate magnet (a), the same when reaction is run in the fringing field  $H_r = 1000$  G of the A-60 magnet (b), and a rather unusual simulation with one E line as calculated for this field (c). The difference between (a) and (b) must be due to relaxation during the time the sample dwells in the earth's field (about 1 sec). Although spectrum (b) still does not show E, the trend is in the right direction.

The spectra calculated for the methyl doublet of isopropylchloride show also deviations from experiment (figure 11), most seriously for the 100 G case. Values of  $\lambda$  close to unity gave the best results.

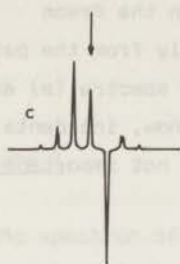


**Figure 10.** Spectrum of the methine proton ( $\delta$  4.13 ppm) of isopropylchloride, resulting from photolysis of DIK in  $\text{CCl}_4$ , in a field  $H_r = 1000$  G of a separate magnet (a), and in the fringing field (1000 G) of the spectrometer magnet (b). A computer simulation is shown on top (c).

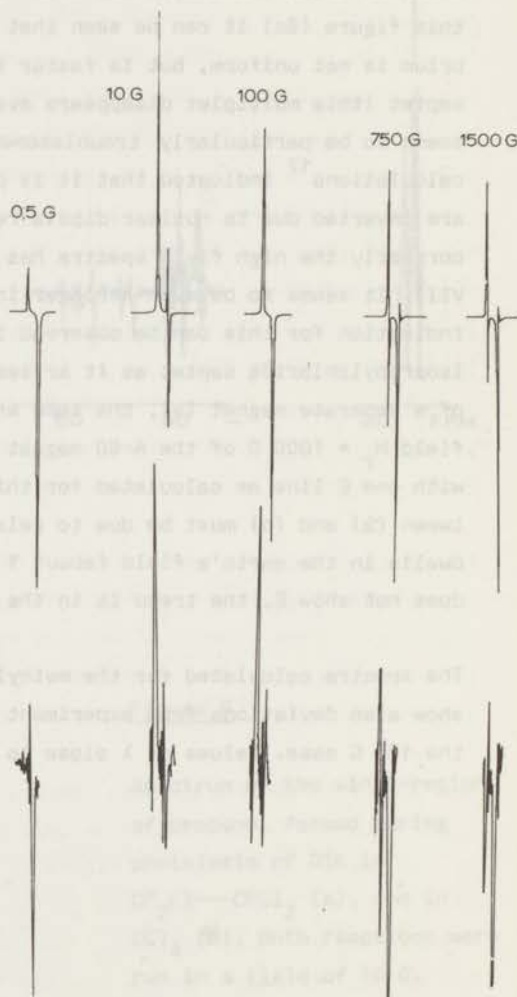
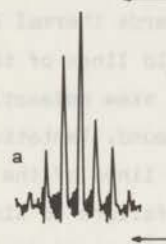


**Figure 11.**

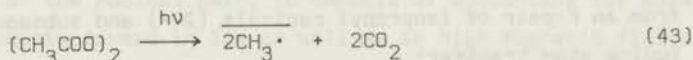
Spectra of the isopropylchloride methyl doublet after irradiation of DIK in  $\text{CCl}_4$ , in various fields as indicated in the figure. Experimental (a) and simulated (b) spectra are shown.

### 4.3 Thermal and Photochemical Decomposition of Acetyl Peroxide.

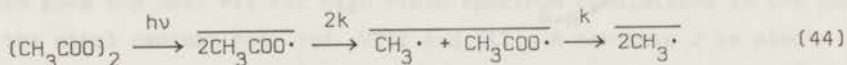
During irradiation of a solution of acetyl peroxide (AP) in  $\text{CCl}_4$  in high field (14 kG), no polarization was observed, in contrast to the thermal decomposition (cf. XI<sup>19</sup>). Irradiation in low magnetic fields resulted in polarization for ethane: E in the region  $H_r \sim 0 - 200$  G, with a maximum at 40 G, changing to A for  $H_r > 200$  G and slowly decreasing at higher fields. This behaviour is just as expected for a positive J and a negative  $A_H$  (the methyl radical has  $A_H = -23$  G =  $-4.0 \cdot 10^8$  radians/sec).

When irradiation was carried out in the presence of acetophenone, in fields  $H_r < 200$  G, we observed the a reversal of the ethane polarization (A-effect), indicating, that acetophenone acts as a triplet sensitizer for the decomposition of AP (similar to propionyl peroxide, cf. IV<sup>20</sup>). However, the effects were small, compared to the direct photolysis and we have not yet observed polarizations in fields  $H_r > 200$  G.

The thermal decomposition was carried out by heating a solution of AP in hexachloroacetone to  $120^\circ$  in a separate magnet and rapidly quenching the reaction in a bath of liquid nitrogen. The ethane line resulting from the thermal reaction exhibited qualitatively the same behaviour as in the case of photolysis, but in addition showed an increasing E effect in fields higher than about 2000 G, due to the pair  $\text{CH}_3 \cdot \text{CH}_3\text{COO} \cdot$  ( $\Delta g$  effect). The difference between the polarization in the thermal and photochemical reaction is probably due to a more rapid formation of the pair  $2\text{CH}_3 \cdot$  in the photolysis. This may occur either via concerted homolysis:



or via more rapid decarboxylation of "hot" acetoxy radicals:



If the rate of decarboxylation  $k$  would be larger than  $2 \cdot 10^{10} \text{ sec}^{-1}$  no observable polarization would be expected in the high field range. In accordance with our observations, Sheldon and Kochi<sup>21</sup> recently found

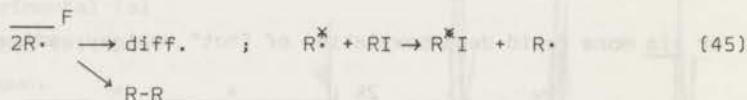
a substantially lower yield of methylacetate in the photolysis of AP, as compared to the thermal decomposition.

The negative ethane polarization at low fields parallels an observation by Garst and Cox<sup>3b</sup>, who reported E for ethane from a methyl radical pair formed in the reaction of methyl iodide with sodium mirror, run in a field of 20 G.

It is remarkable, that a positive value is required for the effective exchange integral of the methyl radical pair ( $T_0$ -state below S-state). We consider the other possible explanations suggested<sup>3b</sup> (polarization due to F-pairs or due to anisotropic electron-nuclear interactions) highly unlikely in the case of the thermal reaction, in view of the good simulation results obtained for products of <sup>13</sup>C-methyl radicals in high fields (cf. XI). F-polarization in the photolysis of AP in CCl<sub>4</sub> is also excluded, because of the observed reversal of polarization in the presence of acetophenone. A positive J would not have been anticipated, especially considering the case of the similar ethyl radical pair, where a negative J could accommodate the results (section 4.1).

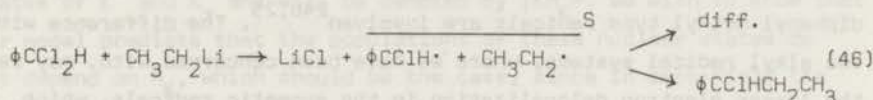
#### 4.4 Other work.

Ward et al<sup>2</sup> have reported polarization if isopropyl iodide, present during decomposition of benzoyl peroxide in the earth's field. The observed pattern, an E sextet for the methine proton and an E/A doublet (E smaller than A) for the methyl group, is in accordance with escape from an F-pair of isopropyl radicals (2R<sup>•</sup>) and subsequent thermoneutral iodine atom transfer:



In zero-field E and A "n-1 multiplets" are expected:  $\Gamma_{me} = + - + - + + = +$ , E/A. The presence of the E line in the methyl doublet is reproduced by a computer simulation taking  $H_r = 0.5$  G and  $0.5 < \lambda < 1.0$ . It is probably not caused by deviations from an adiabatic behaviour during transfer.

Another system reported in this paper<sup>2</sup> involves the formation of 1-chloro-1-phenylpropane in the reaction of  $\alpha,\alpha$ -dichlorotoluene with ethyllithium:



The 1-proton showed an E triplet, both when the reaction was run in the earth's field and in "zero field"<sup>22</sup>. We have simulated this system with  $H_r = 0$  and with  $H_r = 0.5$  G and in both cases an E triplet, with lines of about equal intensities, was obtained for the methine proton. Apparently the inner lines of multiplets vanish in zero-field only when but two groups of equivalent nuclei are present in the product. We note, that the population of the zero-field levels still occurs uniformly within the K-manifolds; however this does not lead to "n-1 multiplets" when more than two groups are present.

Fischer and Lehnig<sup>23</sup> have studied the field dependence of the benzene line during decomposition of benzoyl peroxide. The E effect in high fields changed to A at lower fields. This behaviour would require a negative J in our model.

## 5. Conclusions.

The diffusion model of CIDNP, extended to include mixing of S with all three T states of the radical pair, is capable of accounting for polarization in products formed in low as well as in high magnetic fields. It seems necessary to retain a non-zero effective exchange integral in this model. The magnitude of J was found to be consistent with values which gave the best fit for high field spectrum simulations in the case of the ethyl radical pair (cf. VIII and XII). A non-zero J is also necessary to reproduce the peculiar oscillations of the polarization versus magnetic field curve in the case of chloroform formed in the photoreaction of diisopropyl ketone in  $\text{CCl}_4$  (figure 7), and in the case of ethane from acetyl peroxide.

Little or no information on the actual behaviour of J in diffusing radical pairs is available from other sources. Adrian<sup>24</sup> has set J = 0. This value or at least values much lower than the hf. parameters seem to give good results for high field spectrum simulations in cases where benzyl or diphenyl methyl type radicals are involved<sup>24b,25</sup>. The difference with the alkyl radical systems, where we have been concerned with, may reflect the larger electron delocalization in the aromatic radicals, which, if anything, would be expected to decrease J for a given interradsical separation. It may be noted that our averaging procedure selects those pairs which have a shorter than average separation. This is obvious in the case of recombination products because there we are concerned with pairs that eventually react. It is, however, also true for escape products in our treatment<sup>26</sup>.

It is interesting that the chemically significant parameter  $\lambda$  can be obtained from the low field CIDNP spectra. Our results for small radicals show that  $\lambda$  is close to unity. For larger radicals one might expect smaller values for  $\lambda$ , since it becomes less probable that the orientation, favourable for reaction, is attained during an encounter.

Furthermore, it appears from the low field spectra, that adiabatic behaviour during sample transfer between magnets is closely obeyed, in the case that nmr coupling constants are of the order 6-7 Hz. For coupling constants of about 1 Hz, however, departures may occur and this may partly be the cause of some of the differences between the experimental and simulated spectra of propene (figure 6 and 8).

#### APPENDIX. Populations of zero-field levels.

The Hamiltonian for a radical pair in zero-field becomes (cf. eq. 1):

$$H_{RP} = -J\left(\frac{1}{2} - S_1 \cdot S_2\right) + S_1 \cdot \sum_j^a A_j I_j + S_2 \cdot \sum_K^b A_K I_K \quad (A1)$$

A total spin operator can be defined as  $\underline{F} = \underline{S} + \underline{K}$ , where  $\underline{S} = \underline{S}_1 + \underline{S}_2$  and  $\underline{K} = \sum_i I_i$  ( $\underline{K}$  is the total nuclear spin operator). The nuclear Hamiltonian for the reaction product is simply

$$\underline{H}^P = \sum_{i>j} J_{ij} I_i \cdot I_j \quad (A2)$$

which is diagonal in the K-representation<sup>27</sup> because  $[\underline{H}^P, K^2] = 0$  and  $[\underline{H}^P, K_z] = 0$ . Therefore, the nuclear states of the product are eigenstates of  $K^2$  and  $K_z$  and will be denoted by  $|KM_K\rangle$ . We wish to show that our model predicts that the populations of these nuclear states do not depend on  $M_K$ , which should be the case, since in zero-field the system is rotationally invariant.

The zero-field CIDNP problem can be treated most conveniently in a basis  $|SM_S KM_K\rangle$ . Using this basis the formalism of section 2 can be applied. Since  $\underline{H}_{RP}$  commutes with  $F^2$  and with the components of  $\underline{F}$ ,

$$[\underline{H}_{RP}, F^2] = 0 \quad , \quad [\underline{H}_{RP}, \underline{F}] = 0 \quad (A3)$$

the eigenstates of the radical pair can be characterized by F and M (M is the eigenvalue of  $F_z$ ); the elements of the eigenvector matrix  $\underline{T}$  (eq. 5) are essentially Clebsch-Gordon coefficients. The matrix  $\underline{Q}^P$  appearing in eq. (11) becomes  $\underline{Q}^P = \underline{E}_S \otimes \underline{I}$  ( $\underline{I}$  is the unit matrix of order L) and therefore eq. (19) now reads

$$V_{v1}^P = T_{1v;1} \quad (A4)$$

As a result, we have for the population of state  $|1v\rangle = |00KM_K\rangle$  in the case of a S-precursor (cf. eq. 24):

$$P_{v'}^S = \lambda(p - m \sum_{r=1,j} T_{1r;1} T_{1r;j} T_{1v;1} T_{1v;j} \sqrt{2\pi\omega_{j1}}) \quad (A5)$$

the Clebsch-Gordon coefficient  $T_{1v;1} = \langle 00KM_K | FM \rangle$  has non-zero values for  $M = M_K, F = K$ , which restricts the sum over l and j to states with the same K and  $M_K$ . However, the coefficients  $\langle 00KM_K | KM_K \rangle$  are all equal to unity<sup>28</sup> and therefore do not depend on  $M_K$ . Furthermore,  $\omega_{j1}$  can be written

$$\omega_{j1} = |\omega_j - \omega_1| = |(\underline{H}_{RP})_{jFM} - (\underline{H}_{RP})_{1F'M'}| = |(\underline{H}_{RP})_{jKM_K} - (\underline{H}_{RP})_{1KM_K}| \quad (A6)$$

By using the fact that  $H_{RP}$  commutes with the components of  $F$  (eq.A3) it is easy to show<sup>29</sup> that the diagonal matrix elements  $(H_{RP})_{JKM_K}$  are independent of  $M_K$ . Thus the populations  $P_v^S$  do not depend on  $M_K$  either, and are all equal within a K-manifold. Since we have shown that the polarization from S and T-precursors is opposite (eq.27), the same will hold in the case of a T-precursor.

#### References and Footnotes

1. M. Lehnig and H. Fischer, Z. Naturforsch., 24a, 1771 (1969).
2. H.R. Ward, R.G. Lawler, H.Y. Loken and R.A. Cooper  
J. Amer. Chem. Soc., 91, 4928 (1969).
- 3.(a) J.F. Garst, R.H. Cox, J.T. Barbas, R.D. Roberts, J.I. Morris  
and R.C. Morrison, ibid., 92, 5761 (1970);  
(b) J.F. Garst and R.H. Cox, ibid. p. 6389.
4. S.V. Rykov, A.L. Buchachenko and V.I. Baldin,  
Zhur. Strukt. Khim., 10, 928 (1969).
5. J. Bargon and H. Fischer, Z. Naturforsch., 22a, 1556 (1967).
- 6.(a) G.L. Closs, J. Amer. Chem. Soc. 91, 4552 (1969)  
(b) G.L. Closs and A.D. Trifunac, ibid. 92, 2183 (1970).
7. R. Kaptein and L.J. Oosterhoff, Chem. Phys. Letters,  
4, 195, 214 (1969).
8. R. Kaptein, part VIII, to be published.
- 9.(a) S.H. Glarum, paper presented at the 159th National Meeting  
of the American Chemical Society, Houston, Feb. 1970.  
(b) S.H. Glarum, personal communication.
10. cf. P.L. Corio, "Structure of High-Resolution NMR Spectra",  
Academic Press, New York, 1966, p. 480.
11. R.M. Noyes, J. Amer. Chem. Soc., 78, 5486 (1956).
12. A. Abragam, "The Principles of Nuclear Magnetism", Oxford  
University Press, 1961, chapter II.
13. One might think of arranging the directions of  $H_r$  and  $H_o$  exactly  
opposite to each other, so that a negatively polarized sample  
in  $H_r$ , would show enhanced absorption in  $H_o$ . However, when the  
transfer time is 1 sec, the transverse components of the  
magnetic field would have to be less than 0.037 mG during transfer.

This condition would not appear to be easily satisfied in practice.

14. R. Kaptein, part XII to be published.
15. J.A. den Hollander, R. Kaptein and P.A.T.M. Brand, part VII, to be published.
16. A. Hudson and H.A. Hussain, Mol. Phys., **16**, 199 (1969).
17. A more detailed study of this relaxation problem is in progress.
18. In case of reaction in zero-field intramolecular dipole relaxation does not alter the populations in zero-field, because transitions between different K-manifolds are forbidden and levels within a given K-manifold have already equal populations.
19. R. Kaptein, J. Brokken-Zijp, F.J.J. de Kanter and L.J. Oosterhoff, part XI, to be published.
20. R. Kaptein, J.A. den Hollander, D Antheunis and L.J. Oosterhoff, Chem. Comm., 1687 (1970).
21. R.A. Sheldon and J.K. Kochi, J. Amer. Chem. Soc., **92**, 4395 (1970).
22. In this experiment the earth's field was shielded such that the residual field was in the milligauss range, H.R. Ward and R.G. Lawler, personal communication.
23. H. Fischer and M. Lehnig, personal communication.
24. (a) F.J. Adrian, J. Chem. Phys., **53**, 3374 (1970);  
(b) F.J. Adrian, personal communication.
25. G.L. Cross, personal communication.
26. We use the same distribution function  $f(t)$  as has been used in the case of P-products. We have considered other functions as well, e.g.  $\exp[-kt]$ , where  $k$  is a rate constant for disappearance of the radicals. However, it can be verified, that this does not lead to S-T<sub>±</sub> polarization, when  $k < \omega$ , which normally will be the case. Therefore, in our opinion, polarization in escape products is due to those pairs, which have undergone at least one unreactive reencounter, and originates from S-T transitions during the time between birth and reencounters. For this reason the function  $f(t)$  appears in eq.(33).
27. cf. ref. 10 p. 177.
28. A. Messiah, "Quantum Mechanics", North Holland, Amsterdam, Volume II, p. 1058.
29. cf. ref. 28 p. 569.

## CHAPTER XI

### CHEMICALLY INDUCED DYNAMIC NUCLEAR POLARIZATION XI THERMAL DECOMPOSITION OF ACETYL PEROXIDE.

By R. Kaptein, J. Brokken-Zijp and F.J.J. de Kanter.

(Department of Theoretical Organic Chemistry,  
University of Leiden, P.O. Box 75, Leiden,  
The Netherlands).

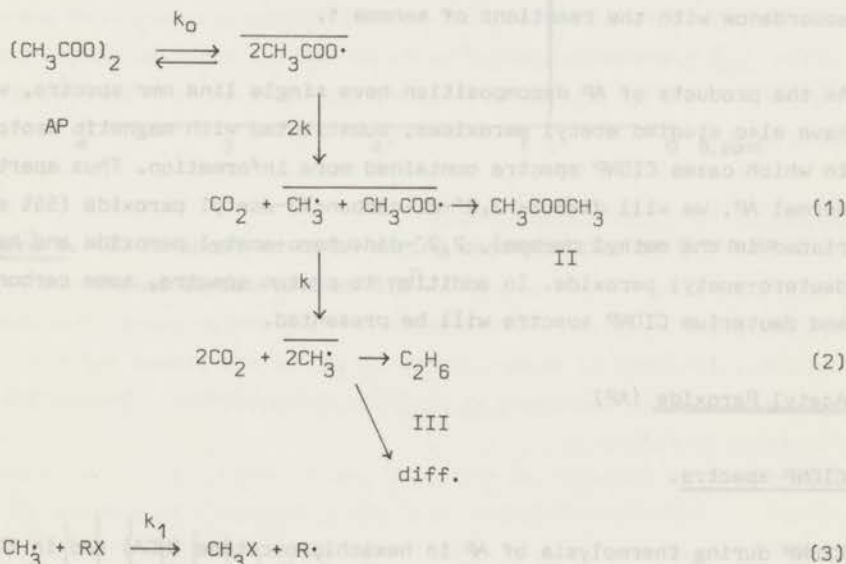
#### 1. Introduction.

The decomposition of acetyl peroxide (AP) is one of the most extensively investigated homolytic reactions. We have therefore chosen to study this reaction with nmr<sup>1</sup> in order to test current theories of CIDNP and to see whether nuclear polarization can help to answer some of the remaining questions concerning the reaction mechanism.

In most solvents the thermal decomposition of AP,  $\text{CH}_3\overset{\text{O}}{\parallel}\text{C}-\text{O}-\text{O}-\overset{\text{O}}{\parallel}\text{CCH}_3$  follows first order kinetics with a rate constant very similar to a number of other acyl peroxides<sup>2</sup>. This has been taken as evidence<sup>3</sup> for the fact that the primary step is formation of a pair of acetoxy radicals by simple O-O bond scission; this is substantiated by a study of oxygen and deuterium isotope effects<sup>4,5</sup>. Szwarc and coworkers<sup>3</sup> suggested that methylacetate and ethane were formed by a "cage" reaction, following decarboxylation of the very unstable acetoxy radical. This was inferred from their observation that these products were always formed in solution, but not in the gas-phase.<sup>18</sup> O-scrambling found in both peroxide<sup>4</sup>

and methylacetate<sup>4,6</sup> from specifically labeled AP supports the intermediacy of short-lived acetoxy radicals. Cage recombination of acetoxy radicals may be responsible for the observed viscosity dependence of the overall decomposition rate<sup>7</sup>. Recent work<sup>8</sup> has shown that <sup>18</sup>O-scrambling in the peroxide itself is also partly due to [3,3] and possibly [1,3] sigmatropic rearrangements in AP, which are, however, of no concern for us here.

Thus, from these and other studies a mechanistic picture has emerged for the thermal decomposition of AP in "inert" solvents, which is now favoured by most workers, and which is summarized in scheme 1.



Scheme 1.

RX denotes the solvent or some other substrate, to be specified later on. The bars indicate radical pairs with correlated electron spins, derived from a common parent molecule. The rate constant,  $k$ , for the decarboxylation of the acetoxy radical has been estimated to be of the order  $10^9 - 10^{10} \text{ sec}^{-1}$  by Szwarc<sup>3</sup>. Eirich and coworkers<sup>7</sup>, applying a theoretical model for geminate recombination, have found a value  $k = 1.6 \cdot 10^9 \text{ sec}^{-1}$  at  $60^\circ$  and an activation energy of 6.6 kcal/mole from product studies. Thus the time-scale of the decarboxylation process is

of the same order as that of geminate recombination<sup>9</sup>, which renders this system particularly interesting from the point of view of CIDNP, since effects of the successive pairs will be observable.

In preceding parts<sup>10</sup> we have incorporated Noyes theory of geminate diffusive recombination<sup>9,11</sup> into a previously given formalism<sup>12</sup> of the radical pair theory of CIDNP. This theory has been independently proposed by Closs<sup>13</sup>. Competitive reactions have been treated in part IX, within the framework of the diffusion model and the case of AP has already been shortly discussed as an example<sup>10b</sup>. It will be shown presently, that CIDNP spectra obtained during thermolysis of AP are in accordance with the reactions of scheme 1.

As the products of AP decomposition have single line nmr spectra, we have also studied acetyl peroxides, substituted with magnetic isotopes, in which cases CIDNP spectra contained more information. Thus apart from normal AP, we will discuss 2,2'-di-carbon-13-acetyl peroxide (55% enriched in the methyl carbon), 2,2'-dideutero-acetyl peroxide and hexa-deutero-acetyl peroxide. In addition to proton spectra, some carbon-13 and deuterium CIDNP spectra will be presented.

## 2. Acetyl Peroxide (AP)

### 2.1 CIDNP spectra.

CIDNP during thermolysis of AP in hexachloroacetone (HCA) and in thiophenol has been reported in part I. Bargon and Fischer have discussed the reaction of AP in dimethylphthalate<sup>14</sup>. A 60 Mc spectrum of a 0.1 M solution of AP ( $\delta$  2.11 ppm) in HCA at 110° is shown in figure 1. Emission (E) is observed for ethane ( $\delta$  0.83 ppm) and methylacetate ( $\text{OCH}_3$ , 3.54 ppm) and enhanced absorption (A) for methylchloride ( $\delta$  2.94 ppm) and methane ( $\delta$  0.18 ppm). At higher temperatures the E signal at 1.60 ppm becomes more clearly visible; we have tentatively assigned this line to 1,1,1,3,3-pentachlorobutan-2-one, on the analogy with results for isopropyl and *t*-butyl radicals, where A for pentachloroacetone has been observed. This E line can be observed in figure 2. This fish-bone shows the development of this system in time.

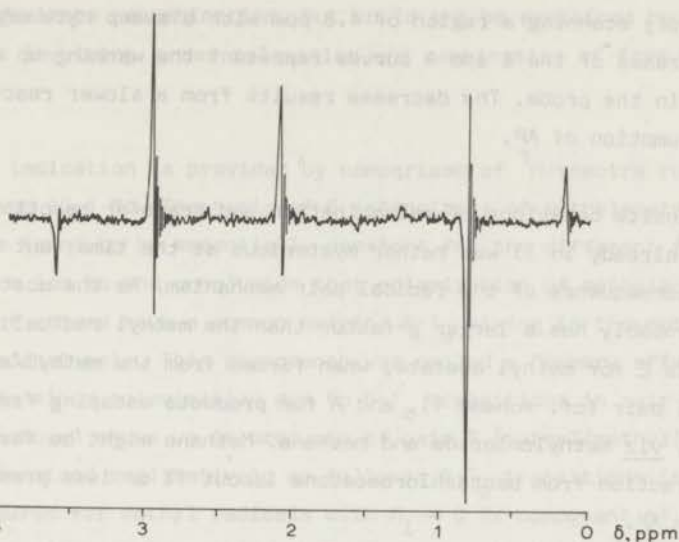


Figure 1. 60 Mc spectrum taken during decomposition of 0.1 M AP in hexachloroacetone at  $110^{\circ}$ .

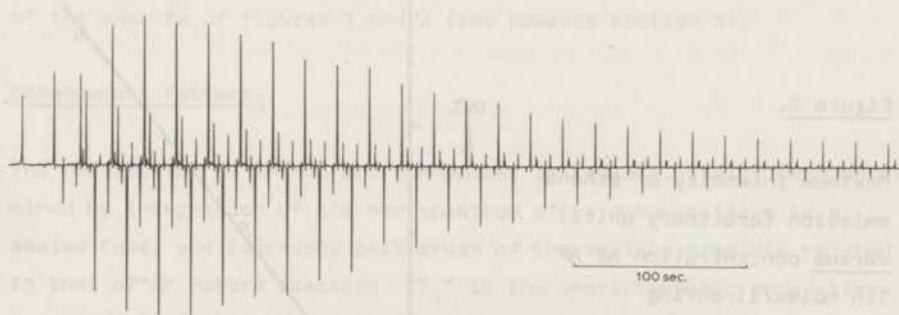


Figure 2. Time-development of the polarization during decomposition of AP in HCA at  $120^{\circ}$ , obtained by repeatedly sweeping through a region of 4.8 ppm.

The spectrum has been run at  $120^{\circ}$  on a Varian HA-100 spectrometer, by repeatedly scanning a region of 4.8 ppm with a sweep rate of 25 Hz/sec. The increase of the E and A curves represent the warming up of the sample in the probe. The decrease results from a slower reaction due to consumption of AP.

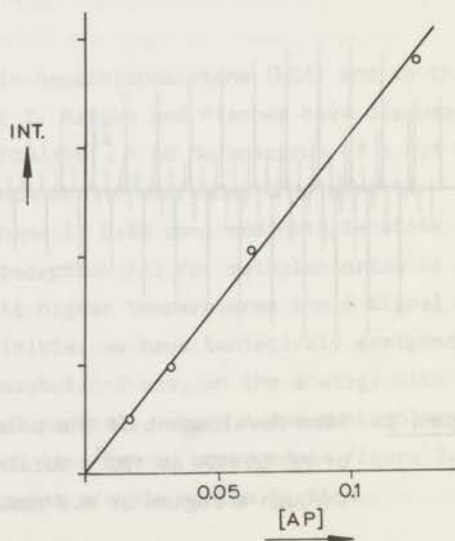
The opposite behaviour of recombination and transfer reaction products, (noted already in I) was rather mysterious at the time, but is a natural consequence of the radical pair mechanism. As the acetoxy radical most probably has a larger g-factor than the methyl radical, the theory predicts E for methyl acetate, when formed from the methyl/acetoxy radical pair (cf. scheme 1), and A for products escaping from recombination, *viz* methylchloride and methane. Methane might be formed by H-abstraction from pentachloroacetone (about 1% or less present in HCA) or from AP.

## 2.2 Origin of the ethane polarization.

The E effect for ethane cannot be due to S-T<sub>0</sub> mixing in the methyl radical pair, because no net effects can arise from pairs of equivalent radicals. In order to ascertain the origin of the ethane emission, we have studied its dependence on peroxide concentration. The results are presented in figure 3.

Figure 3.

Maximum intensity of ethane emission (arbitrary units) versus concentration of AP (in moles/l) during decomposition in HCA.



The linear dependence is expected for a polarization mechanism associated with geminate recombination, but could not be explained by other mechanisms involving cross-relaxation and combination of free methyl radicals.

A further indication is provided by comparison of  $^1\text{H}$ -spectra run at 100, 60, and 15.1 Mc. The ratio of E intensities of methylacetate and ethane was found to be essentially constant for the different fields. Thus we are led to the conclusion that polarization of methylacetate and that of ethane have a common origin:  $S-T_0$  mixing in the methyl/acetoxo radical pair. This phenomenon was called a "memory effect" in part IX, since polarization due to  $S-T_0$  transitions in pair 2 (methyl/acetoxo) shows up in products of pair 3 (methyl/methyl). This can be understood qualitatively as follows:  $S-T_0$  transitions in pair 2 are favoured for methyl radicals with  $M_1 > 0$  (z-component of nuclear spin). As during decarboxylation the electron spins (and nuclear spins) will not change, there will be born more methyl radical pairs with  $M_1 < 0$  in the singlet state, giving rise to emission for ethane.

A disproportionation reaction of the type



would give similar polarization. It cannot be excluded on the basis of the spectra of figures 1 and 2 (see however section 3).

### 2.3 Enhancement factors.

The results for AP in HCA are summarized in table 1. Yields were determined by integration of the nmr spectrum after decomposition in a sealed tube, and represent peak areas of the various products related to that of AP before reaction. " $T_1$ " is the characteristic decay-time for the polarization, determined by saturation recovery of the polarized lines, during the reaction. In this way both spin-lattice relaxation and escape of gaseous products from the sample are accounted for in " $T_1$ ".

Table 1. Decomposition of 0.1 M AP in HCA at 110° (100 Mc).

products	$\delta$ (ppm)	yield % (a)	"T <sub>1</sub> "(sec) (b)	V <sub>r</sub> (c)
AP	2.11 N <sup>(d)</sup>			
methylacetate (OCH <sub>3</sub> )	3.54 E	32	9	-44
(CCH <sub>3</sub> )	1.96 N			
ethane	0.83 E	5	11	-168
methylchloride	2.94 A	41	7	+192
methane	0.18 A	6		
pentachlorobutanone <sup>(e)</sup>	1.60 E	<0.5		
acetic acid	2.02 N	11		
acetic anhydride	2.16 N	3		
other products		2		

(a) Determined from nmr integration after decomposition in sealed tube; estimated relative error  $\pm 10\%$ .

(b) Determined from saturation recovery during decomposition.

(c) Calculated from eq. (5); estimated error  $\pm 20\%$ .

(d) N: not enhanced.

(e) tentative assignment.

V<sub>r</sub> is the enhancement factor per molecule AP decomposed, introduced previously<sup>10</sup>; it is simply related to experimental quantities:

$$V_r = \frac{I - I^0}{I(AP_t)T_1k_0} \quad (5)$$

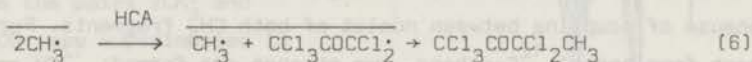
where the observed intensity, I, the thermal equilibrium intensity, I<sup>0</sup>, and the intensity of the precursor, I(AP<sub>t</sub>), are measured at time t', the time of maximum enhancements. The rate constant for AP decomposition<sup>15</sup> is k<sub>0</sub> = 2.5 · 10<sup>-3</sup> sec<sup>-1</sup> at 110°. It was necessary to allow for I<sup>0</sup> only in the case of methylacetate, where I<sup>0</sup> has been set equal to the intensity of the acetate CH<sub>3</sub> group. Since only one CH<sub>3</sub> fragment is responsible for the polarization<sup>16</sup>, half the intensity of

the AP signal has been taken for  $I(AP_t)$ .

It can be noted that the yield of ester is much larger than that of ethane, while the reverse is true for the polarization. It is interesting to compare the experimental ratio of the enhancement factors for methylacetate and ethane,  $V'_{II}/V'_{III}(\text{exp}) = 0.26$ , with predictions of the theory. In part IX a calculation has been made for a one-proton pair, with parameters pertaining to this case. For  $k$  (rate of decarboxylation) between  $10^9$  and  $10^{10} \text{ sec}^{-1}$ , it was found that  $V'_{II}/V'_{III}(\text{theor}) = 0.17-0.10$ . If the experimentally observed ester yield is used ( $P_{II} = 0.32$  in eq. 24 of IX) these values become  $0.27 - 0.13$ . For  $k = 2 \cdot 10^9 \text{ sec}^{-1}$  the enhancement factor calculated for the ester would be  $V'_{II} = -50$  (close to the observed value of  $-44$ ) and the calculated ratio  $V'_{II}/V'_{III}(\text{theor}) = 0.19$ , in reasonable agreement with the observed 0.26.

The intensity of the methylchloride A-line depends on  $k_1$  (rate constant for chlorine abstraction from HCA by methyl radicals) and also on the relaxation time of methyl radicals. The rate constant  $k_1$  has been measured<sup>18</sup> and would have a value  $k_1 = 2 \cdot 10^4 \text{ l/mole sec}$  at  $110^\circ$ . If methyl radicals disappear predominantly by reaction with the solvent, their life-time would be  $(k_1 [\text{HCA}])^{-1} = 7.7 \cdot 10^{-6} \text{ sec}$ . Relaxation times of radicals are usually in the range  $10^{-5} - 10^{-4} \text{ sec}$  (longer times have even been inferred from CIDNP spectra<sup>19,20</sup>), so that the life-time of the methyl radical could well be shorter than its relaxation time, giving polarization of about the same magnitude, but opposite to that of ethane and methylacetate.

The E-effect attributed to pentachlorobutanone deserves some comment. This effect would be compatible with recombination of singlet-correlated methyl/pentachloroacetyl radical pairs (we measured  $g_{\text{pentachloroacetyl}} = 2.0080$  by esr):



Since this pair is formed after about 4 microseconds (on the average), we would have another example of long-time spin-correlation effects of the type discussed in IX.

Formation of acetic acid and acetic anhydride (as indicated by nmr and glc) is somewhat surprising. The mechanism by which these products are formed is not known.

### 3. 2,2'-Di-carbon-13-acetyl Peroxide ( $^{13}\text{C-AP}$ ).

Sofar CIDNP spectra were in reasonable agreement with the reactions of scheme 1, but other possibilities were not excluded. For instance, reaction (4) might also account for the ethane emission. The results of  $^{13}\text{C-AP}$  show that this cannot be an important route to ethane.

#### 3.1 $^1\text{H}$ -spectrum.

The 100 Mc  $^1\text{H}$  nmr spectrum taken during decomposition of 0.22 M  $^{13}\text{C-AP}$  in HCA at 110 $^\circ$  is shown in figure 4a. As the  $^{13}\text{C}$ -enrichment of the methyl carbon atom is only  $55 \pm 1\%$  (from nmr), the same lines appear as in figure 1 (cf. table 1) due to products of  $^{12}\text{CH}_3$  radicals. In addition lines belonging to products of  $^{13}\text{CH}_3$  radicals appear. Since the  $^{13}\text{C}$  nucleus has spin  $I = \frac{1}{2}$  the spectra of methylacetate, methylchloride, peroxide and methane, containing  $^{13}\text{CH}_3$  fragments, consist of doublets flanking the  $^{12}\text{C}$ -species: methylacetate ( $\text{OCH}_3$ ),  $J_{\text{CH}} = 146$  Hz, E + E/A; methylchloride,  $J_{\text{CH}} = 150$  Hz, A/E + A;  $^{13}\text{C-AP}$ ,  $J_{\text{CH}} = 131$  Hz; methane,  $J_{\text{CH}} = 124$  Hz, A/E + A. From the  $^{13}\text{C}$ -methylacetate doublet (E lines with unequal intensities) the g-factor of the acetoxy radical can be obtained. Calculations with an exchange integral  $|J| = 5 \cdot 10^8$  radians/sec gave the best fit with  $\Delta g = 0.0032 \pm 0.0002$  for the methyl/acetoxy radical pair, which implies  $g_{\text{acetoxy}} = 2.0058 \pm 0.0002$  ( $g_{\text{methyl}} = 2.0026$ , cf. ref. 21). The g-factor of this very unstable radical will not easily be obtained from esr.

The spectrum of ethane<sup>22</sup> in the region 0 - 1.8 ppm is more complex, because of coupling between nuclei of both  $\text{CH}_3$  fragments. Furthermore, apart from normal  $^{12}\text{C}$ -ethane, two ethanes are formed:  $^{12}\text{CH}_3$ - $^{13}\text{CH}_3$  and  $^{13}\text{CH}_3$ - $^{13}\text{CH}_3$ . The nuclear coupling constants<sup>22</sup> are:  $J_{\text{CH}} = 125.0$  Hz,  $J_{\text{CCH}} = -4.5$  Hz,  $J_{\text{CC}} = 34.6$  Hz, and  $J_{\text{HCCH}} = 8.0$  Hz. Computer simulations have been made, following the procedures given in VIII.

Figure 4a.

100 Mc  $^1\text{H}$ -spectrum of the decomposition of 0.22 M  $^{13}\text{C}$ -AP (55% enriched) in HCA at  $110^\circ$ . A simulation of the ethane spectrum, calculated with the parameters of the methyl radical pair (see text) is shown on top.

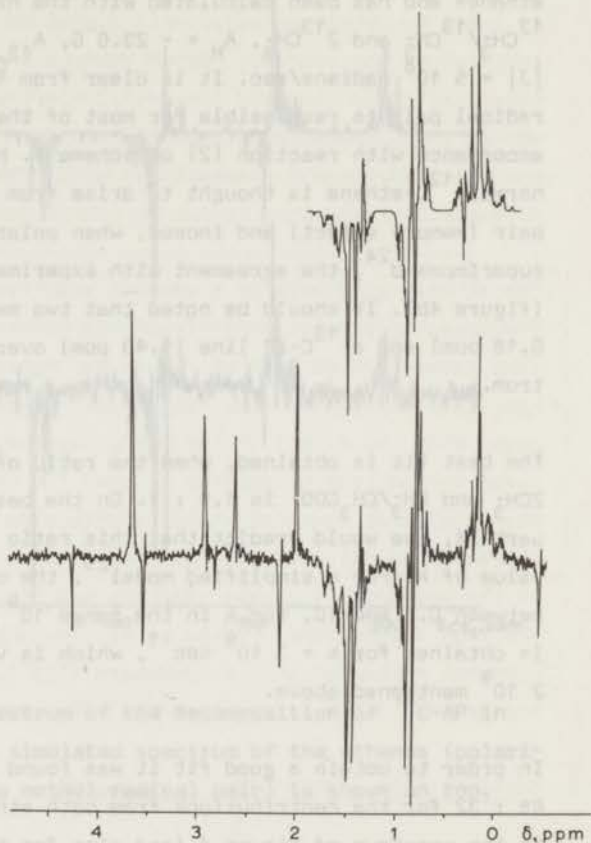


Figure 4b.

Simulation of the ethane  $^1\text{H}$ -spectrum from  $^{13}\text{C}$ -AP. Contributions of polarization from the pairs  $2\text{CH}_3\cdot$  and  $\text{CH}_3/\text{CH}_3\text{COO}\cdot$  are superimposed in proportion 1.9 : 1.



The simulation of figure 4a is a superposition of both  $^{13}\text{C}$  containing ethanes and has been calculated with the hf. parameters of the pairs  $^{12}\text{CH}_3/^{13}\text{CH}_3$  and  $2^{13}\text{CH}_3$ ,  $A_{\text{H}} = -23.0 \text{ G}$ ,  $A_{^{13}\text{C}} = +38.3 \text{ G}^{23}$ , and with  $|J| = 5 \cdot 10^8$  radians/sec. It is clear from figure 4a, that the methyl radical pair is responsible for most of the ethane polarization, in accordance with reaction (2) of scheme 1. However, the E effect of normal  $^{12}\text{C}$ -ethane is thought to arise from the methyl/acetoxyl radical pair (memory effect) and indeed, when polarization from this pair is superimposed<sup>24</sup>, the agreement with experiment becomes even better (figure 4b). It should be noted that two methane lines (at 0.80 and 0.18 ppm) and a  $^{13}\text{C}$ -AP line (1.43 ppm) overlap with the ethane spectrum.

The best fit is obtained, when the ratio of contributions from the pairs  $2\text{CH}_3$  and  $\text{CH}_3/\text{CH}_3\text{COO}\cdot$  is 1.9 : 1. On the basis of the theory given in part IX, one would predict that this ratio is rather sensitive to the value of  $k$ . For a simplified model<sup>25</sup>, the calculated ratio varies between 0.8 and 10, for  $k$  in the range  $10^9 - 10^{10} \text{ sec}^{-1}$ . The value 1.9 is obtained for  $k = 3 \cdot 10^9 \text{ sec}^{-1}$ , which is very close to the value  $2 \cdot 10^9$  mentioned above.

In order to obtain a good fit it was found to be necessary to use a ratio 68 : 32 for the contributions from both ethanes ( $^{12}\text{C} - ^{13}\text{C} : ^{13}\text{C} - ^{13}\text{C}$ ) to the spectrum of figure 4 (and also for the  $^{13}\text{C}$  spectrum, figure 5), instead of the statistically expected ratio 63 : 37. The discrepancy seems somewhat large to be explained by a kinetic isotope effect for the decarboxylation of the acetoxyl radical, although this would be expected to give an effect in the right direction ( $k_{^{12}\text{C}} > k_{^{13}\text{C}}$ , cf. ref. 26). We have not pursued this point further. For  $^{13}\text{CH}_3\text{Cl}$ , the pairs  $2\text{CH}_3$  and  $\text{CH}_3/\text{CH}_3\text{COO}\cdot$  contribute about equally to the spectrum. The relatively larger effect due to the last pair, as compared to the case of ethane, is to be expected, since in the "escape" product the net effects of methylacetate must be balanced as well as those of ethane.

### 3.2 $^{13}\text{C}$ -spectrum.

The 15.1 Mc  $^{13}\text{C}$ -spectrum ( $H_0 = 14 \text{ kG}$ ) during decomposition of  $^{13}\text{C}$ -AP in HCA at  $124^\circ$  is shown in figure 5a.

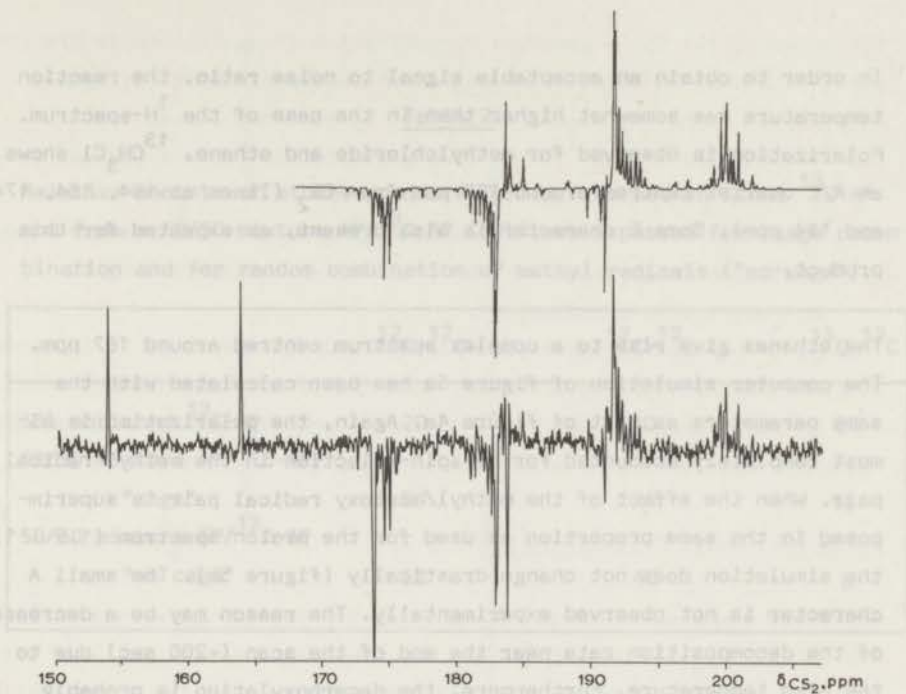


Figure 5a. 15.1 Mc  $^{13}\text{C}$ -spectrum of the decomposition of  $^{13}\text{C}$ -AP in HCA at  $124^\circ$ . A simulated spectrum of the ethanes (polarization from the methyl radical pair) is shown on top.

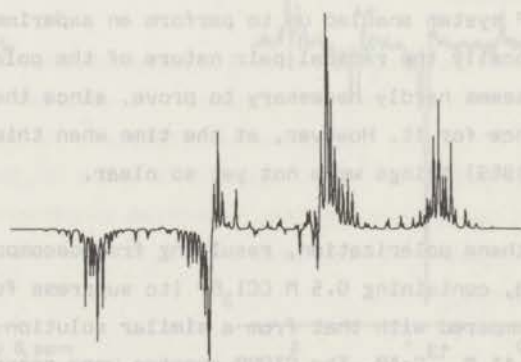


Figure 5b. Simulation of the ethane  $^{13}\text{C}$ -spectrum from  $^{13}\text{C}$ -AP. Contributions of polarization from the pairs  $2\text{CH}_3$  and  $\text{CH}_3/\text{CH}_3\text{COO}$  are superimposed in proportion 1.9: 1.

In order to obtain an acceptable signal to noise ratio, the reaction temperature was somewhat higher than in the case of the  $^1\text{H}$ -spectrum. Polarization is observed for methylchloride and ethane.  $^{13}\text{CH}_3\text{Cl}$  shows an A/E quartet centred around 169 ppm from  $\text{CS}_2$  (lines at 154, 164, 174 and 184 ppm). Some E character is also present, as expected for this product.

The ethanes give rise to a complex spectrum centred around 187 ppm. The computer simulation of figure 5a has been calculated with the same parameters as that of figure 4a. Again, the polarization is almost completely accounted for by spin-selection in the methyl radical pair. When the effect of the methyl/acetoxyl radical pair is superimposed in the same proportion as used for the proton spectrum (1.9 : 1), the simulation does not change drastically (figure 5b). The small A character is not observed experimentally. The reason may be a decrease of the decomposition rate near the end of the scan (~200 sec) due to the high temperature. Furthermore, the decarboxylation is probably somewhat faster at this temperature ( $124^\circ$ ), and consequently a ratio higher than 1.9 : 1 for the pairs  $2\text{CH}_3\cdot$  and  $\text{CH}_3\cdot/\text{CH}_3\text{COO}\cdot$  would be required.

### 3.3 50/50 Mixture enriched/non-enriched AP.

The AP system enabled us to perform an experiment, which proves unequivocally the radical pair nature of the polarization. At present this seems hardly necessary to prove, since there is abundant convincing evidence for it. However, at the time when this experiment was carried out (1969) things were not yet so clear.

The ethane polarization, resulting from decomposition of 0.22 M  $^{13}\text{C}$ -AP in HCB, containing 0.5 M  $\text{CCl}_3\text{Br}$  (to suppress formation of methane), was compared with that from a similar solution containing 0.11 M AP and 0.11 M  $^{13}\text{C}$ -AP. The CIDNP spectra were recorded under as nearly as possible identical conditions for both cases. The results are shown in figure 6. The ratio's, in which the contributions from three ethane polarizations is expected to change in the case of different polarization mechanisms, is presented in table 2.

Table 2.

Relative amounts of ethane products formed from 55% enriched  $^{13}\text{C}$ -AP and from a 50/50 mixture AP/ $^{13}\text{C}$ -AP (55%), as expected for "cage recombination and for random combination of methyl radicals ("no-cage").

	$^{12}\text{C}-^{12}\text{C}$	$^{12}\text{C}-^{13}\text{C}$	$^{13}\text{C}-^{13}\text{C}$
55% enriched $^{13}\text{C}$ -AP	20	50	30
50/50 mixture AP/ $^{13}\text{C}$ -AP			
" cage "	60	25	15
50/50 mixture AP/ $^{13}\text{C}$ -AP			
" no cage "	52	40	8

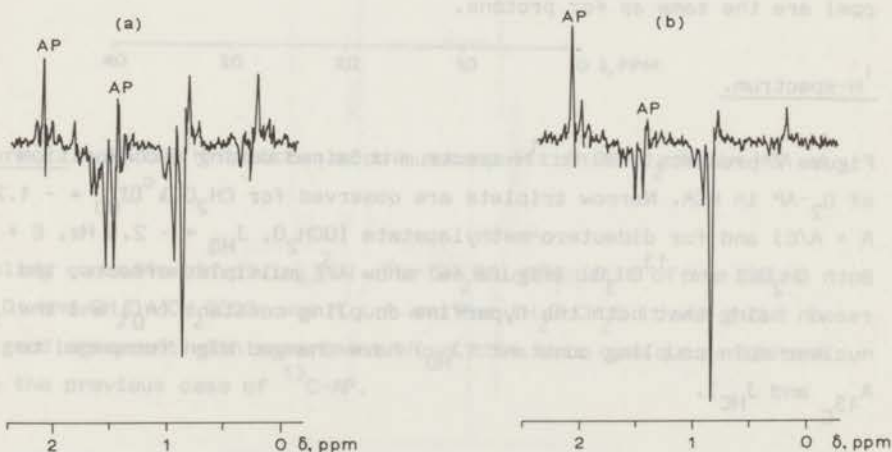


Figure 6. 100 Mc  $^1\text{H}$ -spectra of the decomposition of 0.22 M  $^{13}\text{C}$ -AP in hexachlorobutadiene with  $\text{CCl}_3\text{Br}$  (a) and of a mixture of 0.11 M AP and 0.11 M  $^{13}\text{C}$ -AP in the same solvent (b).

The expectations for a geminate recombination ("cage") process are compared with one, in which polarized ethane would be formed by random encounters. Comparing figure 6a and 6b, it can be observed that (i) intensities of the  $^{13}\text{C}$  containing ethanes in (b) are reduced by a factor  $\frac{1}{2}$  as compared to (a), and (ii) relative intensities of lines belonging to different ethanes are unaltered (e.g. lines of the "doublet" at 1.5 ppm belong to different ethane molecules).

This is in perfect agreement with the second line of table 2. It shows, without using any theory of CIDNP, that the ethane polarization results from a "cage" process, and rules out any mechanism acting in free methyl radicals, such as the original cross-relaxation mechanism.

#### 4. Dideutero-acetyl Peroxide ( $\text{D}_2\text{-AP}$ ).

Deuterium has a spin  $I = 1$ . The ratio of the nuclear g-factors of  $^2\text{D}$  and  $^1\text{H}$  is  $g_{\text{D}}/g_{\text{H}} = 0.154$ . Therefore the coupling constants  $A_{\text{D}}$  (in the radicals) and  $J_{\text{HD}}$  (in the products) are smaller than the corresponding  $A_{\text{H}}$  and  $J_{\text{HH}}$  by a factor 6.5 ( $A_{\text{D}} = -3.54$  in the  $\text{CH}_2\text{D}\cdot$  radical<sup>23</sup>). Both  $^1\text{H}$ - and  $^2\text{D}$ -spectra have been examined. Deuterium chemical shifts (in ppm) are the same as for protons.

#### 4.1 $^1\text{H}$ -spectrum.

Figure 7 presents a 60 Mc  $^1\text{H}$ -spectrum obtained during decomposition of  $\text{D}_2\text{-AP}$  in HCA. Narrow triplets are observed for  $\text{CH}_2\text{DCl}$  ( $J_{\text{HD}} = -1.7$  Hz,  $A + A/E$ ) and for dideutero-methylacetate ( $\text{OCH}_2\text{D}$ ,  $J_{\text{HD}} = -2.5$  Hz,  $E + E/A$ ). Both  $\text{CH}_2\text{DCl}$  and  $^{13}\text{CH}_3\text{Cl}$  (figure 4a) show A/E multiplet effects, the reason being that both the hyperfine coupling constant ( $A_{\text{D}}$ ) and the nuclear spin coupling constant ( $J_{\text{HD}}$ ) have changed sign (compared to  $A_{^{13}\text{C}}$  and  $J_{\text{HC}}$ ).

Again, the spectrum of 1,2-di-deuteroethane is more complex. Nuclear coupling constants in  $\text{CH}_2\text{D}-\text{CH}_2\text{D}$  are:  $J_{\text{HH}}$  (vicinal) = + 8.0 Hz,  $J_{\text{DD}}$  (vicinal) = + 0.19 Hz,  $J_{\text{HD}}$  (geminal) = - 1.6 Hz, and  $J_{\text{HD}}$  (vicinal) = + 1.22 Hz. The simulated spectra of figure 7a have been calculated with the same parameters as used in the previous sections (except for

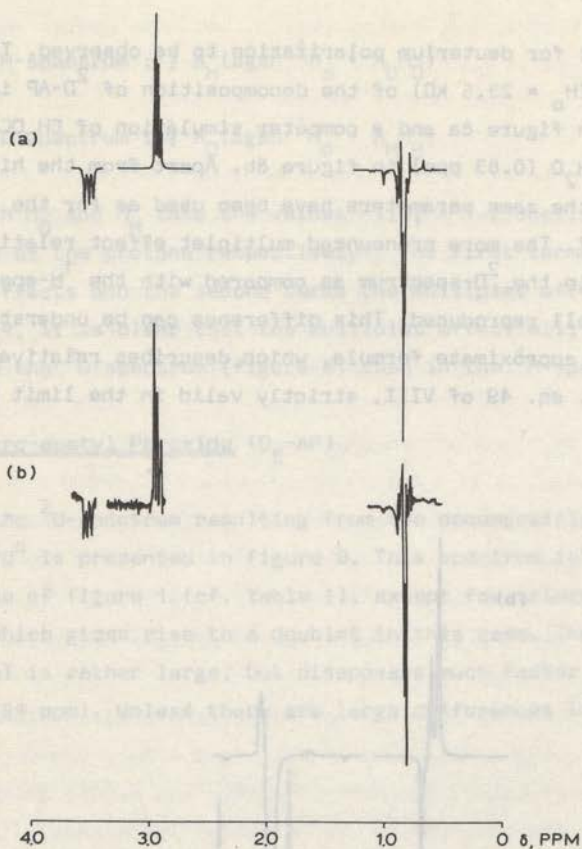


Figure 7. 60 Mc  $^1\text{H}$ -spectrum of the decomposition of  $\text{D}_2\text{-AP}$  in HCA at  $110^\circ$ .

coupling constants involving  $^2\text{D}$ ). For  $\text{CH}_2\text{DCI}$  the ratio of the pairs  $2\text{CH}_2\text{D}^*$  and  $\text{CH}_2\text{D}^*/\text{CH}_2\text{DCO}^*$  was 1 : 1 and for  $\text{CH}_2\text{D}-\text{CH}_2\text{D}$  it was 1.9 : 1. The good agreement with experiment shows that this case is consistent with the previous case of  $^{13}\text{C-AP}$ .

#### 4.2 $^2\text{D}$ -spectrum.

Due to the quadrupole moment of the deuterium nucleus, the relaxation times of lines in  $^2\text{D}$ -spectra are somewhat shorter than in the corresponding  $^1\text{H}$ -spectra. Usually they lie in the range 0.5 - 5 sec $^{27}$ , which

is not too short for deuterium polarization to be observed. The 15.4 Mc  $^2\text{D}$ -spectrum ( $H_0 = 23.5$  kG) of the decomposition of  $^2\text{D}$ -AP in HCA at  $120^\circ$  is shown in figure 8a and a computer simulation of  $\text{CH}_2\text{DCl}$  (2.94 ppm) and  $\text{CH}_2\text{D}-\text{CH}_2\text{D}$  (0.83 ppm) in figure 8b. Apart from the higher magnetic field the same parameters have been used as for the simulation of figure 7. The more pronounced multiplet effect relative to the net effect in the  $^2\text{D}$ -spectrum as compared with the  $^1\text{H}$ -spectrum (figure 7) is well reproduced. This difference can be understood by considering the approximate formula, which describes relative CIDNP intensities (cf. eq. 49 of VIII, strictly valid in the limit of large  $|J|$ ):

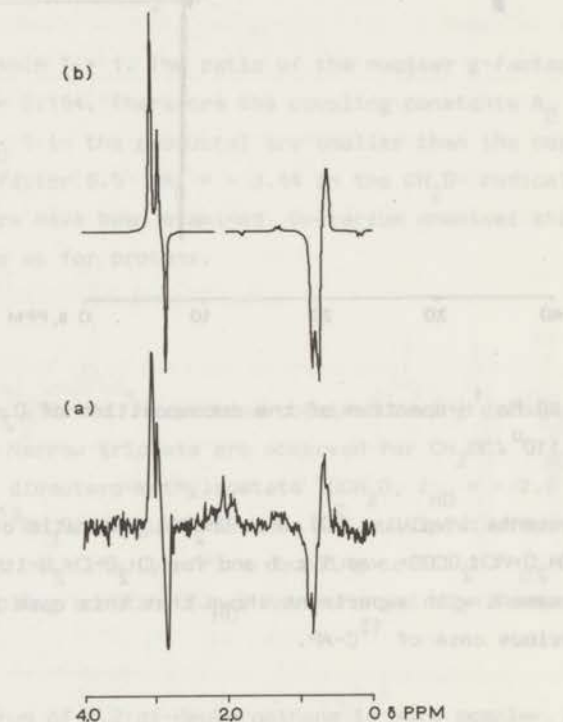


Figure 8. 15.4 Mc  $^2\text{D}$ -spectrum of the decomposition of  $\text{D}_2$ -AP in HCA at  $120^\circ$ .

$$\text{For the } ^1\text{H-spectrum : } \frac{1}{2} A_H (\Delta g \beta h^{-1} H_O + A_D M_D) \quad (7a)$$

$$\text{For the } ^2\text{D-spectrum : } \frac{1}{2} A_D (\Delta g \beta h^{-1} H_O + A_H M_H) \quad (7b)$$

where both  $M_D$  and  $M_H$  take the values  $-1, 0, +1$  (labelling the states of  $^2\text{D}$  and of the protons respectively). The first terms in (7) represent the net effects and the second terms the multiplet effects. Since  $A_D/A_H = 0.154$ , it is clear that the multiplet effect will be relatively larger in the  $^2\text{D}$ -spectrum (figure 8) than in the  $^1\text{H}$ -spectrum (figure 7).

5. Hexadeutero-acetyl Peroxide ( $\text{D}_6\text{-AP}$ )

The 15.4 Mc  $^2\text{D}$ -spectrum resulting from the decomposition of  $\text{D}_6\text{-AP}$  in HCA at  $120^\circ$  is presented in figure 9. This spectrum is very similar to the one of figure 1 (cf. table 1), except for trideuteromethane ( $\text{CD}_3\text{H}$ ), which gives rise to a doublet in this case. The  $\text{CD}_3\text{H}$  signal (0.18 ppm) is rather large, but disappears much faster than that of  $\text{CD}_3\text{Cl}$  (2.94 ppm). Unless there are large differences in relaxation

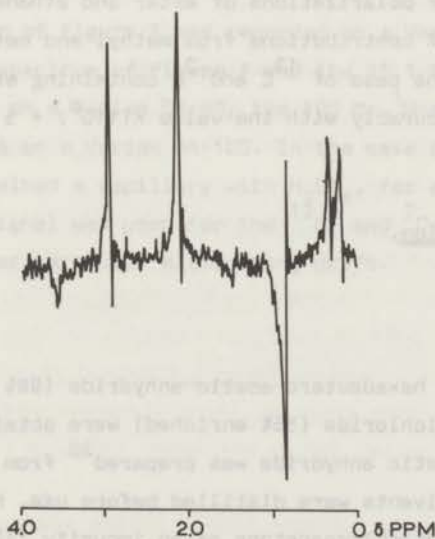


Figure 9. 15.4 Mc  $^2\text{D}$ -spectrum of the decomposition of  $\text{D}_6\text{-AP}$  in HCA at  $120^\circ$ .

times, this indicates that H-atom abstraction from pentachloroacetone (about 1% present) is much faster than Cl-atom abstraction from HCA.

## 6. Conclusions.

On the basis of the reaction mechanism of scheme 1, radical pair theory is able to account for the observed CIDNP spectra during decomposition of acetyl peroxide and of  $^{13}\text{C}$ -enriched and deuterated analogues. Ethane formation by reaction (4) and similarly formation of methylacetate by disproportionation of acetoxy radicals, which has been considered<sup>3</sup>:



are not likely to be of major importance, if these reactions contribute at all.

A rate constant for the decarboxylation of acetoxy radicals,  $k_2 = 3 \cdot 10^9 \text{ sec}^{-1}$  seems to be compatible with

- (i) the absolute enhancement of methylacetate polarization,
- (ii) the ratio of polarizations of ester and ethane (memory effect) and
- (iii) the ratio of contributions from methyl and methyl/acetoxy radical pairs, in the case of  $^{13}\text{C}$  and  $^2\text{D}$  containing ethanes.

This compares favourably with the value  $k(110^\circ) = 5 \cdot 10^9 \text{ sec}^{-1}$ , obtained by Eirich<sup>7</sup>.

## 7. Experimental section.

### Reagents.

Acetic anhydride, hexadeutero-acetic anhydride (98% enriched), and 2-carbon-13-acetylchloride (55% enriched) were obtained commercially; 2,2'-dideutero-acetic anhydride was prepared<sup>28</sup> from ketene and  $\text{D}_2\text{O}$  (cf. ref. 29). Solvents were distilled before use. Hexachloroacetone contained some pentachloroacetone as an impurity (1% or less).

## Peroxides.

Acetyl peroxide, hexadeutero- and dideutero-acetyl peroxide were prepared from the anhydrides following the procedure of Price and Morita<sup>30</sup> (addition of  $\text{Na}_2\text{O}_2$  and water to a solution of the anhydride in ether while keeping the temperature below  $5^\circ$ , washing the ethereal layer in aqueous  $\text{NaHCO}_3$ , and drying over  $\text{Na}_2\text{SO}_4$ ). The synthesis of acetyl peroxide from acetylchloride by this method, without special precautions gave low yields of peroxide (10-15%). However, by varying the reaction conditions somewhat, the yield could be boosted to 80%. The following procedure was used for the preparation of 2,2'-di- $^{13}\text{C}$ -acetyl peroxide: To a solution of 0.44 g 2- $^{13}\text{C}$ -acetylchloride in 3.5 ml ether, cooled to  $-15^\circ$ , was added 0.45 g  $\text{Na}_2\text{O}_2$ . Four drops of water were added and the mixture was stirred during 40 min at  $-10^\circ$ . After adding 3 ml chilled ether the solution was decanted and the ethereal layer was washed with 10% aqueous  $\text{NaHCO}_3$  and with 5%  $\text{NaCl}$  solution, and dried over  $\text{MgSO}_4$ . The yield was 80%, as determined by iodometric titration<sup>31</sup>.

## NMR spectra.

The 60 Mc spectrum of figure 1 was recorded on a Varian A-60 spectrometer. The 60 Mc spectrum of figure 7 and the 15.1 Mc  $^{13}\text{C}$ -spectrum (fig. 5) were run on a Varian DA-60; the 100 Mc  $^1\text{H}$ -spectra and the 15.4 Mc  $^2\text{D}$ -spectra on a Varian HA-100. In the case of the 100 Mc spectra sample tubes contained a capillary with  $\text{H}_2\text{SO}_4$ , for an internal lock signal. No lock signal was used for the  $^{13}\text{C}$ - and  $^2\text{D}$ -spectra; these were recorded after carefully eliminating drift.

## References and Footnotes.

- 1.(a) Presented in part at the CIDNP symposium of the ACS meeting in Houston, Feb. 1970.
- (b) A preliminary account for this work was given in part I, R. Kaptein, Chem. Phys. Letters, 2, 261 (1968).
2. R.C.P. Cubbon, in "Progress in Reaction Kinetics", Volume 5, ed. G. Porter, Pergamon, Oxford, 1970, p. 29.
- 3.(a) M. Szwarc, in "Peroxide Reaction Mechanisms", ed. J.O. Edwards, Interscience, New York, 1962, p. 153;
- (b) A. Rembaum and M. Szwarc, J. Amer. Chem. Soc. 77, 3486 (1955);
- (c) L. Herk, M. Feld and M. Szwarc, ibid. 83, 2998 (1961).
4. J.W. Taylor and J.C. Martin, ibid., 89, 6904 (1967).
5. T. Koenig and R. Cruthoff, ibid., 91, 2562 (1969).
6. T. Kashiwagi, S. Kozuka and S. Oae, Tetrahedron, 26, 3619 (1970).
7. W. Braun, L. Rajbenbach and F.R. Eirich, J. Phys. Chem., 66, 1591 (1962).
8. M.J. Goldstein and H.A. Judson, J. Amer. Chem. Soc. 92, 4119 (1970).
- 9.(a) R.M. Noyes, ibid., 77, 2042 (1955);
- (b) R.M. Noyes, ibid., 78, 5486 (1956).
- 10.(a) R. Kaptein, part VIII, to be published;
- (b) R. Kaptein, part IX, to be published.
11. cf. F.J. Adrian, J. Chem. Phys., 53, 3374 (1970).
12. R. Kaptein and L.J. Oosterhoff, Chem. Phys. Letters, 4, 195, 214 (1969).
- 13.(a) G.L. Closs, J. Amer. Chem. Soc., 91, 4552 (1969);
- (b) G.L. Closs and A.D. Trifunac, ibid., 92, 2183 (1970).
14. J. Bargon and H. Fischer, Z. Naturforsch. 23a, 2109 (1968).  
The emission line at 0.79 ppm reported in this paper has been erroneously assigned to methane (instead of ethane).
15. The apparent rate constant (from disappearance of the AP signal has been corrected for an estimated 20% cage return of acetoxy radicals.
16. The hf. coupling constant  $A(\text{CH}_3)$  in the acetoxy radical is not known, but will probably be comparable to  $A(\text{CH}_3)$  in the 2-methyl allyl radical<sup>17</sup> (3.19 G), thus much smaller than  $A_{\text{H}} = -23$  G in the methyl radical.

17. P.J. Krusic and J.K. Kochi, J. Amer. Chem. Soc., 90, 7157 (1968).
18. D.M. Tomkinson, J.P. Galvin and H.O. Pritchard, J. Phys. Chem. 68, 541 (1964).
19. G.L. Closs and D.R. Paulson, J. Amer. Chem. Soc., 92, 7229 (1970).
20. M. Lehnig and H. Fischer, Z. Naturforsch. 25a, 1963 (1970).
21. H. Fischer, "Magnetic properties of free radicals", Landolt-Börnstein, New Series, Group II, Vol. 1, ed. K. -H. Hellwege, Springer, Berlin (1965).
- 22.(a) R.M. Lynden-Bell and N. Sheppard, Proc. Roy. Soc., A 269, 385 (1962);
- (b) D.H. Graham and C.E. Holloway, Can. J. Chem., 41, 2114 (1963).
23. R.W. Fessenden, J. Phys. Chem., 71, 74 (1967).
24. Both  $^1\text{H}$ - and  $^{13}\text{C}$ -hf. coupling constants of the methyl carbon in the acetoxy radical have been set equal to zero. Trial calculations with  $A_{\text{H}}$  and  $A_{^{13}\text{C}}$  of the order of 3 G did not change the spectrum significantly.
25. The calculations have been performed for a one-proton pair with  $\Delta g = -0.0032$  (for the methyl/acetoxy radical pair) and a two-nuclei pair  $^{12}\text{C-H/R}\cdot$  (for the methyl radical pair) on the basis of eq. 24 of IX. Other parameters used:  $|J| = 5 \cdot 10^8$  rad/sec,  $m' = 10^{-6} \text{ sec}^{\frac{1}{2}}$ ,  $p = \frac{1}{2}$ ,  $\lambda_{\text{III}} = 1$ ,  $P_{\text{II}} = 0.32$  and the hf. parameters of the  $^{13}\text{CH}_3$  radical.
26. L. Melander, "Isotope Effects on Reaction Rates", Ronald Press Co., New York, 1960, chap. 7.
27. J.A. Glasel, J. Amer. Chem. Soc., 91, 4569 (1969).
28. We thank Mr. R. Wijting for the preparation of this anhydride and of di- and hexadeutero-acetyl peroxide.
29. F.I. Andersen, Nature, 173, 541 (1954).
30. C.C. Price and H. Morita, J. Amer. Chem. Soc., 75, 3685 (1953).
31. C.D. Wagner, R.H. Smith and E.D. Peters, Ind. Eng. Chem. Anal. Ed. 19, 979 (1947).

CHAPTER XII

CHEMICALLY INDUCED DYNAMIC NUCLEAR POLARIZATION XII  
THERMAL DECOMPOSITION OF ALIPHATIC ACYL PEROXIDES.

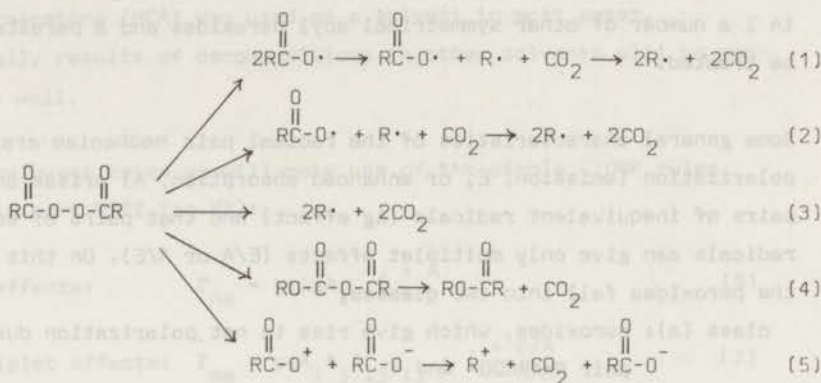
By R. Kaptein

(Department of Theoretical Organic Chemistry,  
University Leiden, P.O. Box 75, Leiden,  
The Netherlands).

1. Introduction.

This work describes a CIDNP study of the reactions of aliphatic acyl peroxides  $(RCOO)_2$ . In non-polar solvents the thermal decomposition of these peroxides is predominantly homolytic<sup>1</sup>; they provide a convenient source of alkyl radicals. The kinetics of peroxide decompositions have been reviewed by Cubbon<sup>2</sup> recently.

Decomposition rates of the straight-chain acyl peroxides are all similar to those of acetyl and benzoyl peroxides (activation energy ~ 30 kcal/mole), indicating one-bond homolysis as the first step. In contrast, the  $\alpha$ -branched peroxides and those, where R is stabilized by resonance, decompose faster, which is considered as evidence for concerted two or three-bond cleavage<sup>3</sup>. These latter peroxides are known to have polar decomposition routes available as well<sup>4</sup>. In addition, induced decomposition may occur. Disregarding this for the moment the modes of decomposition are summarized in scheme 1.



Scheme 1.

The acyloxy radicals (RCOO·), intermediates in reaction (1) and (2), rapidly decarboxylate to give alkyl radicals. Reaction (4) gives the "carboxyl inversion" product<sup>4</sup>, which is usually not very stable and decomposes further to give the ester. Routes (4) and (5) are often referred to as "polar".

Interestingly, Walling et al.<sup>5</sup> have recently suggested that reactions (2) - (5) (in the case of the more rapidly decomposing peroxides) all proceed via a common intermediate, a tight ion pair-radical pair, which would give both the rearranged carboxyl inversion product, and, upon diffusive separation in apolar media, a radical pair. It should be noted, that according to our theoretical picture of CIDNP<sup>6</sup>, no information on the initial stages of the process can be obtained by this technique. Only after some diffusion has occurred (say after at least  $10^{-10}$  sec) observable polarization is generated, by the combined effects of nuclear spin dependent intersystem-crossing and "spin-selection"<sup>7</sup> at reencounters (only singlet (S) pairs recombine). Of course, only homolytic reactions (1) - (3) can lead to polarization in the reaction products.

A preliminary account of the present work has been given previously<sup>8</sup> (part I). Since at that time radical pair theory<sup>9,10,6</sup> did not yet exist, interpretations of CIDNP spectra given in I, are necessarily incomplete or incorrect. They will now be reconsidered in the light

of the new theoretical developments. In addition to systems discussed in I a number of other symmetrical acyl peroxides and a preester will be treated.

Some general characteristics of the radical pair mechanism are that net polarization (emission, E, or enhanced absorption, A) arises only from pairs of inequivalent radicals ( $\Delta g$  effect) and that pairs of equivalent radicals can give only multiplet effects (E/A or A/E). On this basis, the peroxides fall into two classes:

class (a): peroxides, which give rise to net polarization due to the pair  $R\cdot/RCOO\cdot$  and

class (b): peroxides, which exhibit only multiplet effects due to the pair  $2R\cdot$  (of course, net effects could arise in this case due to solvent derived radicals).

The decarboxylation of acyloxy radicals is a competitive reaction of the type discussed in IX<sup>11</sup>. According to the theory<sup>11</sup> one would estimate that the acyloxy radical has to live longer than about  $10^{-10}$  sec in order to give rise to observable net effects. For instance, acetyl peroxide<sup>8,12</sup> and benzoyl peroxide<sup>13</sup> would fall in class (a). As will be shown below, other cases where the acyloxy radicals give rise to net polarization are peroxides with R = cyclopropyl, vinyl and methyl substituted vinyl. The other peroxides studied here would belong to class (b).

We will frequently make use of computer simulation of CIDNP spectra, by the procedure described in VIII. The magnitudes of the isotropic hyperfine (hf.) coupling constants, needed for the simulations, were known from esr in most cases<sup>14</sup>. As to the signs of these hf. parameters, it has been established<sup>15</sup>, that in planar  $\pi$ -electron alkyl radicals  $\alpha$ -hydrogens have a negative sign and  $\beta$ -hydrogens a positive sign (CIDNP spectra confirm this once again). For non-planar and  $\sigma$ -radicals the situation is not so simple and in some cases unknown signs could be determined from the CIDNP spectra, e.g. for cyclopropyl, cyclopropyl-carbinyl and the vinyl radicals. The g-factors of the  $R\cdot$  radicals differ only slightly from the free electron g-factor (alkyl  $g = 2.0026$ , vinyl  $g = 2.0022$ ). A value of 2.006 has been used for the g-factor of the acyloxy radicals (cf. XI). Simulated spectra have been calculated with  $|J| = 5 \times 10^8$  radians/sec, if not stated otherwise.

Hexachloroacetone (HCA) was used as a solvent in most cases. Occasionally results of decompositions in other solvents will be mentioned as well.

In some relevant cases we will make use of the simple CIDNP rules derived in part VIII (eq.52):

$$\text{for net effects: } \Gamma_{ne} = \mu c \Delta g A_i \left\{ \begin{array}{l} + A \\ - E \end{array} \right. \quad (6)$$

$$\text{for multiplet effects: } \Gamma_{me} = \mu c A_i A_j J_{ij} \sigma_{ij} \left\{ \begin{array}{l} + E/A \\ - A/E \end{array} \right. \quad (7)$$

where the symbols have meanings as defined in VIII.

## 2. Aliphatic Acyl peroxides.

Acetyl peroxide (AP) has been discussed separately<sup>12</sup>. Propionyl peroxide (PPO), butyryl, isobutyryl, isovaleryl and pivaloyl peroxide have R = ethyl, propyl, isopropyl, 2-methylpropyl (isobutyl) and t-butyl respectively. The hf. coupling constants of these radicals<sup>16</sup>, given in table 1, have been used in the computer calculations.

Table 1.

Hyperfine coupling constants of alkyl radicals, in gauss (cf. ref.16).

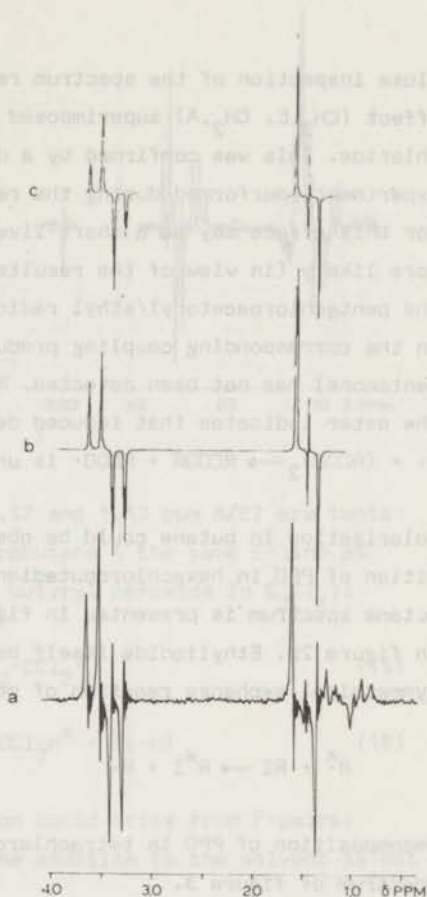
Radical	$A_\alpha$	$A_\beta$	$A_\gamma$
$\text{CH}_3\dot{\text{C}}\text{H}_2$	- 22.4	+ 26.9	
$\text{CH}_3\text{CH}_2\dot{\text{C}}\text{H}_2$	- 22.1	+ 33.2	0.38
$(\text{CH}_3)_2\dot{\text{C}}\text{H}$	- 22.1	+ 24.7	
$(\text{CH}_3)_2\text{CH}\dot{\text{C}}\text{H}_2$	- 22.0	+ 35.1	(a)
$(\text{CH}_3)_3\dot{\text{C}}$		+ 22.7	

(a) probably less than 0.5 G.



Figure 1.

60 Mc spectrum taken during decomposition of propionyl peroxide in HCA (a), with computer simulations for ethylchloride, calculated with  $|J| = 5 \cdot 10^8$  rad/sec (b) and with  $J = 0$  (c).



$\delta(\text{CH}_2)$  3.52,  $\delta(\text{CH}_3)$  1.47 ppm, A/E multiplets, in figure 1b and c. Mainly due to the greater solubility of ethylchloride as compared to butane in HCA, the former gives rise to much stronger signals than butane,  $\delta(\text{CH}_2)$  1.30,  $\delta(\text{CH}_3)$  0.90 ppm, E/A. The effective exchange integral,  $J$ , which enters the theory, has been varied in this case, in order to assess the importance of the magnitude of  $J$ . For comparison, simulated spectra with  $J = 0$  (fig.1c) and  $|J| = 5 \cdot 10^8$  radians/sec (fig.1b) are shown. The latter value is compatible with low field experiments<sup>18</sup> and with the 15.1 Mc spectrum<sup>6</sup>. It can be seen that a non-zero value is needed to account for the larger enhancements for the outer lines of the  $\text{CH}_2$  quartet<sup>19</sup>.

Close inspection of the spectrum reveals that there is a small net effect ( $\text{CH}_3, \text{E}; \text{CH}_2, \text{A}$ ) superimposed on the multiplet effects in ethylchloride. This was confirmed by a double-resonance (spin-decoupling) experiment, performed during the reaction. The radical pair responsible for this effect may be a short-lived propionyloxy/ethyl pair, but more likely (in view of the results for AP and isobutyryl peroxide) the pentachloroacetyl/ethyl radical pair (cf. scheme 2). Polarization in the corresponding coupling products (ethylpropionate or pentachloropentanone) has not been detected. Non-observation of polarization in the ester indicates that induced decomposition of the type  $\text{R}\cdot + (\text{RCOO})_2 \rightarrow \text{RCOOR} + \text{RCOO}\cdot$  is unimportant.

Polarization in butane could be observed more clearly during decomposition of PPO in hexachlorobutadiene, containing 1 M ethyliodide. The butane spectrum is presented in figure 2a and a satisfactory simulation in figure 2b. Ethyliodide itself became also polarized (A/E) due to a symmetrical exchange reaction of polarized ethyl radicals<sup>20</sup>



Decomposition of PPO in tetrachloroethylene at  $110^\circ$  resulted in the spectrum of figure 3.

Figure 2.

100 Mc spectrum of butane formed during decomposition of PPO in the presence of ethyliodide (a) and a computer simulation with  $|J| = 5 \cdot 10^8$  rad/sec (b).

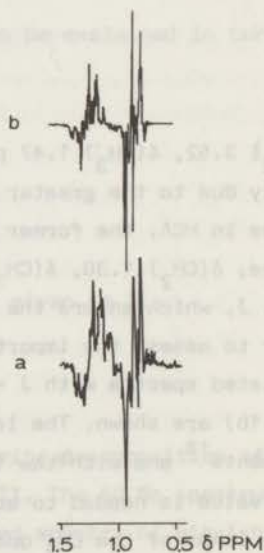
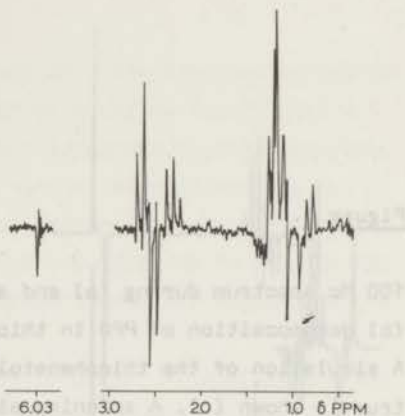
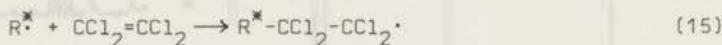


Figure 3.

100 Mc spectrum resulting from the decomposition of PPO in tetrachloroethylene.



The enhanced lines ( $\delta$  6.03 ppm, E; 2.57 and 1.13 ppm A/E) are tentatively assigned to 1,1,2,2-tetrachlorobutane (the same E-line at 6.03 ppm was observed in the case of butyryl peroxide in  $C_2Cl_4$ ):



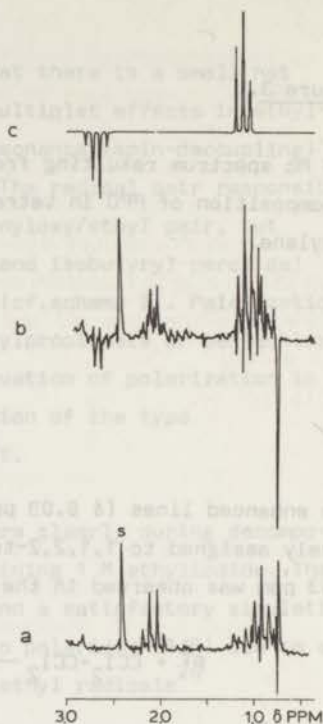
The E effect for the abstracted proton could arise from F-pairs:

$\Gamma_{ne} = + + - + = -$ , indicating that the addition to the solvent is not very fast.

Finally, the reaction of PPO in thiophenol at  $110^{\circ}$  gives rise to the spectrum shown in figure 4b. Polarization of butane is completely suppressed, indicating that thiophenol is a powerful radical scavenger. Polarized products are thiophenetole ( $\phi SR$ ) and ethane (RH). The reactions (13) can account for this, polarization originating from recombination and escape from the ethyl/thiophenoxy radical pair. A value  $g = 2.0071$  was needed for the simulation of thiophenetole ( $\delta(CH_2)$  2.68 ppm E,  $\delta(CH_3)$  1.12 ppm A), considerably higher than the value quoted in ref. 14,  $g = 2.0040$ . The discrepancy may be partly due to nuclear relaxation (cf. VII and X). The ethane emission is caused by the fact that the positively coupled  $CH_3$  protons in the ethyl radical are in the majority. High yields of unpolarized propionic acid ( $\delta(CH_2)$  2.09,  $\delta(CH_3)$  0.93 ppm) are obtained; the mechanism by which it is formed is not clear.

Figure 4.

100 Mc spectrum during (a) and after (b) decomposition of PPO in thiophenol. A simulation of the thiophenetole spectrum is shown (c). A spinning sideband of the solvent peak is indicated by S.



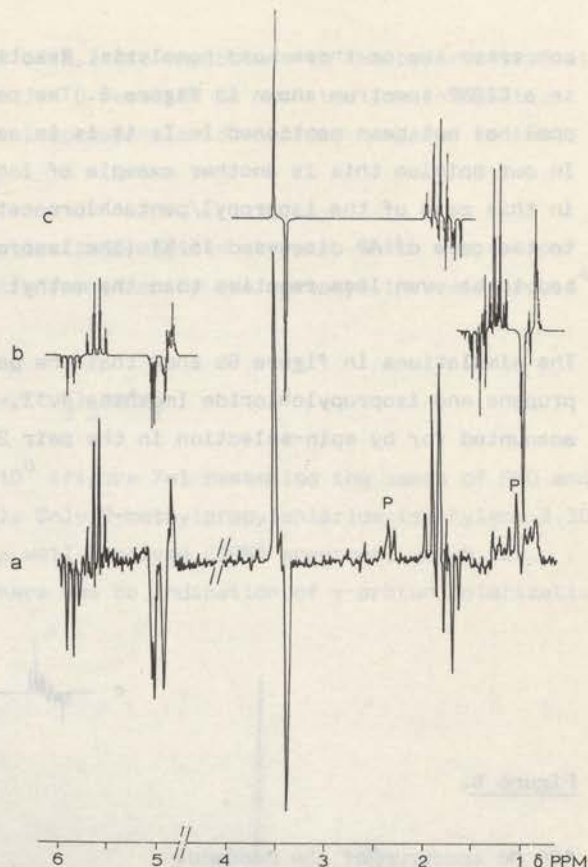
## 2.2 Butyryl peroxide $R\cdot = \text{CH}_3\text{CH}_2\dot{\text{C}}\text{H}_2$

This peroxide behaved very similar to PPO. The 100 Mc spectrum obtained during decomposition in HCA at  $110^\circ$  is shown in figure 5a (cf. I). The simulations (fig. 5b) for n-propylchloride ( $\alpha$   $-\text{CH}_2$  3.44,  $\beta$   $-\text{CH}_2$  1.82 ppm) propene (methylene 4.84, methine 5.70 ppm) and propane (methylene 1.32, methyl 0.85 ppm) are based on the reactions of scheme 2 (disproportionation and escape from the pair  $2R\cdot$ ). Agreement of calculated with observed relative intensities is good. The small net A effect for the central line of the propylchloride triplet may have the same origin as the net effects for ethylchloride.

The hf. constant of the  $\gamma$ -protons (0.38 G) is too small to give observable effects in the CIDNP spectrum. This is reflected in the normal relative intensities within the propene methine quartets. Also, polarization was not observed for these protons, but the high field region

Figure 5.

100 Mc spectrum obtained during decomposition of butyryl peroxide in HCA (a) and computer simulations of propene and propane (b) and of n-propylchloride (c). Lines due to the peroxide are indicated by P.



is obscured by many overlapping signals; polarized hexane may be present as well.

When the decomposition is carried out in thiophenol, an E triplet at 2.92 ppm is observed due to the S-CH<sub>2</sub> protons of propylthiophenolate ( $\phi$ SCH<sub>2</sub>CH<sub>2</sub>CH<sub>3</sub>). The same arguments apply here as in the case of PPO, as to the explanation of this effect.

### 2.3 Isobutyryl peroxide. R<sup>•</sup> = CH<sub>3</sub>CHCH<sub>3</sub>

The reaction of this peroxide in the presence of CCl<sub>3</sub>Br has been treated in VI<sup>21</sup> and its kinetics in IX<sup>11</sup>. The activation energy for decomposition (27.3 kcal/mole<sup>22</sup>) is lower than in the preceding cases, indicating

concerted two or three-bond homolysis. Reaction in HCA at 80° results in a CIDNP spectrum shown in figure 6. The polarization of PCA (6.74 ppm) has not been mentioned in I; it is in accord with reaction (11). In our opinion this is another example of long enduring spin-correlation, in this case of the isopropyl/pentachloroacetyl radical pair, similar to the case of AP discussed in XI (the isopropyl radical would be expected to be even less reactive than the methyl radical).

The simulations in figure 6b show that the polarizations of propene, propane and isopropylchloride (methine 4.12, methyl 1.46 ppm) are well accounted for by spin-selection in the pair 2R•.

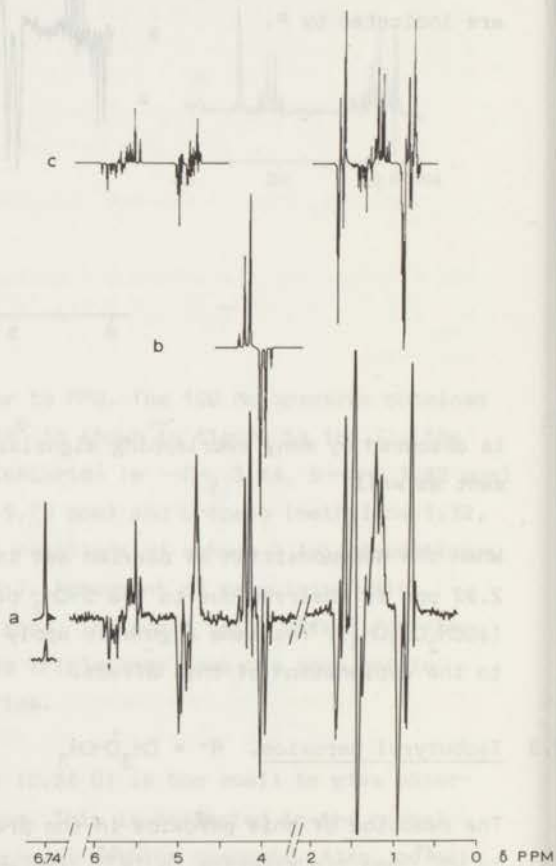


Figure 6.

100 Mc spectrum of the decomposition of isobutyryl peroxide in HCA (a) and computer simulations of isopropylchloride (b) and of propene and propane (c).

There may be contributions of 2,3-dimethylbutane to the polarization at 0.9 ppm. Calculations with  $J = 0$  resulted in much too low intensities for the outer lines of the isopropylchloride septet, compared to the inner lines.

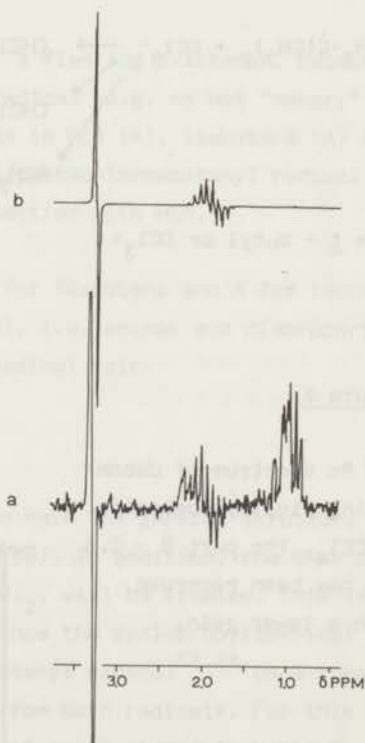
A major product was the ester, isopropylisobutyrate, which was not polarized, in keeping with its formation by the carboxyl inversion route<sup>4c,5</sup> (reaction 4).

2.4 Isovaleryl Peroxide.  $R^{\bullet} = (\text{CH}_3)_2\text{CH}\dot{\text{C}}\text{H}_2$

Decomposition in HCA at 110<sup>o</sup> (figure 7a) resembled the cases of PPO and butyryl peroxide (class b). Only 2-methylpropylchloride (methylene 3.30, methine 1.95 ppm) showed a well resolved CIDNP spectrum, which is simulated in figure 7b. There was no indication of  $\gamma$ -proton polarization.

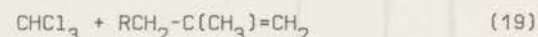
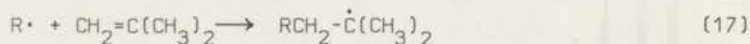
Figure 7.

100 Mc spectrum of the decomposition of isovaleryl peroxide in HCA (a) and a computer simulations of 2-methylpropylchloride.



2.5 Pivaloyl peroxide.  $R^\bullet = (\text{CH}_3)_3\dot{\text{C}}$

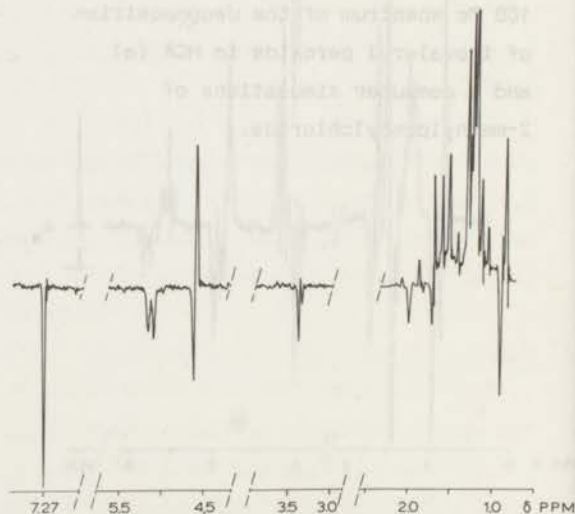
This extremely unstable peroxide decomposed rapidly at room temperature. The CIDNP spectrum resulting from decomposition in  $\text{CCl}_4$  ( $30^\circ$ ) is shown in figure 8. The products isobutane (methyl 0.89 ppm) and isobutene (methylene 4.60, methyl 1.71 ppm) show E/A multiplets as expected from the theory. Note that for isobutene this is due to a negative nuclear spin coupling constant (cf. VIII). Isobutane exhibits a second order multiplet effect (E/A, A/E) superimposed on the E/A effect, as discussed in VIII. Apart from chloroform at 7.26 ppm, E, there are a number of E lines at 1.99, 3.35 and 5.10 ppm, which have not been assigned. We suggest that these lines belong to coupling and/or disproportionation products of secondary radicals formed by addition to isobutene:



$R^\bullet = t$ -butyl or  $\text{CCl}_3^\bullet$

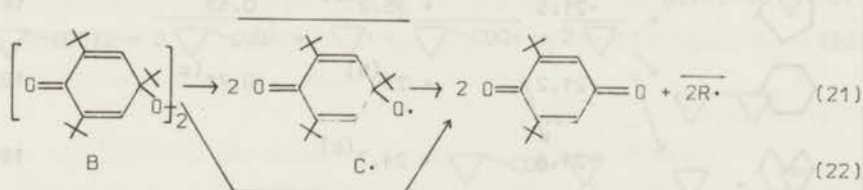
Figure 8.

100 Mc spectrum of decomposing pivaloyl peroxide in  $\text{CCl}_4$ . The part 0 - 2.5 ppm has been recorded with a lower gain.



E effects for all protons would result from free radical encounters (F-type), since the hf. parameters in the secondary radical will be positive:  $\Gamma_{ne} = + + - +, = -$ . The chloroform E signal is probably also due to reactions (18) and (19) and not to disproportionation of  $\text{CCl}_3\cdot$  with t-butyl radicals, because isobutene does not show E.

In part I we reported reactions of t-butyl radicals generated from bis (1,3,5-tri-t-butyl-2,5-cyclohexadienone) peroxide (B). An interpretation of the spectra given in I can be given now. The polarizations during reaction in HCA ( $130^\circ$ ) are in accord with the reactions of scheme 2 with  $\text{R}\cdot = \text{t-butyl}$ . Decomposition may proceed by (21) or by direct formation of the t-butyl radical pair (22):



If radical  $\text{C}\cdot$  exists, it can have only a fleeting existence, because no polarization is observed due to this radical (e.g. no net "memory" effect in isobutane). Rather large net effects in PCA (A), isobutene (A) and t-butylchloride (E) due to the t-butyl/pentachloroacetyl radical pair indicate a relatively fast transfer reaction with HCA.

Reaction in thiophenol gave rise to E for isobutane and A for isobutene, which is consistent with reactions (13), i.e. escape and disproportionation from the t-butyl/thiophenoxy radical pair.

### 3. Alicyclic Acyl Peroxides.

The peroxides discussed in this section have the general structure  $[(\text{CH}_2)_{n-1}\text{CHCOO}]_2$  where  $n = 3-7$  (ring size). In addition, the case of cyclopropylacetylperoxide,  $(\triangle\text{CH}_2\text{COO})_2$ , will be treated. This latter peroxide constitutes a special case, since the cyclopropylcarbonyl radical undergoes a rearrangement to the butenyl radical<sup>23,24</sup> on a time-scale such as to give rise to CIDNP effects from both radicals. For this reason, the hf. parameters of the butenyl radical are included in table 2, together with those of the cycloalkyl radicals.

Table 2.

Hyperfine coupling constants of cycloalkyl and butenyl radicals, in gauss.

Radical	$A_\alpha$	$A_\beta$	$A_\gamma$	ref.
	- 6.5 <sup>(a)</sup>	+ 23.4 <sup>(a)</sup>		16
	-21.2	+ 36.7	1.12	16
	-21.5	+ 35.2 <sup>(b)</sup>	0.53	16
	-21.2	+ 23 <sup>(b)</sup>	0.71 <sup>(c)</sup>	16
	-21.8	+ 24.7 <sup>(b)</sup>		16
	-20.7	+ 2.55 <sup>(a)</sup>	2.98(anti) 2.01(syn)	24a
$\text{CH}_2=\text{CH}\dot{\text{C}}\text{H}_2\text{CH}_2$	-22.2	+ 28.5	0.61 <sup>(d)</sup>	24a

(a) sign determined from CIDNP (this work).

(b) average of two types of  $\beta$ -hydrogen coupling constants.

(c)  $\delta$ -protons.

(d) an additional splitting of 0.35 G was observed due to coupling with one  $\delta$ -proton<sup>24a</sup>.

The chemistry of these peroxides has been studied by Hart<sup>25</sup> and coworkers. Only cyclopropylcarbonyl peroxide ( $n=3$ ) belongs to class (a) and shows polarization for the corresponding ester. The spectra obtained during thermolysis of the 4 to 7 membered ring acyl peroxides in HCA have very similar characteristics. Polarization of the cycloalkylchlorides (A/E) and cycloalkenes is most prominent. Assignments are given in tables 3 and 4.

The cycloalkanes produced during reaction in thiophenol all showed single E lines.

3.1 Cyclopropanecarbonyl peroxide.  $R\cdot = \triangle$

Strongly polarized spectra were encountered during decomposition of cyclopropanecarbonyl peroxide in HCA at 115° (figure 9a). The peak assignments are given in table 3. The PCA signal at 6.74 ppm is not enhanced (impurity). All net effects are probably generated in the cyclopropyl/cyclopropylcarboxyl radical pair:

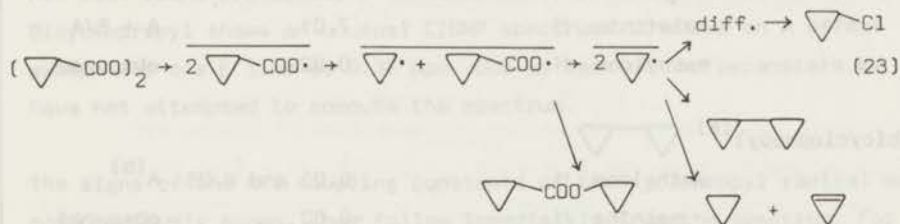


Figure 9.

100 Mc spectrum of the decomposition of cyclopropane-carbonyl peroxide in HCA (a) and simulated spectra of the ester (cyclopropyl cyclopropanecarboxylate) (b), and of cyclopropylchloride (c).

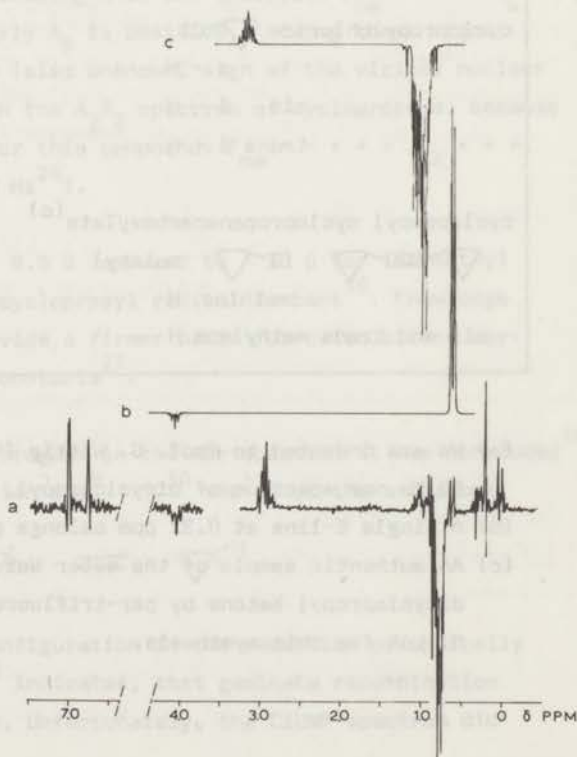


Table 3.

Assignment of CIDNP spectrum of the decomposition of cyclopropanecarbonyl peroxide in HCA (figure 9).

product		$\delta$ (ppm)	polarization	
cyclopropane		0.22	A	
cyclopropene		olefinic H	7.01	A + E/A
		methylene H	0.92	obscured
bicyclopropyl <sup>(a)</sup>		methylene H	0.00 and 0.25	A <sup>(b)</sup>
		methine H	-0.80	obscured
cyclopropylchloride		$\alpha$ - H	2.96	A
		cis $\beta$ - H	0.74	E
		trans $\beta$ - H	0.87	E
cyclopropyl cyclopropanecarboxylate <sup>(c)</sup>		(O  moiety)		
		methine H	4.05	E
		cis and trans methylene H	0.60	A

(a) We are indebted to Prof. G. Wittig (Heidelberg) for a copy of a 60 Mc nmr spectrum of bicyclopropyl.

(b) A single E-line at 0.32 ppm belongs probably also to this compound.

(c) An authentic sample of the ester was prepared by oxidation of dicyclopropyl ketone by per-trifluoro-acetic acid. We thank Mr. C. M. Lok for this synthesis.

As shown in IX, this reaction sequence can account for net polarization in bicyclopropyl, cyclopropane and cyclopropene (memory effect). It is therefore unnecessary to invoke a reaction of the type



The E/A effect observed for cyclopropene is probably due to the pair  $2 \nabla\cdot$ . For the simulations of figure 9b (ester) and 9c (cyclopropylchloride) a g-value of 2.0073 has been used for the acyloxy radical. Coupling or disproportionation products of cyclopropyl radicals have not been found previously<sup>25a</sup> in decompositions carried out at 70°. Bicyclopropyl shows an unusual CIDNP spectrum: it shows an A effect except for one E line at 0.32 ppm. Due to lack of nmr parameters we have not attempted to compute the spectrum.

The signs of the hf. coupling constants of the cyclopropyl radical were not previously known. They follow immediately from the spectrum. For instance, for the  $\alpha$ -proton, showing A in the chloride:  $\Gamma_{ne} = - - - A_\alpha = +$ , hence  $A_\alpha$  is negative. Similarly  $A_\beta$  is positive. Knowing these signs, it is possible to derive the (also unknown) sign of the vicinal nuclear spin coupling constant  $J_{AX}$  in the  $A_2X_2$  spectrum of cyclopropene, because of the E/A effect observed for this compound:  $\Gamma_{me} = - + + - J_{AX} + = +$ , hence  $J_{AX}$  is positive (+ 1.8 Hz<sup>26</sup>).

The small magnitude of  $A_\alpha$  (- 6.5 G compared to - 23 G for the methyl radical) indicates that the cyclopropyl radical is bent<sup>16</sup>. Knowledge of the sign of  $A_\alpha$  should provide a firmer basis for calculations correlating geometry with hf. constants<sup>27</sup>.

From the equivalence of  $\beta$ -hydrogens in the esr spectrum it was concluded<sup>16</sup> that there is a rapid inversion ( $10^9 - 10^{10} \text{ sec}^{-1}$ ) at the  $\alpha$ -C atom:



The observed retention of configuration in the reduction of optically active cyclopropylbromides<sup>28</sup> indicates, that geminate recombination competes with this inversion. Unfortunately, the CIDNP spectrum did

not permit an estimate of the rate of inversion. It appears, however, that this problem could be studied in suitably substituted cyclopropanecarbonyl peroxides.

Decomposition in thiophenol or other hydrogen donors resulted in a strong E line for cyclopropane.

3.2 Cyclobutanecarbonyl peroxide R• =  $\square^{\bullet}$

This peroxide decomposed conveniently at 110° in HCA (figure 10, table 4). Polarization for PCA, cyclobutene and cyclobutylchloride

Table 4.

Assignments of CIDNP spectra of the decomposition of cyclic acyl peroxides, with n-membered ring  $[(\text{CH}_2)_{n-1}\text{CHCOO}]_2$  (n = 4-7) in HCA.

Product	n = 4 δ (ppm)	n = 5 δ (ppm)	n = 6 δ (ppm)	n = 7 δ (ppm)
cycloalkene (a)				
olefinic H	5.90 A + E/A	5.61 A+E/A	5.56 E/A <sup>(b)</sup>	5.64 E/A <sup>(b)</sup>
allylic H	-2.5 obscured	2.29 E/A	-2.0 obsc.	-2.1 obsc.
cycloalkylchloride				
α - H	4.30 A/E	4.27 A/E	3.38 A/E	4.09 A/E
β - H	-2.2-2.5 A/E	1.96 A/E	-1.7 A/E	-1.7 A/E
PCA <sup>(c)</sup>	6.74 A	6.74 A	6.74 strong A	6.74 A

(a) cycloalkane signals at 1.92, 1.48, 1.41 and 1.51 ppm for n = 4-7 were not enhanced.

(b) complex pattern.

(c) pentachloroacetone.

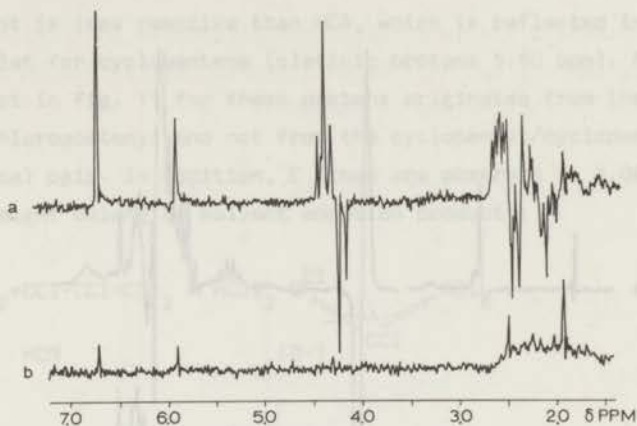


Figure 10. 100 Mc spectrum of cyclobutanecarbonyl peroxide during (a) and after (b) decomposition in HCA.

is manifest. The region between 1.5 and 2.5 ppm shows a complex polarized spectrum, predominantly due to the chloride, overlapping with lines of other products, which we have not attempted to unravel. Reactions of scheme (2) can account for the observed polarization. The cyclobutyl radical probably has a planar geometry at the  $\alpha$ -C atom. A/E effects in cyclobutylchloride confirm the opposition of signs of  $A_\alpha$  and  $A_\beta$  expected for this geometry.

### 3.3 Cyclopentane carbonyl peroxide $R\cdot =$ C1CCC(C1)O

Figure 11 shows the spectrum obtained during decomposition of the 5-membered ring peroxide. Polarization is essentially similar to the previous case (cf. table 4). The spectrum shows somewhat more detail: the allylic protons of cyclopentene are observable at 2.29 ppm; each line of the "triplet" shows an E/A effect (positive nuclear coupling constant). Note, however, that the main splitting is due to the homo-allylic protons, which have a hf. coupling constant too small to affect the spectrum ( $\gamma$ -protons). The single line of cyclopentane at 1.48 ppm is not enhanced. Scheme 2 accounts for the polarizations.

Decomposition of this peroxide in hexachlorobutadiene (HCB) resulted in a spectrum, partially shown in figure 12.

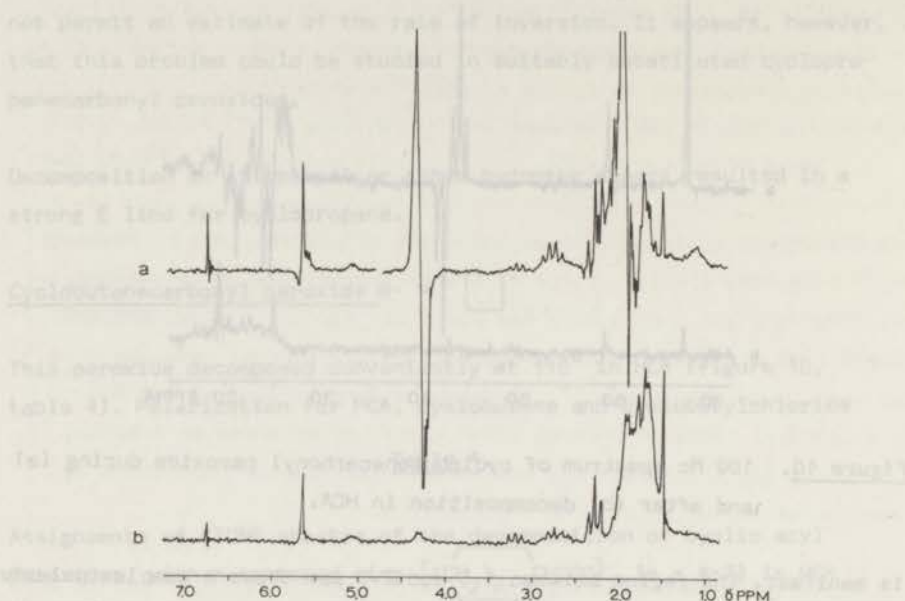


Figure 11. 100 Mc spectrum of cyclopentanecarbonyl peroxide during (a) and after (b) decomposition in HCA

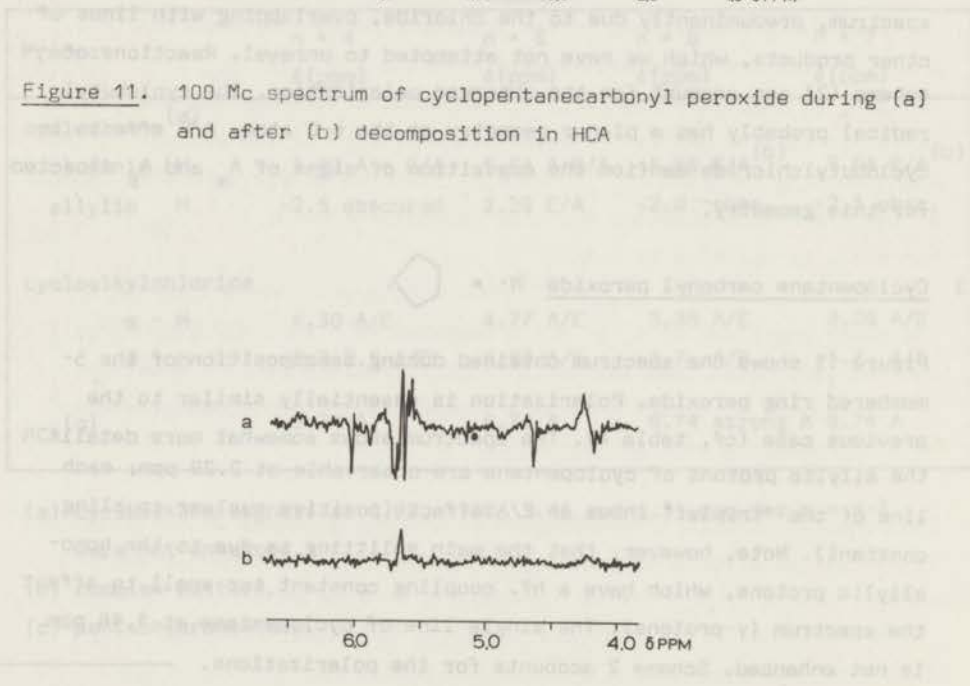
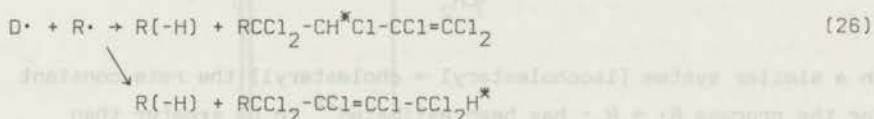
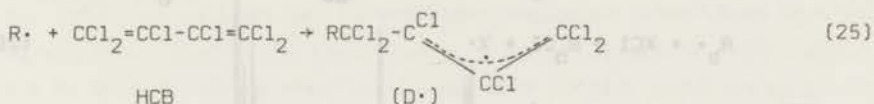


Figure 12. 100 Mc spectrum taken during (a), and after (b) decomposition of cyclopentanecarbonyl peroxide in hexachlorobutadiene.

This solvent is less reactive than HCA, which is reflected in a pure E/A multiplet for cyclopentene (olefinic protons 5.60 ppm). Apparently the A effect in fig. 11 for these protons originates from the cyclopentyl/pentachloroacetyl and not from the cyclopentyl/cyclopentylcarboxyl radical pair. In addition, E lines are observed at 6.06 and 4.68 ppm, that might belong to solvent addition products:



The allyl type radical D· can be expected to give two disproportionation products. Both E lines occurred in all α-branched peroxides, decomposed in HCB. Theory predicts E effects for F-pairs with Δg < 0, in accord with reactions (25) and (26).

The cases of the cycloalkancarboxyl peroxides with n = 6 and 7 resembled those with n = 4 and 5 (cf. table 4); spectra are not shown. The high field region was rather structureless. The α-proton of the chloride showed A/E effects. In the case of the cyclohexyl radical in particular, a strong A effect for PCA was observed. The spectra of products of the n = 4-7 cycloalkyl radicals did not permit an evaluation of the rate of ring inversion, which tends to average out the β-proton hf. couplings. This process is probably fast on the CIDNP time-scale<sup>16</sup>.

### 3.4 Cyclopropylacetyl peroxide $R\cdot = \triangle-\text{CH}_2\cdot$

The decomposition of this peroxide has been described by Hart *et al.*<sup>25</sup>. The faster rate of decomposition as compared to other cycloalkylacetyl peroxides has been ascribed to resonance stabilization of the cyclopropylcarbinyl radical and concerted peroxide bond cleavage (reactions 2 and/or 3). High yields of ester (unpolarized) are indicative of significant contributions by a polar reaction path.



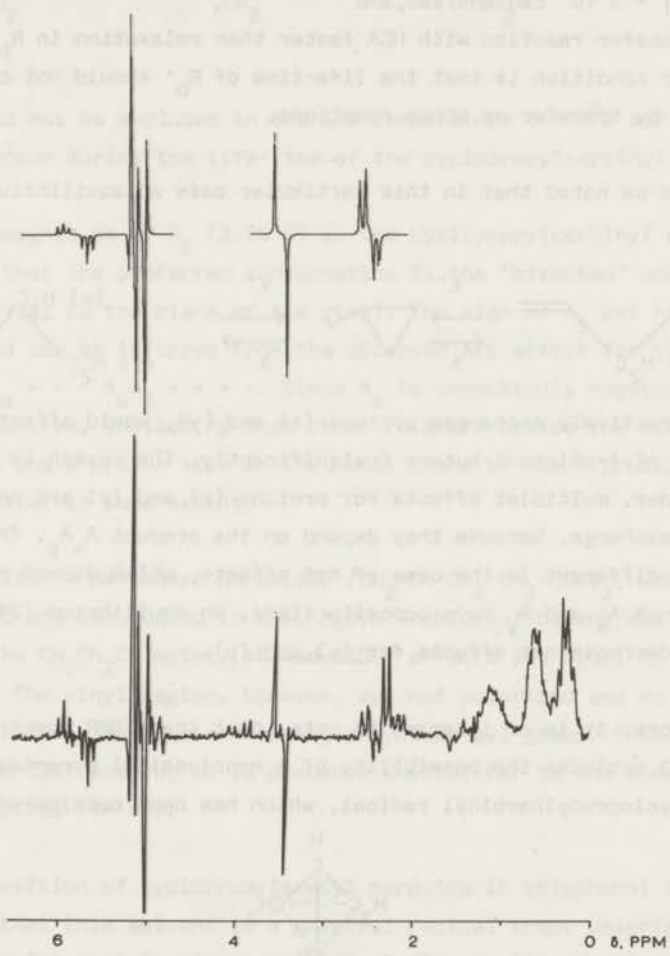
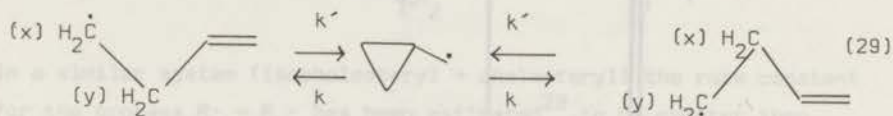


**Figure 13.** 100 Mc spectrum obtained during decomposition of cyclopropaneacetyl peroxide in HCA. A simulated spectrum of 4-chloro-1-butene is shown on top.

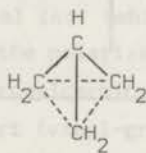
- (i) equal diffusive behaviour for  $R_a^{\cdot}$  and  $R_b^{\cdot}$ ,
  - (ii) equal efficiencies of recombination during encounters for the pairs  $2R_a^{\cdot}$ ,  $R_a^{\cdot}/R_b^{\cdot}$  and  $2R_b^{\cdot}$ ,
  - (iii)  $|J| = 5 \cdot 10^8$  radians/sec, and
  - (iv) transfer reaction with HCA faster than relaxation in  $R_b^{\cdot}$ .
- A further condition is that the life-time of  $R_b^{\cdot}$  should not be shortened too much by transfer or other reactions.

It should be noted that in this particular case an equilibrium of the type<sup>31</sup>



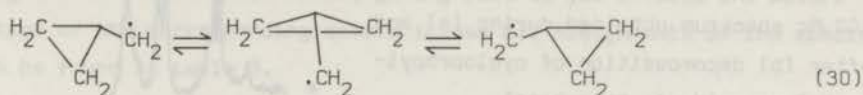
which effectively exchanges protons (x) and (y), would affect the CIDNP spectrum of 4-chloro-1-butene insignificantly. The reason is that in first order, multiplet effects for protons (x) and (y) are not affected by this exchange, because they depend on the product  $A_x A_y$ . The situation would be different in the case of net effects, which depend on  $\Delta g A_x$  and  $\Delta g A_y$ . Since  $A_x$  and  $A_y$  have opposite signs, an equilibrium (29) would tend to decrease net effects for (x) and (y).

Furthermore, it is of interest to note, that the CIDNP spectrum of figure 13 excludes the possibility of a nonclassical pyramidal structure of the cyclopropylcarbinyl radical, which has been considered<sup>32</sup>:



The high symmetry of this structure would result in a correlation of the CH-proton with all the other protons, whereas in the spectrum of this proton (5.76 ppm) only correlation with the vinyl  $\text{CH}_2$  protons is observed, as reflected in the almost normal intensities within the A and E triplets. Of course, this conclusion confirms the evidence from esr, but is obtained much more readily.

Similarly, a rate process of the type



which could not be excluded in the low temperature ( $-150^\circ$ ) esr work<sup>24a</sup>, does not occur during the life-time of the cyclopropylcarbinyl radical.

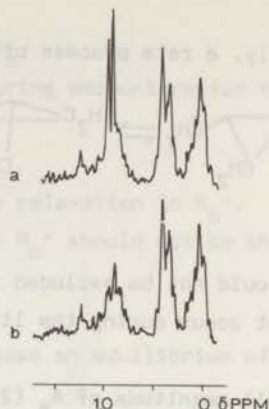
The small magnitude of  $A_\beta$  (2.55 G) in the cyclopropylcarbinyl radical indicates that the preferred conformation is the "bisected" one ( $\pi$  orbital parallel to the plane of the ring). The sign of  $A_\beta$  was hitherto unknown and can be inferred from the observed A/E effect for the methine proton:  $\Gamma_{\text{me}} = - - A_\alpha A_\beta + + = -$ . Since  $A_\alpha$  is undoubtedly negative,  $A_\beta$  must be positive, indicating that other rotamers beside the bisected one, where the  $\beta$ -proton sits in the nodal plane of the  $\pi$  orbital, are also populated to some extent.

For comparison 4-pentenoyl peroxide,  $(\text{CH}_2=\text{CH}-\text{CH}_2-\text{CH}_2-\text{COO})_2$ , was synthesized and decomposed in HCA. Again 4-chloro-1-butene was a major product. The  $\text{CH}_2\text{CH}_2\text{Cl}$  moiety showed CIDNP effects identical to those of figure 13. The vinyl region, however, was not polarized and no effects were detected for species containing a cyclopropyl group. Thus, if the equilibrium (29) occurs, it is probably shifted far to the side of the butenyl radical ( $k \gg k'$ ).

The decomposition of cyclopropylacetyl peroxide in thiophenol (figure 14) confirmed that this solvent is a powerful radical trap: polarization occurs only for methylcyclopropane ( $\text{CH}_3$  0.98 ppm, A) and not for unsaturated products. Apparently H-abstraction competes effectively with rearrangement. The A effect is in agreement with reactions (13).

Figure 14.

100 Mc spectrum obtained during (a) and after (b) decomposition of cyclopropylacetyl peroxide in thiophenol.



4.  $\alpha$ -Unsaturated Acyl peroxides.

These peroxides of this type will be examined, which generate vinyl and methyl substituted vinyl radicals during decomposition. The hf. parameters of these radicals are given in table 5.

Table 5.

Hyperfine coupling constants of vinyl-type radicals (in gauss).

Radical	$A_\alpha$	$A_\beta$	$A(\text{CH}_3)$	ref.
$\text{CH}_2=\dot{\text{C}}\text{H}$	+ 13.4 <sup>(a)</sup>	+ 68.5(trans) + 34.2(cis)		16,33a
$\text{CH}_2=\dot{\text{C}}-\text{CH}_3$		+ 57.9(trans) + 32.9(cis)	+ 19.5 <sup>(a)</sup>	16
$\text{CH}_3-\text{CH}=\dot{\text{C}}\text{H}$ <sup>(b)</sup>	+ 13	+ 51 <sup>(c)</sup>	- 7.5 $\pm$ 2	

(a) sign determined by CIDNP (this work).

(b)  $A_\alpha$  and  $A_\beta$  assumed to be similar to the vinyl radical;  $A(\text{CH}_3)$  determined from CIDNP (see text).

(c) average value of  $A_\beta(\text{cis})$  and  $A_\beta(\text{trans})$ , for a rapidly inverting radical.

The vinyl radicals have  $g = 2.0022$ . The acyloxy radicals have relatively long life-times in these cases, giving rise to net effects and polarization of the corresponding esters (class a). Assignments of the spectra can be found in table 6.

4.1 Acrylyl peroxide  $R\cdot = \text{CH}_2\overset{\cdot}{\text{C}}\text{H}$

This hazardous peroxide (see experimental section) was decomposed in HCA at  $110^\circ$ . The CIDNP spectrum of figure 15 shows net effects for vinyl-chloride (E), vinylacrylate (A), ethylene (A) and acetylene (A) (cf. table 6). In runs at higher temperatures small effects in the region 5.10 - 5.20 ppm were observed, probably due to small amounts of butadiene. The observed polarizations can be explained in terms of a reaction sequence similar to reactions (23) for cyclopropyl. Net effects arise from the vinyl/acyloxy radical pair. Here again, the A effects for ethylene and acetylene are probably another manifestation of the memory effect (cf. IX) and do not imply a reaction analogous to (24).

A serious but unsuccessful attempt has been made to simulate the characteristic pattern of CH-proton of the ester at 7.20 ppm, using the hf.

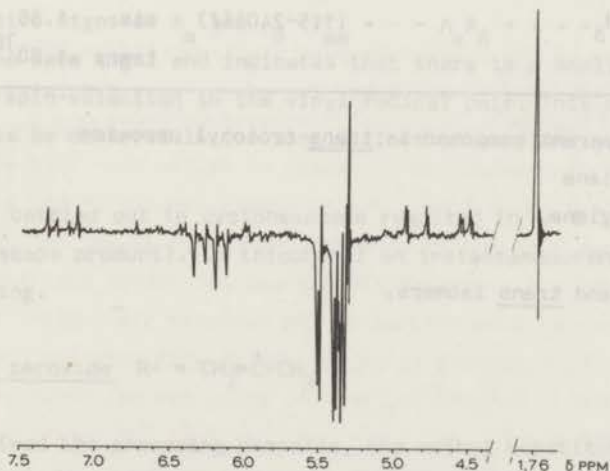


Figure 15. 100 Mc spectrum of the decomposition of acrylyl peroxide in HCA.

Table 6.

Assignments of CIDNP spectra obtained during decomposition of  $\alpha$ -unsaturated acyl peroxides  $(RCOO)_2$  in HCA.

products	R•	$CH_2=\dot{C}H$ $\delta$ (ppm)	$CH_2=\dot{C}-CH_3$ $\delta$ (ppm)	$CH_3-CH=\dot{C}H^{(a)}$ $\delta$ (ppm)
RH		5.31 <sup>(b)</sup> A		
R(-H)		1.76 <sup>(c)</sup> A	4.60 <sup>(d)</sup> A	
RC1	$\alpha$ -H	6.26 E+E/A		cis <sup>(e)</sup> 5.97 E trans <sup>(e)</sup> 5.90 E
	cis $\beta$ -H	5.48 E	5.05	5.75 E
	$\beta$ -H	5.39 E	5.06 }E(+A/E)	5.84 E
	CH <sub>3</sub>		2.06 E+A/E	cis -1.70 trans -1.65 } A
RCOOR				
	(OR moiety) $\alpha$ -H	7.20 A		cis <sup>(e)</sup> trans }-6.9 A
	cis $\beta$ -H	4.86 A		4.81 A
	trans $\beta$ -H	4.55 A	}4.8-4.9 A	5.32 A
	CH <sub>3</sub>		(1.5-2.0)(?)	cis -1.55 trans -1.60 }E(?)

(a) The parent compound is trans-crotonyl peroxide

(b) ethylene

(c) acetylene

(d) allene

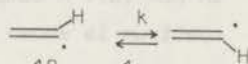
(e) cis and trans isomers.

parameters of table 5, varying  $\Delta g$  and  $J$  and considering fast and slow exchange of  $\beta$ -protons in the vinyl radical. All sorts of patterns could be calculated for this proton, except the experimentally observed one (outer lines more enhanced than inner lines). We have therefore not given a simulation in figure 15. The failure may be due to relaxation in the product.

Yet, a number of conclusions may be drawn:

(i) Both  $\alpha$  and  $\beta$ -hydrogens have positive hf. coupling constants (e.g. for the ester:  $\Gamma_{ne} = - + - A = +$ ,  $A_\alpha$  positive). For  $A_\alpha$  both positive<sup>33,27a</sup> and negative<sup>27b</sup> signs have been predicted theoretically. The positive signs are in accordance with esr measurements on vinyl radicals trapped in a neon matrix<sup>34</sup> and on oriented substituted vinyl radicals<sup>35</sup>.

(ii) Equal intensities of cis and trans  $\beta$ -hydrogens of the ester indicate that the inversion process



is fast on the CIDNP time scale ( $k > 10^{10} \text{ sec}^{-1}$ ).

A range for  $k \sim 3 \cdot 10^7 - 3 \cdot 10^9 \text{ sec}^{-1}$  has been inferred from low temperature esr work<sup>16</sup> ( $-170^\circ - -104^\circ$ ).

(iii) The small E/A effect in vinylchloride is also in accordance with positive signs of  $A_\alpha$  and  $A_\beta$  ( $\Gamma_{me} = - - A_\alpha A_\beta + + = +$ ,  $A_\alpha$  and  $A_\beta$  of the same sign) and indicates that there is a small contribution from spin-selection in the vinyl radical pair. This cannot of course be observed in the single lines of ethylene and acetylene.

Experiments carried out in cyclohexanone resulted in an E line for ethylene (escape product). In thiophenol an instantaneous reaction set in upon mixing.

#### 4.2 Methacrylyl peroxide $R \cdot = \text{CH}_2=\dot{\text{C}}-\text{CH}_3$

Having survived the preceding peroxide, the methyl substituted analogues appeared to be more stable. The CIDNP spectrum of the decomposition of methacrylyl peroxide in HCA at  $110^\circ$  is given in figure 16a (table 6). The spectrum shows enhancements for 2-chloropropene and probably for the ester, 2-propenyl methacrylate; other products contribute to the

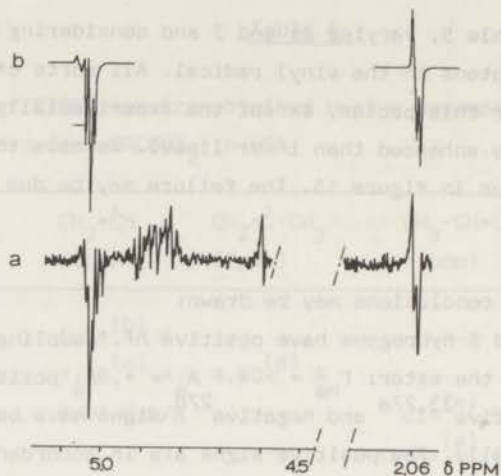


Figure 16. 100 Mc spectrum of the decomposition of methacrylyl peroxide in HCA (a). A computer simulation of the 2-chloropropene spectrum is shown on top (b) (see text).

lines at 4.8-4.9 ppm as well. The single A line at 4.60 ppm has been tentatively assigned to allene ( $\text{CH}_2=\text{C}=\text{CH}_2$ ). In addition, many lines appeared in the region 1.5-2.0 ppm which have not been assigned.

The simulation of the 2-chloropropene spectrum (figure 16b) is a superposition of two spectra calculated for escape from the pairs  $\text{R}\cdot/\text{RCOO}\cdot$  ( $\Delta g = 0.0036$ ) and  $2\text{R}\cdot$  in the ratio 5 : 4. This indicates that decarboxylation of the methacryloxy radical is faster than that of the acryloxy radical, most likely due to steric effects of the  $\alpha$ -methyl group. The fact that A/E appears for the methyl group, but vanishes almost completely for the methylene group was rather puzzling at first. It is, however, well reproduced by the computer simulation. This E + A/E effect for 2-chloropropene is in accordance with negative nuclear coupling constants between  $\text{CH}_2$  and  $\text{CH}_3$  group and all positive signs for the hf. parameters:  $\Gamma_{\text{me}} = - - + + - + - -$ , A/E. The positive sign for  $\text{A}(\text{CH}_3)$  is due to hyperconjugation similarly to the signs of  $\text{A}_\beta$  in alkyl radicals. In the isoelectronic acetyl radical ( $\text{CH}_3-\dot{\text{C}}=\text{O}$ )  $\text{A}(\text{CH}_3)$  has also been found to be positive (cf. part VII). The spectrum does not show sufficient detail to discriminate between fast and slow methyl group

inversion in the 1-methylvinyl radical, although somewhat better results were obtained in the fast exchange limit (average value for  $\text{CH}_2$  hf. constants). At  $-172^\circ$  the inversion has been found<sup>16</sup> to be slow compared to the hf. interactions.

#### 4.3 Trans-Crotonyl peroxide $\text{R}\cdot = \text{CH}_3\text{-CH}=\dot{\text{C}}\text{H}$

Decomposition of the trans peroxide in HCA at  $110^\circ$  resulted in a mixture of about equal amounts of cis and trans products (figure 17a, table S), showing that inversion of the  $\alpha$ -hydrogen of the 2-methylvinyl radical is fast, as in the case of the vinyl radical. Simulated spectra of cis and trans esters ( $\beta$ -protons) and a superposition of cis and trans 1-chloropropene ( $\alpha$  and  $\beta$ -protons) are shown in figure 17b. The esr spectrum of the 2-methylvinyl radical has not been reported, to our knowledge. Assuming that  $A_\alpha$  and  $A_\beta$  are similar to those of the vinyl

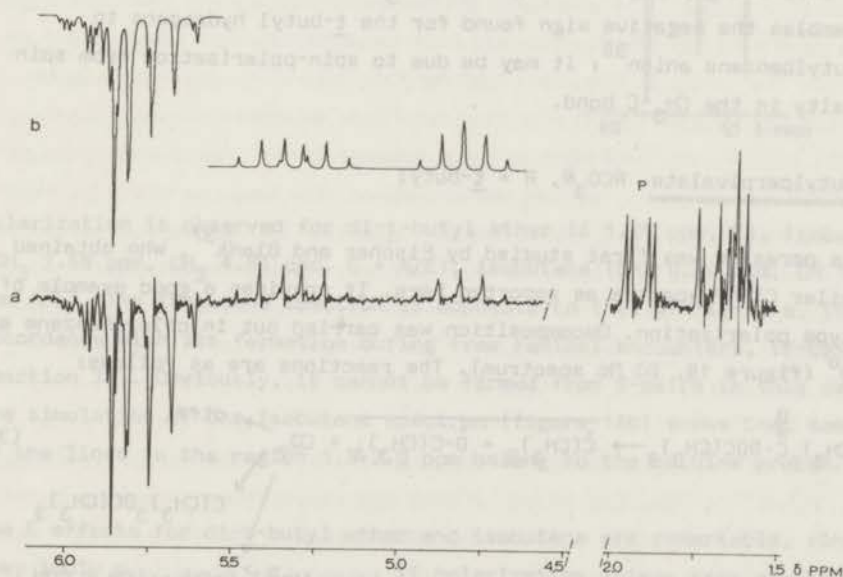


Figure 17. 100 Mc spectrum of the decomposition of trans-crotonyl peroxide in HCA (a) and computer simulations (b) for 1-chloropropene (cis and trans superimposed) and for cis and trans 1-propenyl esters of trans-crotonic acid. Peroxide peaks are indicated by P.

radical, we have taken  $A_\alpha = +13$  G and  $A_\beta = +51$  G for a rapidly inverting radical. The methyl region is unclear due to overlapping of cis and trans ester, cis and trans chloride and possibly coupling and disproportionation products. However, A lines at 1.65 and 1.70 belong to 1-chloropropene and hence a negative sign of  $A(\text{CH}_3)$  is implied,  $\Gamma_{ne} = - - - A(\text{CH}_3) = +$ ,  $A(\text{CH}_3) < 0$ . The magnitude of  $A(\text{CH}_3)$  can be estimated through its effect on the spectrum of the  $\alpha$  and  $\beta$  protons. For 1-chloropropene we considered only escape from the pair  $\text{R}\cdot/\text{RCOO}\cdot$ . The best results were obtained with  $A(\text{CH}_3) = -7.5$  G and  $\Delta g = 0.004$  (cf. figure 17b). However, the uncertainties are considerable in this case: (i) unknown  $\Delta g$ , (ii) unknown hf. constants, (iii) there may be small contributions from the pair  $2\text{R}\cdot$ , (iv) amounts of cis and trans products need not be exactly equal and (v) effects of relaxation neither in the radical nor in the product were considered. Therefore, the choice of parameters may not be unique and the uncertainty in the magnitude of  $A(\text{CH}_3)$  may be rather large. Yet, the surprisingly negative sign of  $A(\text{CH}_3)$  seems to be unambiguous. It resembles the negative sign found for the t-butyl hydrogens in t-butylbenzene anion<sup>36</sup>; it may be due to spin-polarization from spin density in the  $\text{CH}_3\text{-C}$  bond.

5. t-Butylperpivalate  $\text{RCO}_2\text{R}$ ,  $\text{R} = \text{t-butyl}$

This perester was first studied by Fischer and Blank<sup>37</sup>, who obtained similar CIDNP spectra as reported here. It provides a good example of F-type polarization. Decomposition was carried out in chlorobenzene at  $110^\circ$  (figure 18, 60 Mc spectrum). The reactions are as follows:

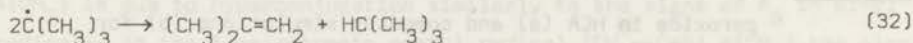
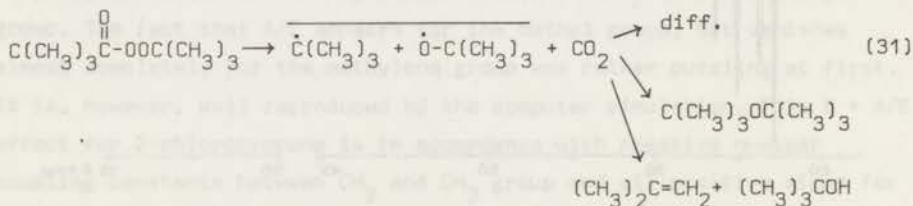
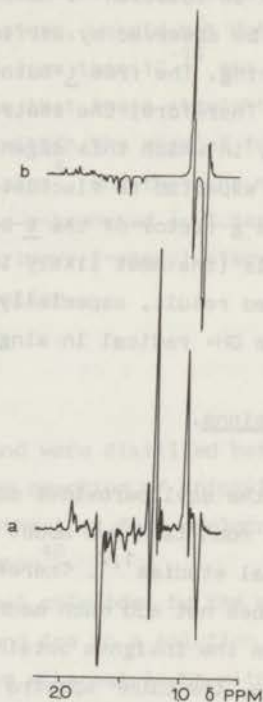


Figure 18.

60 Mc spectrum of the decomposition of t-butylperpivalate in chlorobenzene (a) and a computer simulation of the spectrum of isobutane (b).



Polarization is observed for di-t-butyl ether ( $\delta$  1.25 ppm, E), isobutene ( $\text{CH}_3$  1.68 ppm,  $\text{CH}_2$  4.61 ppm, E + A/E), isobutane ( $\text{CH}_3$  0.90 ppm, CH 1.73 ppm A/E). The isobutane spectrum is opposite to that of figure 8, in accordance with its formation during free radical encounters, (F-case, reaction 32). Obviously, it cannot be formed from S-pairs in this case. The simulation of the isobutane spectrum (figure 18b) shows that some of the lines in the region 1.3-2.0 ppm belong to the methine proton.

The E effects for di-t-butyl ether and isobutene are remarkable, since they imply  $g_{\underline{t}\text{-butoxy}} < g_{\underline{t}\text{-butyl}}$ , if polarization arises from reaction (31):  $\Gamma_{ne} = - + \Delta g + = - . \Delta g > 0$ . The alternative, polarization from free radical encounters is considered to be very unlikely for these products. It should be noted that polarization in di-t-butyl ether must be due to the t-butyl fragment, since the hydrogen hf. interactions should be much larger in the t-butyl than in the t-butoxy radical.

Several claims have been reported of esr observations of the t-butoxy radical in solution<sup>38</sup>. However, it seems likely<sup>39</sup> that this radical cannot be observed by esr in the liquid state, due to extreme line broadening. The free t-butoxy radical has an orbitally degenerate ground state. Therefore, the isotropic g-factor in solution will depend upon the way in which this degeneracy is lifted by interactions with the solvent, and is expected to fluctuate very strongly<sup>39</sup>. Our finding, that the average g-factor of the t-butoxy radical is smaller than that of alkyl radicals (the most likely interpretation of figure 18) is a rather unexpected result, especially in view of the observed<sup>14</sup>  $g = 2.0094$  for the OH· radical in single crystals of ice.

## 6. Conclusions.

Since the acyl peroxides constitute a class of thoroughly studied compounds much is known about their reaction mechanisms from careful chemical studies<sup>1,2</sup>. Therefore, it is hardly surprising that the present work does not add much mechanistic information. Rather CIDNP seems to confirm the insights obtained earlier, or, depending upon one's point of view, the CIDNP spectra of the reactions studied here constitute strong support for the radical pair theory. In all cases where esr parameters and reaction mechanisms are known, the spectra could be explained by this theory. In some cases unknown signs of hf. parameters could be obtained from the spectra (for cyclopropyl, cyclopropylcarbinyl and the vinyl type radicals). Similarly, the unknown sign of the nuclear spin coupling constant in cyclopropene could be determined. This could be done very easily with the help of the rules (6) and (7).

The rate of decarboxylation of acyloxy radicals is susceptible of study with CIDNP. Our spectra indicate that the rate decreases in the order  $R \cdot > CH_3 \cdot > CH_2 = \dot{C} - CH_3 > \triangle \cdot \sim CH_2 = \dot{C}H > CH_3 - CH = \dot{C}H$  where  $R \cdot$  is alkyl or cycloalkyl other than methyl and cyclopropyl. The longer life-time of the acyloxy radical in the last four cases is not unreasonable, in view of the high bond strength to cyclopropyl and vinyl moieties. Conjugation with the carbonyl group may also stabilize the acyloxy radicals in these cases. When  $R \cdot$  is a secondary, tertiary or resonance stabilized radical, it is doubtful that the acyloxy radicals exist outside the primary cage,

if at all. The difference between the acetoxy radical (R=methyl, part XI) and the straight chain acyloxy radicals, is noteworthy. In spite of carefully looking for enhancements in the esters, we did not detect any polarization in these cases. A life-time of less than  $10^{-10}$  sec is indicated by this non-observation. It may be that these straight chain aliphatic acyloxy radicals also exist only within the cage of formation, possibly as ion pair-radical pair intermediates<sup>5</sup>, and that the mechanism of ester formation is similar to that of the  $\alpha$ -branched acyl peroxides. Results of a  $^{18}\text{O}$ -labelling study with the primary  $\delta$ -phenylvaleryl peroxide<sup>4d</sup> seem also to point in this direction.

## 7. Experimental section.

Acyl chlorides were obtained commercially and were distilled before use. Cyclopropaneacetylchloride was obtained from reaction of thionylchloride with cyclopropaneacetic acid, which was synthesized from cyclopropane-carbonyl chloride by an Arndt-Eistert reaction<sup>40</sup>.

Acyl peroxides were synthesized from the acyl chlorides by the general procedure of Kharash<sup>41</sup> (addition of  $\text{Na}_2\text{O}_2$  and ice to a solution of the acyl chloride in ether at  $-5^\circ$ , washing the ethereal layer with cold aqueous bicarbonate and ice-water, drying over  $\text{Na}_2\text{SO}_4$ ). The purity of the peroxides was over 95% as determined by nmr. This procedure was satisfactory except for pivaloyl peroxide, due to its instability, even at  $0^\circ$ . The following procedure (cf.ref. 42) was used for the preparation of pivaloyl peroxide: A solution of 0.55 moles of pyridine and 30 ml ether was cooled to  $-10^\circ$ ; 0.15 mole 30%  $\text{H}_2\text{O}_2$  was added at such a rate that the temperature did not exceed  $0^\circ$ . The mixture was rapidly stirred and 0.2 moles of pivaloyl chloride in 30 ml ether was added in 15 min, while the temperature was kept below  $-15^\circ$ . The reaction mixture was stirred for an additional 2 hr at  $-20^\circ$  and neutralized with chilled dilute  $\text{H}_2\text{SO}_4$  solution. The water layer was then frozen out at  $-40^\circ$ , in a methanol- $\text{CO}_2$  bath. The ethereal layer was decanted, washed with 20 ml 5%  $\text{NaHCO}_3$  solution chilled to  $-10^\circ$ , and the water layer again frozen to  $-40^\circ$ . This was repeated two times with a 10%  $\text{NaCl}$  solution as well. The ethereal layer was dried over  $\text{Na}_2\text{SO}_4$  and stored at  $-80^\circ$ . Small portions were concentrated on a rotary evaporator at  $-15^\circ$  before use.

Acrylyl peroxide was found to be very unstable. It exploded frequently, even in ethereal solution, presumably due to a chain reaction involving addition to the double bond. None of the other peroxides showed this lability.

t-Butylperpivalate was prepared as described by Bartlett and Hiatt<sup>43</sup>.

Solvents were distilled before use. Hexachloroacetone contained less than 1% pentachloroacetone as an impurity.

NMR spectra. 60 Mc spectra were recorded on a Varian A-60 spectrometer; 100 Mc spectra on a Varian HA-100 spectrometer. A capillary with  $H_2SO_4$  was used as a lock signal for the HA-100 spectra. CIDNP spectra were run about 60 sec after putting a 0.2 M peroxide solution in the preheated spectrometer probe. Deoxygenating samples did not have any effect; dissolved oxygen is consumed during the first stages of the reaction. This resulted often in narrower lines during and just after the reaction than before.

#### References and Footnotes.

1. See for a general discussion: C. Walling, "Free Radicals in Solution", John Wiley, New York, N.Y., 1963, chap. 10.
2. R.C.P. Cubbon in "Progress in Reaction Kinetics", Vol.5, ed. G. Porter, Pergamon, Oxford, 1970, p. 29.
3. M. Szwarc in "Peroxide Reaction Mechanisms", ed. J.O. Edwards, Interscience, New York, N.Y., 1962, p. 153.
4. (a) F.D. Greene, H.P. Stein, C.C. Chu and F.M. Vane, J. Amer. Chem. Soc., **86**, 2080 (1964);  
(b) C. Walling, H.N. Moulden, J.H. Waters and R.C. Neuman, ibid. **87**, 518 (1965);  
(c) R.C. Lamb, J.G. Pacifici and P.W. Ayers, ibid., **87**, 3928 (1965);  
(d) T. Kashiwagi, S. Kozuka and S. Dae, Tetrahedron, **26**, 3619 (1970).
5. C. Walling, H.P. Waits, J. Milovanovic and C.P. Pappiaonou, J. Amer. Chem. Soc., **92**, 4927 (1970).

6. R. Kaptein, part VIII, to be published.
7. This term has been introduced by H.R. Ward, paper presented at the CIDNP Symposium of the 159th National Meeting of the American Chemical Society, Houston, Feb. 1970.
8. R. Kaptein, part I, Chem. Phys. Letters, 2, 261 (1968).
9. (a) G.L. Closs, J. Amer. Chem. Soc., 91, 4552 (1969);  
 (b) G.L. Closs and A.D. Trifunac, ibid., 92, 2183 (1970).
10. R. Kaptein and L.J. Oosterhoff, Chem. Phys. Letters, 4, 195, 214 (1969).
11. R. Kaptein, part IX, to be published.
12. R. Kaptein, J. Brokken-Zijp and F.J.J. de Kanter, part XI, to be published.
13. H. Fischer and J. Bargon, Accounts Chem. Research, 2, 110 (1969).
14. H. Fischer, "Magnetic properties of free radicals", Landolt-Börnstein, New Series, Group II, Vol 1, ed. K.-H. Hellwege, Springer, Berlin (1965).
15. cf. A. Carrington and A.D. McLachlan, "Introduction to Magnetic Resonance", Harper and Row, New York, (1967), chap. 6.
16. R.W. Fessenden and R.H. Schuler, J. Chem. Phys., 39, 2147 (1963).
17. The esr spectrum of the pentachloroacetyl radical consists of 5 lines due to coupling with 2 chlorine atoms with  $A_{Cl} = 3.02$  G. The g-factor is 2.0080. The radical was generated by the decomposition of benzoyl peroxide in HCA. We are indebted to Mr. F.J.J. de Kanter for taking the esr spectrum.
18. R. Kaptein and J.A. den Hollander, part X, to be published.
19. Adrian has advocated the use of  $J = 0$ , cf. F.J. Adrian, J. Chem. Phys., 53, 3374 (1970).
20. (a) H.R. Ward, R.G. Lawler and R.A. Cooper, Tetrahedron Letters, 69, 527 (1969);  
 (b) A.R. Lopley, Chem. Comm., 64 (1969).
21. R. Kaptein, F.W. Verheus and L.J. Oosterhoff, part VI, to be published.
22. J. Smid and M. Szwarc, J. Chem. Phys., 29, 432 (1958).
23. C. Walling, "Molecular Rearrangements", ed. P. de Mayo, Volume I, Interscience, New York, (1963), chap. 7.
24. (a) J.K. Kochi, P.J. Krusic and D.R. Eaton, J. Amer. Chem. Soc., 91, 1877 (1969);

- 24.(b) R.A. Sheldon and J.K. Kochi, ibid., 92, 4395 (1970).
- 25.(a) H. Hart and D.P. Wyman, ibid., 81, 4891 (1959);  
(b) H. Hart and R.A. Cipriani, ibid., 84, 3697 (1962).
26. K.B. Wiberg and B.J. Nist, ibid., 83, 1226 (1961).
- 27.(a) R.S. Drago and H. Petersen, ibid., 89, 5774 (1967);  
(b) T. Yonezawa, T. Kawamura and H. Kato, Bull. Chem. Soc. Jap., 43, 74 (1970).
- 28.(a) H.M. Walborsky and C.J. Chen, J. Amer. Chem. Soc., 89, 5499 (1967);  
(b) J. Jacobus and D. Pensak, Chem. Comm., 400 (1969);  
(c) L.J. Altman and T.R. Erdman, Tetrahedron Letters, 4891 (1970).
29. D.J. Carlsson and K.U. Ingold, J. Amer. Chem. Soc., 90, 7047 (1968).
30. Authentic 4-chloro-1-butene was synthesized from cyclopropylcarbinol, cf. J.D. Roberts and R.H. Mazur, J. Amer. Chem. Soc., 73, 2509 (1951). We thank Mrs. M. Fráter-Schröder for the synthesis of this compound and that of cyclopropylacetyl peroxide.
31. L.K. Montgomery and J.W. Matt, ibid., 89, 3050, 6556 (1967).
32. T.A. Halgren, M.E.H. Howden, M.E. Medof and J.D. Roberts, ibid., 89, 3051 (1967).
- 33.(a) E.L. Cochran, F.J. Adrian and V.A. Bowers, J. Chem. Phys., 40, 213 (1964);  
(b) J.A. Pople, D.L. Beveridge and P.A. Dobosh, J. Amer. Chem. Soc., 90, 4201 (1968).
34. P.H. Kasai, E.B. Whipple, ibid., 89, 1033 (1967).
35. M. Iwasaki and B. Eda, J. Chem. Phys., 52, 3837 (1970).
36. E. de Boer and H. van Willigen, in "Progress in NMR Spectroscopy", Volume 2, ed. J.W. Emsley, J. Feeney and L.H. Sutcliffe, Pergamon, Oxford, (1967), chap. 3.
37. H. Fischer and B. Blank, personal communication.
- 38.(a) L.H. Piette and W.C. Landgraf, J. Chem. Phys., 32, 1107 (1960);  
(b) S. Weiner and G.S. Hammond, J. Amer. Chem. Soc., 91, 2182 (1969).
39. M.C.R. Symons, ibid., 91, 5924 (1969).
40. J.H. Turnbull and E.S. Wallis, J. Org. Chem., 21, 663 (1956).
- 41.(a) M.S. Kharash, S.S. Kane and H.C. Brown, J. Amer. Chem. Soc., 63, 526 (1941);  
(b) M.S. Kharash, J. Kuderna and W. Nudenberg, J. Org. Chem., 19, 1283 (1954).

42. J.K. Kochi and P.E. Mocadlo, ibid., 30, 1134 (1965).
43. P.D. Bartlett and R.R. Hiatt, J. Amer. Chem. Soc., 80, 1398 (1958).

## SAMENVATTING.

Wanneer men een kernspin resonantie (nmr) spectrum meet van een oplossing, waarin een radicaal reactie optreedt, kunnen de producten, die daarbij gevormd worden, aanzienlijk versterkte absorptie en ook emissie lijnen te zien geven. Deze effecten werden in 1967 bij toeval ontdekt door Bargon, Fischer en Johnsen in Darmstadt en door Ward en Lawler in Providence (USA). Dit verschijnsel werd aangeduid met de naam "Chemically Induced Dynamic Nuclear Polarization" (CIDNP) en vormt het onderwerp van dit proefschrift.

De in 1967 gepubliceerde theorie van CIDNP (gebaseerd op gecombineerde kern-electron relaxatie in vrije radicalen) bleek niet te voldoen. Daarom werd door ons naast de experimentele ook de theoretische kant van dit onderwerp bestudeerd. Dit heeft geleid tot een betere verklaring van de CIDNP effecten, die ook door Closs (Chicago) onafhankelijk gevonden werd, en die nu vrij algemeen aanvaard is.

In deze "radicaal paar theorie" worden de verschijnselen toegeschreven aan overgangen tussen singulet en triplet toestanden van radicaal paren. De overgangen worden geïnduceerd door interacties van kernspins met electronen spins. Alhoewel de kernspin toestanden hierbij niet veranderen (althans in hoog magnetisch veld) beïnvloeden zij wel de singulet-triplet overgangswaarschijnlijkheid en daardoor ook de reactie kans van het radicaal paar, aangezien recombinitie gewoonlijk alleen vanuit de singulet toestand kan geschieden. De populaties van de kernspin niveaus van recombinitie producten maar ook die van de producten van ontsnappende radicalen, krijgen hierdoor grote afwijkingen van thermisch evenwicht, hetgeen in de nmr spectra tot uitdrukking komt als emissie of versterkte absorptie.

Deze theorie, waarvan de basis gelegd wordt in Hst. II en III, wordt toegepast ter verklaring van de CIDNP effecten, die optreden bij de fotolyse (direct en gesensibiliseerd) van acyl peroxiden (Hst. IV); bij een reactie, waarin een biradicaal als intermediair optreedt (Hst. V); bij de ontleding van isobutyryl peroxide in aanwezigheid van verschillende concentraties  $\text{CCl}_3\text{Br}$ , waarbij omkeer van de

polarisatie optreedt (Hst. VI); en bij photochemische reacties van diisopropyl keton, in welk geval een nieuwe photoreactie met  $\text{CCl}_4$  ontdekt werd (Hst. VII).

Een vollediger discussie van de theorie wordt gegeven in Hst. VIII. Rekening wordt gehouden met de diffusie van radicaal paren, door toepassing van een "random walk" diffusie model van Noyes. Een uitbreiding hiervan voor de beschrijving van snelle radicaal reacties, die concurreren met "kooi"-recombinatie, wordt gegeven in Hst. IX, waar ook enige voorbeelden besproken worden.

De magneetveld afhankelijkheid van CIDNP is het onderwerp van Hst. X. Het blijkt, dat bij reacties in lage magneetvelden rekening gehouden moet worden met de drie laagste triplet toestanden van het radicaal paar (in hoog veld slechts met één). Enkele eigenaardige effecten, zoals oscillaties in de veld afhankelijkheid van de polarisatie, kunnen dan verklaard worden.

Tenslotte worden thermische ontledingen van acyl peroxiden behandeld, acetyl peroxiden in Hst. XI en een serie andere peroxiden in Hst. XII. De reactie, waarbij het cyclopropylcarbiny radical gevormd wordt, dat zich omlegt tot het 3-butenyl radicaal, is er een voorbeeld van, hoeveel informatie een CIDNP spectrum kan geven over reactiemechanisme en structuur van radicalen.



#### ACKNOWLEDGEMENT.

It is a pleasure to acknowledge many stimulating conversations with Professors H. Fischer, H.R. Ward, R.G. Lawler and G.L. Closs, by which this work has greatly benefited. These and other investigators, Prof. A.R. Lepley, Dr. S.H. Glarum, Dr. A.M. Trozzolo and Dr. F.J. Adrian, have generously made available their results prior to publication.

Special thanks are due to Mr. J.A. den Hollander for the pleasant cooperation on several parts of this work and for numerous discussions on other parts.

I also wish to thank Dr. T.A. van Santen for illuminating discussions on some delicate theoretical problems and Mrs. Dr. M. Fráter-Schröder for helpful suggestions and excellent experimental assistance.

For their skilful help with the experiments I am greatly indebted to my coworkers: H.F. Poort, G.J. van Kampenhout, C.M. Lok, J. Valk, Mrs. J. Brokken-Zijp, G.A. van Albada, H.J. de Jong, P.C.M. van Rossum, F.J.J. de Kanter, D. Antheunis, P.A.T.M. Brand, R.L.C. Wijting, F.W. Verheus, and J.P.M. van der Ploeg.

Mrs. L.G.A. Meijer-te Meij has kindly read parts of the manuscript and corrected the English.

CURRICULUM VITAE

Na het behalen van het eindexamen gymnasium- $\beta$  in 1958, begon ik in dat jaar met de studie in de schei- en natuurkunde aan de Rijksuniversiteit te Leiden. Het kandidaatsexamen (letter e) werd in juni 1962 afgelegd. De studie werd voortgezet onder leiding van Prof. Dr. L.J. Oosterhoff. Tentamens voor theoretische natuurkunde en wiskunde werden afgelegd na het volgen van colleges van de hoogleraren Dr. S.R. de Groot, Dr. J.A.M. Cox, Dr. P.W. Kasteleijn en Dr. C. Visser. Het doctoraal examen met hoofdvak Theoretische Organische Chemie volgde november 1965. Van juni 1963 tot november 1965 vervulde ik een kandidaats assistentschap aan de afdeling Theoretische Organische Chemie, dat daarna overging in een doctoraal assistentschap. Vanaf februari 1968 ben ik aan deze afdeling verbonden als wetenschappelijk medewerker.

